Vietnamese-German University

COPYRIGHT WARNING

This paper is protected by copyright. You are advised to print or download **ONE COPY** of this paper for your own private reference, study and research purposes. You are prohibited having acts infringing upon copyright as stipulated in Laws and Regulations of Intellectual Property, including, but not limited to, appropriating, impersonating, publishing, distributing, modifying, altering, mutilating, distorting, reproducing, duplicating, displaying, communicating, disseminating, making derivative work, commercializing and converting to other forms the paper and/or any part of the paper. The acts could be done in actual life and/or via communication networks and by digital means without permission of copyright holders.

The users shall acknowledge and strictly respect to the copyright. The recitation must be reasonable and properly. If the users do not agree to all of these terms, do not use this paper. The users shall be responsible for legal issues if they make any copyright infringements. Failure to comply with this warning may expose you to:

VGU Vietnamese-German University

- Disciplinary action by the Vietnamese-German University.
- Legal action for copyright infringement.
- Heavy legal penalties and consequences shall be applied by the competent authorities.

The Vietnamese-German University and the authors reserve all their intellectual property rights.

Copyright

Vietnamese German University

Faculty of Engineering

Effect of longitudinal reinforcement distribution on the shear strength of slender reinforced concrete members without shear reinforcement

Thesis

Submitted for the Degree of
Bachelor in Civil Engineering and Construction Management

Author

Hung Nguyen Viet

Matriculation No.: 10721002 (VGU), 555542 (HBC)

Supervisors

Dr.-Ing. habil. Ngoc Linh Tran (VGU)

Prof. Dr.-Ing. Christian Kulas (HBC)

August 11, 2026

Hung Nguyen Viet

Effect of longitudinal reinforcement distribution on the shear strength of slender reinforced concrete members without shear reinforcement

Vietnamese German University, Faculty of Engineering
Civil Engineering and Construction Management Program

Thesis No.: BCE-2026-04

This thesis is available for public access at the library of Vietnamese-German University (VGU). A digital version of the thesis may also be archived in the institutional repository of VGU, subject to the university's publication and copyright policies. For further information regarding access or citation, readers are encouraged to contact the university library.

VGU
Vietnamese-German University

Vietnamese-German University

HBC. HOCHSCHULE BIBERACH UNIVERSITY OF APPLIED SCIENCES

HUNG NGUYEN VIET	555542	BCE 8.semester
Name of the student (capital letters)	Matriculation-No.	Degree program and semester

Declaration of independent authorship of the bachelor's thesis

VGU Vietnamese-German University

I hereby declare, in accordance with § 27a para. 7 of the examination regulations, that I have independently authored my bachelor's thesis and have not used any sources or aids other than those specified by me.

31.07.2026	Huy
Place, date	Signature

Foreword

This thesis was carried out at the Vietnamese German University within the Civil Engineering and Construction Management program, Faculty of Engineering. First and foremost, I would like to express my sincere gratitude to my supervisors Dr.-Ing. habil. Ngoc Linh Tran and Prof. Christian Kulas for their valuable guidance, constructive comments, and continuous support throughout the development of this thesis. Their knowledge and experience greatly contributed to the completion of this work.

I would also like to thank lecturer Dr. Hung Nguyen Dinh and lab engineer Mr. Ven Phan Lam for their technical guidance and valuable assistance during the experimental work. My appreciation also goes to my fellow students for their cooperation and support in preparing and conducting the experiments.

Finally, I am deeply grateful to my family and friends for their encouragement, patience, and support during my studies.

VGU
Vietnamese-German University

Abstract

Due to the lack of shear reinforcement, the behavior of reinforced concrete non-stirrup beams relies on the mutual interaction between longitudinal reinforcement and concrete, thus the specific parameters of both materials cannot be calculated independently. Longitudinal reinforcement for a long time has been verified its important role in deciding the effectiveness of shear transfer mechanisms such as dowel action, aggregate interlock, uncracked compression zone... and even size effect. Not only reinforcement ratio, the changes in layout, size of bar, reinforcing materials bring about significant changes in shear resistance of non-stirrup beams. In this thesis, a shear test was conducted among four non-stirrup beams to investigate the influence of longitudinal reinforcement on shear capacity. Four beams contain different numbers of longitudinal reinforcement pairs with ratio 2.6% and 3.8% corresponding to concrete cover thickness 24 mm and 74 mm. Simultaneously, the calculation of shear resistance is established for 4 testing specimens and 784 specimens in DafStb Heft 597 to evaluate the accuracy and precision, according to five different methods, concentrating on the new European standard EN 1992-1-1:2023 and other models such as CSA A23.3:2019, simplified *m*SM, iterative *m*SM, and iterative SMCFT. These methods are stretching across three fundamental theories: Critical Shear Crack Theory, simplified Modified Compression Field Theory, and pure mechanical Shear Model. As result, the experiment initially demonstrates the effectiveness of longitudinal reinforcement in controlling cracks and enhancing shear resistance after critical state, while resultant critical shear strengths of four beams are quite identical. Both approaches of *m*SM obtain the highest overall accuracy and precision, while the iterative SMCFT also yields the mean prediction close to unity.

VGU
Vietnamese-German University

Zusammenfassung

Aufgrund der fehlenden Querkraftbewehrung wird das Tragverhalten von Stahlbetonbalken ohne Bügel maßgeblich durch das Zusammenwirken von Längsbewehrung und Beton bestimmt. Daher können die relevanten Einflussparameter beider Werkstoffe nicht unabhängig voneinander betrachtet werden. Die Längsbewehrung spielt nachweislich eine wesentliche Rolle für die Wirksamkeit verschiedener Querkrafttragmechanismen, darunter die Dübelwirkung, die Rissverzahnung und die ungerissene Betondruckzone, sowie für den Größeneffekt. Nicht nur der Bewehrungsgrad, sondern auch Änderungen der Bewehrungsanordnung, des Stabdurchmessers und des Bewehrungswerkstoffs können die Querkrafttragfähigkeit von Balken ohne Querkraftbewehrung erheblich beeinflussen. Im Rahmen dieser Arbeit wurden Querkraftversuche an vier Balken ohne Bügelbewehrung durchgeführt, um den Einfluss der Längsbewehrung auf die Querkrafttragfähigkeit zu untersuchen. Die vier Versuchsbalken wiesen unterschiedliche Anzahlen paarweise angeordneter Längsbewehrungsstäbe auf. Die Bewehrungsgrade betrugen 2,6% beziehungsweise 3,8%, während die zugehörigen Betondeckungen 24 mm beziehungsweise 74 mm betrugen. Parallel dazu wurde die Querkrafttragfähigkeit sowohl für die vier untersuchten Versuchskörper als auch für 784 in DAfStb-Heft 597 dokumentierte Versuchskörper berechnet, um die Genauigkeit und Zuverlässigkeit von fünf unterschiedlichen Berechnungsverfahren zu bewerten. Im Mittelpunkt standen dabei die neue europäische Norm EN 1992-1-1:2023 sowie die Modelle nach CSA A23.3:2019, die vereinfachte mechanical Shear Model (*m*SM), die iterative *m*SM und die iterative Simplified Modified Compression Field Theory (SMCFT). Diese Verfahren basieren auf drei grundlegenden theoretischen Ansätzen: der Critical Shear Crack Theory, der vereinfachten Modified Compression Field Theory und rein mechanischen Shear Model. Die Versuchsergebnisse zeigen zunächst, dass die Längsbewehrung die Rissbildung wirksam begrenzt und die Querkrafttragfähigkeit nach Erreichen des kritischen Zustands erhöht. Beide Ansätze der *m*SM erreichen die höchste Gesamtgenauigkeit und Präzision, während die iterative SMCFT zudem eine mittlere Vorhersage nahe eins liefert.

VGU
Vietnamese-German University

Notation

$A_{ct,ef}$	Effective concrete tensile area
A_s, A_{sl}	Area of tensile longitudinal reinforcement
a	Shear span, distance from support to load application point
a/d	Span-to-depth ratio
a_{cs}	Effective shear span with respect to control section in EN 1992-1-1:2023
a_g	general notation of aggregate size
$a_{g,max}$	Maximum size of coarse aggregate
a_v	Mechanical shear span in EN 1992-1-1:2023
b	Width of cross-section
b_w	Web width of cross-section
BFRP	Basalt fiber reinforced polymer
CoV	Coefficient of variation
c	Depth of compression zone
CSCT	Critical Shear Crack Theory
D	Sieve size or aggregate particle size
D_{lower}	Smallest value of the upper sieve size D, consider the coarsest fraction of aggregates in concrete
D_{max}, d_g	Maximum aggregate size
d	Effective depth of cross-section
d_{dg}	Size parameter describing the failure zone roughness
d_{g0}	Reference aggregate-size or roughness value, taken as 16 mm
d_0	Transition size in the simplified *mSM* formulation
d_v	Effective shear depth in CSA A23.3-19
EC2	Eurocode 2
E_c	Young's modulus of concrete
E_s	Young's modulus of steel
f_c, f_c'	General notation for concrete compressive strength
f_{ck}	Characteristic concrete compressive strength
f_{ct}	Concrete tensile strength
$f_{ct,ef}$	Effective concrete tensile strength
f_y	Yield strength or tensile strength of reinforcing steel
f_{yd}	Design yield strength of longitudinal reinforcement
G_F	Fracture energy of concrete

Vietnamese-German University

GFRP	Glass fiber reinforced polymer
h	Overall depth of the cross-section
$h_{ct,ef}$	Effective tensile concrete depth, taken as $2.5(h-d)$ in the thesis
κ	Factor accounting for the location and kinematics of critical shear crack, defined in the CSCT refined model
k_b	Concrete-reinforcement bond factor in the crack-spacing equation
$k_x = \frac{x}{d}$	Relative depth of the compression zone
L	Total length of beam
l_{ch}	Characteristic length of concrete
$MCFT$	Modified Compression Field Theory
mSM	mechanical Shear Model of Tran (2020)
mSM*	Iterative calculation following mechanical Shear Model of Tran (2020)
M	Bending moment
M_{Ed}	Design action value of bending moment
M_{fl}	Comparative flexural moment calculated by steel tensile strength f_y = 345 MPa, used as the reference value in Kani's experiment
M_u	Experimental ultimate moment in Kani's experiment
min θ, max θ	Minimum and maximum values of the experimental-to-calculated ratio θ
n_1, n_2	Numbers of bars corresponding to ϕ_{s1} and ϕ_{s2}
P	Concentrated applied load
P_{cr}	Load at the critical shear-cracking state
P_{ult}	Ultimate load
SD	Standard deviation
SMCFT	Simplified Modified Compression Field Theory
SMCFT*	Iterative calculation following Simplified Modified Compression Field Theory
s_{cr}, $s_{cr,1}$, $s_{cr,2}$	Crack spacing
s_{ze}	Equivalent crack spacing in SMCFT
s_z	Crack spacing parameter dependent on crack control characteristics of longitudinal reinforcement in CSA A23.3-19
s_{ze}	Equivalent crack spacing parameter in CSA A23.3-19
V	Shear resistance force
V_c	Concrete shear resistance or calculated shear resistance force, depending on the model
V_{cc}	Shear-resistance contribution of the concrete compression zone in mSM
V_{cr}	Shear force defined at critical cracking state

VGU Vietnamese-German University

V_{ct}	Shear capacity of the tensile zone in *m*SM
V_{Ed}	Design value of the applied shear force.
V_{exp}	Experimentally measured shear resistance
$V_{initial}$	Initial assumed shear-force value in the iterative calculation
V_u, V_{ult}	Ultimate shear force
w	Crack opening or crack width
w_c	Limit crack width, considered in *m*SM
w_{cr}	Horizontal crack width at the tensile reinforcement
x	Depth of the compression zone
x_A	Position of the critical shear crack in the CSCT
z	Internal lever arm used in the shear check; EC2 takes $z = 0.9d$
z_c	Lever arm in *m*SM model, $z_c = d(1 - k_x/3)$
α_E	Factor taking into account the aggregate type
β	Factor accounting for shear resistance of cracked concrete in CSA A23.3-19
β_t	Coefficient to access mean strain over length between two cracks depending on the type of loading
γ_v	Partial factor for shear resistance in the EC2 section
δ_θ	Coefficient of variation CoV
ε	Longitudinal strain at control depth in CSCT
ε_1	Principal tensile strain
ε_s	Strain in the longitudinal reinforcement
ε_x	Reference longitudinal strain in CSCT and SMCFT
ε_{cm}	Mean concrete strain between cracks
ε_{cr}	Strain at cracking, f_{ct}/E_c
ε_{sm}	Mean reinforcement strain between cracks
η_e	Modular ratio between steel and concrete, generally understood as E_s/E_c
θ	Inclination angle of the compressive stress field in MCFT as well as the experimental-to-calculated ratio V_{exp}/V_c
κ	Curvature of the cracked cross-section
λ	Light-weight concrete factor in CSA A23.3-19; as well as shear span-to-depth ratio in *m*SM
λ_s	Effective span-to-depth ratio in the simplified *m*SM formulation
μ_θ	Mean value of θ
ν	Poisson's ratio of concrete
ρ, ρ_l, ρ_s	Longitudinal tensile reinforcement ratio
ρ_z	Transverse or web reinforcement ratio in the SMCFT formulation
$\rho_{s,ef}$	Effective reinforcement ratio, $A_s/A_{ct,ef}$

German University

σ	Normal or tensile stress
σ_s	Stress in the reinforcement at the cracked section
σ_x	Normal stress in concrete in the x direction
σ_y	Normal stress in concrete in the y direction
$\sigma_1,\ \sigma_2$	Principal stresses
$\sigma_{ct}(w)$	Residual tensile stress of concrete expressed as a function of crack opening
τ	Shear stress
τ_{bm}	Mean bond stress in the k_b formulation
τ_{Ed}	Design resistance shear stress
τ_{Rc}	Shear stress resistance of members without shear reinforcement without partial factor
τ_{Rd}	Design shear resistance stress
τ_{max}	Maximum shear stress
τ_{Rdc}	Shear stress resistance of members without shear reinforcement according to EC2
$\tau_{Rdc,min}$	Minimum shear-stress resistance of a member without shear reinforcement
ϕ_c	Concrete resistance factor in CSA A23.3-19
ψ	Solidity factor; taken as $\psi = 2/3$ for the compression zone

VGU
Vietnamese-German University

Contents

Foreword **iii**

1 Introduction **1**

1.1 Motivation . . . 1

1.2 Scope of the work . . . 2

1.3 Research objective . . . 2

1.4 Structure of the thesis . . . 3

2 Literature review **5**

2.1 Shear failure and transfer mechanisms . . . 5

2.2 Parameters affecting shear capacity . . . 9

2.3 Role of longitudinal reinforcement in shear capacity . . . 11

2.4 Background of EN 1992-1-1:2023 . . . 14

2.5 Research gap . . . 18

VGU
Vietnamese-German University

3 Experimental program **22**

3.1 Test specimens . . . 22

3.2 Material . . . 23

3.3 Casting procedure . . . 24

3.4 Instrumentation and test procedure . . . 25

3.4.1 Determination of concrete properties . . . 25

3.4.2 Shear test . . . 27

3.5 Experimental result . . . 29

4 Predictive calculation **37**

4.1 Iterative calculation formulation . . . 37

4.1.1 Modified Compression Field Theory . . . 37

4.1.2 Model *m*SM . . . 39

4.2 Simplified calculation formulation . . . 43

4.2.1 Model EN 1992-1-1:2023 . . . 43

4.2.2 Model CSA A23.3:2019 . . . 44

4.2.3 Model *m*SM . . . 45

4.3 Detailed calculation 46
4.3.1 Simplified calculation 46
4.3.2 Iterative calculation 53
4.4 Application of structural analysis software 54
4.4.1 Response-2000 software 54
4.4.2 INCA2 software 56
4.4.3 Additional application of Response-2000 software 58

5 Discussion **62**
5.1 Comparison between experimental result and predictive calculation 62
5.1.1 Four testing VGU beams 62
5.1.2 Database of 784 beams 64
5.2 General discussion 76
5.2.1 Discussion of experimental results 76
5.2.2 Evaluation of shear design models 79
5.2.3 Recommendation 81

6 Conclusion **83**

Bibliography **85**

Appendix A **91**

Appendix B **94**

Appendix C **98**

Appendix D **100**

VGU
Vietnamese-German University

List of Figures

2.1 *(a) Stress trajectories in a homogeneous beam of rectangular section and (b) potential crack pattern* [7], *reproduced* 5

2.2 *Flexural- and web-shear crack in beam* [11] 6

2.3 *Shear failure modes* [7] 6

2.4 *Aggregate interlock, uncracked compressive zone, residual tensile stress, and dowel action* [26] 8

2.5 *Arch action* [27] 8

2.6 *Two sides of splitting specimens with aggregates protrude out of cementitious matrix of low- and high strength concrete after splitting test* [28] 9

2.7 *An example of dowel action in reinforced concrete circular column* [29] 9

2.8 *Influence of beam effective depth and maximum aggregate size on the normalized shear strength of reinforced concrete beams without shear reinforcement* [36] . . 11

2.9 *Model of Walraven: Shear stress and normal stress transfer through crack by the increase of crack width and relative slip* [40] 11

2.10 *Kani's valley of diagonal failure* [1], *reproduced* 13

2.11 *Comb/Teeth model of Kani* [1] 13

2.12 *Smooth and deformed steel bars using in the test of 8 beams* [1] 13

2.13 *Result of 8 beams to examine the bonding capacity of longitudinal reinforcement, reproduced* [1], *reproduced* 13

2.14 *Load-deformation graph for 32 MPa beam with longitudinal reinforcement ratio 0.5%, 1%, 2%* [45], *reproduced* 14

2.15 *Shear stress of beams using glass fiber reinforced polymer* [46], *reproduced* . . . 14

2.16 *Influence of crack pattern in shear strength of beams: Tests EA1 with deformed bars and EB1 with smooth bars by Leonhardt and Walther* [43] 15

2.17 *Penetration of crack into diagonal compressive strut: Tests BP0 without spiral reinforcement and BP2 with spiral reinforcement by Muttoni et al.* [16] 15

2.18 *Comparison of shear strength calculated by CSCT (hyperbolic) and experiment results (black dots) of 150 slender normal- to high-strength beams without stirrup under concentrated load* [16] 17

2.19 *Types of cracks: primary flexural crack A, secondary flexural crack B, dowelling crack D, and aggregate interlock E* [49] 18

VGU Vietnamese-German University

2.20 *A typical example of Critical Development 1, 2, 3, and 4 corresponding with beam SC52, SC59, SC65, and SC62 respectively* [49] . . . 18
2.21 *Failure envelopes of RC beams under point loading (f_c = 20–100 MPa, d_g = 8–32 mm, ρ = 0.5–3%, d = 200–2000 mm, and a/d = 3–8), assuming critical shear crack location at 0.5a and power-law failure criterion* [52] . . . 20
2.22 *Comparison of original CSCT hyperbolic and power-law (with different span-to-depth ratio a/d) failure criterion* [53], *reproduced* . . . 20

3.1 *Cross-section of four testing beams* . . . 23
3.2 *Procedure of casting four experiment beams* . . . 24
3.3 *Cutting specimen* . . . 26
3.4 *Cutting specimen* . . . 26
3.5 *Splitting test* . . . 26
3.6 *Compressive test* . . . 26
3.7 *Cross-section of a specimen in splitting test* . . . 26
3.8 *Specimen after compressive test* . . . 26
3.9 *Elastic modulus of concrete test* . . . 27
3.10 *Specimen after elastic modulus test* . . . 27
3.11 *White painting and gridlines drawing on finished beams* . . . 28
3.12 *Instrumentation installation and setup of beam on testing frame* . . . 29
3.13 *Installation of strain gauge on longitudinal reinforcement* . . . 29
3.14 *Record of cracks in beam V26.01 after shear failure: primary flexural crack (yellow), crack splitting along longitudinal reinforcement (green), and critical shear crack (red)* . . . 32
3.15 *Record of cracks in beam V26.02 after shear failure: primary flexural crack (yellow), crack splitting along longitudinal reinforcement (green), and critical shear crack (red)* . . . 32
3.16 *Record of cracks in beam V26.03 after shear failure: primary flexural crack (yellow), crack splitting along longitudinal reinforcement (green), and critical shear crack (red)* . . . 32
3.17 *Record of cracks in beam V26.04 after shear failure: primary flexural crack (yellow), crack splitting along longitudinal reinforcement (green), and critical shear crack (red)* . . . 32
3.18 *Load–mid-span deflection graph of four experiment beams* . . . 33
3.19 *Photograph of actual crack patterns and corresponding crack diagrams of test beam V26.01, V26.01-1 (top) shows the left side of the beam, while V26.01-2 (bottom) shows the right side* . . . 34

Vietnamese-German University

3.20 *Photograph of actual crack patterns and corresponding crack diagrams of test beam V26.02, V26.02-1 (top) shows the left side of the beam, while V26.02-2 (bottom) shows the right side* . . . 34
3.21 *Photograph of actual crack patterns and corresponding crack diagrams of test beam V26.03, V26.03-1 (top) shows the left side of the beam, while V26.03-2 (bottom) shows the right side* . . . 35
3.22 *Photograph of actual crack patterns and corresponding crack diagrams of test beam V26.04, V26.04-1 (top) shows the left side of the beam, while V26.04-2 (bottom) shows the right side* . . . 35
3.23 *Critical shear crack (red line) of beam V26.01 penetrates into compressive zone in stable manner* . . . 36
3.24 *Aggregate interlock cracks (red line) spread from primary flexural crack (blue line) and propagate both sides of beam V26.02* . . . 36
3.25 *Potential shear crack (blue line) and secondary critical shear crack formed after failure (red line), in beam V26.03* . . . 36
3.26 *Critical shear crack (red line) of beam V26.04* . . . 36

4.1 *Fifteen equations of Modified Compression Field Theory* [56] . . . 39
4.2 *Load-deformation of typical beam under shear failure* [39] . . . 40
4.3 *Shear force and bending moment diagram of beam under concentrated load* . . . 48
4.4 *Cross-section of four testing beams on software Response-2000* . . . 55
4.5 *Compressive zone (dark grey zone) and tensile zone (grey zone) of cross-section of four testing beams V26.01, V26.02, V26.03, and V26.04 in INCA2 software* . . . 57
4.6 *Cross-sections of three beams GB58, GB54, and GB56 in experiment of Cholostiakow et al., reproduced* [59] . . . 58
4.7 *Cross-sections of six beams without stirrups are investigated for the influence of side reinforcement using Response-2000* . . . 60
4.8 *Crack patterns and crack width predicted by Response-2000 of six beams without shear reinforcement* . . . 61

5.1 *Experimental-to-calculated shear resistance ratio graph of four testing beams* . . . 64
5.2 *Distribution of experimental-to-calculated shear strength ratios of 784 beams among five methods* . . . 66
5.3 *Longitudinal reinforcement ratio versus experimental-to-calculated shear strength ratio for 784 beams among five methods* . . . 68
5.4 *Longitudinal reinforcement diameter versus experimental-to-calculated shear strength ratio for 784 beams among five methods* . . . 69

VGU Vietnamese-German University

5.5 *Effective depth versus experimental-to-calculated shear strength ratio for 784 beams among five methods* 70
5.6 *Shear span-to-effective-depth ratio versus experimental-to-calculated shear strength ratio for 784 beams among five methods* 71
5.7 *Concrete compressive strength versus experimental-to-calculated shear strength ratio for 784 beams among five methods* 72
5.8 *Maximum aggregate size versus experimental-to-calculated shear strength ratio for 784 beams among five methods* 73
5.9 *Influence of six parameters on the ratio V_{ct}/V_{cc} predicted by the iterative mSM* . 75

A.1 *Formwork used in the experiment* 91
A.2 *Longitudinal reinforcement details in the experiment* 92
A.3 *Procedure of experimental works* 92
A.4 *Support and equipment used in the experiment* 93
A.5 *Shear test procedure* 93
B.1 *Bending moment-shear force interaction diagram of four experiment beams predicted by CSA 2014 (blue line) and MCFT (red line) on Response-2000 software* . 94
B.2 *Bending moment-shear force interaction diagram of three beams GB58, GB54, and GB56 predicted by CSA 2014 (blue line) and MCFT (red line) on Response-2000 software* 95
B.3 *Moment-curvature diagram of four experiment beams, produced by INCA2 software* 96
B.4 *Stress of cross-section calculated by INCA2 for four experiment beams* 97

Vietnamese-German University

List of Tables

3.1 *Geometry and longitudinal reinforcement ratio of four experiment beams* 23
3.2 *Components of concrete mix* 23
3.3 *Results of concrete compressive and tensile splitting test* 33
3.4 *Ultimate and critical loads and shear forces recorded for the four specimens* . . . 33

4.1 Shear equations 46
4.2 *Section properties, loading, and geometry of the four testing beams* 47
4.3 *Longitudinal reinforcement used in four testing beams* 48
4.4 *Concrete properties of four testing beams* 48
4.5 *Shear resistance force of four testing beams calculated by EN 1992-1-1:2023* . . . 50
4.6 *Shear resistance force of four testing beams calculated by CSA A23.3:2019* 51
4.7 *Shear resistance force of four testing beams calculated by simplified mSM formulation* 52
4.8 *Shear resistance force of the four testing beams calculated using the iterative SMCFT and mSM approaches* 54
4.9 *Shear resistance of the four testing beams in relation to MCFT calculated by Response-2000 software, CSA A23.3-19 (simplified MCFT), and iterative SMCFT approach* 55
4.10 *Relative depth of the compression zone of the four test beams calculated using INCA2 and mSM* 56
4.11 *Curvature of the four test beams calculated using INCA2 and mSM* 56
4.12 *Mechanical properties of GFRP and BFRP reinforcement used in specimens GB58, GB54, and GB56* 59
4.13 *Comparison between experimental and Response-2000 shear strength predicted for original specimens GB58, GB54, and GB56* 59
4.14 *Relevant parameters of six beams without stirrups investigated for the influence of side reinforcement using Response-2000* 60
4.15 *Results of shear resistance and crack spacing recorded at the bottom of the beams for six specimens analyzed using Response-2000* 60

5.1 *Shear strength of four testing beams, calculated by EC2-2025, CSA A23.3-19, simplified mSM, iterative SMCFT*, iterative mSM* and MCFT by Response2000* . 63

5.2 *Mean value, standard deviation and coefficient of variation of results calculated by EC2-2025, CSA A23.3-19, simplified mSM, iterative SMCFT*, iterative mSM* and MCFT by Response2000, for shear strength of four testing beams* 63
5.3 *Comparison of shear strength calculation for database of 784 beams among 5 methods* 65

B.1 *Material properties used in Response-2000 software* 94
C.1 *General characteristics of the database* 98
C.2 *Minimum and maximum values of six investigated parameters in the database* . 98
C.3 *Frequency distribution of the experimental-to-calculated shear resistance ratios, adopted in Figure 5.2* 99
D.1 *Key parameters obtained from the final iteration of the mSM calculation* 102
D.2 *Key parameters obtained from the final iteration of the SMCFT calculation* . . . 102

VGU
Vietnamese-German University

1. Introduction

1.1 Motivation

In structural engineering, besides flexural design, an important factor that has notable influences on structural behavior and the stability of concrete structure is shear in beam. Once internal stresses caused by shear forces are not precisely considered in the design, shear failure may occur. Shear fracture arises when principal tensile stress reaches concrete tensile strength, particularly at critical section. Shear failure is typically accompanied with sudden, brittle and unpredictable action; lack of ductility and with little or no warning before happens [1].

Therefore, shear strength of reinforced concrete members in the past decades has been widely studied in literature and experiment on its potential catastrophic collapse. This has led to the development of various mechanical shear models. For instance, the 45° Truss model was developed by Ritter (1899) to analyze a post-cracking behavior of beam and was refined by Mörsch (1908) [2]. Following Ritter-Mörsch truss analogy, after hundred years evolution, Schlaich et al. proposed the Strut and Tie model by considering beam and discontinuity region of beam [3]. In the late 1980s, Muttoni and Schwartz introduced Critical Shear Crack theory (CSCT) that shear capacity is governed by critical shear crack and its kinematic [4]. In 1986, Michael Collins and Frank Vecchio improved the Modified Compression Field theory (MCFT) with the involvement of concrete tensile stresses of cracked concrete and defined inclined angle [5]. These models establish the theoretical foundation for evaluating shear behavior and predicting shear failure in concrete members.

VGU
Vietnamese-German University

Mostly shear stresses of modern concrete members are resisted by transverse reinforcement (stirrups), whereas the behavior of members without shear reinforcement is “a different ball game altogether”. The lack of stirrups requires greater reliance on other shear transfer mechanisms of materials according to different cracking stages. This complex characteristic gives rise to a lack of an obvious practical shear model that can wholly describe the actual shear behavior and the shear strength of reinforced concrete members without stirrups still remains an interesting and intriguing topic for further investigation.

In recent years, the second generation of Eurocode 2 (EC2) has been introduced with a new

breakthrough of the significant improvement in shear and punching design. The shear design now develops based on the mechanical model Critical Shear Crack theory (CSCT) integrating with experimental calibration, instead of purely relying on empirical formulations as previous. The refinement is expected to assess the shear and punching resistance of concrete members more accurately and enhance ease of use compared to the current EC2. However, despite the theoretical background, the shear formulations proposed in the new EC2 follow a semi-empirical approach, thus this model may not accurately reflect the actual shear behavior. The empirical correction factors in these formulations were calibrated from variety of experiments, which may be true in simple cases but cannot be applied synchronously to some special cases such as special concrete types, structure under fatigue, distinctive reinforcement arrangements, complex-shaped structure... Therefore, this limitation emphasizes the need for further empirical study into shear resistance design of concrete members focusing on the applicability, calibration, and safety margins of this design standard.

1.2 Scope of the work

VGU
Vietnamese-German University

This bachelor thesis concentrates on the theoretical study of shear capacity following the second generation of EC2. The so-called new or second version (generation) of EC2 mentioned in this thesis is of European version EN 1992-1-1:2023 and German version DIN EN 1992-1-1:2025-09 (published on September 2025) [6]. The primary purpose is to experimentally investigate the shear capacity of normal-strength concrete and normal-steel beams without stirrups and punching shear is probably excluded. Both theoretical and experimental investigation are constrained to slender members ($a/d > 2.5$), specifically rectangular beams. The shear test was carried on under simply supported beams subjected to concentrated loading, with their bottom longitudinal steel reinforcement detailed in multi-layers. Besides, there is no involvement of axial forces or pre-stressed concrete technique in this test.

1.3 Research objective

In the context of the second generation of EC2, this bachelor's thesis aims at evaluating the influence of longitudinal reinforcement distribution on the shear resistance of slender reinforced concrete members without shear reinforcement. This aim is attainable through the following

objectives:

- Review of the proposed shear strength model of the new EC2 (EN 1992-1-1-23), mechanical Shear Model (*m*SM), and Canadian standard (CSA A23.3-19) and their mechanical backgrounds. The predictive calculation is implemented among these three models as well.
- The shear test of non-stirrup beams containing different flexural reinforcement and its arrangements is conducted to record and analysis the relative shear behavior in practice.
- Conduct a comparison between predictive calculation and experimental results of shear strength in order to assess the degree to which these shear models reflects practical phenomenon.

The overview and actual data of the behavior of non-stirrup beams with varied reinforcement detailing are collected from the experiment. From these, the predictive calculations from selected models are performed. Therefore, the accuracy and reliability as well as prediction capability of considered shear strength models are examined through this thesis. As a result, conclusions will be drawn regarding to the impact of reinforcing steel distribution to the shear capacity of reinforced concrete members without stirrups. To achieve the research objective, this bachelor's thesis addresses the following research questions:

VGU
Vietnamese-German University

- How do longitudinal steel reinforcement ratio and arrangement contribute to the shear capacity of slender reinforced concrete members without shear reinforcement?
- How accurate and consistent are the EN 1992-1-1:2023, *m*SM, and CSA A23.3:2019 standard following iterative and simplified approaches in predicting the shear capacity of slender reinforced concrete members without shear reinforcement?

1.4 Structure of the thesis

The material presented in this thesis is divided into 6 chapters.

- The first section "**Introduction**" is about an overview of motivation, scope of the work, research aim and objective of bachelor thesis.
- Part 2 "**Literature Review**" concentrates on comprehensive literature review on shear failure and transfer mechanisms, influencing parameters affecting shear capacity of

concrete members without transverse reinforcement. In particular, this section provides a detailed review of the Critical Shear Crack theory, which is utilized in EN 1992-1-1:2023 and the role of longitudinal reinforcement in shear capacity, as these concepts form the central focus of the research. Drawing on these findings, the research gap addressed in this thesis is identified.

- Part 3 "**Experiment**" introduces a practical shear test of four normal-strength beam specimens with different longitudinal arrangement, aiming to investigate the actual shear behavior and relevant factors governing shear capacity of members without stirrups. The overall results and behavior of reinforced concrete beams without stirrups are described in this section.
- Part 4 "**Predictive Calculation**" provides the overall review among background theories and formulation of the Modified Compression Field Theory (MCFT), and mechanical principles, which are utilized respectively in the Canadian standard and *m*SM (2020) models; as well as review two simplified formulations in EN 1992-1-1:2023 and CSA A23.3:2019. Based on available experiment database and researched theories, the predictive computation of relevant factors and shear strength of 4 experimental and 784 database beam specimens are performed. This section provides a detailed breakdown step by step analysis, assumptions, iterative calculation, and execution procedures to create a database for the subsequent comparison with experimental results.
- Part 5 "**Discussion**" summarizes the comparative analysis between the experimental result and calculated predictions of three selected codes. Thereafter, a thorough discussion is presented to highlight key findings of the experiment, evaluate comparison outcomes and each shear prediction model; and offer recommendations.
- Part 6 "**Conclusion**" concludes the research work and presents further remarks of the thesis.

Weimar Bauhaus-University

2. Literature review

2.1 Shear failure and transfer mechanisms

In structural beam design, cracks occur once the principal tensile stress exceeds the tensile strength of concrete. The principal tension stresses acting in an uncracked beam are described through curved lines or stress trajectories on the surface (Figure 2.1). It can be observed that continuous curves plot the flow of compressive and tensile stress within a loaded structure, in which the tangent to these tensile trajectories defines the direction of principal tensile stress. Because concrete is weak at tension, cracks develop perpendicular to these maximum tensile curves as exceed concrete tensile strength. At middle bottom of beam, stress trajectories are horizontal, causing vertical flexural cracks. When moving toward supports, the increase of shear force orients the direction of principal tensile stresses into diagonal angle, causing diagonal cracks.

VGU
Vietnamese-German University

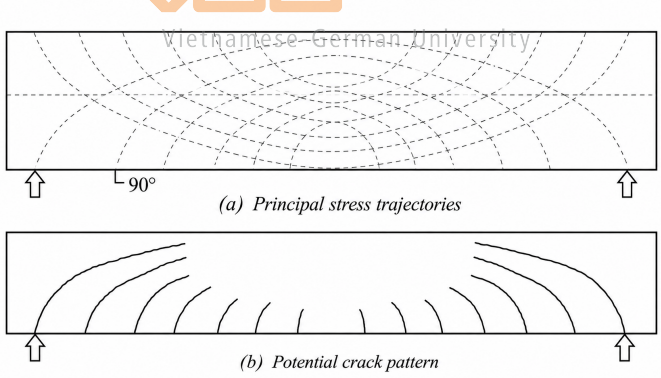

Figure 2.1: *(a) Stress trajectories in a homogeneous beam of rectangular section and (b) potential crack pattern* [7], *reproduced*

Shear failure is decided by inclined crack, which could be mainly described as web-shear and flexural-shear crack [8] (Figure 2.2). Web-shear cracks rarely occur in beam and they usually develop near inflection points of a continuous beam or adjacent to restraints of a simple beam. In most cases, flexural cracks initiate vertically at the section of large bending moment and then propagate diagonally into compression zone, forming shear-flexural cracks. When these cracks form in the shear span, the shear capacity of beam declines since shear stress transferring through crack is limited. Based on dimensions, geometries, loading, reinforcement

ratio and structural properties of concrete members, the shear failure could be described as diagonal tension failure, shear compression failure, shear tension failure, web crushing failure and arch rib failure (Figure 2.3) [9], [10]. The most commonly observed case in slender beams is diagonal tension failure, when a diagonal crack propagates over the whole cross-section leading to collapse. This mode of failure usually happens in beams with limited flexural reinforcement. Beams with sufficient reinforcement amount but low or without stirrup may cause shear compression failure. In this case, cracks also develop diagonally but form an uncracked compressive zone above crack's tip, in which global failure occurs by crushing of this zone. Shear tension failure is governed by cracks that spread along the longitudinal reinforcement due to worse bonding condition or lack of anchorage of steel bars. Web crushing and arch rib failure are observed as dominant in thin web or deep beams. For slender beams without shear reinforcement, flexural cracks develop early, followed by the rapid penetration of shear-flexural cracks to the top of beam; the resultant sudden failure is referred to as diagonal tension failure [7].

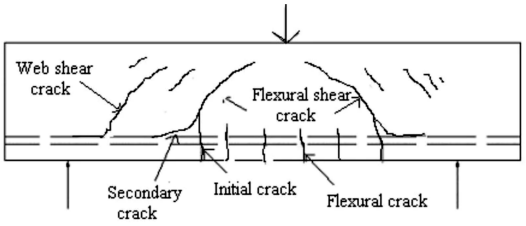

Figure 2.2: *Flexural- and web-shear crack in beam* [11]

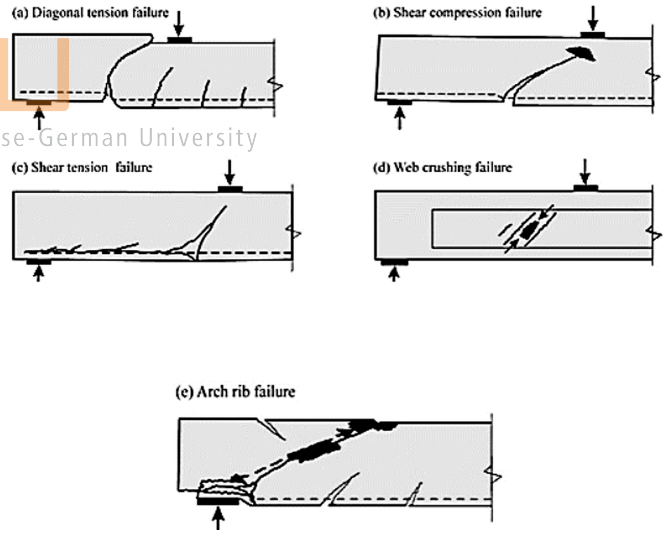

Figure 2.3: *Shear failure modes* [7]

The 1973 ASCE-ACI Committee 426 reported that shear stresses transfer within cracked beam mostly through five mechanisms: concrete residual tensile stress, arch action, uncracked compressive zone, aggregate interlock, and dowel action (Figure 2.4, 2.5) [12], and are widely accepted toward application. These mechanisms could be divided into arch action and as-beam shear transfer action. However, it should be notice that the relevant importance of these shear transfer mechanisms are dissimilarly evaluated by different researcher in their development

method.

- ***Residual tensile stress of concrete***: this can be simply understood as a small portion of concrete sticking two sides of a crack, usually after the crack initiates, which allows shear stresses are transferred through the crack. This mechanism originates from the softening behavior of concrete, the tensile stress capacity decreases gradually after reaching its peak, resulting from the development from micro to macro crack [13], [14]. It is a higher possibility to transfer shear stress through small cracks, however, it is limited to the crack openings larger than 2 mm [15].
- ***Arch action***: usually happens after beam action fails, allowing shear stresses are transferred directly from load point to support through internal, compressive, conceptual arching model rather than flexural action. After cracking, the uncracked compressive zone functions as a diagonal compressive or elbowed shape strut to transfer stress from load point to support. In combination, thanks to dowel action, longitudinal reinforcement acts as tensile tie that carries ideally uniform tensile force between supports and its impact relies on the effectiveness of concrete-steel bonding capacity, anchorage, and cracking pattern. For non-stirrup beams, arch action is considered as the consequence of critical shear crack through the formation of direct and elbow-shaped strut [16]. A typical example is (very) short or deep beam, whose shear span a is less than twice effective depth d.
- ***Uncracked compressive zone***: after the deformation of tension zone, uncracked concrete above crack's tip still owns abilities to resist shear stress, which shares about 20% to 40% of overall shear capacity. The contribution of this zone is decided by the depth of compressive zone. For slender beams, the effect of uncracked concrete is relatively small, since cracks tend to extend higher that shifts a neutral axis upward and narrows the depth of compressive zone.
- ***Aggregate interlock***: aggregate interlock describes the shear transfer capacity wherein protruding aggregates such as gravel, crushed stone, sand... on one crack's side interlock physically with cementitious matrix of the opposite side. Examples of broken aggregate particles on two surfaces of splitting test specimens for high- and low-strength concrete are shown in Figure 2.6. Aggregate interlock prevents the sliding between two cracking interfaces, which is governed by several factors such as roughness of crack surface,

crack width, aggregate size, concrete strength... Through the experiment on beams without shear reinforcement, Albrecht and Schnell demonstrated that 51% of load causing critical shear failure were carried by aggregate interlock [17]; while Fenwick defined that aggregate interlock resisted up to 70% of bonding force between inclined crack by comparing normal beam with the one have smooth aggregate crack surface [18].

- ***Dowel action***: when inclined crack expands, the shear capacity of concrete at crack is replaced by flexural reinforcement, where longitudinal steel bars bridging through concrete cracks, act like dowel to resist the sliding between crack's interface (Figure 2.7). This effect could be explained by three mechanisms: steel yielding and concrete crushing beneath dowel, concrete cover splitting, and other defect conditions [19]. Previous studies illustrated that dowel action contributes up to 9% shear transfer of deep beam [20], while this mechanism accounts for 15% to 25% of total shear capacity [21] [22]. Theoretically, there are two failure types of dowel action: crushing of concrete and slippage of diagonal cracks with the latter being dominant for beams without shear reinforcement [23].

In summary, in addition to flexural action, the shear capacity of beams without stirrups does not depends on single factor, but on the complex combination between several mechanisms. These transfer mechanisms provides the secondary line of defense with its limitation governed by widening and slipping of cracks, which eventually lead to major shear failure. However, diagonal cracked beam was illustrated as being capable of transferring shear stresses mainly through aggregate interlock, uncracked compressive zone, and dowel action [24] [25].

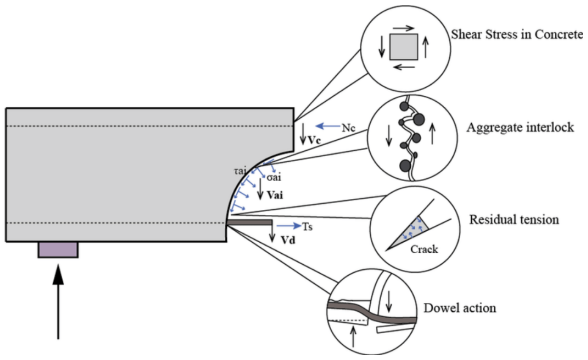

Figure 2.4: *Aggregate interlock, uncracked compressive zone, residual tensile stress, and dowel action* [26]

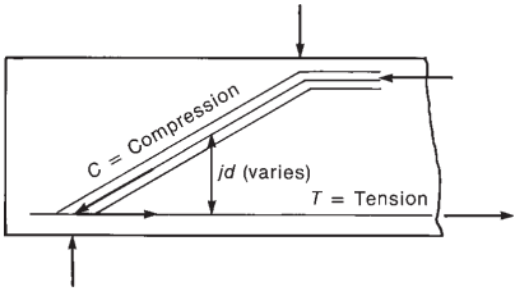

Figure 2.5: *Arch action* [27]

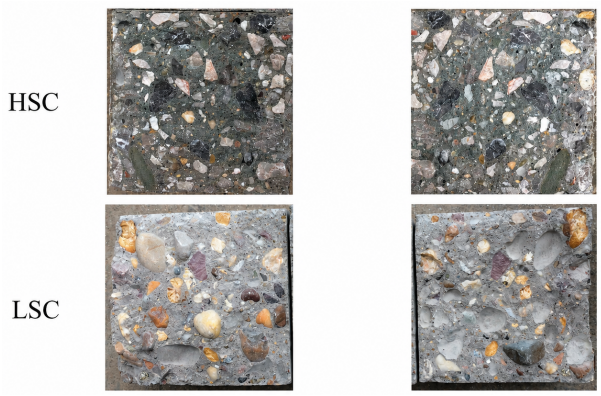

Figure 2.6: *Two sides of splitting specimens with aggregates protrude out of cementitious matrix of low- and high strength concrete after splitting test* [28]



Figure 2.7: *An example of dowel action in reinforced concrete circular column* [29]

2.2 Parameters affecting shear capacity

Concrete strength importantly presents among most of design codes in calculating shear capacity of members without web reinforcement. There is a clear correlation between load bearing capacity and concrete strength: higher-strength concrete offers a direct proportional increase in the shear capacity. The shear capacity increases proportionally with square root of concrete compressive strength f_c or effective concrete tensile strength $f_{ct,ef}$ in many current formulations. Several tests are conducted on beams with and without shear reinforcement corresponding with various outcomes: shear strength increases considerably with compressive strength [30], or shear stress decreases once compressive strength exceeds 34.5 MPa [31]. Some other opinions suggest that the role of compressive strength is insignificant and may ignore in the analysis of inclined shear failure or shear strength [32] [33].

Size effect, Kani (1967) pioneered in investigating the effect of member size on shear strength by testing several experiments beams without shear reinforcement with distinct effective depth d, longitudinal reinforcement ratio ρ_l and span-to-depth ratio a/d. This investigation has demonstrated the noticeable influence of a/d ratio on the ability of shear resistance and has figured out the important ratio a/d at 2.5 [34]. Shioya (1989) carried out a variety of large beams tests with depth 100 mm to 3,000 mm and finally concluded that the shear capacity of members was limited by the increase of member size and the decrease of aggregate size [35]. This conclusion could also be observed from Figure 2.8, which was developed by Collins and Kuchma (1999) [36]. The graph illustrated the normalized shear strength of the similar

reinforcement ratio, concrete compressive strength and steel tensile strength with effective depth varying from 101.6 mm to 2997.2 m (4" to 118") and black dots above each figure show the relevant strength. Further research was also conducted to provide experimental supplements for the importance of member size in shear capacity [37] [38]. Furthermore, the size phenomenon in beams without shear reinforcement demonstrates superiority rather than stirrup beams.

Strain effect, a key parameter in many shear strength models is the longitudinal tensile strain ε_x, which reflects the role of deformation state in shear capacity, besides material and geometrical properties. The main idea of CSCT is that width of critical shear crack is proportional to the longitudinal tensile strain ε_x and the effective depth d. The increase of longitudinal strain corresponds with the opening of inclined cracks width w, reducing the transfer of stress across crack and diminishing several shear transfer mechanisms such as aggregate interlock and concrete residual tensile stress. In the new EC2 and *m*SM models, crack width is expressed as the product of the crack spacing and difference between the mean strains of concrete and reinforcement [6] [39], while the reference strain is chosen to evaluate at mid-height of cross-section in MCFT or at about $0.6d$ in CSCT [5] [16]. In simplified equations, the longitudinal strain of concrete is usually neglected, instead, the reference strain of member is estimated by the strain of longitudinal reinforcement ε_s.

VGU
Vietnamese-German University

Aggregate size correlates closely with beams without shear reinforcement characterized by aggregate interlock and size effect. The increase of aggregate size improves the roughness of crack interface, allowing higher shear stress transfer through crack. Walraven (1980) exemplified from his experiment that the shear stresses allowed to transfer through cracks of maximum particle size D = 32 mm better than the one with D = 16 mm, because crack width expands and relative slip between two surfaces of crack increases (Figure 2.9) [40]. As previously presented in Figure 2.8, Collins and Kuchma (1999) examined the shear strength of beams without reinforced concrete varying aggregate size from 2.54 to 25.4 mm and followed similar trend with the former. However, in case of light-weight and high-strength concrete, coarse aggregates are split up by cracks and crack surface becomes smoother, which lowers the influence of this effect in beams [36].

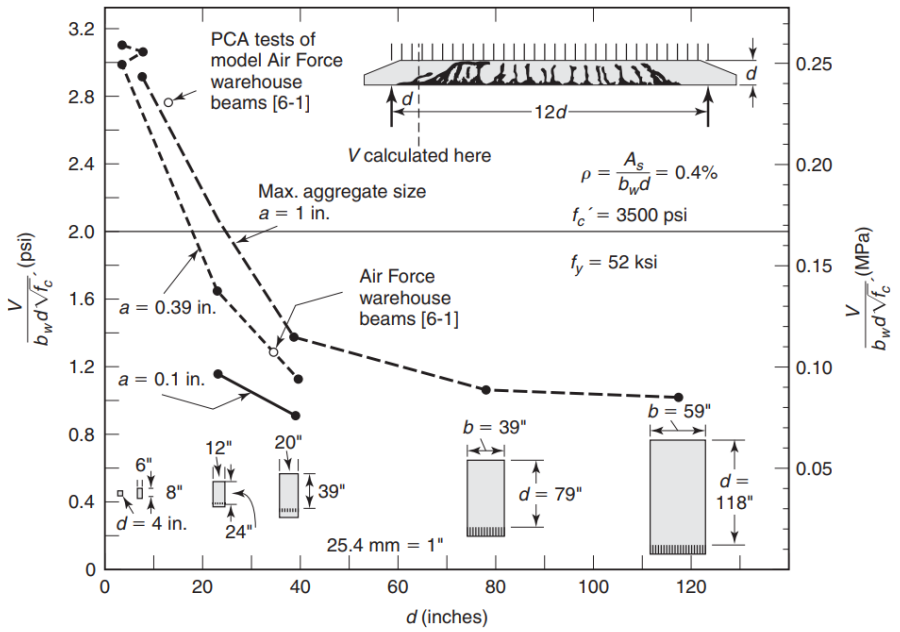

Figure 2.8: *Influence of beam effective depth and maximum aggregate size on the normalized shear strength of reinforced concrete beams without shear reinforcement* [36]

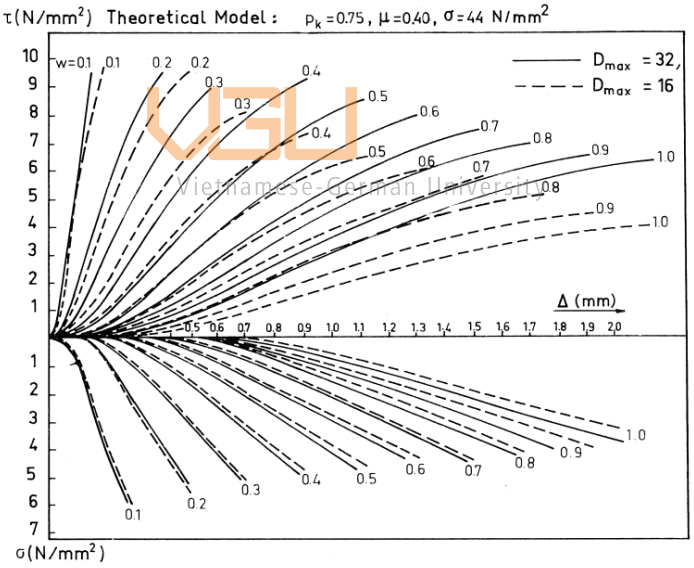

Figure 2.9: *Model of Walraven: Shear stress and normal stress transfer through crack by the increase of crack width and relative slip* [40]

2.3 Role of longitudinal reinforcement in shear capacity

The flexural cracks tend to appear earlier and extend wider into the beam due to small reinforcement ratio, which affects to the shear-transfer possibility along inclined crack through dowel action or crack's interface [41]. That's why the increase of longitudinal reinforcement ratio is expected to enhance aggregate shear transfer by controlling crack width. Besides, higher

reinforcing steel ratio also improves the dowel action by providing larger dowel area and reducing tensile stresses in the surrounding concrete. Taylor (1972) illustrated the impact of dowel action to shear resistance is remarkably related to the layout of longitudinal reinforcement, in which the shear capacity of members reinforced by two layers of reinforcing steel bars is about 40% higher than the one with single layer containing two bars of the same diameter [42]. On the other hand, earlier experiments by Leonhardt and Walther (1962) reported a decrease in beam plasticity strength as diagonal cracks penetrated deeper into the theoretical diagonal strut [43]. The larger longitudinal reinforcement ratio inhibits deeper penetration of flexural cracks within beams and can better control the opening of crack width, hence improving shear resistance stress [41] [44]. This feature also contributes to reduce the size effect in shear. With the same geometry, Collin and Kuchma (1999) found out that shear capacity of beam without side longitudinal reinforcement along depth decreases inversely with higher depth, while the other remains constant shear resistance as side reinforcement limits the formation and widening of shear cracks [36].

Furthermore, the correlation between longitudinal reinforcement and span-to-depth ratio on shear capacity was well-known by the study of Kani (1966). He has conducted 11 test series among 133 non-stirrup beams with different reinforcement ρ and span-to-depth a/d ratio to examine the impact of steel proportion on shear strength [32]. As results, he presented the graph called "valley of diagonal failure" or Kani's valley in Figure 2.10. The dimensionless indicator of beam strengths M_u/M_{fl} was employed with experimental ultimate bending moment at failure M_u and comparative flexural failure M_{fl}. The so-called valley is bounded by D (diagonal failure) and T (transition to flexure), wherein the left side of D and the right side of T attain full flexural capacity and no diagonal crack expects beyond T. With higher ρ_l, beam must be very slender to reach full flexural capacity. The minimum value about 54% of beam capacity can be obtained at the intersection a/d = 2.5. From 2.5 to 6, the structure is inclined to behave like a "beam" with flexural and shear mechanism, so-called beam action. Kani explained the working mechanism in this region as a comb, whose spine is uncracked compressive zone and concrete teeth is the section between two flexural cracks, working as a cantilever beam with "support" penetrated into compressive zone (Figure 2.11) [1].

Kani also illustrated the effect of reinforcement bonding on crack spacing with an interesting result, better bond conditions resulted in lower diagonal load capacity [1]. This was verified by the Stuttgart test of 8 beams with the same reinforcement, concrete strength, geometry but

VGU Vietnamese-German University

using smooth and ribbed steel bars (Figure 2.12). The shear capacity of smooth-bar beams is about 1.31 – 1.93 times higher than the defected one (Figure 2.13). In addition, Angelakos (1999) studied three 32 MPa beams without stirrups DB0.530, DB130, and DB230 with reinforcement ratio ranging from 0.5%, 1%, and 2% [45]. By the growth of steel ratio, the stiffness of beams also increased as in Figure 2.14, while smaller bond splitting was recorded. Consequently, the diagonal shear at failure became steeper and crack width was smaller leading to higher shear capacity 165.1 kN, 185.1 kN, and 272.1 kN. The change in reinforcement material and arrangement is also significantly affected the shear behavior of beams without shear reinforcement. Beams reinforced with glass fiber reinforced polymer bars (ρ_l = 1% and 1.8%) in two layers made diagonal shear failure slower, thereby increasing shear capacity by 28% (Figure 2.15) [46].

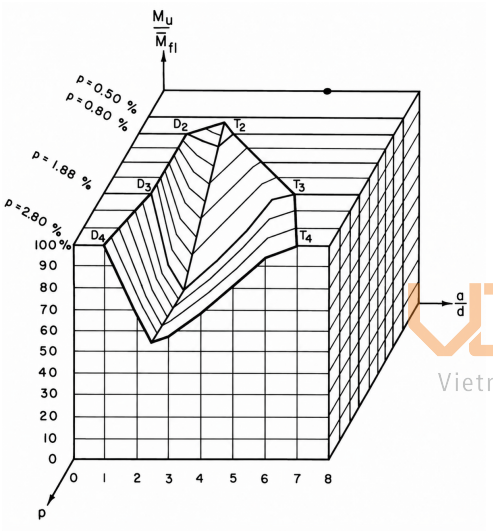

Figure 2.10: *Kani's valley of diagonal failure* [1], *reproduced*

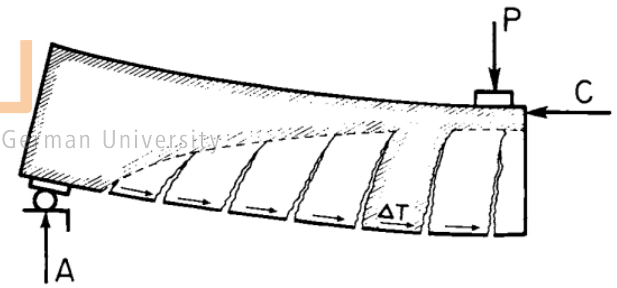

Figure 2.11: *Comb/Teeth model of Kani* [1]

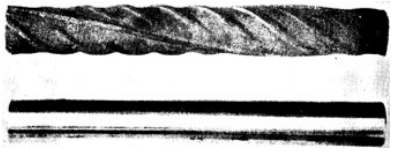

Figure 2.12: *Smooth and deformed steel bars using in the test of 8 beams* [1]

Type of loading	Corresponding beams		Reinforcement		Load at failure, kips		Ratio of capacities
	Deformed bars	Smooth bars	p, percent	No. of bars	Deformed bars	Smooth bars	smooth bars deformed bars
Concentrated loads	EA1	EB1	1.90	2	26.4	51.0	1.93
$\frac{a}{d}$ = 2.78	EA2	EB2	1.88	5	33.5	44.6	1.33
Uniformly distributed load	GA1	GB1	1.90	2	55.2	76.0	1.38
	GA2	GB2	1.88	5	65.3	85.7	1.31

Figure 2.13: *Result of 8 beams to examine the bonding capacity of longitudinal reinforcement, reproduced* [1], *reproduced*

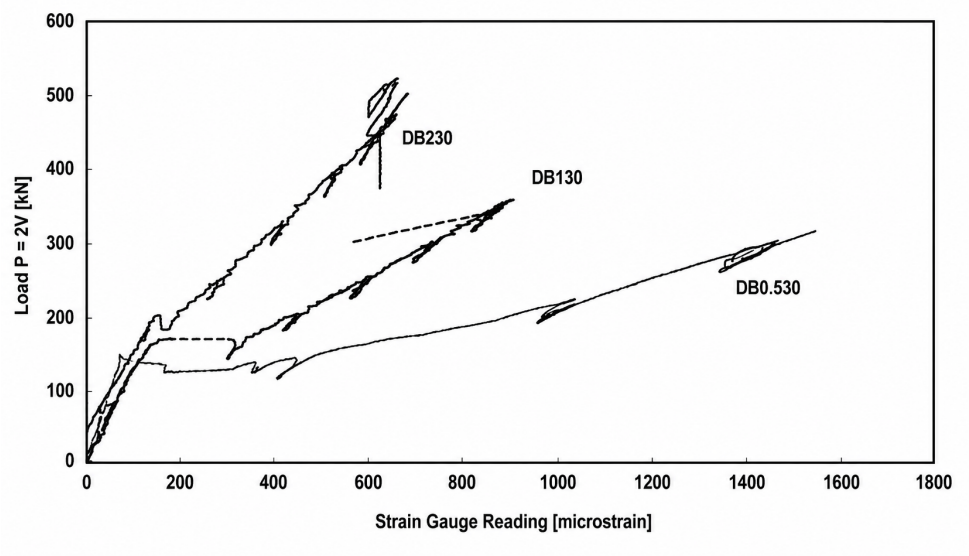

Figure 2.14: *Load-deformation graph for 32 MPa beam with longitudinal reinforcement ratio 0.5%, 1%, 2%* [45], *reproduced*

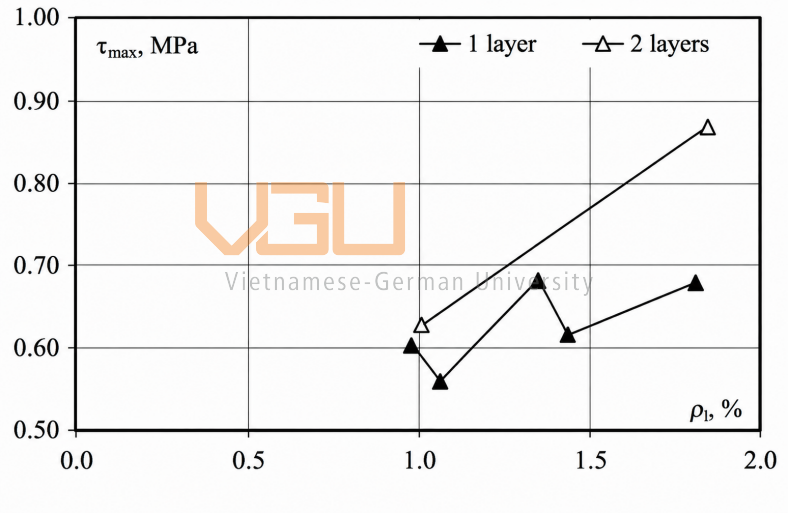

Figure 2.15: *Shear stress of beams using glass fiber reinforced polymer* [46], *reproduced*

2.4 Background of EN 1992-1-1:2023

The second generation of EC2 is currently refined based on theoretical background of Critical Shear Crack Theory. The CSCT was introduced by Muttoni (1985) to propose a draft design Swiss code [47], which oriented for punching shear of slab-column connection as well as beams and one-way slabs with or without shear reinforcement. It can be simply explained that shear strength of members without shear reinforcement is decided by the expansion of critical shear crack and its kinematic. The development of critical shear crack may lead to the new shear transfer mechanism after failure, arching action, which is activated through the form of

elbow-shaped strut and direct strut by aggregate interlock [16].

The concept of critical shear crack has been illustrated by the author using the same aforementioned Stuttgart test of Leonhardt and Walther (1962). As shown in Figure 2.16, beam EA1 and EB1 were cast respectively with deformed and smooth steel bars [43]. Beam EA1 failed at about 50% of its calculated plastic strength, while beam EB1 reached about 86%. This difference can be attributed to the propagation of a diagonal crack into the theoretical compression strut of beam EA1. In contrast, only a few of flexural cracks formed within the beam EB1 due to the absence of bonding stress. Muttoni et al. (1986) provided further evidence supporting this idea, that the spiral reinforcement in beam BP2 was nevertheless not able to carry shear stress, but limit inclined crack penetrating along the compression strut, allowing BP2 to reach its full computed plastic capacity, while BP0 reached only about 50% [48] (Figure 2.17).

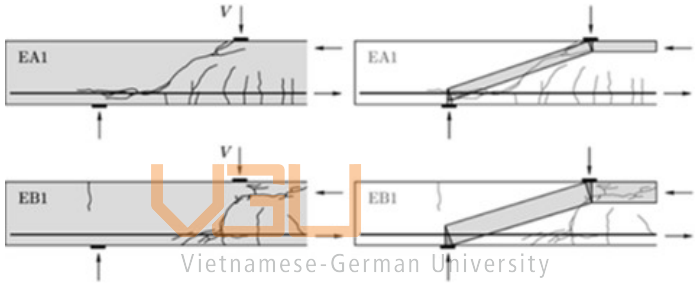

VGU
Vietnamese-German University

Figure 2.16: *Influence of crack pattern in shear strength of beams: Tests EA1 with deformed bars and EB1 with smooth bars by Leonhardt and Walther* [43]

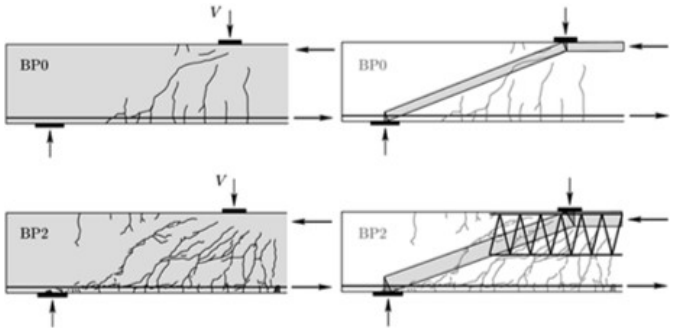

Figure 2.17: *Penetration of crack into diagonal compressive strut: Tests BP0 without spiral reinforcement and BP2 with spiral reinforcement by Muttoni et al.* [16]

This theory focuses on fundamental assumption, that critical crack width w governed by the strain in control depth ε and effective depth d. The size effect is therefore naturally reflected through a physical interpretation, members with higher depth suffer larger crack width and lower shear strength. Similarly, the higher increase in longitudinal strain results in larger crack opening, leading to structure failure.

$$w \propto \varepsilon \cdot d \tag{2.1}$$

The CSCT offers the shear strength through the function of concrete compressive strength f_c, and the function of crack width w and its interface's roughness (largest aggregate size d_g) [16] as follows:

$$\frac{V_c}{b\,d} = \sqrt{f_c} \cdot f(w, d_g) \tag{2.2}$$

For reference strain, the control section of beams under concentrated load is chosen at $d/2$ from the loading point due to load introduction, since the shear force is constant over the span and the bending moment approaches extreme value at mid-span, result in wider cracks. The reference strain is examined at 0.6 of effective depth d from the top fiber and cross-section remains plan. The roughness in CSCT is defined as $d_{g0} + d_g$, with minimum aggregate size d_{g0} equal to 16 mm, since the interface between cracks is not perfectly smooth and shear stress can be transfer through rough cementitious matrix. The reference strain without axial forces is described in Equation 2.3.

$$\varepsilon = \frac{M}{b\,d\rho E_s\left(d - \frac{c}{3}\right)} \frac{0.6d - c}{d - c} \tag{2.3}$$

where M is the bending moment, d effective depth, b width of section, ρ longitudinal reinforcement ratio, E_s elastic modulus of steel and c is depth of compression zone.

In overall, the shear strength of CSCT for beams without shear reinforcement is as follows:

$$\frac{V}{b\,d\sqrt{f_c}} = \frac{1}{6} \frac{2}{1 + 120\dfrac{\varepsilon d}{16 + d_g}} = \frac{0.3}{1 + \varepsilon d \dfrac{120}{16 + d_g}} \tag{2.4}$$

From the basic assumption of crack width, the CSCT normalized shear strength is defined by a hyperbolic curve that clearly describes the progressive reduction in shear strength as critical crack width increases. The validation against 150 testing beams showed that the CSCT curve asymptotes closely with black points of testing results, confirming its accuracy and

reliability in practice (Figure 2.18).

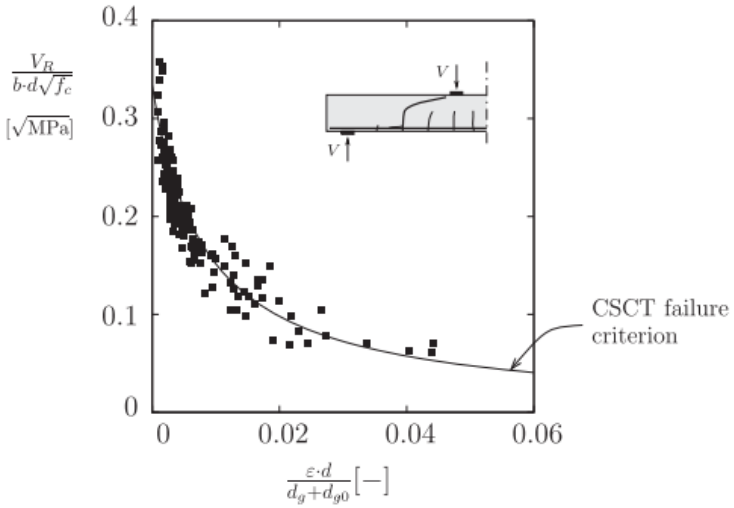

Figure 2.18: *Comparison of shear strength calculated by CSCT (hyperbolic) and experiment results (black dots) of 150 slender normal- to high-strength beams without stirrup under concentrated load* [16]

Following the context of critical shear crack, Cavagnis et al. proposed a refined CSCT model that considers the pattern of cracks after or right before failure through an experimental campaign on 20 beams [49]. The refined model is expected to be well applied for one-way slab and beams without stirrups, in which pattern, location, and kinematics of shear cracks were evaluated in shear test by more modern technique: high-resolution photography. In the first test, there were 13 non-stirrup beams under different loading conditions and beam setup with the same longitudinal reinforcement ratio (included both compressive and tensile reinforcement). The observed cracks during this test were categorized into primary flexural crack A, secondary flexural crack B, dowelling crack D, and aggregate interlock E (Figure 2.19). From these categorizes, the author divided the development of critical shear crack into 4 types: (Type 1) Potential shear crack allowing direct strut action to develop, (Type 2) Failures follow a stable propagation of a critical shear crack, (Type 3) Failures driven by loss of aggregate interlock capacity due to development of an interlock crack, and (Type 4) Failures driven by merging of primary flexural cracks. An example of crack development Type 1 to 4 could be seen through crack diagrams of beam SC52, SC59, SC65, and SC62 respectively (Figure 2.20). As results, four as-beam shear transfer mechanisms aggregate interlock, residual tensile stress, uncracked compressive zone, and dowel action are identified by its governing role corresponding to each failure modes. The effective mechanisms are governed by cracking state, pattern, and development.

VGU
Vietnamese-German University

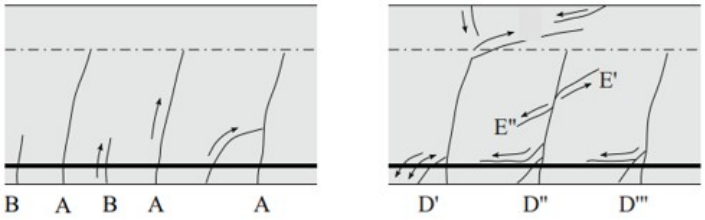

Figure 2.19: *Types of cracks: primary flexural crack A, secondary flexural crack B, dowelling crack D, and aggregate interlock E* [49]

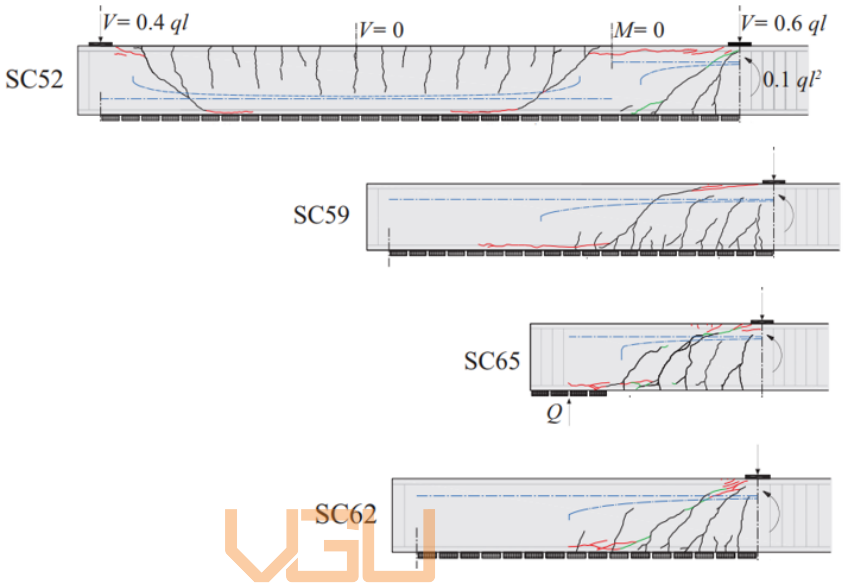

Figure 2.20: *A typical example of Critical Development 1, 2, 3, and 4 corresponding with beam SC52, SC59, SC65, and SC62 respectively* [49]

2.5 Research gap

The shear strength of members without shear reinforcement depends on several interacting shear transfer mechanisms, accordingly various approaches have been developed to explain this behavior. After more than a century of development, the problem of shear resistance of reinforced concrete structure remains a controversial topic regarding the reliability and accuracy of each shear model. In reality, there was a notable argument between researcher groups Dönmez & Bažant and Muttoni & Ruiz about the accuracy and scientific background of the Critical Shear Crack Theory. Dönmez et al. concluded that the CSCT depends on six hypotheses that lack physical justification and apply one-dimensional elastic beam theory to a multi-dimensional nonlinear fracture problem [50]. Additionally, his finite element analysis also defined that energy dissipation was concentrated in the region near main shear crack rather than within the crack opening, suggesting in contrast with CSCT that crack width

does not control failure. The author of CSCT, Muttoni and Ruiz also defended their theory by providing experimental evidences and core mechanical models [51]. From other perspective, Bentz and Foster provided an independent aspect by evaluating experimental data in the last 30 years and demonstrates the capable of accurately predicting shear strength of mechanical models depending on the development of cracks, such as MCFT or CSCT [49]. These groups of authors also represent three large background theories of shear strength: energetic fracture mechanics, CSCT, and MCFT.

In addition, from the aforementioned Cavagnis's test, the shear capacity of beams without shear reinforcement embedded on patterns of crack is described through a refined closed-form equation, which is employed in the new EC2 [52]. The refinement still reflected the basic idea of CSCT, thus integrating the involvement of various shear transfer mechanisms decided by the location and shape of crack, through the coefficient κ. The closed-form formulation is simplified from an iterative calculation of the refined CSCT model, estimating the contribution of four shear transfer mechanisms and opening of crack width through load-deformation relationship. To enhance ease of use, shear strength of limited specimens (described in Figure 2.21) using these refined formulations is performed through a narrow region (grey area) and the closed-form equation (hyperbolic) is derived by power law (Equation 2.4), which covered in this failure envelope. Similarly, coefficient κ in the CSCT closed-form formula is also derived from an equation, whose curves match or coincide within certain ranges with those of original model. In the new EC2, span-to-depth ratio a/d is also chosen at 4, since the power-law failure criterion at this range mostly matches the original CSCT failure criterion (Figure 2.22) [53]. From these mentioned points, it is indisputable that the new shear formulation of EC2, despite relying on CSC theory, is mainly developed following semi-empirical approach, and the simplification still depends on several assumptions and limited to a certain range of related parameters. Hence, this process may rely significantly on specific experimental framework and experience of researchers. This may lead to ambiguity and inaccuracies regarding contributing roles of shear transfer mechanisms and the behavior of non-stirrup beams in reality.

VGU
Vietnamese-German University

$$\frac{V_c}{b\,d\sqrt{f_c}} = \kappa \left(\frac{d_{dg}}{\varepsilon_s d}\right)^{1/2} \tag{2.5}$$

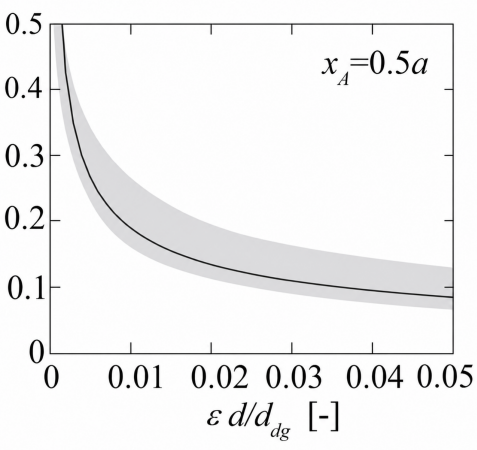

Figure 2.21: *Failure envelopes of RC beams under point loading (f_c = 20–100 MPa, d_g = 8–32 mm, ρ = 0.5–3%, d = 200–2000 mm, and a/d = 3–8), assuming critical shear crack location at 0.5a and power-law failure criterion* [52]

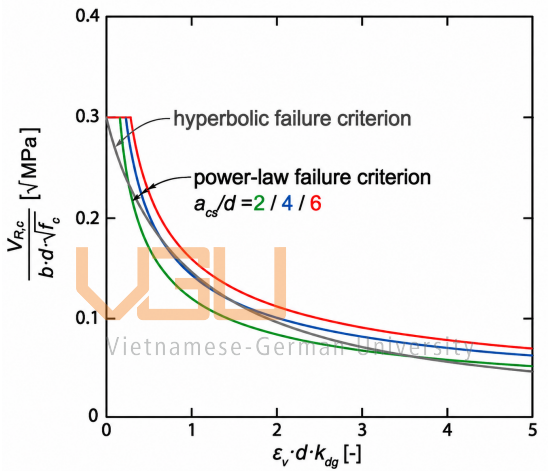

Figure 2.22: *Comparison of original CSCT hyperbolic and power-law (with different span-to-depth ratio a/d) failure criterion* [53], *reproduced*

On the other hand, several studies presented above have emphasized the important role of longitudinal reinforcement in shear transfer mechanisms by controlling crack development [41] [42] [43] [45] and thus also size effect [1]. Although the influence of longitudinal reinforcement ratio on the shear resistance has been widely investigated, there was limited research that has separated the effect of longitudinal reinforcement distribution. In particular, the effect of bar layers, number of bars, thickness of bottom concrete cover... on shear capacity of slender concrete beams without shear reinforcement remains an open topic of research, specifically within the calculation framework of the second generation EC2. This gap is especially significant considering that the shear resistance by CSCT continues to be the center of discussion among major background theories. For these reasons, this thesis is expected to contribute to experimental investigation of the new EC2 provision, particularly with respect to the influence

of longitudinal reinforcement on the shear resistance of reinforced concrete beams without stirrups. The calculations of beams without shear reinforcement relied on three theoretical backgrounds CSCT, MCFT, and pure mechanical principles are generally evaluated as well in terms of accuracy and reliability.

VGU
Vietnamese-German University

3. Experimental program

Under the scope of bachelor thesis, the shear test was conducted in order to evaluate the actual shear behavior until failure of non-stirrup beams with distinct longitudinal reinforcement arrangement. The main purpose is to investigate the influence of longitudinal reinforcement by modifying reinforcement ratio, steel bars arrangement as well as thickening concrete cover of beams. The test was carried out through four normal-strength concrete beam specimens with different cross-section dimensions and longitudinal reinforcement ratios. These differences aim at investigating specific shear behavior of each chosen reinforcement ratio, thus, the expected conclusion shall be drawn from the comparison between experimental results and predictive calculation in the role of longitudinal reinforcement. The test was conducted at the civil engineering laboratory of Vietnamese German University - VGU.

3.1 Test specimens

VGU
Vietnamese-German University

The test was conducted among four specimens, marked as V26.01, V26.02, V26.03, and V26.04. They all had rectangular cross-section with dimension 150 x 250 mm and 150 x 300 mm, while the length was 1,500 mm with effective working length 1,200 mm (Figure 3.1). Sections had different arrangements of four to six 16 mm diameter steel bars, which resulted in two different longitudinal reinforcement ratios 2.6% and 3.8%. The steel reinforcement was arranged in multi-layers at 210 mm effective depth, same span-to-depth ratio a/d of 2.86 and there was no shear reinforcement included.

Specifically, pairs V26.01/V26.02 and V26.03/V26.04 were designed with reinforcement ratios of 2.6% and 3.8% respectively, and the thickness of the concrete cover for beams within the same pair was changed to 24 mm and 74 mm. On the other hand, pair V26.01/V26.03 and V26.02/V26.04 retain the same cross-sectional dimensions but change steel bars arrangement, increasing from 2 to 3 pairs of reinforcement. This experimental design optimizes the research objectives allowing comparison of the combined effects of reinforcement ratio, reinforcement arrangement, and concrete cover. The specimen detail is described in Table 3.1.

Table 3.1: *Geometry and longitudinal reinforcement ratio of four experiment beams*

Specimen	Dimension (mm)	a (mm)	d (mm)	a/d	ρ_l (%)
V26.01	250 x 150 x 1,500	600	210	2.86	2.6
V26.02	300 x 150 x 1,500	600	210	2.86	2.6
V26.03	250 x 150 x 1,500	600	210	2.86	3.8
V26.04	300 x 150 x 1,500	600	210	2.86	3.8

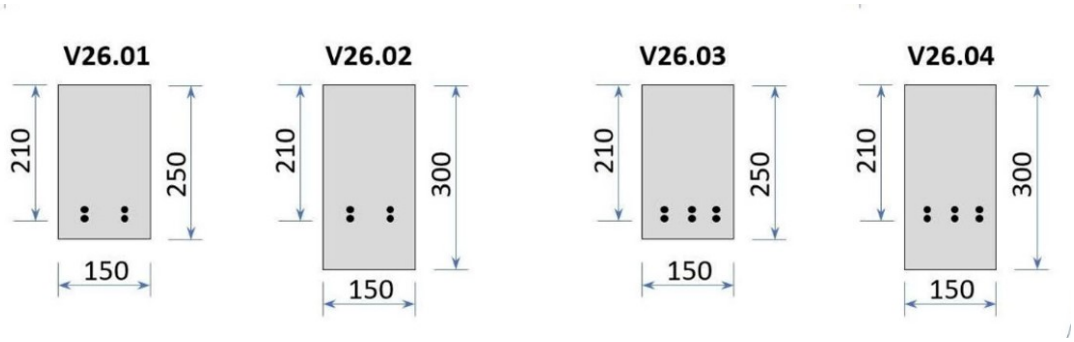

Figure 3.1: *Cross-section of four testing beams*

3.2 Material

The concrete mix was designed to achieve a compressive strength of C30/37, whose materials used were measured and prepared, including B350 steel bars diameter 16 mm, crushed stone, sand, the accelerating admixture Sika CTP 432, and cement. Maximum size of coarse aggregates is 16 mm and minimum size is 2 mm, which were not through sieving analysis to determine but obtained directly from the supplier. The use of admixture accelerates the hydration reaction, allowing the concrete to reach its initial strength rapidly and simultaneously for a reduction in water content while maintaining ideal strength. To ensure the consistency and quality, concrete was mixed by several batches, which the specified concrete components are quantified as in Table 3.2. The actual concrete strengths and elastic modulus are determined by tests after 28 days.

VGU
Vietnamese-German University

Table 3.2: *Components of concrete mix*

Component	Quantity per 0.05 m^3 concrete
Cement	21.6 kg
Crushed stone	54.5 kg
Sand	28.7 kg
Water	7.2 liter
Admixture	216 gram

3.3 Casting procedure

The casting process included the preparation of the formwork, installation of the reinforcement, and concrete placement. The reinforcement was arranged according to the designed beam configuration and fixed in the required position. Concrete was then mixed, poured into the formwork, and compacted to ensure uniform spreading and remove entrapped air. In addition, cylindrical specimens with a diameter of 150 mm were cast to determine the concrete strength and elastic modulus. Further details of the experimental work are provided in Appendix A.

Regarding curing condition, the beams were stored outdoors under roof to avoid direct sunlight and rainfall. The laboratory environment is characterized by hot and humid condition with relative humidity ranging 66% to 76% and ambient temperature fluctuating 21°C to 33°C. After 28 days of curing, the formwork was removed and the testing procedure was conducted.



Figure 3.2: *Procedure of casting four experiment beams*

3.4 Instrumentation and test procedure

3.4.1 Determination of concrete properties

After releasing the mold, the cylinder specimens were flattened at both ends by concrete cutting saw (Figure 3.3 & 3.4). This step ensures that the compressive load distributes evenly over the cross section, applies directly at the center, and avoid early destruction of samples. Specimen test was conducted under compressive test and splitting test using universal testing machine. The compressive test indicates the maximum compressive load concrete sample can bear before deformation, in which the cylinder specimen 150 x 300 mm is placed central vertically between the loading platens and gradually subjected to compression until failure (Figure 3.6 & 3.8). Maximum load at failure is recorded and divided by cross-section area of specimen equal to concrete compressive strength f_c. In contrast, the specimen in splitting test lies horizontally between loading platens. Testing specimen was also cut down to 150 x 160 mm to match the length of platens allowing uniformly distributed load alongside. The machine continues loading until a sudden vertical crack propagates along the cross-section, splitting the cylinder into two halves (Figure 3.5 & 3.7). Concrete tensile strength f_{ct} was calculated by load at peak recorded at failure. Similarly to compressive test, the cylinder concrete specimen was now equipped with longitudinal compressometer 150 mm, which two metal rings are tightened at the top and bottom of specimen (Figure 3.9 & 3.10). Two linear displacement transducers are installed on one ring against the other. From the displacement of sensors and load data of compressive machine, the elastic modulus can be determined by the division of stress by strain.

VGU
Vietnamese-German University

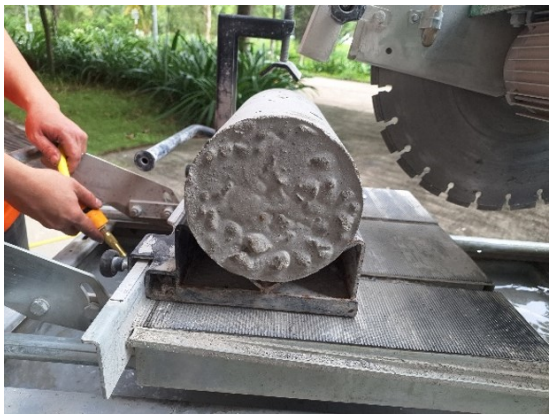

Figure 3.3: *Cutting specimen*



Figure 3.4: *Cutting specimen*



Figure 3.5: *Splitting test*



Figure 3.6: *Compressive test*



Figure 3.7: *Cross-section of a specimen in splitting test*



Figure 3.8: *Specimen after compressive test*



Figure 3.9: *Elastic modulus of concrete test*



Figure 3.10: *Specimen after elastic modulus test*

3.4.2 Shear test

VGU
Vietnamese-German University

Preparation for the test required painting all beams white and drawing a grid pattern to ensure accurate observations (Figure 3.11). During shear test, the beam was setup as a simply supported beam, lying on two roller supports. Due to the massive size of beam, the roller support were reproduced by welding I-shaped steel beam with cylindrical steel bar. As could be seen from Figure 3.12, there are two loading plates made of steel plates and rubber between structure and supports. Placing a concrete beam directly onto a cylindrical steel bar creates line contact, reducing middle contact surface. This small line contact causes peak stress at support reactions. The loading plates help expanding contact surface preventing early concrete crushing at this position before bending or shearing happens. Since the beam surface is not perfectly straight but rugged, rubber pad between steel and concrete eliminates instability as well as generate a uniform pressure distribution across the entire interface by smoothing out the rough surface.

At the loading point, a loading hydraulic jack was applied to the beam through a round steel bar and bearing plate. This steel bar acts as a roller, so that the beam rotates freely beneath it when it sags, ensuring that applying force is always ideally concentrated vertical. Similarly at supports, the steel and rubber pad allow distributing force evenly and preventing localized beam fracture.

Aiming to record longitudinal reinforcement strain and displacement of beam, the measuring

equipment was installed at certain designated position. Linear displacement transducers at both ends and the midpoint of the beam indicated the total vertical displacement. Longitudinal reinforcement displacement was also recorded by strain gauges attached to steel bars in beams V26.01 and V26.03 (Figure 3.13). Steel bar was sanded to remove outer zinc coating before attaching measuring grid to steel surface. The summarization of employed measuring devices is as follows:

- 3 linear displacement transducers at both end and middle bottom of beam
- 4 strain gauges attached with longitudinal steel bars in beam V26.01 and V26.03
- Load cell of testing hydraulic jack

After being properly aligned on the testing frame, four beams were subjected gradually to concentrated loading until complete failure, during which time the structural response was recorded through physical observation and videotaping. All cracks were detected and marked with relevant loading magnitude.



Figure 3.11: *White painting and gridlines drawing on finished beams*

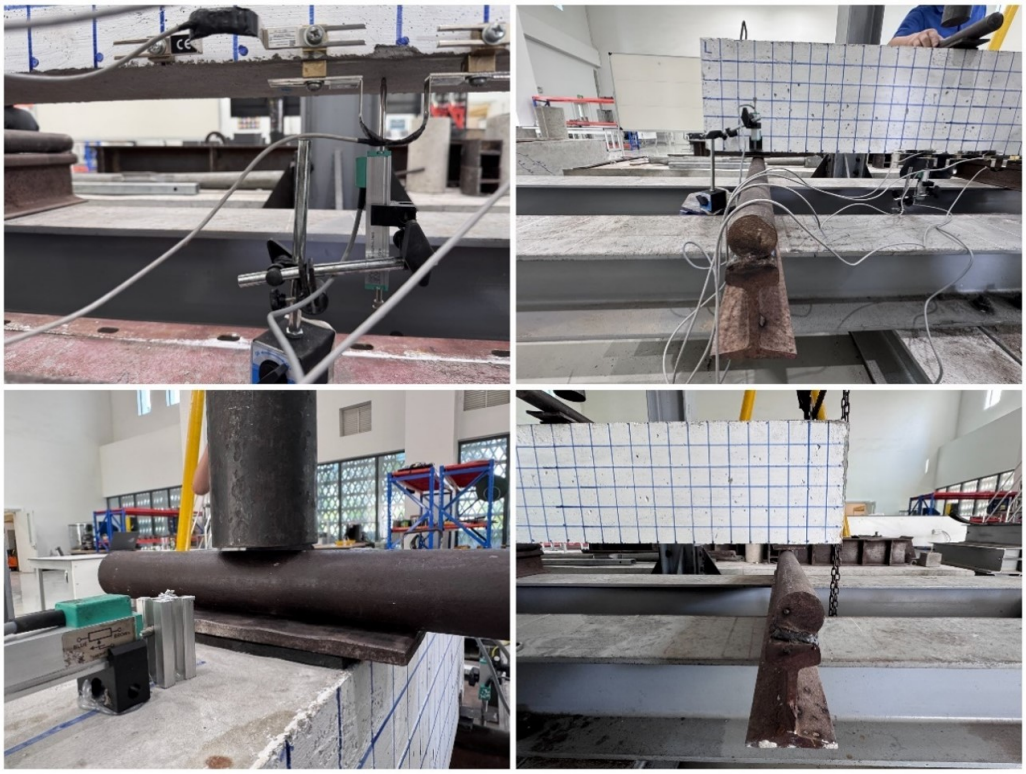

Figure 3.12: *Instrumentation installation and setup of beam on testing frame*



Figure 3.13: *Installation of strain gauge on longitudinal reinforcement*

3.5 Experimental result

As expected, all test specimens failed in shear, with tension shear failure being the dominant mode. In theory, the formation of critical shear crack limits the ability of beam to transfer shear stress through crack, followed by global shear failure. This failure is typically catastrophic, brittle and occurs without warning. General crack diagrams of four beams are also shown through series of picture in Figure 3.19 to 3.22. In summary, the overall observation of crack patterns among four testing specimens is described as follows:

- **Beam V26.01** (Figure 3.14): within the first range of 60 kN, there was a few observed flexural cracks distributed evenly along the middle bottom of beam. When load exceeded 80 kN, these cracks tended to develop vertically but not too high into compressive zone and no new flexural crack was recorded. Alternatively, a critical shear crack penetrated diagonally toward loading point at 120 kN and developed notably upon this threshold. As load increased, the main crack width expanded rapidly spreading upwards loading point and stretching along the longitudinal reinforcement toward a support. The beam completely failed at 127 kN due to crushing of the concrete zone above crack's tip, followed by rapid expansion of the critical shear crack. The failure is governed by the critical shear crack and fails by tension shear failure.
- **Beam V26.02** (Figure 3.15): the number of flexural and shear cracks at bottom and web of beam is generally quite limited. Despite containing a similar reinforcement ratio to V26.01, the specimen exhibited an early flexural crack at 20 kN at mid-span of tension zone, whose height is about equal to concrete cover due to thicker concrete layer and be subjected to largest bending moment. The structure only showed a second flexural crack at 50 kN before spreading diagonally into compressive zone at 80 kN. After 90 kN, shear cracks appeared densely within the web and a critical shear crack suddenly formed at 115 kN, propagating upward from the bottom of beam. The main crack width expanded rapidly reaching the loading point and extended along tensile reinforcement, causing failure at 119 kN since the critical crack splits the beam in half. The failure of specimen is classified as diagonal tension failure.
- **Beam V26.03** (Figure 3.16): there is the only and first diagonal crack recorded in V26.03 at 100 kN, which does not become critical, propagating rapidly vertically upward to compression zone. This crack experiences a tendency similar to beam V26.01, as it continues to branch and propagate toward loading point and along longitudinal reinforcement. The beam failed due to concrete crushing above crack's tip, while the secondary critical shear crack formed on the opposite side of beam. The failure in this case is not governed by critical shear crack and fails at compression shear failure.
- **Beam V26.04** (Figure 3.17): in similar to beam V26.02, due to large height, the first crack appeared very early at mid-span of beam and developed vertically upwards. At 70 kN, vertical cracks were recorded at two adjacent points, approximately at one-fourth beam length and developed diagonally. As load increased, more diagonal cracks were formed

VGU
Vietnamese-German University

in the web, combining with previous flexural crack to form a central arc. From here, two splitting cracks developed backwards towards two supports. Under increasing load, there was no further cracks recorded until global failure occurs at 175 kN by concrete crushing at loading point. Tension shear failure is recorded in this case.

Normally, displacement at two ends of beam is used to eliminate errors caused by displacement of support system, by the subtraction of middle-span for average of both-end displacement. However, due to equipment disturbance, the relevant mid-span deflection to each loading magnitude is assumed to be the main displacement in this test. The load-deflection graphs of four beams are shown in Figure 3.18. When observing the load and mid-span deformation graph of four beams, the curve increases steadily before witnessing a significant load drop, after which they either continue to grow or decline until failure. This load drop corresponds to the sudden formation of the main diagonal shear crack, in which the shear resistance stress of experiment V_{cr} is recorded at this point. Simultaneously, this value is further confirmed by recording actual moment the diagonal crack developed. Table 3.3 also shows the result of compressive and tensile strength of cylinder concrete specimens. Table 3.4 shows the summarization of ultimate and critical load of four testing specimens. The development, location, and shape of critical shear cracks are shown in Figure 3.23 to Figure 3.26. Due to error of equipment and data disturbance, the recorded values of longitudinal reinforcement strain from strain gauges is not utilized in the presented study.

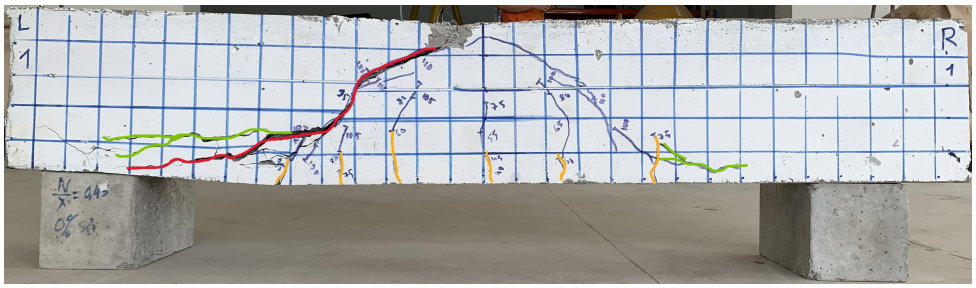

Figure 3.14: *Record of cracks in beam V26.01 after shear failure: primary flexural crack (yellow), crack splitting along longitudinal reinforcement (green), and critical shear crack (red)*



Figure 3.15: *Record of cracks in beam V26.02 after shear failure: primary flexural crack (yellow), crack splitting along longitudinal reinforcement (green), and critical shear crack (red)*



Figure 3.16: *Record of cracks in beam V26.03 after shear failure: primary flexural crack (yellow), crack splitting along longitudinal reinforcement (green), and critical shear crack (red)*

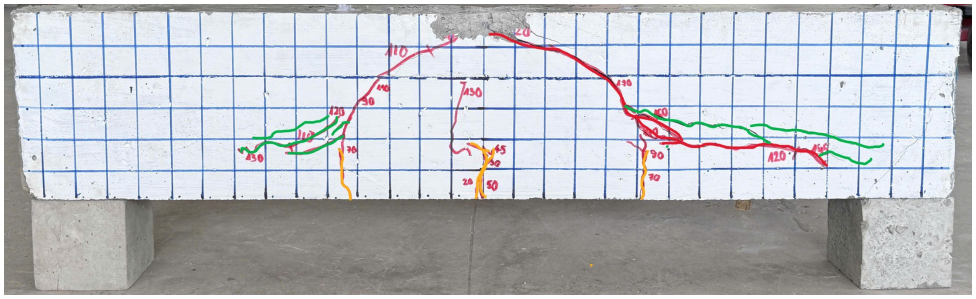

Figure 3.17: *Record of cracks in beam V26.04 after shear failure: primary flexural crack (yellow), crack splitting along longitudinal reinforcement (green), and critical shear crack (red)*

Table 3.3: *Results of concrete compressive and tensile splitting test*

Test	Maximum load (kN)	Area (mm^2)	Concrete strength (MPa)
Compressive test	998.78	17,671.46	56.52
Splitting tensile test	169.38	24,300	6.97

Table 3.4: *Ultimate and critical loads and shear forces recorded for the four specimens*

Specimen	ρ_l (%)	P_{cr} (kN)	V_{cr} (kN)	P_{ult} (kN)	V_{ult} (kN)
V26.01	2.6	120	60	127	63.5
V26.02	2.6	115	57.5	119	59.5
V26.03	3.8	123	61.5	148	74
V26.04	3.8	125	62.5	175	87.5

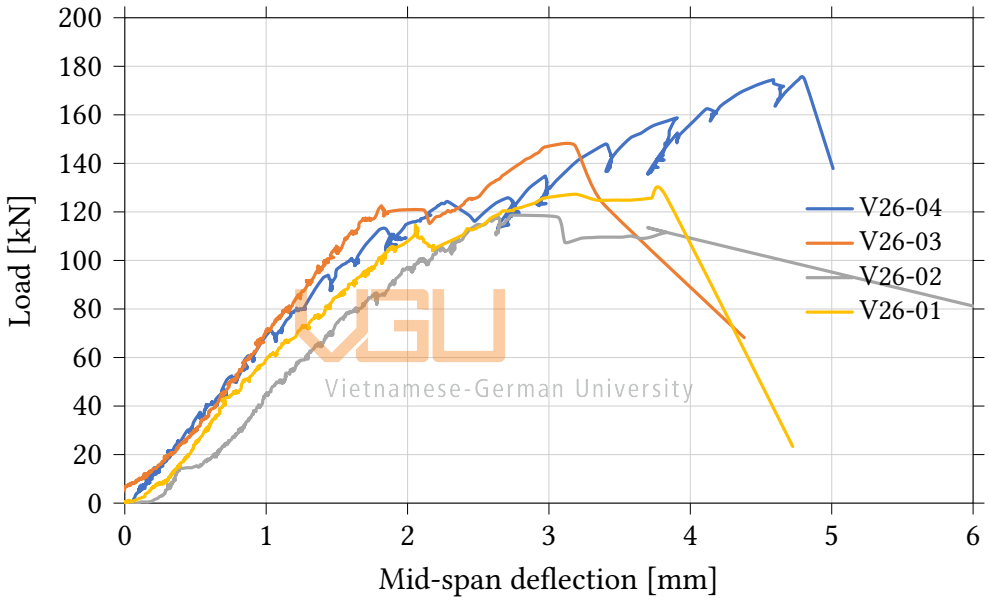

Figure 3.18: *Load–mid-span deflection graph of four experiment beams*

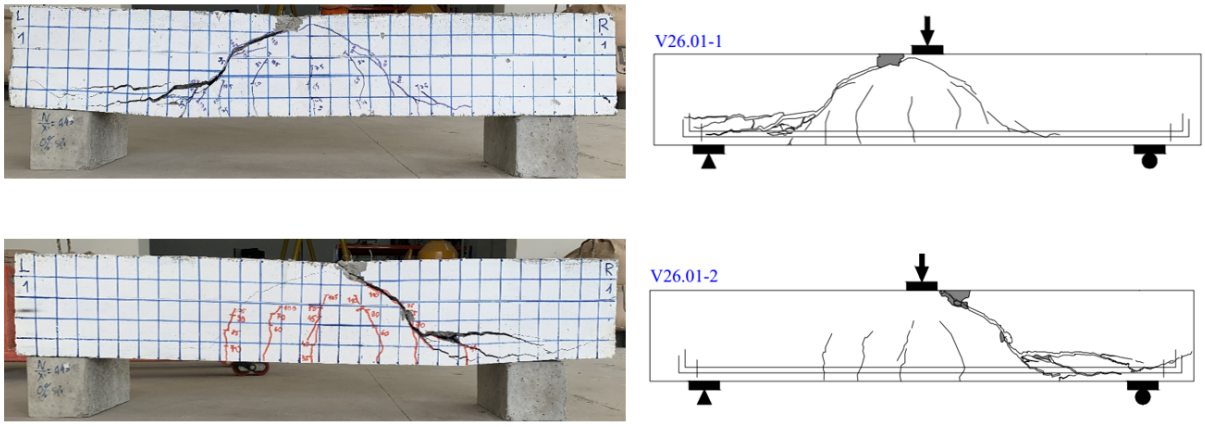

Figure 3.19: *Photograph of actual crack patterns and corresponding crack diagrams of test beam V26.01, V26.01-1 (top) shows the left side of the beam, while V26.01-2 (bottom) shows the right side*

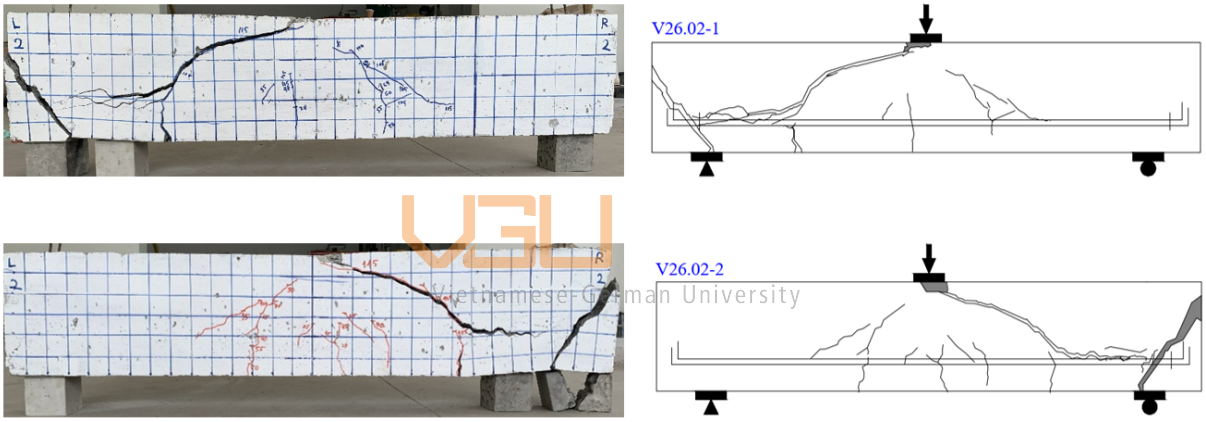

VGU
Vietnamese-German University

Figure 3.20: *Photograph of actual crack patterns and corresponding crack diagrams of test beam V26.02, V26.02-1 (top) shows the left side of the beam, while V26.02-2 (bottom) shows the right side*

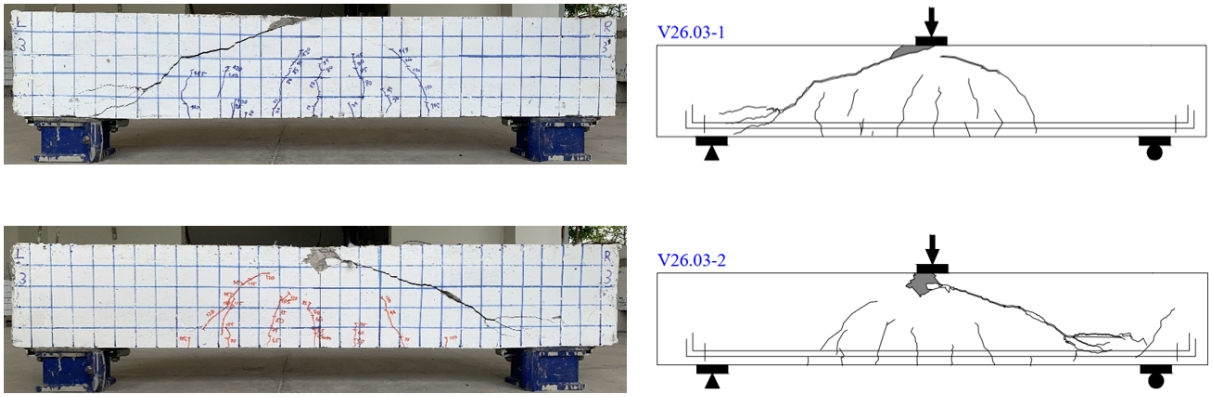

Figure 3.21: *Photograph of actual crack patterns and corresponding crack diagrams of test beam V26.03, V26.03-1 (top) shows the left side of the beam, while V26.03-2 (bottom) shows the right side*

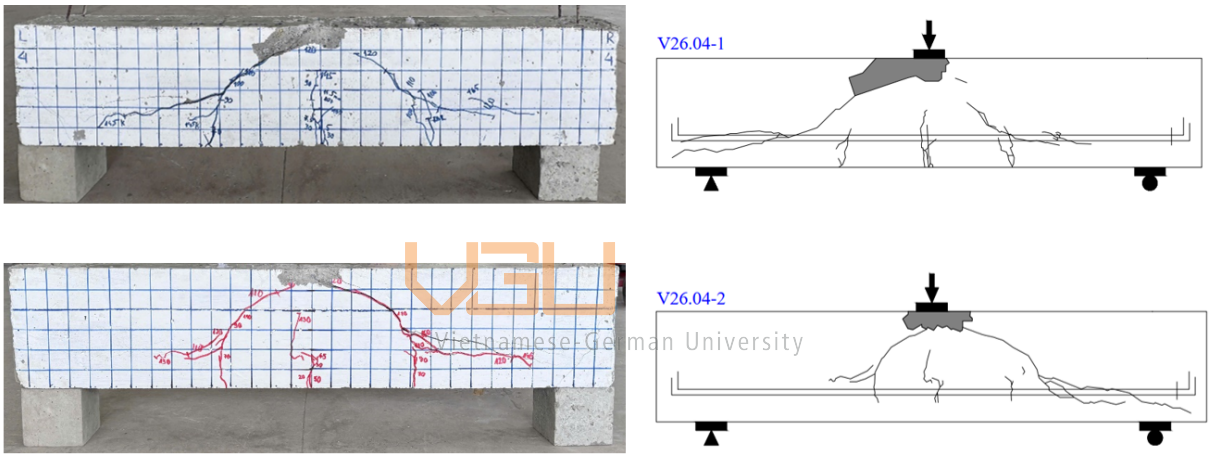

VGU
Vietnamese-German University

Figure 3.22: *Photograph of actual crack patterns and corresponding crack diagrams of test beam V26.04, V26.04-1 (top) shows the left side of the beam, while V26.04-2 (bottom) shows the right side*

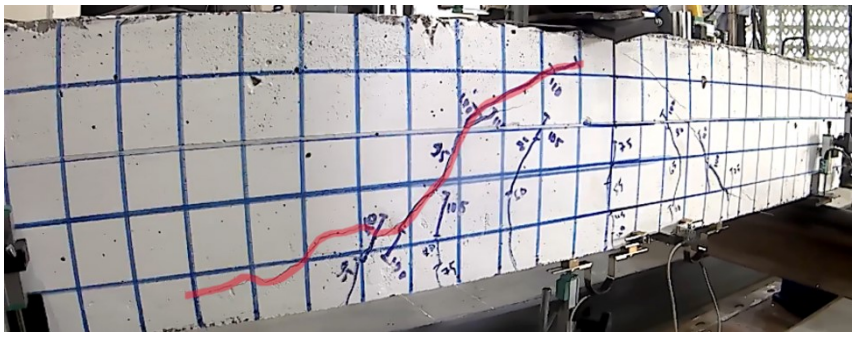

Figure 3.23: *Critical shear crack (red line) of beam V26.01 penetrates into compressive zone in stable manner*

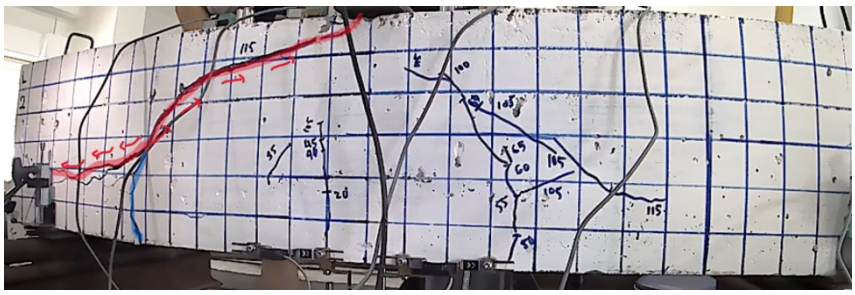

Figure 3.24: *Aggregate interlock cracks (red line) spread from primary flexural crack (blue line) and propagate both sides of beam V26.02*

VGU
Vietnamese-German University

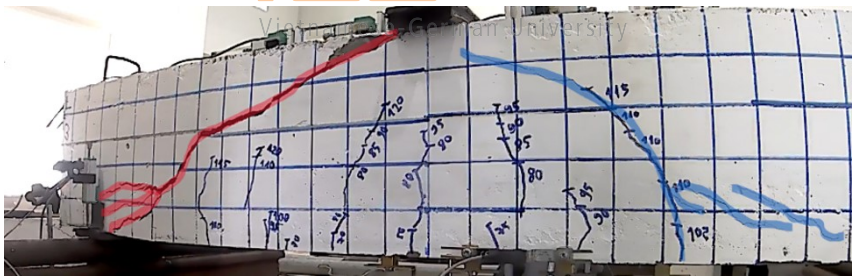

Figure 3.25: *Potential shear crack (blue line) and secondary critical shear crack formed after failure (red line), in beam V26.03*

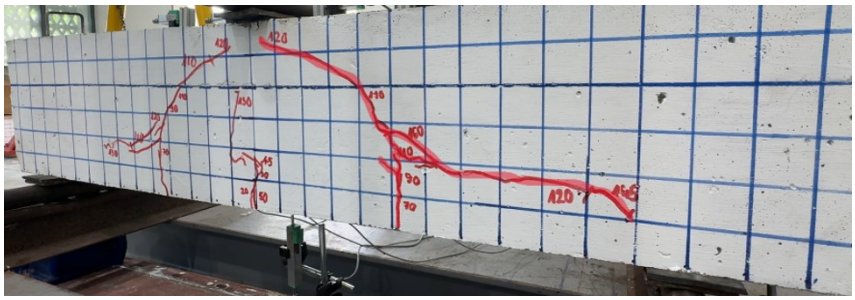

Figure 3.26: *Critical shear crack (red line) of beam V26.04*

4. Predictive calculation

This section provides the overall review of underlying theories, including Shear Failure Theory in *m*SM, and Simplified Modified Compression Field Theory, which require iterative calculation approach in shear capacity of slender beams without shear reinforcement. The theory Critical Shear Crack underlying in new version of EC2 only requires iterative calculation for members subjected to axial loads. Besides, the three selected shear design models with simplified approach are also presented, particularly EN 1992-1-1:2023, *m*SM and CSA A23.3-19. All formulations are served the calculation process in the upcoming section.

4.1 Iterative calculation formulation

4.1.1 Modified Compression Field Theory

VGU
Vietnamese-German University

The MCFT was the refined version on the basis of the original Compression Field Theory (CFT) in the 1970s by Mitchell and Collins, a model initially introduced for predicting the behavior of reinforced concrete beams under shear and torsion [54]. The development of CFT was the turning point in the analysis of concrete structure, that formerly depended on the 45° Truss model by Ritter and Mörsch at the end of 19th century. Rather than assuming that the longitudinal reinforcement and concrete form a 45° truss, CFT claims this angle was variable based on reinforcement ratio and load configuration. In CFT, post-cracking concrete is assumed to act as a diagonal compressive field, which was effective in carrying shear forces. The inclination angle of this field is determined following the Tension Field Theory of Wagner (1929), which explained the shear of thin metal web girders being carried by a field of diagonal tension and the compression-resisted capacity of thin web is negligible [55]. Similarly, after cracking, the concrete in the CFT tended not to carry tension, with shear being transferred through a diagonal compression field. This made the theoretical calculation overly conservative and predicted results were typically lower than reality. On the other hand, the MCFT took into account for the concrete tensile stresses between cracks. Both models were derived under compatibility condition, equilibrium condition and stress-strain relationships under average stresses and strains from Figure 4.1. The significant changes recorded in the modified CFT are:

consideration of local stress at crack and defined diagonal angle of concrete compressive field.

The widespread application of MCFT was well-known through the paper of Bentz et al. (2008), suggesting the simple closed-form formulation of this complex model [56]. This method offers a simple and general design method for reinforced concrete members with high accuracy as the original theory. The shear strength of members without shear reinforcement depends on the longitudinal strain ε_x and crack spacing s_{ze}, which was described through factor β. These two factors are mentioned as strain effect factor and size effect factor in MCFT, where the independence of two mentioned factors are neglected for simplification and β can be expressed through the product of a strain factor and a size factor. Besides, it is conservative when minimizing the inclination angle θ for members without shear reinforcement, leading to the outstanding role of longitudinal reinforcement.

The shear strength formulation V of reinforced concrete members without stirrups in simplified MCFT is as follows:

$$V = \left(\beta\sqrt{f_c} + \rho_z f_y \cot\theta\right) b\, d \tag{4.1}$$

VGU
Vietnamese-German University

where β tensile stress factor in the cracked concrete, θ inclined angle of diagonal compressive stress, f_c concrete compressive strength, f_y steel tensile strength, ρ_z web reinforcement ratio.

The factor β and angle θ are calculated by the formula:

$$\beta = \frac{0.4}{1 + 1500\varepsilon_x}\frac{1300}{1000 + s_{ze}} \tag{4.2}$$

$$\theta = (20^\circ + 7000\varepsilon_x)\left(0.88 + \frac{s_{xe}}{2500}\right) \leq 75^\circ \tag{4.3}$$

where ε_x average longitudinal strain, s_{ze} crack spacing parameter [57], and are expressed through equation:

$$\varepsilon_x = \frac{\frac{M}{d_v} + V}{2E_s A_s} \tag{4.4}$$

$$s_{ze} = \frac{35 s_z}{a_g + 15} \tag{4.5}$$

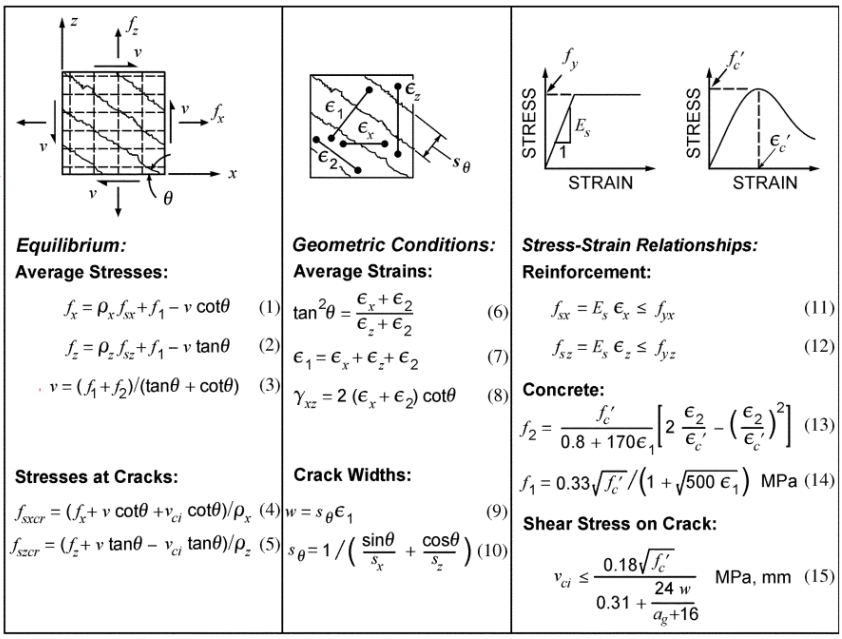

Figure 4.1: *Fifteen equations of Modified Compression Field Theory* [56]

4.1.2 Model *m*SM

The *m*SM model was introduced by Tran (2020), whose proposed shear model was derived from mechanics-based principles and refined by the involvement of actual value of relevant parameters such as facture energy G_F, concrete tensile strength f_{ct}, crack width w_{cr} and crack spacing s_{cr} without requiring empirical modification, rather than experience value [39]. In this model, reinforced concrete members are assumed to govern by flexural-shear crack and considered as slender to very slender members (a/d beyond 2.5). The develop of cracks separates the mutual role between compressive and tensile zone, leading to the instability of structure. The shear capacity is investigated at the end of 2nd crack stage, when the shear-resistance mechanism differs in the presence of concrete residual tensile stresses, crack-induced shear stresses, and trivial dowel action (Figure 4.2). At this 2nd crack state, cracks do not surpass the neutral axis and the shear stress in the uncracked concrete zone follows a parabolic distribution, peaking at the neutral axis.

VGU
Vietnamese-German University

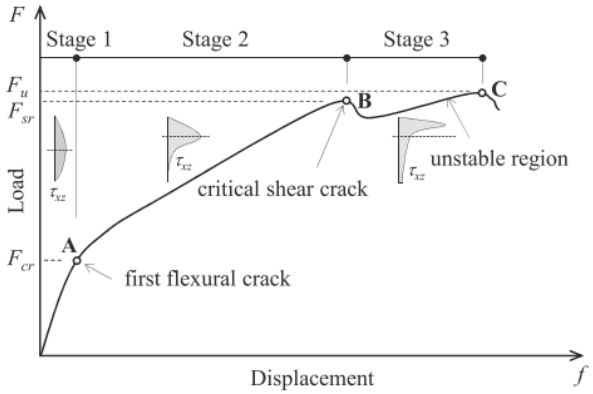

Figure 4.2: *Load-deformation of typical beam under shear failure* [39]

The total shear capacity is formulated by summing the individual combination of compressive and tensile zone, in which the capacity of the compression zone is described in Equation 4.6, with k_x relative depth x/d of compression zone and solidity factor $\psi = 2/3$. Additionally, despite of formed crack, the tension zone still contributes to the overall shear capacity through aggregate interlock action and shear-transferred through cracks, which are decided by the opening of crack width w_{cr} and crack spacing s_{cr}. If cracks open wider, aggregate bonding is ineffective and the shear strength of this zone becomes zero. The shear capacity of tensile zone is described as follows Equation 4.7. The integration in this equation represents for the amount of energy dissipates over area unit of crack, when crack is opening; known as fracture energy G_F. The consideration of fracture energy G_F in the equation allows for a natural reflection of the aggregate size effect.

VGU
Vietnamese-German University

$$V_{cc} = \frac{2}{3}\tau_{max}\, b\, d k_x \tag{4.6}$$

$$V_{ct} = b\, d \frac{1 - k_x}{w_{cr}} \int_0^{w_a} \sigma_{ct}(w)\, d_w = b\, d \frac{1 - k_x}{w_{cr}} G_F \tag{4.7}$$

The author used the basic equilibrium condition to determine the shear stress distribution over the cross-section. As mentioned above, cracks occur once the principal tensile stress exceeds the tensile strength of concrete. Considering a pure shear stress state, there is no longitudinal concrete stress σ_x or normal concrete stress σ_z. In this state, in the 45-degree direction, the maximum shear stress τ_{max} coincides with the principal directions σ_1 and σ_2, but following reverse direction, $\tau_{max} = \sigma_1 = -\sigma_2$. From this condition, the principal shear strain is expressed through Hooke's law as follows:

$$\varepsilon_1 = \frac{\sigma_1}{E_c}(1 + \nu) \tag{4.8}$$

Considering the Saint-Venant theory of maximum principal strain, crack occurs once principal tensile strain reaches strain at crack $\varepsilon_1 = \varepsilon_{cr} = f_{ct}/E_c$. Besides, the principal tensile stress at failure shall be equal to effective concrete tensile strength $\sigma_1 = f_{ct,ef}$. As a result, the effective concrete tensile strength could be derived as follows:

$$f_{ct,ef} = f_{ct}\frac{1}{1+\nu} \tag{4.9}$$

Because $\tau_{max} = \sigma_{1,2} = f_{ct,ef}$, the total shear capacity of members without shear reinforcement could be derived as:

$$V_c = \frac{2}{3} f_{ct,ef} b\, d \left(k_x + \frac{1.5 G_F}{f_{ct,ef} w_{cr}} (1 - k_x) \right) \tag{4.10}$$

The proposed shear model implies the experimental value of effective tensile strength $f_{ct,ef}$, facture energy G_F and elastic modulus E_c. Otherwise, the formulations using compressive strength f_c are suggested as below:

Concrete tensile strength

$$f_{ct} = 0.3(f_{ck})^{2/3}, \qquad f_{ck} \leq 50\,\text{MPa} \tag{4.11}$$

$$f_{ct} = 1.1(f_{ck})^{1/3}, \qquad f_{ck} > 50\,\text{MPa} \tag{4.12}$$

VGU
Vietnamese-German University

Effective concrete tensile strength with Poisson's ratio ν = 0.2

$$f_{ct,ef} = f_{ct}\frac{1}{1+\nu} = 0.83 f_{ct} \tag{4.13}$$

Elastic modulus of concrete

$$E_c = \alpha_E\, 21500 \left(\frac{f_c}{10} \right)^{1/3} \tag{4.14}$$

Fracture energy

$$G_F = 0.03 f_c^{0.18} a_g^{0.32} \tag{4.15}$$

where a_g accounts for the largest size of aggregate in concrete mixture, which is not splitting by concrete cracks. Alternatively, if it is known that aggregate particles fracture during splitting test, the minimum aggregate size is used.

Since wider crack opening weakens the total shear capacity, crack spacing s_{cr} and crack width w_{cr} shall be precisely estimated. The process of calculating these two parameters is

described below:

$$w_{cr} = s_{cr}\left(\varepsilon_{sm} - \varepsilon_{cm}\right) \tag{4.16}$$

where $\varepsilon_{sm} - \varepsilon_{cm}$ is the difference of average strain between steel and concrete through crack, can be calculated as:

$$\varepsilon_{sm} - \varepsilon_{cm} = \frac{1}{E_s}\left[\sigma_s - \beta_t \frac{f_{ct}}{\rho_{s,ef}}\left(1 + \eta_e \rho_{s,ef}\right)\right] \geq \left(1 - \beta_t\right)\frac{\sigma_s}{E_s} \tag{4.17}$$

where β_t is a factor dependent on load duration, taken as 0.6 for short-term loading; $\rho_{s,ef}$ is the effective reinforcement ratio $A_s/A_{ct,ef}$, considering effective height $h_{ct,ef} = 2.5(h - d)$; η_e is the ratio of elastic modulus between steel E_s and concrete E_c; the reinforcement stress σ_s and reinforcement strain $\varepsilon_s = \sigma_s/E_s$ can be calculated as follows:

$$\sigma_s = \frac{M}{z_c A_s} \tag{4.18}$$

$$\varepsilon_s = \kappa d(1 - k_x) \tag{4.19}$$

where lever arm $z_c = d(1 - k_x/3)$, κ is the curvature at cracked section, and k_x is the relative depth of compression zone, determined as follows:

VGU Vietnamese-German University

$$\kappa = \frac{2M}{E_c b\, d^3 k_x^2 \left(1 - \frac{k_x}{3}\right)} \tag{4.20}$$

$$k_x = \left(\sqrt{1 + \frac{2}{\eta_e \rho_s}} - 1\right)\eta_e \rho_s \tag{4.21}$$

The model utilizes an author-developed equation for primary crack spacing s_{cr} to overcome limitations of empirical modification and inflexible application in current methods, incorporating a mechanical model of the bond between concrete and reinforcement.

$$s_{cr} = \max\left(s_{cr,1}, s_{cr,2}\right) \tag{4.22}$$

where

$$s_{cr,1} = 0.75d(1 - k_x) \tag{4.23}$$

$$s_{cr,2} = \frac{1.5\phi_s}{4k_b \rho_{s,ef}} \tag{4.24}$$

with

$$k_b = \frac{\tau_{bm}}{f_{ct}} = 0.97 \left(\frac{1 + \eta_e \rho_{s,ef}^2}{\rho_{s,ef}} \frac{\phi_s}{E_s} \right)^{1/4} \sqrt{\frac{f_c^{3/4}}{f_{ct}}} \tag{4.25}$$

where ϕ_s equivalent steel bar diameter, when there are more than 2 sizes of steel bar used, this parameter can be calculated by:

$$\phi_{s,eq} = \frac{n_1 \phi_{s1}^2 + n_2 \phi_{s2}^2 + \cdots}{n_1 \phi_{s1} + n_2 \phi_{s2} + \cdots} \tag{4.26}$$

4.2 Simplified calculation formulation

4.2.1 Model EN 1992-1-1:2023

The European Committee for Standardization introduced the second generation of Eurocode 2 (EN 1992-1-1:2023), which was subsequently adopted in Germany as DIN EN 1992-1-1:2025-09, published in September 2025. Different from previous generation, the shear capacity of members without shear reinforcement now relies on the mechanical model Critical Shear Crack Theory with design coefficient, instead of using purely empirical formulation in Eurocode 2004 [6] [53]. Several assumptions adopted in this new version are: the steel elastic modulus E_s is set equal to 200 GPa, the inner level arm of internal forces is defined as $z = 0.9d$ and the effective shear span $a_{cs} = 4d$, where d is the effective depth of cross-section.

In EN 1992-1-1:2023, the verification of shear capacity obeys the following criterion as follows:

$$\tau_{Rd} \geq \tau_{Ed} = \frac{V_{Ed}}{b_w z} > \tau_{Rdc,min} \tag{4.27}$$

where z level arm for shear stress calculation defined as $z = 0.9d$. The minimum shear stress resistance $\tau_{Rdc,min}$ is defined at the elastic state of steel reinforcement $\varepsilon_v = f_y/E_s$, calculated as follows:

$$\tau_{Rdc,min} = \frac{11}{\gamma_V} \sqrt{\frac{f_{ck}}{f_{yd}} \frac{d_{dg}}{d}} \tag{4.28}$$

in which γ_V is the partial factor for shear resistance without shear resistance, can be found in Clause 4.3.3(1); f_{ck} is the characteristic cylinder compressive strength of concrete; f_{yd} is the design yield strength of flexural reinforcement; d is the effective depth of cross-section; d_{dg} is the size parameter describing the crack and failure zone roughness, depending on concrete type and its aggregate size, is taken as:

- 16 mm + $D_{\text{lower}} \leq 40$ mm for concrete strength $f_{\text{ck}} \leq 60$ MPa
- 16 mm + $D_{\text{lower}}(60/f_{\text{ck}})^2 \leq 40$ mm for concrete strength $f_{\text{ck}} > 60$ MPa

D_{lower} is the smallest value of the upper sieve size D in an aggregate, considering the coarsest fraction of aggregates in the concrete. In case of D_{max} is known, D_{lower} can be replaced by D_{max}.

The design value of shear stress resistance of members without shear reinforcement is expressed through equation:

$$\tau_{\text{Rdc}} = \frac{0.66}{\gamma_{\text{V}}} \left(100 \rho_{\text{l}} f_{\text{ck}} \frac{d_{\text{dg}}}{d} \right)^{1/3} \tag{4.29}$$

where γ_{V} is the partial factor for shear design, ρ_{l} is the longitudinal reinforcement ratio, which is calculated as $\rho_{\text{l}} = A_{\text{sl}}/b_{\text{w}}d$; A_{sl} is the effective area of tensile reinforcement; b_{w} is the width of cross-section. In case of the effective shear span a_{cs} of linear member smaller than $4d$, the value of d may be replaced by the mechanical shear span a_{v}:

$$a_{\text{v}} = \sqrt{\frac{a_{\text{cs}}}{4} d} \tag{4.30}$$

$$a_{\text{cs}} = \left| \frac{M_{\text{Ed}}}{V_{\text{Ed}}} \right| \geq d \tag{4.31}$$

VGU Vietnamese-German University

4.2.2 Model CSA A23.3:2019

The design of members without shear reinforcement relies on the simplified MCFT [57], which is expressed through the shear resistance attributed to the concrete V_{c}:

$$V_{\text{c}} = \phi_{\text{c}} \lambda \beta \sqrt{f'_{\text{c}}}\, b_{\text{w}} d_{\text{v}} \tag{4.32}$$

where ϕ_{c} is the resistance factor for concrete, λ factor accounting for low-density concrete, b_{w} minimum effective web with, d_{v} effective shear depth (taken larger than $0.9d$ or $0.72h$), and factor β for shear resistance of cracked concrete. For simplification, the yield strength of longitudinal reinforcement f_{y} does not exceed 400 MPa, the concrete compressive strength does not exceed 60 MPa, the nominal maximum coarse aggregate size larger than 20 mm and the value β for members without shear reinforcement is:

$$\beta = \frac{230}{1000 + d_{\text{v}}} \tag{4.33}$$

However, the effective shear depth d_v shall be replaced by equivalent crack spacing parameter s_{ze} to consider the influence of aggregate size:

$$s_{ze} = \frac{35 s_z}{15 + a_g} \tag{4.34}$$

where s_z crack spacing, shall be taken as d_v or the maximum vertical distance between longitudinal layers in the presence of skin reinforcement; a_g specified nominal maximum size of coarse aggregate. Some notable points shall be considered:

- In the determination of V_c, the square root of f'_c shall not exceed 8 MPa and the value of β need not to be taken less than 0.05.
- The equivalent crack spacing parameter s_{ze} may gain a value of $0.85 s_z$ at minimum. In the case of skin reinforcement, the minimum value of reinforcement area is $0.003 b_w s_z$.

4.2.3 Model *m*SM

The *m*SM formulation introduced above requires iterative approach, because several factors are dependent on each other and crack width w_{cr} is unknown, to ascertain the most accurate results. On the other hand, a simple approach is also provided for this model [39], by means of omitting the mean concrete strain at crack ε_{cm} in Equation 2.2. By now, the crack width is rewritten to the product of reinforcement strain ε_s and crack spacing s_{cr}, performing the size effect in the mathematical expression. The crack spacing s_{cr} and reinforcement strain ε_s are calculated respectively following Equation 4.22 and 4.19; the bending moment is taken by the product of shear force V_c and shear span $a - d$; and then plug these factors into Equation 4.10. As a result, the simple equation of shear capacity without shear reinforcement is as follows:

$$V_c = \frac{1}{3} f_{ct,ef} b d k_x \left(1 + \sqrt{1 + \frac{d_0}{d}}\right) \tag{4.35}$$

where parameter d_0 is defined by:

$$d_0 = 2 l_{ch} \frac{3 - k_x}{\lambda_s (1 - k_x)} \tag{4.36}$$

with lambda λ_s states for effective span-to-depth ratio a/d, characteristic length l_{ch} is as follows:

$$l_{ch} = \frac{E_c G_F}{f_{ct,ef}^2} \tag{4.37}$$

For simply supported beams under concentrated load, the effective shear span-to-depth ratio λ_s can be taken as $a/d - 1$.

4.3 Detailed calculation

The overall equations applied to calculate shear resistance following five methods are described in Table 4.1 below:

Table 4.1: Shear equations

Shear model	**Shear equation**
EN 1992-1-1:2023	$V_c = 0.66 \left(100 \rho_l f_c \frac{d_{dg}}{d}\right)^{1/3} b_w z$
CSA A23.3:2019	$V_c = \beta \sqrt{f_c'}\, b_w d_v$
*m*SM simplified	$V_c = \frac{1}{3} f_{ct,ef} b\, d\, k_x \left(1 + \sqrt{1 + \frac{d_0}{d}}\right)$
SMCFT iterative	$V_c = \beta \sqrt{f_c'}\, b_w d_v$
*m*SM iterative	$V_c = \frac{2}{3} f_{ct,ef} b\, d \left(k_x + \frac{1.5 G_F}{f_{ct,ef} w_{cr}} (1 - k_x)\right)$

VGU Vietnamese-German University

4.3.1 Simplified calculation

Based on design codes and shear theories presented in the previous section, predictive calculations are performed to create a database for comparison with experimental results. Two main calculation approaches are utilized: a simplified method following EN 1992-1-1:2023, CSA A23.3-19, and *m*SM; and an iterative calculation method required for simplified MCFT and *m*SM. The purpose is to determine expected "mean shear strength" of slender beams without stirrup, which is achieved by assuming the safety factor as 1 and defining mechanical parameters experimentally among all design codes. The detail calculations include 4 experimental specimens and 784 specimens from DAfStb Heft 597 database of the German Committee for Structural Concrete [58]. Among 784 specimens, there are 40 cases subjected to distributed load, while the others subjected to concentrated load. These 784 rectangular beams without

shear reinforcement were tested by more than 70 researcher groups during the period 1953 to 2011. The relevant parameters and calculation results of shear capacity of four beam specimens without shear reinforcement are summarized in this section and the results on Excel of 784 specimens in DAfStb could be found in Appendix D. The missing information required for the DAfStb calculation is assumed to be identical to that of the four testing specimens.

This dataset is proceeded using Excel VBA to optimize synchronous computation and enhance accuracy for the large number of specimens. While relevant figures of 784 database specimens are fully provided in database, certain assumptions are made for four experimental specimens. Ideally, all relevant material properties such as concrete compressive strength, steel tensile strength or elastic modulus are determined from actual tests. However, due to experimental limitation, the elastic modulus of steel E_s is assumed to be 197,000 MPa, maximum & minimum aggregate size is taken as 2 and 16 mm, Poisson's ratio ν as 0.2 and concrete tensile strength f_{ct} is calculated from experimental compressive strength f_c = 56.52 MPa using Equation 4.11. Remarkably, since aggregate particles are split on the surfaces of splitting test specimens, maximum aggregate size $a_{g,max}$ is employed to calculate shear strength of four testing specimens regarding two approaches of *m*SM.

VGU Vietnamese-German University

The four specimens V26.01, V26.02, V26.03, and V26.04 were designed for the shear tests described in the previous section; their geometries, cross-sections, and loading are summarized in Table 4.2.

Table 4.2: *Section properties, loading, and geometry of the four testing beams*

Specimen	**Section properties**				**Loading and geometry**		
	b	h	A	A_w	L	a	a/d
	mm	mm	mm^2	mm^2	mm	mm	–
V26.01	150	250	37,500	31,500	1,500	600	2.86
V26.02	150	300	45,000	31,500	1,500	600	2.86
V26.03	150	250	37,500	31,500	1,500	600	2.86
V26.04	150	300	45,000	31,500	1,500	600	2.86

Table 4.3 and 4.4 provide the relevant information of longitudinal reinforcement and concrete applied to four testing specimens.

Regarding the boundary conditions, the beams are set up under a simply supported beam subjected to concentrated load. The corresponding bending moment and shear force diagrams are presented in Figure 4.3. For analytical calculations, the magnitude of concentrated load in is taken as the maximum failure load recorded during the laboratory shear tests.

Table 4.3: *Longitudinal reinforcement used in four testing beams*

Specimen	**Longitudinal reinforcement**						
	ϕ_s	No. bar	d	E_s	f_y	A_{sl}	ρ_l
	mm	–	mm	MPa	MPa	mm^2	–
V26.01	16	4	210	197,000	350	804.25	0.026
V26.02	16	4	210	197,000	350	804.25	0.026
V26.03	16	6	210	197,000	350	1,206.37	0.038
V26.04	16	6	210	197,000	350	1,206.37	0.038

Table 4.4: *Concrete properties of four testing beams*

Specimen	**Concrete**							
	a_g	$a_{g,max}$	v	f_c	f_{ct}	E_c	Method	n_e
	mm	mm	–	MPa	MPa	MPa	–	E_s/E_c
V26.01	2	16	0.2	56.52	0	28,737	cyl/sp	6.86
V26.02	2	16	0.2	56.52	0	28,737	cyl/sp	6.86
V26.03	2	16	0.2	56.52	0	28,737	cyl/sp	6.86
V26.04	2	16	0.2	56.52	0	28,737	cyl/sp	6.86

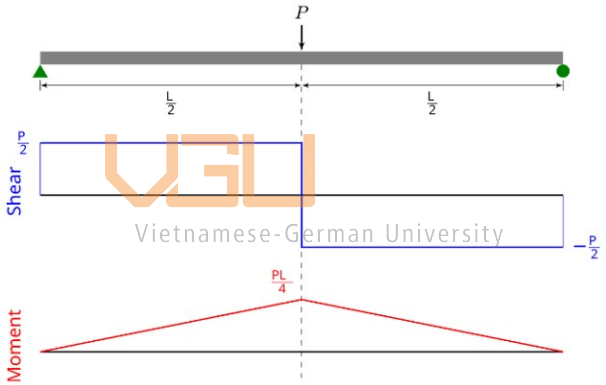

Figure 4.3: *Shear force and bending moment diagram of beam under concentrated load*

The relevant bending moment and shear force of simply supported beam subjected to concentrated load is described as:

$$M = \frac{PL}{4} \tag{4.38}$$

$$V = \frac{P}{2} \tag{4.39}$$

$$M = \frac{P}{2}(a - d) \tag{4.40}$$

From the preliminary information, beam V26.01 is taken as an example for the calculation of experiment specimens following three simplified shear design model: EN 1992-1-1:2023, CSA A23.3:2019, and *m*SM. The shear capacity of remaining three specimens V26.02, V26.03, and V26.04 will be predicted by the same way. The detailed verification of shear resistance

subjected to concentrated load may be conducted for control sections that are outside a distance d from the support reaction and loading point. In this case, the shear capacity of all specimens is evaluated at distance $a - d$ from the support.

1. **Simplified shear capacity calculation following EN 1992-1-1:2023**

In EN 1992-1-1:2023, the shear stress resistance of reinforced concrete beam V26.01 without shear reinforcement following is calculated by the formula:

$$\tau_{\mathrm{Rc}} = 0.66 \left(100 \rho_{\mathrm{l}} f_{\mathrm{c}} \frac{d_{\mathrm{dg}}}{d} \right)^{1/3}$$

in which the longitudinal reinforcement ρ_{l} is 0.026, f_{c} is determined from compressive test as 56.52 MPa, effective depth d as 210 mm, and maximum aggregate size D_{max} as 16 mm. As the shear span a = 600 mm smaller than four times effective depth $4d$ = 840 mm, the value d in Equation 4.29 should be replaced by mechanical shear span a_{v}. The mechanical shear span a_{v} and size parameter d_{dg} is calculated as follows:

$$a_{\mathrm{v}} = \sqrt{\frac{a-d}{4} d} = \sqrt{\frac{600-210}{4} 210} = 143.1 \text{ mm}$$

Vietnamese-German University

$$d_{\mathrm{dg}} = 16 + D_{\mathrm{max}} = 16 + 16 = 32 \text{ mm}$$

Then, substitute mechanical shear span a_{v} and size parameter d_{dg} into the formula, the shear resistance stress of beam V26.01 is:

$$\tau_{\mathrm{Rc}} = 0.66 \left(100 \cdot 0.026 \cdot 56.52 \cdot \frac{32}{143.1} \right)^{1/3} = 2.11 \text{ MPa}$$

The following shear resistance force of beam V26.01 is:

$$V_{\mathrm{Rc}} = \tau_{\mathrm{Rc}} b_{\mathrm{w}} z = \tau_{\mathrm{Rc}} b_{\mathrm{w}} 0.9 d = 2.11 \cdot 150 \cdot 0.9 \cdot 210 = 59.82 \text{ kN}$$

The following steps are applied to the remaining three beams by Excel software, due to rounding condition, the results are more accurate than hand calculation and the results are shown in the table below:

Table 4.5: *Shear resistance force of four testing beams calculated by EN 1992-1-1:2023*

Specimen	**EN 1992-1-1:2023**
	V_c [kN]
V26.01	59.57
V26.02	59.57
V26.03	68.19
V26.04	68.19

2. Simplified shear capacity calculation following CSA A23.3:2019

In CSA A23.3:2019, the shear stress resistance of reinforced concrete beam V26.01 without shear reinforcement following is calculated by the formula:

$$V_c = \beta \sqrt{f'_c}\, b_w d_v$$

in which f'_c is the concrete compressive strength f_c determined from experiment 56.52 MPa (smaller than 60 MPa), width of cross-section b_w is 150 mm, effective shear depth d_v is taken larger than $0.9d$ as equal to $d = 210$ mm, and the factor accounting for shear resistance of cracked concrete β is calculated by Equation 4.33. For members without shear reinforcement and accounting for all aggregate sizes, the value of d_v is replaced by the equivalent crack spacing parameter s_{ze}.

VGU Vietnamese German University

$$\beta = \frac{230}{1000 + d_v}$$

$$s_{ze} = \frac{35 s_z}{15 + a_{g,max}}$$

where crack spacing parameter is taken as $s_z = d_v = 210$ mm and specified nominal maximum size of coarse aggregate $a_{g,max} = 16$ mm. The value of shear resistance of beam V26.01 is as follows:

$$s_{ze} = \frac{35 \cdot 210}{15 + 16} = 237.1 > 0.85 s_z = 0.85 \cdot 210 = 178.5$$

$$\beta = \frac{230}{1000 + d_v} = \frac{230}{1000 + 237.1} = 0.186$$

$$V_c = 0.186\sqrt{56.52} \cdot 150 \cdot 210 = 44.04 \text{ kN}$$

As four experiment beams have the same web width b_w, effective depth d_v, maximum aggregate size $a_{g,max}$, and concrete compressive strength f_c', the shear resistance of four specimens is generally defined at 44.04 kN following CSA A23.03-19.

Table 4.6: *Shear resistance force of four testing beams calculated by CSA A23.3:2019*

Specimen	**CSA A23.3:2019**
	V_c [kN]
V26.01	44.04
V26.02	44.04
V26.03	44.04
V26.04	44.04

3. Simplified shear capacity calculation following *m*SM

In *m*SM, the shear stress resistance of reinforced concrete beam V26.01 without shear reinforcement following is calculated by the formula:

VGU
Vietnamese-German University

$$V_c = \frac{1}{3} f_{ct,ef}\, b\, d\, k_x \left(1 + \sqrt{1 + \frac{d_0}{d}}\right)$$

where compressive tensile strength $f_{ct,ef}$ is from $f_c = 56.52$ MPa and Poisson's ratio $\nu = 0.2$ calculated as follows:

$$f_{ck} = f_c - 8 = 56.52 - 8 = 48.52 \text{ MPa}$$

$$f_{ct} = 0.3\,(f_{ck})^{2/3} = 0.3\,(48.52)^{2/3} = 3.99 \text{ MPa}$$

$$f_{ct,ef} = f_{ct}\frac{1}{1+\nu} = 3.99\frac{1}{1+0.2} = 3.33 \text{ MPa}$$

with reinforcement ratio $\rho = 0.026$ and modular ratio $\eta_e = 6.86$, the relative depth of compression zone k_x is:

$$k_x = \left(\sqrt{1+\frac{2}{\eta_s\rho_s}}-1\right)\eta_e\rho_s = \left(\sqrt{1+\frac{2}{0.026\cdot 6.86}}-1\right)0.026\cdot 6.86 = 0.445$$

The coefficient d_0 is defined by:

$$d_0 = 2l_{ch}\frac{3-k_x}{(\lambda-1)(1-k_x)}$$

with effective shear span-to-depth ratio λ states for span-to-depth ratio $a/d = 2.86$, characteristic length l_{ch} is as follows:

$$G_F = 0.03 f_c^{0.18} a_g^{0.32} = 0.03\cdot 56.52^{0.18}\cdot 2^{0.32} = 0.0774 \text{ N/mm}$$

$$l_{ch} = \frac{E_c G_F}{f_{ct,ef}^{\ 2}} = \frac{28737\cdot 0.0774}{3.33^2} = 201.15 \text{ mm}$$

The parameter d_0 is as:

VGU Vietnamese-German University

$$d_0 = 2l_{ch}\frac{3-k_x}{(\lambda-1)(1-k_x)} = 2\cdot 201.15\frac{3-0.445}{(2.86-1)(1-0.445)} = 993.003$$

The shear resistance of beam V26.01 following simplified *m*SM is as:

$$V_c = \frac{1}{3}\cdot 3.33\cdot 150\cdot 210\cdot 0.445\left(1+\sqrt{1+\frac{993.003}{210}}\right) = 52.8 \text{ kN}$$

The following steps are applied to the remaining three beams by Excel software, due to rounding condition, the results are more accurate than hand calculation and the results are shown in the table below:

Table 4.7: *Shear resistance force of four testing beams calculated by simplified mSM formulation*

Specimen	**Simplified *m*SM**
	V_c [kN]
V26.01	52.37
V26.02	52.37
V26.03	62.03
V26.04	62.03

4.3.2 Iterative calculation

The iterative calculation method in this thesis is implemented for simplified MCFT and *m*SM models by assuming an initial shear resistance force, then subsequently calculating iteratively and comparing until the difference between the final and assumed shear resistance force is minimal. This method is required when such quantities are mutually dependent and cannot be solved directly by single formula. At failure stage, the applied shear force must be equal to the calculated one, so the process of load assumption, deformation calculation, and shear resistance updating needs to be repeated until these two values converge. In *m*SM model, the crack width at failure, which decided by a strain difference between reinforcement and concrete over crack spacing, cannot be determined beforehand and requires iterative calculation. The process of iterative calculation could be found in Appendix D and is described as follows:

1. Define all relevant parameters of concrete and steel f_c, f_{ct}, E_c, E_s and G_F ideally by experiments. If there is missing information, these parameters will be calculated following formulas introduced by Equation 4.11 to 4.15.
2. Choose randomly the initial value of shear capacity $V_{initial}$, for example $V_{initial} = \frac{2}{3} f_{ct,ef} b\, d$. From here, the relevant bending moment M can be calculated at control section $a - d$.
3. Calculate relative depth of compression zone k_x by Equation 4.21 for members without axial force.
4. Calculate crack width w_{cr} and crack spacing s_{cr} by other relevant factors following Equation 4.16 to 4.24.
5. Calculate shear capacity of beam by Equation 4.10, then compared with initial value $V_{initial}$. If two values do not converge, the value of average between initial and estimated shear capacity is used to calculate for next round. This process is repeated until the value tolerance reaches 0.0001 with maximum 1000 loops on Excel.

In simplified MCFT, shear resistance depends on deformation and cracking states of concrete, which in turn are determined by applied internal forces. The process of iteratively calculation could be found in Appendix D and is described as follows:

1. Choose randomly the initial value of shear capacity $V_{initial}$ and then calculate the relevant bending moment M at control section $a - d$.
2. Calculate the relative longitudinal strain ε_x of members with M and $V_{initial}$ by Equation

4.4.

3. From ε_x, calculate the factor accounting for shear resistance of cracked concrete β by Equation 4.2.
4. Calculate shear capacity of beam by Equation 4.1, then compared with initial value $V_{initial}$. The next step of iterative procedure is conducted similarly with Step 5 of *m*SM.

The detailed process of iterative calculation in this thesis is optimized using Excel VBA and could be found in Appendix D. The iterative calculation results for the four experimental beams are summarized on table below.

Table 4.8: *Shear resistance force of the four testing beams calculated using the iterative SMCFT and mSM approaches*

Specimen	**SMCFT Iterative**	***m*SM Iterative**
	V_c [kN]	V_c [kN]
V26.01	56.45	56.41
V26.02	56.45	55.71
V26.03	63.63	68.09
V26.04	63.63	68.09

VGU
Vietnamese-German University

4.4 Application of structural analysis software

4.4.1 Response-2000 software

Response-2000 is the 2D non-linear sectional analysis program of structural analysis, especially reinforced concrete columns and beams following the base of Modified Compression Field Theory. The software is utilized to calculate the strength and ductility of reinforced concrete cross-section subjected shear, moment, and axial load. It is also able to make a prediction of shear strength for complicated sections, hence, the software is applied to calculate the shear capacity of four testing specimens following MCFT methods.

The details of four specimens and its material parameters are modeled to correspond with the condition in predictive calculation (Figure 4.4). More details of this software application could be found in Appendix B. To calculate shear capacity, the software does not consider beam as a homogeneous block, but divides cross-section into several slices. At each certain height y, the software analyzes the resultant stress and strain, that are satisfied the condition of equilibrium condition, compatibility, and constitutive law, shown in Figure 4.1. After inputting

all required information for applied forces, shear span, and support types, Response-2000 generates a bending moment–shear force interaction diagram based on CSA 2014 (blue line) and original MCFT formulation (red line). The shear resistance predicted by MCFT is determined from the red curve at the point where $M/V = a - d = 0.39$, corresponding to the loading condition used in the experiment. The results of shear capacity of 4 beams in experiment are described in Table 4.9. It can be observed that shear resistance predicted by Response-2000 is slightly lower than that obtained using iterative SMCFT method. However, the predicted shear resistance varies among four beams due to differences in cross-sectional depth and longitudinal reinforcement ratio.

Table 4.9: *Shear resistance of the four testing beams in relation to MCFT calculated by Response-2000 software, CSA A23.3-19 (simplified MCFT), and iterative SMCFT approach*

Specimen	**Shear resistance force V_c [kN]**		
	MCFT_Response-2000	SMCFT_CSA 23.3-19	Iterative SMCFT
V26.01	52.28	44.04	56.68
V26.02	58.26	44.04	56.68
V26.03	58.66	44.04	63.63
V26.04	65.66	44.04	63.63

VGU Vietnamese-German University

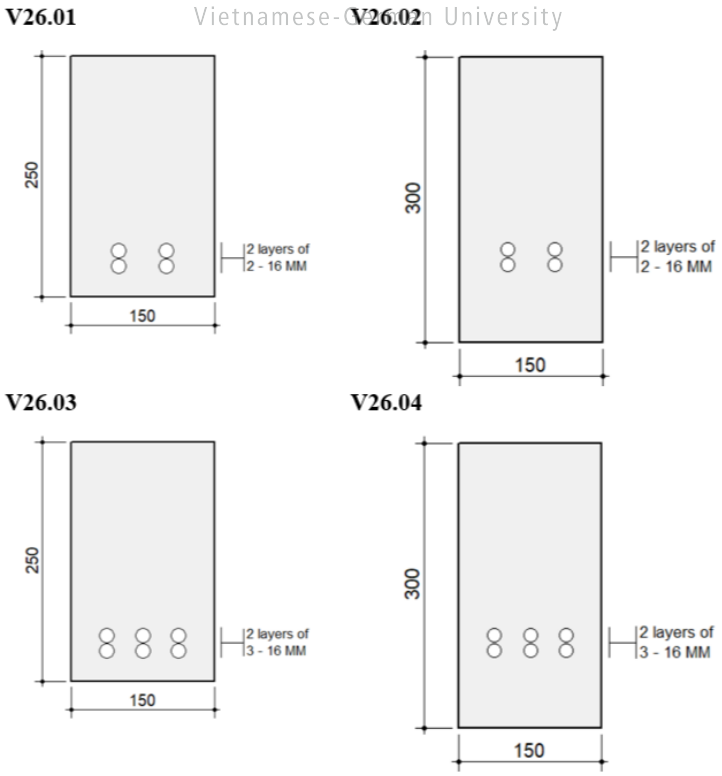

Figure 4.4: *Cross-section of four testing beams on software Response-2000*

4.4.2 INCA2 software

INCA2 is a specialized engineering software applied for the nonlinear calculation and analysis of various types of cross-sections in structural engineering. This software allows users to determine geometric characteristics, material stress-strain states, and check the load-bearing capacity of cross-sections with different geometric shape and material, from conventional reinforced concrete members to complex steel, rigid concrete, and composite structures. The software also enables to generate bending moment-curvature graph, providing important stiffness parameters for nonlinear analysis problems. Parameters related to sectional analysis in *m*SM model are verified by the use of INCA2 (relative depth of compression zone k_x and curvature κ).

Similarly to Response-2000, the details of four specimens and material parameters are modeled on INCA2 to correspond with the condition in predictive calculation. For concrete, the compressive strength, tensile strength, and elastic modulus are inputted similarly with theory, while reinforcement steel is chosen as steel grade S350 of EC2. This cross-section is only subjected to bending moment about y-axis, which is caused by ultimate experiment shear force V_u at control section $a - d$. More details of this software application could be found in Appendix B. The software is based on the Bernoulli-Euler theory that cross-section remain plane when bending. Instead of dividing beam into several small elements like other software, INCA2 employs boundary integration to convert the double integral on the surface into single integral along the polygon boundary of the cross-section and calculates relevant stress, strain.

VGU
Vietnamese-German University

Table 4.10: *Relative depth of the compression zone of the four test beams calculated using INCA2 and mSM*

Specimen	d [mm]	x [mm]	k_x INCA2	k_x *m*SM
V26.01	210	92.1	0.44	0.44
V26.02	210	92.0	0.44	0.44
V26.03	210	106.0	0.50	0.51
V26.04	210	114.2	0.54	0.51

Table 4.11: *Curvature of the four test beams calculated using INCA2 and mSM*

Specimen	M [kNm]	κ_{INCA2} [1/1000 m]	$\kappa_{m\text{SM}}$ [1/1000 m]
V26.01	21.9	6.21	6.62
V26.02	21.7	6.14	6.54
V26.03	26.5	5.82	6.20
V26.04	26.5	4.44	6.20

The moment-curvature of four testing beams are plotted by INCA2, found in Appendix B. By evaluating these graphs, the experimental ultimate bending moments of four beams still lies on linear line of the corresponding section response. It means, cross-sections at failure do not experience the reduction in flexural stiffness or develop to non-linear flexural behavior. The inflection point from linear to nonlinear response may be associated with first flexural crack, longitudinal reinforcement yielding, concrete crushing... With relatively high longitudinal reinforcement ratio and corresponding recorded bending moment, the theoretical flexural capacity of cross-sections is not optimized and governed instead by shear failure, as expected for beams without stirrups.

The depth of compression zone x and relative depth of compression zone $k_x = x/d$ calculated by INCA2 are described in Table 4.10. This coefficient calculated by *m*SM model in Equation 4.21 is about similar with results obtained from INCA2. The sectional response predicted by INCA2 is consistent with cracked elastic concrete section adopted in *m*SM. Both ways consider the same analysis condition, including concrete and steel maintain in linear elastic behavior, neglect concrete tensile stress and axial force. The curvature κ in Table 4.11 is defined from moment-curvature graph of software, at bending moment identified by iterative *m*SM calculation. These values obtained from *m*SM model (Equation 4.20) is nearly identical with the one calculated by the software. The slightly lower value reported by the software is due to its default use of S350 steel, which assumes higher elastic modulus of E_s = 200 GPa.

VGU
Vietnamese-German University

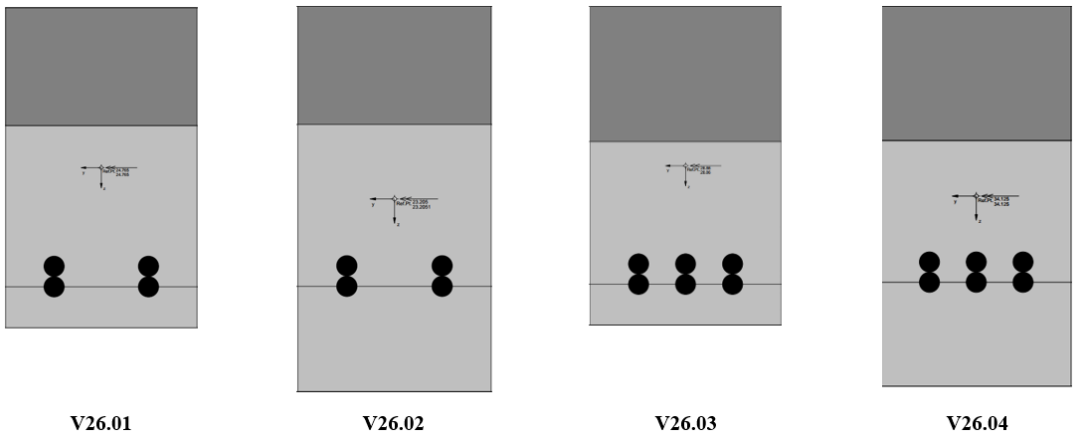

Figure 4.5: *Compressive zone (dark grey zone) and tensile zone (grey zone) of cross-section of four testing beams V26.01, V26.02, V26.03, and V26.04 in INCA2 software*

4.4.3 Additional application of Response-2000 software

This part is conducted additionally to examine the shear strength predictability of Response-2000 for beams with other different longitudinal reinforcement distribution and not in scope of the main finding. Response-2000 is employed to investigate the beams without shear reinforcement, in which longitudinal bars are distributed over the depth of the cross-section. The analysis is conducted for three slender beams without stirrups GB54, GB58, and GB56 from the experiment studied by Cholostiakow et al. [59]. The span-to-depth ratios are 2.65, 2.70, and 2.58, respectively and dimension of cross-section is presented in Figure 4.6.

These three experimental specimens are simulated in Response-2000 with corresponding material properties, geometry, and longitudinal reinforcement arrangements to predict shear strength. The properties of section properties, concrete, longitudinal GFRP, and BFRP reinforcement ratio and properties are summarized in Table 4.12 and 4.14. The results of shear capacity predicted by Response-2000 is shown in Table 4.13.

There is no clear consistent trend defined for these three specimens predicted by Response-2000. For beam GB58, the predicted shear capacity is underestimated with ratio V_{exp}/V_c of 1.288. Similarly, the capacity of GB56 is also underestimated by 12.8%, with predicted and experimental values of respectively 38.266 and 43.9 kN. In contrast, Response-2000 overestimates the shear capacity of GB54 by approximately 19.1%, predicting 37.286 kN compared with the measured value of 31.3 kN. Among the three specimens, GB56 shows the closest agreement with the experimental result, whereas GB58 presents the largest discrepancy.

Vietnamese-German University

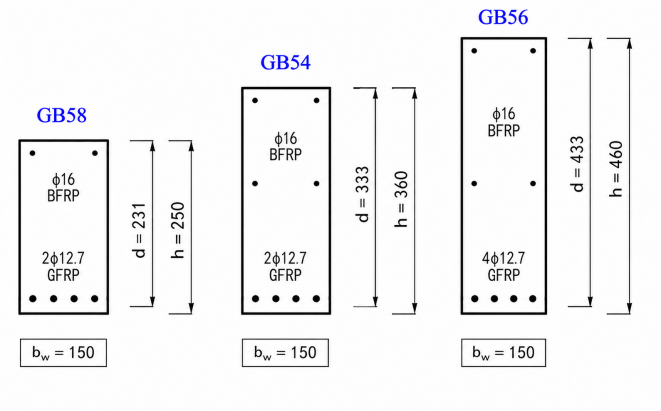

Figure 4.6: *Cross-sections of three beams GB58, GB54, and GB56 in experiment of Cholostiakow et al., reproduced* [59]

Table 4.12: *Mechanical properties of GFRP and BFRP reinforcement used in specimens GB58, GB54, and GB56*

Specimen	**GFRP**	**BFRP**
Elastic modulus [GPa]	46	42
Tensile strength [MPa]	758	1,297

Table 4.13: *Comparison between experimental and Response-2000 shear strength predicted for original specimens GB58, GB54, and GB56*

Specimen	**Experiment**	**Response-2000**	**Ratio**
	V_{exp} **[kN]**	V_c **[kN]**	V_{exp}/V_c
GB58	37.3	28.949	1.288
GB54	31.3	37.286	0.839
GB56	43.9	38.266	1.147

In addition, based on three cross-sections, six beams are analyzed with side reinforcement (GB54*, GB58*, GB56*) and without side reinforcement (GB54-0, GB58-0, GB56-0), while keeping the amount of flexural reinforcement unchanged. In this case, the longitudinal glass fiber reinforced polymer (GFRP) and basalt fiber reinforced polymer (BFRP) bars are replaced by steel reinforcement with tensile strength of 350 MPa, the same with VGU test. All other parameters are identical with original tests of Cholostiakow et al. and members are set up as simply supported beam subjected to concentrated loading (Table 4.14). Besides calculating shear resistance, the maximum bending moment by live load of 40 kNm is assumed at mid-span to investigate crack width and crack spacing. More details of this software application could be found in Appendix B.

As results, the shear resistance, crack spacing at the bottom of the beams, and crack patterns predicted by Response-2000 are presented in Table 4.15 and Figure 4.8. Side longitudinal reinforcement is commonly provided to control crack development along the depth of the beam web. At an assumed maximum mid-span moment of 40 kNm, the beams with side reinforcement GB58*, GB54*, and GB56* exhibit smaller bottom crack spacing than the one without side reinforcement, with values of 216 versus 260 mm, 239 versus 360 mm, and 269 versus 452 mm, respectively. These values correspond to reductions in crack spacing of about 16.9%, 33.6%, and 40.5%. A reduction in crack width is also observed for the GB58*/GB58-0 and GB54*/GB54-0 pairs, whereas the same trend is not evident for GB56*/GB56-0. The predicted shear resistance is higher for all specimens with side reinforcement, increasing from 31.859 to 36.055 kN for GB58*, from 47.905 to 52.230 kN for GB54*, and from 61.122 to 69.485 kN for GB56*, corresponding to increases of approximately 13.2%, 9.0%, and 13.7%, respectively.

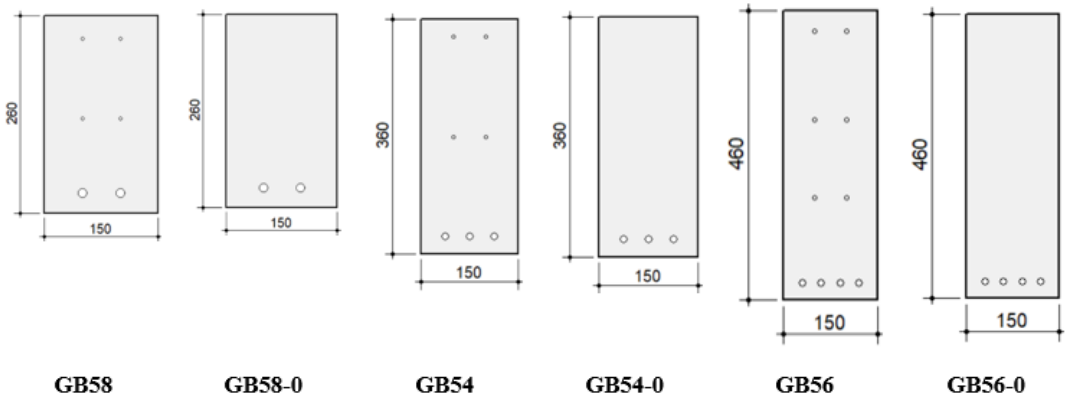

Figure 4.7: *Cross-sections of six beams without stirrups are investigated for the influence of side reinforcement using Response-2000*

Table 4.14: *Relevant parameters of six beams without stirrups investigated for the influence of side reinforcement using Response-2000*

Specimen	a [mm]	a/d	f_c [MPa]	Flexural reinforcement	ρ_l	Side reinforcement
GB58*	620	2.65	36.6	2 ϕ12.7	0.82	4 ϕ6
GB58-0						0
GB54*	900	2.70	30.2	3 ϕ12.7	0.86	4 ϕ6
GB54-0						0
GB56*	1120	2.58	38.0	4 ϕ12.7	0.88	6 ϕ6
GB56-0						0

VGU Vietnamese-German University

Table 4.15: *Results of shear resistance and crack spacing recorded at the bottom of the beams for six specimens analyzed using Response-2000*

Specimen	Shear resistance [kN]	Crack spacing at the bottom of beam [mm]
GB58*	36.055	216
GB58-0	31.859	260
GB54*	52.230	239
GB54-0	47.905	360
GB56*	69.485	269
GB56-0	61.122	452

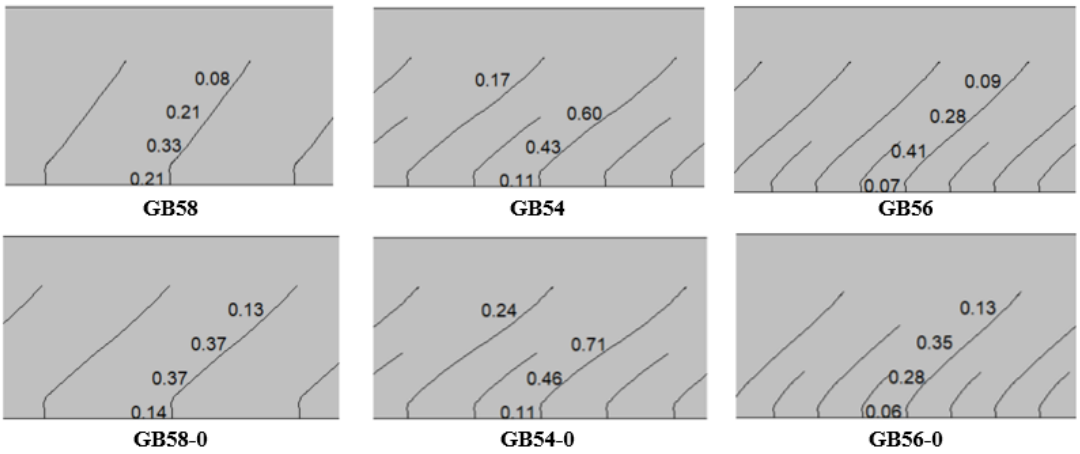

Figure 4.8: *Crack patterns and crack width predicted by Response-2000 of six beams without shear reinforcement*

VGU
Vietnamese-German University

5. Discussion

5.1 Comparison between experimental result and predictive calculation

5.1.1 Four testing VGU beams

From experiment data, predictive shear strength is calculated according to five design provisions by both simplified and iterative approach. The MCFT results obtained from Response-2000 are also included for comparison, however, the main focus still remains on the other five methods. By the aim of providing more comprehensive and objective evaluation, the statistical characteristic including mean value μ_θ, standard deviation SD, and coefficient of variation δ_θ are also provided to evaluate the accuracy and precision of these methods. Specifically, the average ratio between experimental and theoretical shear resistance force $\theta = V_{exp}/V_c$ serves as an indicator for accuracy (values θ above unity indicate conservative predictions), while the CoV is used as measure of precision. The experimental shear resistance used for database evaluation is ultimate shear resistance, while it is critical shear resistance for four testing beams.

The overview of calculated and experimental results of four VGU beams is shown in Table 5.1 and 5.2 summarizes the ratio between experimental and calculated shear strength $\theta = V_{exp}/V_c$ of four testing beams without shear reinforcement, as well as mean value μ_θ, standard deviation, and coefficient of variation δ_θ. The accuracy of five methods is also plotted in graph Figure 5.1. Overall, CSA A23.3-19 provides the most conservative predictions with ratio θ ranging from 1.31 to 1.42. The calculated shear resistances are approximately 24% to 30% lower than experimental values. In this method, shear resistance is determined through factor β, which accounts for crack spacing s_z (assumed to be equal to effective depth d), and maximum aggregate size $a_{g,max}$. Hence, beams with the same effective depth and aggregate size yield similar results, in spite of distinct longitudinal reinforcement ratio and layout. In contrast, EN 1992-1-1-23 predicts shear resistance of beams V26.01 and V26.02 with lower reinforcement ratio 2.6% extremely close to experimental results and its deviation varies only from 1% to 4%.

For beams V26.03 and V26.04 with higher reinforcement ratio 3.8%, this method overestimates shear resistance by 9% to 11% than experiment. This tendency is in contrast to that observed for simplified *m*SM model, which estimates shear resistance relatively accurate for beams with higher reinforcement ratio but underestimates it for 2.6% reinforcement. From safety aspect, the deviation of simplified *m*SM model of four beams remains relatively small, about 13% lower and shear resistance leans toward safety side. In addition, both iterative calculation methods provide relatively similar shear resistance results. For two beams with lower reinforcement ratio V26.01 and V26.02, shear resistance is about 1% to 6% lower than experimental values. Meanwhile, for beams V26.03 and V26.04 with higher reinforcement ratio, the shear resistance is overestimated by up to 11%.

To sum up, CSA A23.3-19 provides the most conservative shear resistance with μ_θ = 1.37. The remaining four methods provides relatively comparable values with mean value μ_θ about 1% to 6% to unity. The iterative SMCFT shows the best overall agreement with experimental results, achieving mean value of 1.01 and low CoV of 0.04.

Table 5.1: *Shear strength of four testing beams, calculated by EC2-2025, CSA A23.3-19, simplified mSM, iterative SMCFT*, iterative mSM* and MCFT by Response2000*

VGU Vietnamese-German University

	Experiment	**EC2-2025**	**CSA A23.3-19**	***m*SM**	**SMCFT***	**MCFT**	***m*SM***
	V_{cr} [kN]	V_c [kN]	V_c [kN]	V_c [kN]	V_c [kN]	V_c [kN]	V_c [kN]
V26.01	60	59.57	44.03	52.37	56.45	52.28	56.41
V26.02	57.5	59.57	44.03	52.37	56.45	58.26	55.71
V26.03	61.5	68.19	44.03	62.03	63.63	58.66	68.09
V26.04	62.5	68.19	44.03	62.03	63.63	65.66	68.09

Table 5.2: *Mean value, standard deviation and coefficient of variation of results calculated by EC2-2025, CSA A23.3-19, simplified mSM, iterative SMCFT*, iterative mSM* and MCFT by Response2000, for shear strength of four testing beams*

Specimen	**EC2-2025**	**CSA A23.3-19**	***m*SM**	**SMCFT***	**MCFT**	***m*SM***
	$\theta = V_{exp}/V_c$	$\theta = V_{exp}/V_c$	$\theta = V_{exp}/V_c$	$\theta = V_{exp}/V_c$	$\theta = V_{exp}/V_c$	$\theta = V_{exp}/V_c$
V26.01	1.01	1.36	1.15	1.06	1.15	1.06
V26.02	0.97	1.31	1.10	1.01	0.99	1.03
V26.03	0.90	1.40	0.99	0.97	1.05	0.90
V26.04	0.92	1.42	1.01	0.98	0.95	0.92
Mean μ_θ	0.95	1.37	1.06	1.01	1.03	0.98
SD	0.05	0.05	0.07	0.04	0.09	0.08
CoV δ_θ	0.051	0.036	0.069	0.040	0.083	0.082

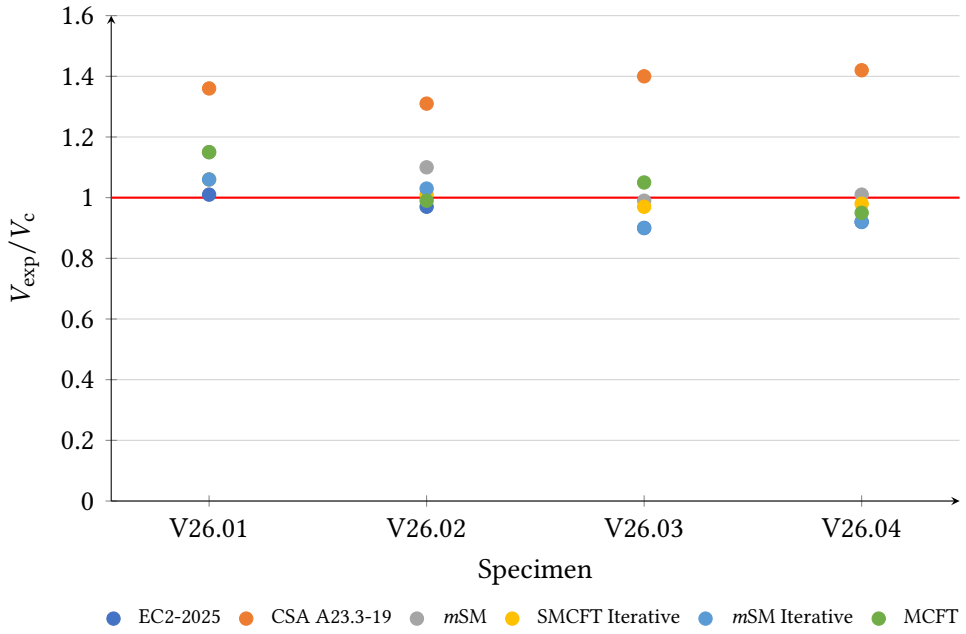

Figure 5.1: *Experimental-to-calculated shear resistance ratio graph of four testing beams*

5.1.2 Database of 784 beams

Concurrently, all shear capacity prediction and evaluation methods are similarly applied to the database of 784 beams to achieve more comprehensive assessment among various specimens. Besides longitudinal reinforcement ratio ρ_l, five other parameters are also investigated versus experimental to predicted shear strength θ, including effective depth d, span-to-depth ratio a/d, diameter ϕ_s, maximum aggregate size $a_{g,max}$, and concrete compressive strength f_c. The limitation of this calculation is that shear resistance of 784 beams in the database are calculated on large scale to establish a general basis for comparison, without fully accounting for specific conditions of regarding material and geometric properties of specimens of every single specimen. Since the critical and ultimate shear resistance of database are not distinguished, missing parameters are assumed, and results are not error-adjusted; the following evaluation is not applicable in all cases.

Table 5.3 presents the overall predictive performance of 784 beams among five calculation methods through mean value θ and coefficient of variation δ_θ. All methods generally provide conservative estimates. Among five considered methods, the simplified and iterative *m*SM show the closest approach to experimental results, with mean values of 1.04 and 1.03. The EC2-2025 and iterative SMCFT also demonstrates satisfactory results, with slightly conservative mean value of 1.09 and 1.12. In similar with 4 VGU beams, CSA A23.3-19 yields the most conservative

results with mean value of 1.40. Figure 5.2 provides a further insight into the distribution of these shear strength predictions. The minimum θ of all methods range from 0.50 to 0.59, indicating the very low rate of unsafe predictions. Both *m*SM methods highlight its dominance by predicting nearly 200 over 784 beams (δ_θ = 0.17 and 0.18) with experimental-to-predicted ratio at unity. Most of predicted *m*SM calculation fluctuates within the range θ from 0.9 to 1.10, while there is a little number of beams calculated with ratio θ from 1.6 to 2. The simplified method of *m*SM is more conservative than the iterative one. Similarly, the majority of EN 1992-1-1:2023 results are concentrated within a relatively narrow interval around θ from 0.9 to 1.3, with limited number of observations extending towards higher ratio. This distribution is consistent with relatively low CoV, suggesting that EC2 provides generally stable predictions with moderate conservative trend. In comparison, the CSA A23.3-19 distribution is shifted considerably toward right side and extends over much wider range. Its histogram shows the general tendency to underestimate actual shear resistance of beams, with most of ratios θ ranging from 1.1 to 1.6. This design standard also exhibits the greatest dispersion, with CoV δ_θ of 0.31 and maximum ratio θ of 3.93. The general method of CSA A23.3-19 (iterative SMCFT) reflects the general pattern of CSA standard, that to be conservative in predicting shear strength. However, the SMCFT improves the scatter of data with CoV δ_θ of 0.20 and 182/784 specimens defined at θ of 1.

VGU
Vietnamese-German University

Overall, the simplified and iterative *m*SM methods provide the highest synergy between accuracy and reliability, followed closely by the new EC2. The iterative SMCFT remains reasonably accurate but exhibits slightly greater dispersion, whereas CSA A23.3-19 shows more pronounced conservative estimation and large data scatter.

Table 5.3: *Comparison of shear strength calculation for database of 784 beams among 5 methods*

	EC2-2025	**CSA A23.3-19**	***m*SM**	**SMCFT Iterative**	***m*SM Iterative**
Mean μ_θ	1.09	1.40	1.04	1.12	1.03
SD	0.20	0.44	0.17	0.23	0.18
CoV δ_θ	0.18	0.31	0.17	0.20	0.18
min θ	0.59	0.56	0.55	0.54	0.50
max θ	2.45	3.93	2.05	2.54	1.93

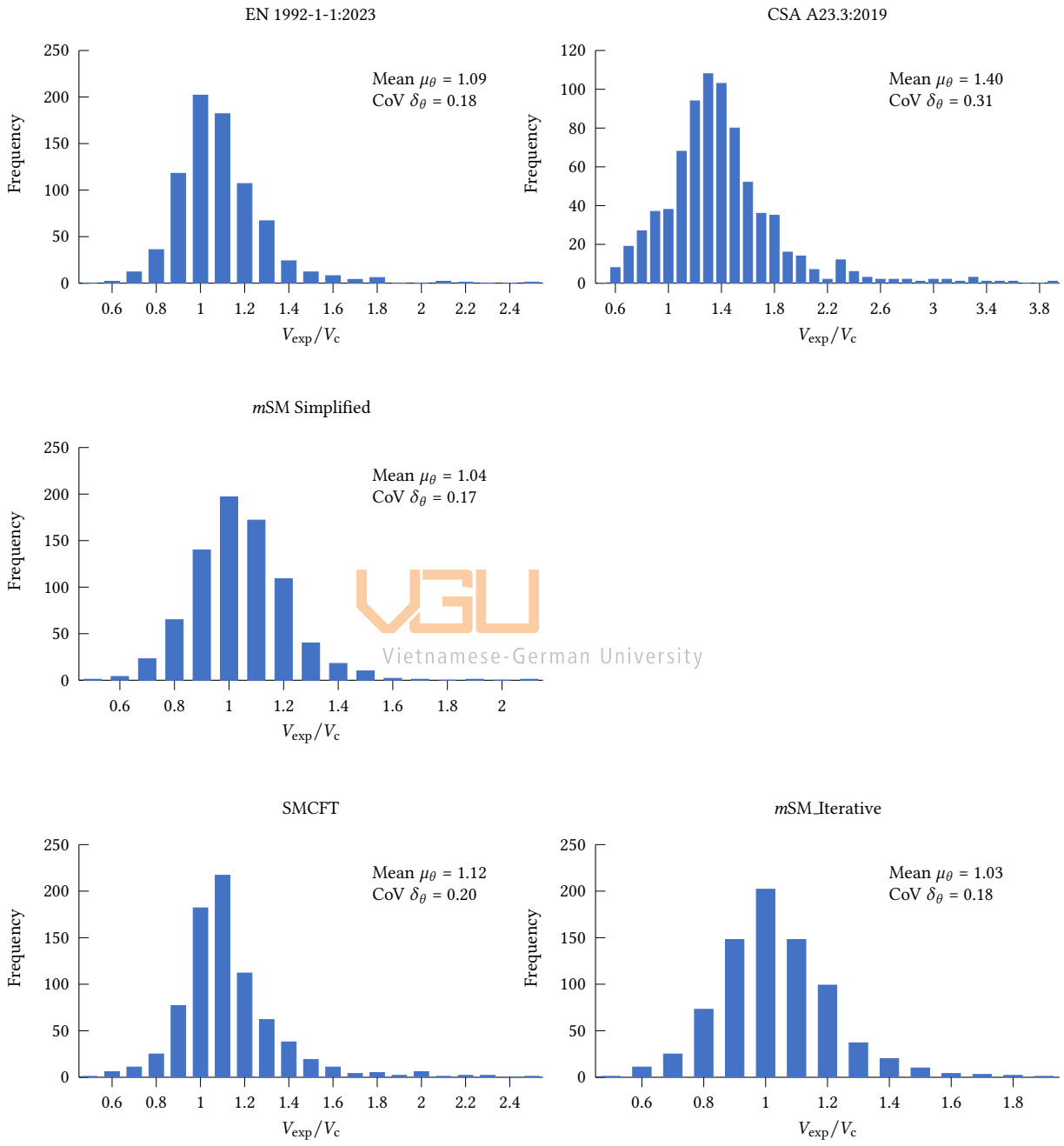

VGU
Vietnamese-German University

Figure 5.2: *Distribution of experimental-to-calculated shear strength ratios of 784 beams among five methods*

Figure 5.3 describes the relationship between the experimental-to-calculated shear strength ratio calculated using 5 different methods and longitudinal reinforcement ratio ρ_l. Although longitudinal reinforcement ratio is not explicitly included in the CSA formulation, the ratio V_{exp}/V_c increases remarkably in proportional with ρ_l, indicating a tendency toward increasingly conservative predictions of shear resistance. In contrast, other four methods remain relatively stable, with most results distributed around the unity line within the range of approximately 0.5 to 1.5. For ρ_l from about 2.5% onwards, the dispersion of all shear strength prediction methods varies larger, leaning toward conservatism. However, the number of cases with underestimated shear resistance are recorded as limited within this range. The longitudinal reinforcement diameter ϕ_s, effective depth d, shear slenderness a/d, and concrete compressive strength f_c are also investigated their relationship versus experimental-to-calculated shear strength, shown from Figure 5.4 to 5.8. In general, the ratio θ tends to decrease as effective depth, span-to-depth ratio, and concrete compressive strength increase. This suggests that the methods shift from underestimating the shear resistance at lower parameter values to predictions closer to experimental results. This trend is most pronounced for CSA A23.3:2019, which produces mostly θ above unity for beams with small effective depths (below 100 mm), a/d from 2 to 3, and low concrete compressive strengths (20 – 30 MPa). As these parameters increase, the CSA predictions generally approach the unity line, whereas EN 1992-1-1:2023, SMCFT, and two *m*SM approaches remain comparatively stable and closed-to unity over most of investigated ranges. The data scatter is relatively greater within very small effective depth d (less than 100 mm). By contrast, both longitudinal reinforcement diameter ϕ_s and maximum aggregate size $a_{g,max}$ do not exhibit clearly consistent tendency versus accuracy, making it difficult to isolate the individual influence of these two parameters based only on scatter plots.

VGU
Vietnamese-German University

To sum up, three parameters d, a/d, and f_c witness more systematic influence on the prediction rather than reinforcement diameter ϕ_s and maximum aggregate size $a_{g,max}$. Among five considered methods, CSA A23.3:2019 tends to be significantly sensitive to these parameter variations, while other approaches are more consistent across the database.

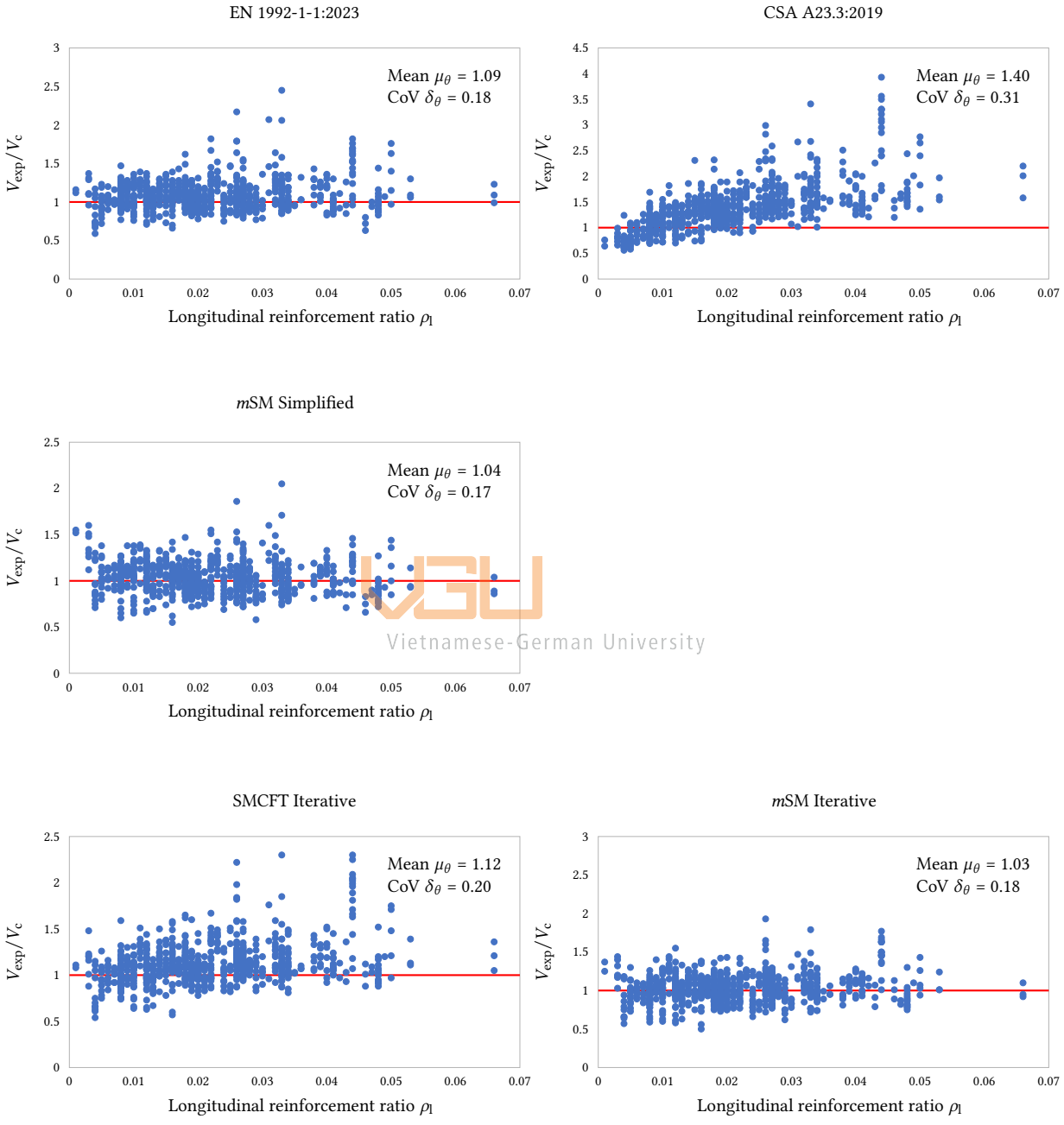

VGU
Vietnamese-German University

Figure 5.3: *Longitudinal reinforcement ratio versus experimental-to-calculated shear strength ratio for 784 beams among five methods*

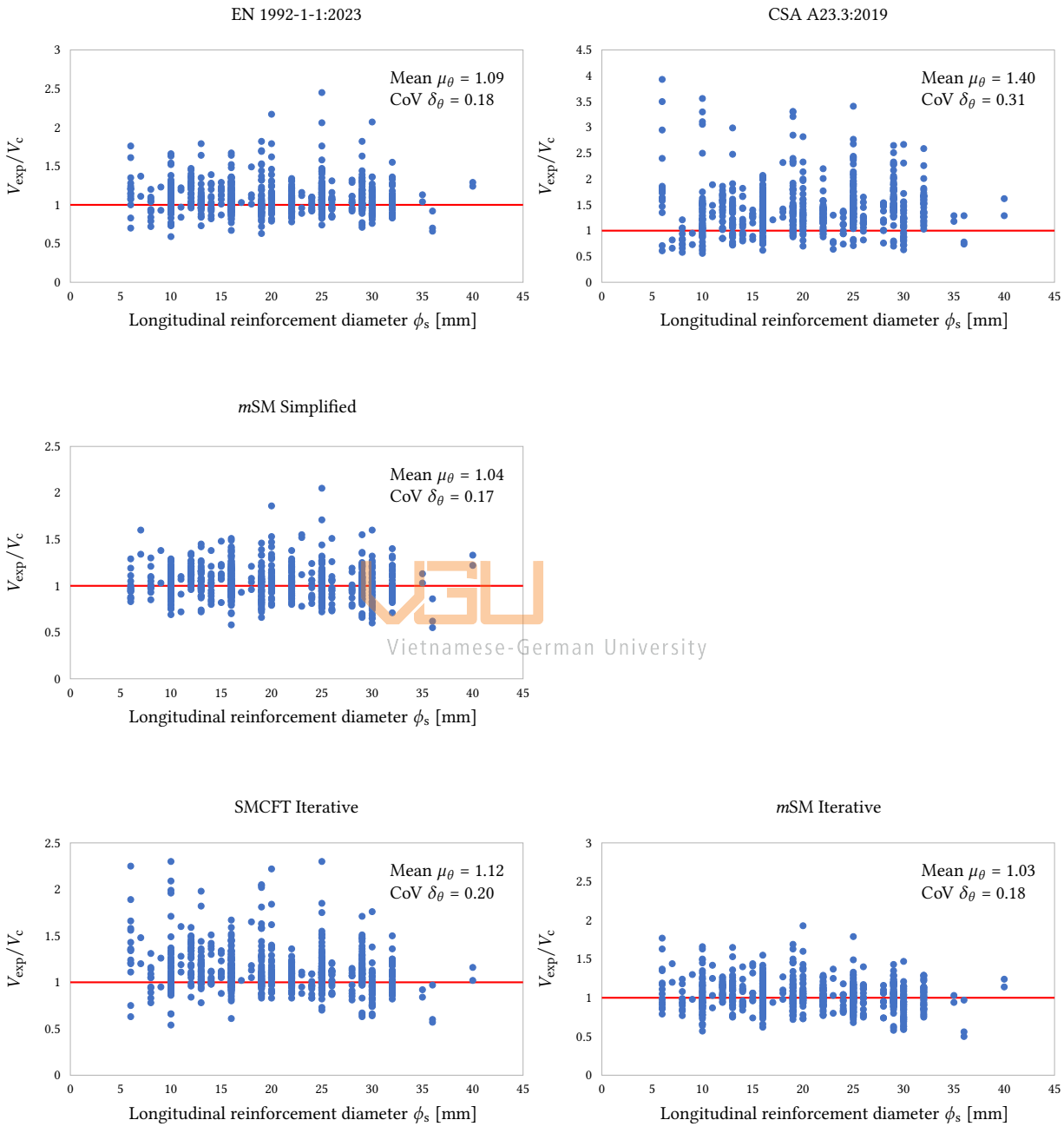

VGU
Vietnamese-German University

Figure 5.4: *Longitudinal reinforcement diameter versus experimental-to-calculated shear strength ratio for 784 beams among five methods*

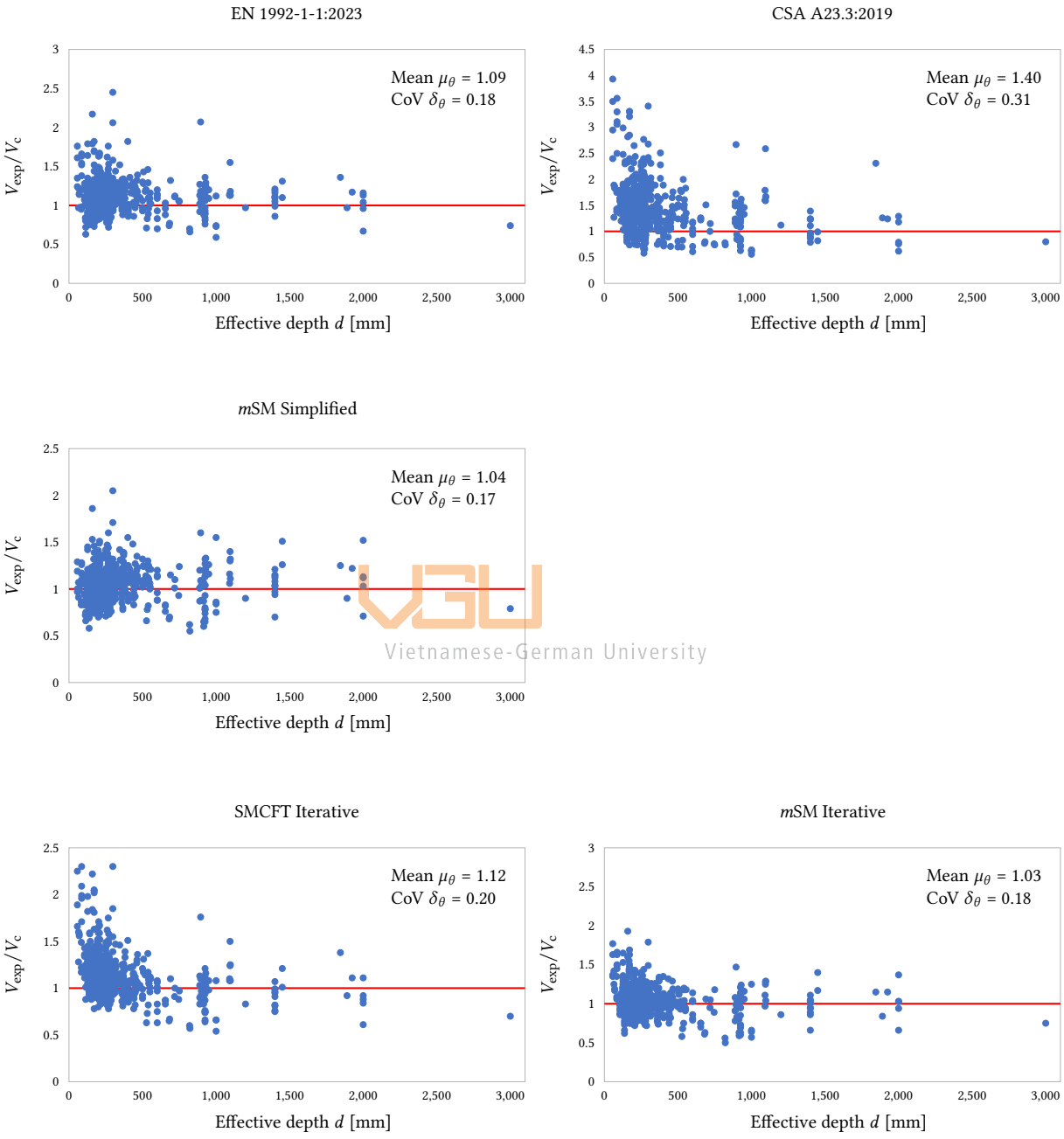

VGU
Vietnamese-German University

Figure 5.5: *Effective depth versus experimental-to-calculated shear strength ratio for 784 beams among five methods*

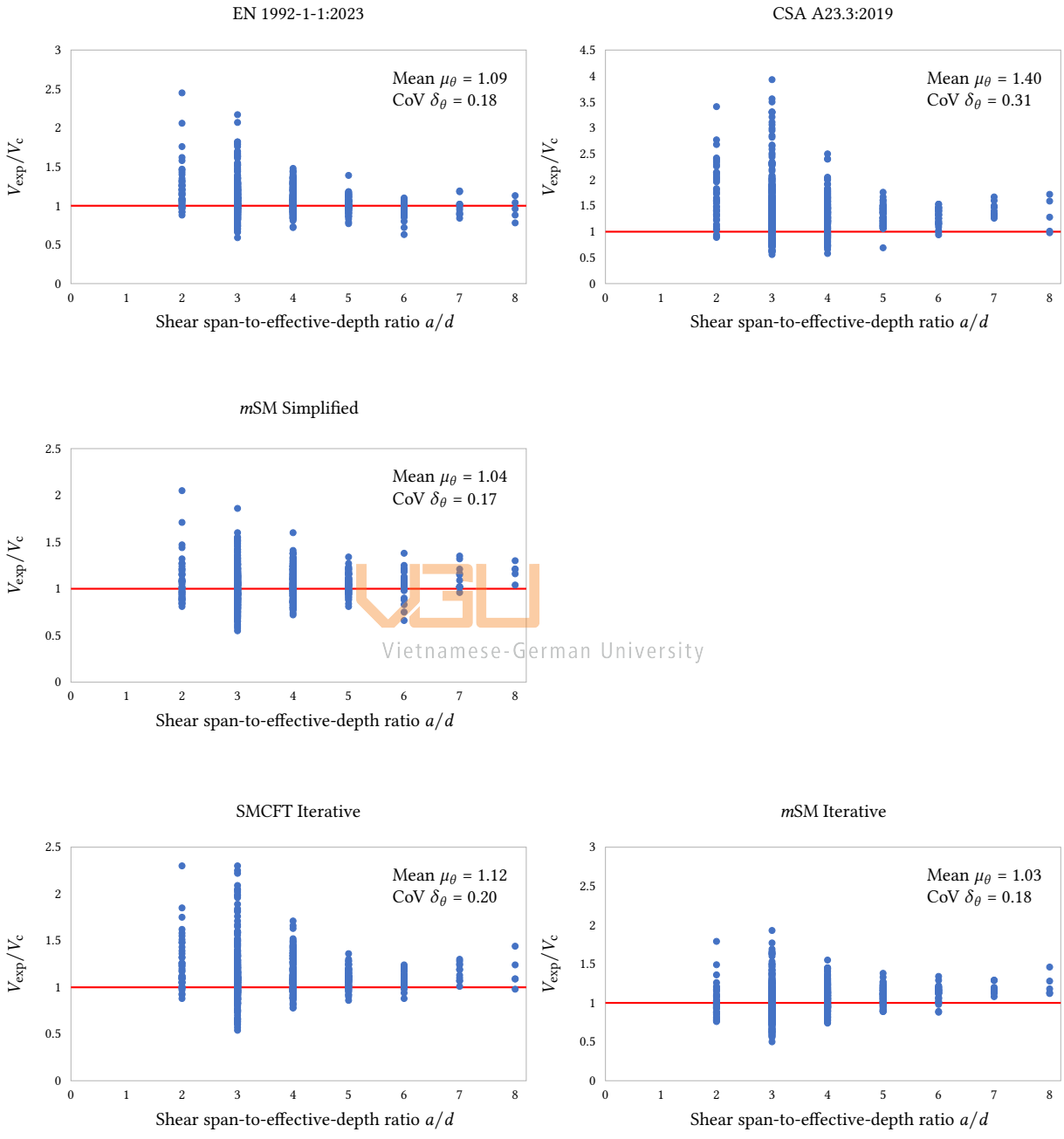

Vietnamese-German University

Figure 5.6: *Shear span-to-effective-depth ratio versus experimental-to-calculated shear strength ratio for 784 beams among five methods*

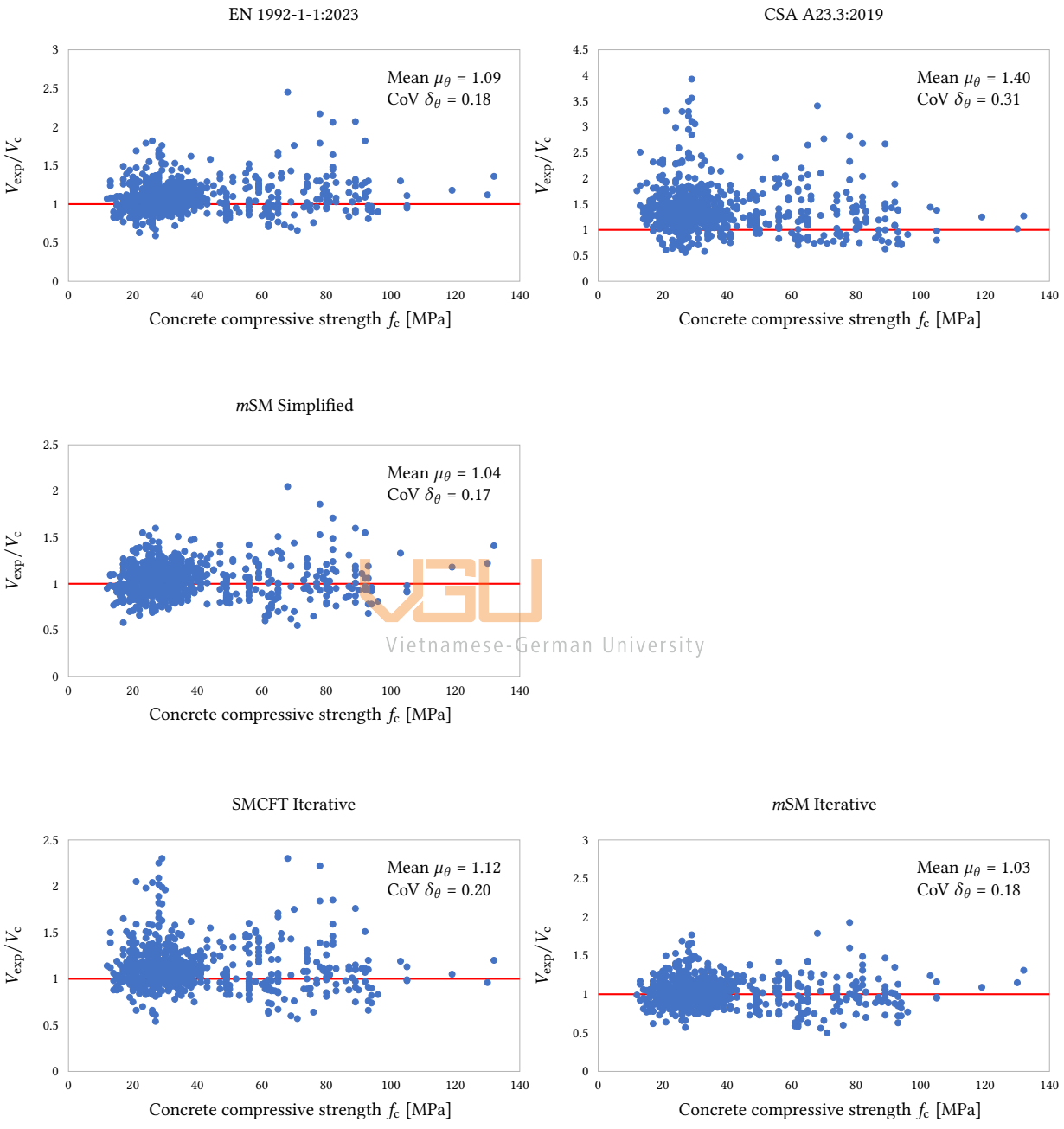

VGU
Vietnamese-German University

Figure 5.7: *Concrete compressive strength versus experimental-to-calculated shear strength ratio for 784 beams among five methods*

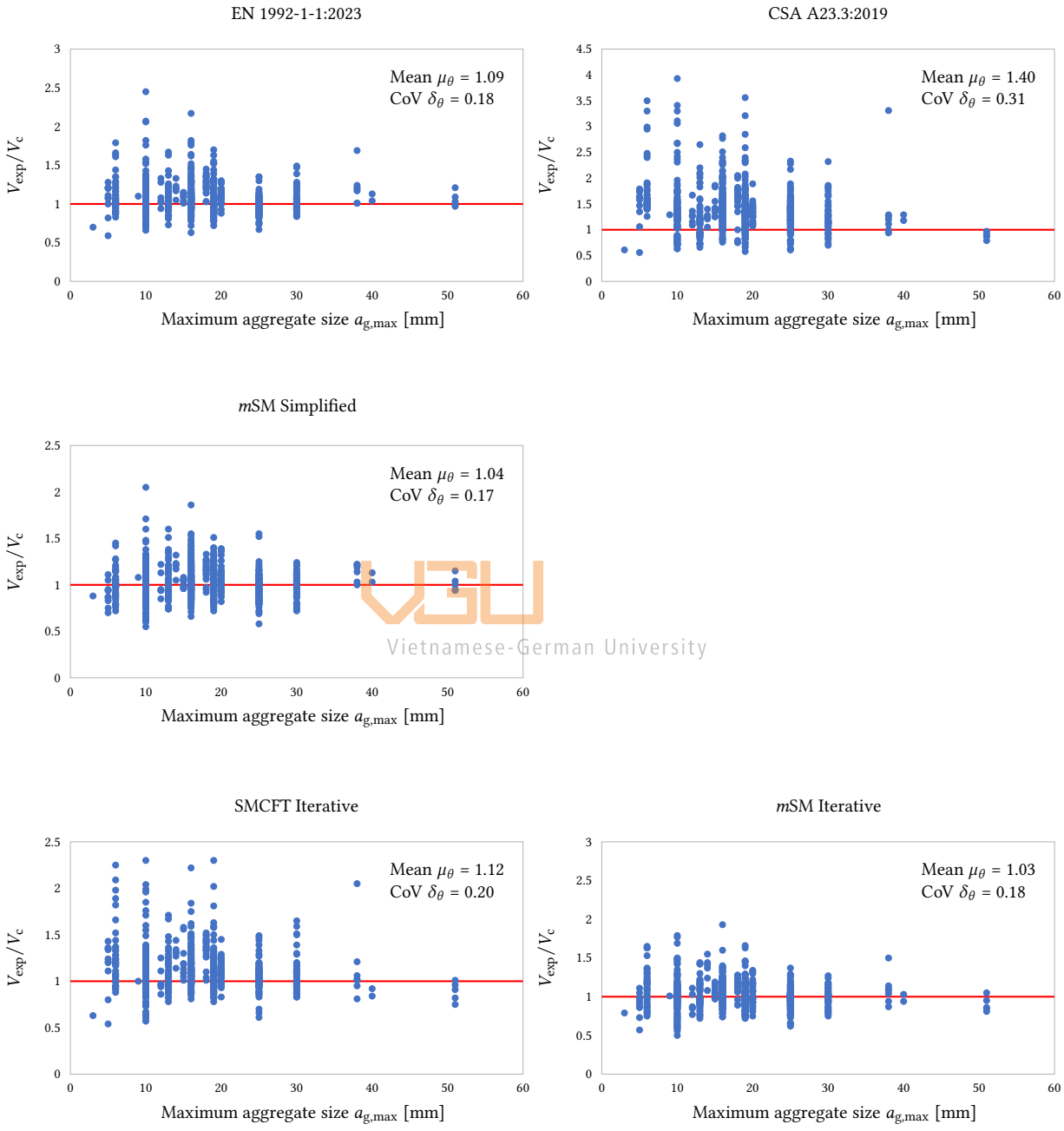

VGU
Vietnamese-German University

Figure 5.8: *Maximum aggregate size versus experimental-to-calculated shear strength ratio for 784 beams among five methods*

Besides, among different shear models considered in this study, *m*SM is the only model that explicitly separates shear resistance into the contributions of tensile zone, V_{ct}, and compressive zone, V_{cc} of concrete members. Therefore, the influence of six investigated parameters on the relative contribution of these two zones can be further evaluated through ratio V_{ct}/V_{cc}, as shown in Figure 5.9.

Regarding longitudinal reinforcement parameters, both increasing longitudinal reinforcement ratio ρ_l generally reduces V_{ct}/V_{cc}, indicating an increasing contribution of the compression zone. More effective longitudinal reinforcement restrains longitudinal strain and crack opening, and shifts neutral axis downward, thereby increasing the effective compression zone. For geometry, the increase of effective depth d generally decreases the relative contribution of tensile zone. In *m*SM, larger effective depth increases crack spacing and thereby influences the critical crack width, reducing the effectiveness of shear transfer through crack in tensile zone. The similar tendency in V_{ct}/V_{cc} is observed with increasing span-to-depth ratio a/d, as larger moment relative to shear increases longitudinal deformation and crack opening, making the contribution of compression zone relatively more dominant. When considering concrete parameters, increasing concrete compressive strength f_c also makes V_{cc} favorable, since stronger concrete enhances the shear resistance developed within uncracked compression zone. On the other hand, maximum aggregate size $a_{g,max}$ and steel bar diameter ϕ_s do not show clear trend toward either compressive or tensile zones.

VGU
Vietnamese-German University

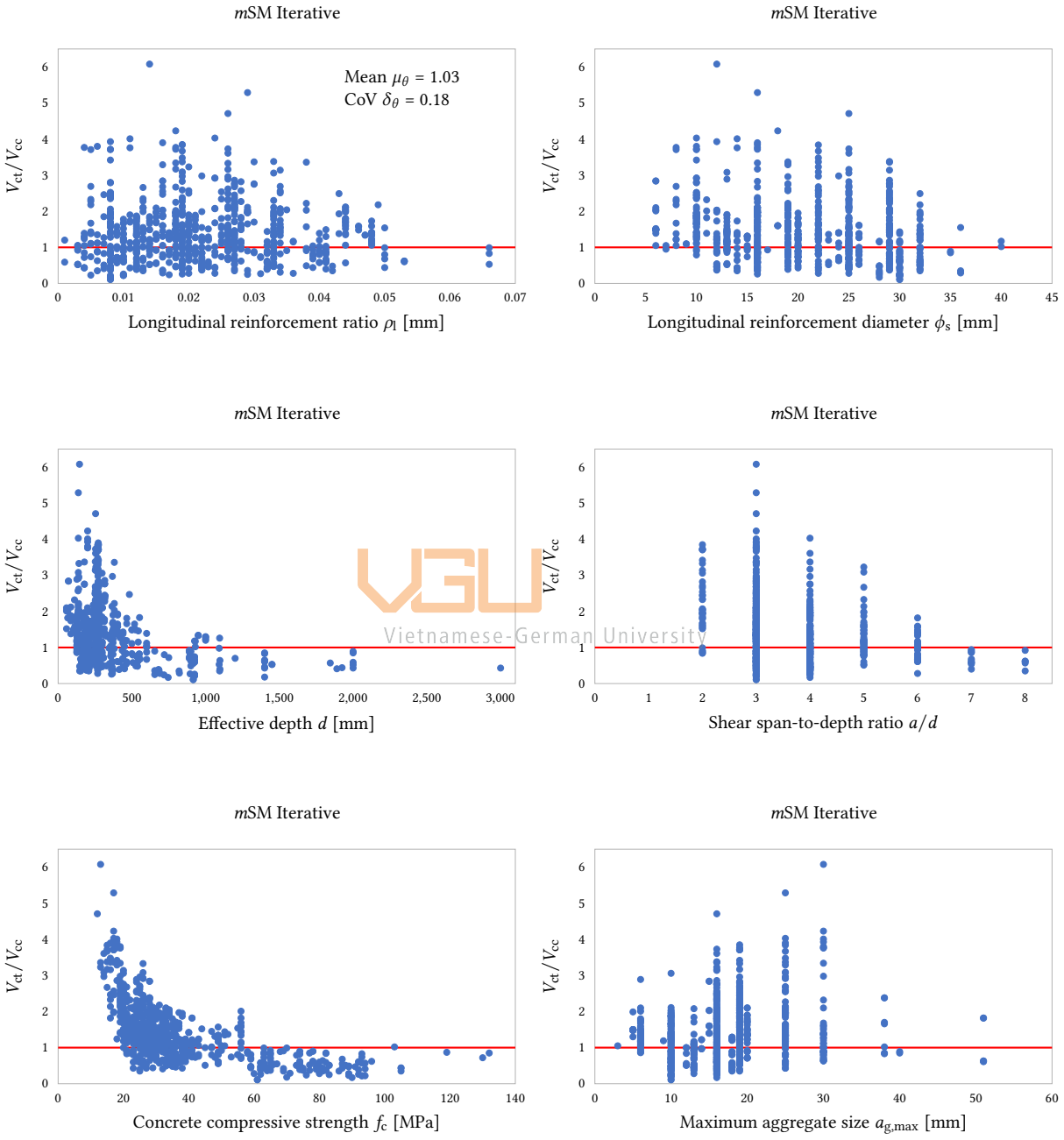

VGU Vietnamese-German University

Figure 5.9: *Influence of six parameters on the ratio V_{ct}/V_{cc} predicted by the iterative mSM*

5.2 General discussion

5.2.1 Discussion of experimental results

The experimental results clearly demonstrate the influence of longitudinal reinforcement detailing on the shear capacity of beams without stirrups. The results support existing theories regarding the role of longitudinal reinforcement in the shear capacity of concrete beams, specifically an increase in reinforcement ratio enhances the shear resistance of the beams. With the same cross-sectional dimensions, the ultimate shear strengths of beams V26.03 and V26.04 are 16.5% and 47.1% higher than those of V26.01 and V26.02, respectively (Table 3.4). The results indicate interaction between longitudinal reinforcement ratio and bottom concrete cover: the increase in ultimate shear capacity associated with higher reinforcement ratio is pronounced for beams with larger concrete cover, while the effect of increasing concrete cover varies depending on reinforcement ratio. The load–deflection curves indicate that all four beams exhibit high stiffness, as its curves rise steeply within deflection below 5 mm (Figure 3.18). These curves of V26.03 and V26.04 continue to rise after the first load drop, while those of V26.01 and V26.02 record a sudden decrease. This indicates that beams with a larger reinforcement ratio maintain greater shear resistance after the formation of critical crack. Specimens V26.01, V26.03, and V26.04 failed in tension shear. A typical case of this failure mode was also observed in very deep beams with low flexural reinforcement ratio, where concrete crushing occurred at the top of the diagonal compression strut. Notably, beam V26.02, with the lowest longitudinal reinforcement ratio 2.6% and largest concrete cover of 74 mm, failed in diagonal tension.

VGU
Vietnamese-German University

Kani's comb model provides a useful first interpretation of the behavior of four testing beams. Both web-shear and flexural-shear cracks in the four beams tend to propagate more or less in the theoretical central arc-like pattern, which is clearly shown in beam V26.04 (Figure 3.22). The "comb teeth" are separated by flexural cracks, subjected to bonding force between concrete and steel and act as individual cantilever beams (Figure 2.11). As load increases, these cantilever beams are free to bend, with largest moment occurring at the fixed end in compressive zone. This model was later refined, as free bending is restrained by friction due to interface roughness and dowel action. Beams are failed when bending moment at fixed end reaches its maximum value or concrete exceeds its compressive strength. However, according to Kani's valley, beams without stirrups with a shear span-to-depth ratio a/d exceeding 2.5

are generally governed by beam action and tend to fail either in diagonal tension or flexure, since members within this range are considered as slender. Tension shear failure is generally recorded in deep beams. Although all four tested beams have the same shear span-to-depth ratio of a/d = 2.86, they mostly exhibit tension shear failure due to variations in longitudinal reinforcement. Furthermore, because the performance of various shear transfer mechanisms and crack patterns remain unclear, this explanation may not be entirely applicable to the behavior observed in four experiment beams.

The CSCT proves to be more appropriate in describing fully the behavior of shear test through critical shear crack development types and relevant shear transfer mechanisms. The shear test shows notable similarities to the experiment of Cavagnis et al. [49]. It should be notice that two experimental programs differ in scope, test setup, and specimen geometry, thus the study by Cavagnis et al. is used as a reference for evaluating the contributions of various mechanisms in four testing beams through crack classifications and critical shear crack development types. The behavior of beams V26.03 and V26.04 could be linked with critical crack development Type 1 "Potential critical shear crack allowing direct strut action to develop" (Figure 3.25 & 3.26) [49]. As previously described, the load-deformation of these two specimens experience a slight load drop before continues increasing. It could be explained that larger flexural reinforcement amount narrows and limits the flexural cracking zone, in which diagonal compressive strut can form within uncracked compressive zone above crack's tip, after the main shear crack has formed. The beam is then subjected to increasing load and fail at about 20% in V26.03 and 40% in V26.04 higher than at load drop (Figure 3.18). The current main shear crack becomes potentially critical, depending on further development. In case of V26.03, the secondary diagonal crack directly from loading point to support occurs after concrete crushing at loading point, while the main shear crack in V26.04 becomes critical leading to failure. In these two specimens, dowelling cracks D initiating from primary flexural crack split along the tensile reinforcement, while there is few aggregate-interlock cracks E observed (Figure 3.16 & 3.17). In this case, uncracked compressive zone in beams V26.03 and V26.04 contribute a dominant role to form compression chord after reaching critical stage. Aggregate interlock is recorded to be minor, since there is no or very small sliding of cracks observed. Dowel action becomes more pronounced at nearly and after failure of beams.

The presence of aggregate interlock could be clearly observed in beam V26.02, belonging to Type 3: "Failures driven by loss of aggregate interlock due to development of interlock crack"

VGU Vietnamese-German University

(Figure 3.24) [49]. Interlock cracks are described as being developed to both sides from flexural crack transferring shear through interface leading to sudden failure. In the Cavagnis' test, this crack is formed at about 99% of maximum load and failure is caused by the penetration of critical shear crack into compressive zone. Beam V26.02 reflects similarly to this type that these aggregate-interlock cracks rapidly penetrate to both sides and cause immediate failure by splitting a beam in half. Similar to beams V26.03 and V26.04, dowel action appears at later stage. The behavior V26.01 could be described practically by development Type 2, stable propagation of critical shear crack into compressive zone (Figure 3.23). In this case, critical shear crack developed from flexural crack propagate with a stable manner at flatter angle from 5 to 30 degrees. Small crack E also branch from this critical crack, following by crack D along tensile reinforcement at nearly the end of load procedure (Figure 3.14). This indicates that both aggregate interlock and dowel action are active in this beam. Notably, for two beams V26.02 and V26.04 with thicker concrete cover, flexural cracks beneath reinforcement already opens widely before failure, recording remarkable dowel action at this stage. Recent experimental studies have employed more advanced techniques such as digital image correlation DIC, acoustic emission AE or 3D scanning to investigate crack kinematics and quantify more explicitly the contribution of various mechanisms. The evaluation of shear transfer mechanisms in this study is mainly based on the observation of crack development, these assessments are only approximate.

VGU
Vietnamese-German University

Overall, the influence of longitudinal reinforcement distribution on the actual behavior of four testing beams could be derived through critical shear crack. Previous studies have primarily focused on two key aspects: location and kinematics of critical shear crack. The crack kinematics are generally characterized by crack opening and rotation, as well as by the propagation and possible redirection of cracks as they approach the loading point. Accordingly, the location of the critical shear crack governs the contribution of uncracked concrete compression zone, whereas the kinematics determine the effectiveness of aggregate interlock, dowel action, and concrete residual tensile strength. This study highlights two important effects of longitudinal reinforcement detailing on the development of the critical shear crack. First, greater concrete cover thickness influences the location of the critical shear crack, causing it to develop farther from the loading point due to wider crack spacing. The influence of concrete cover appears to depend on flexural reinforcement ratio and resulting degree of crack control. Second, higher flexural reinforcement ratio restrains the propagation of flexural cracks into

diagonal cracks, diagonal shear cracks become more dominant within the web instead, and effectively limits the opening of the critical shear crack. Both effects are clearly demonstrated by comparing the experimental response of beam V26.02 with those of the other three specimens. The development of arch action after critical stage in two slender beams V26.03 and V26.04 is attributed to their high longitudinal reinforcement ratio of 3.8%. This substantial reinforcement amount controls the development of shear cracks within the area near loading point and limits their penetration into theoretical diagonal compressive strut. Besides, higher longitudinal reinforcement ratio enhances the contribution of uncracked concrete compression zone, thereby facilitating the formation and maintaining of this compression strut. In contrast, lower reinforcement ratio 2.6% in beam V26.02 displayed in thicker concrete cover 74 mm allows a flexural crack near support to become critical. Accordingly, the crack propagates at a steeper inclination angle and rapidly extends across the entire cross-section, resulting in sudden failure afterward. By comparison, beam V26.03 with reinforcement ratio of 3.8% in smaller concrete cover of 24 mm, becomes difficult to predict the formation of critical shear crack and behavior of beam.

VGU
Vietnamese-German University

5.2.2 Evaluation of shear design models

All five calculation methods discussed in this thesis represent three distinct perspectives on evaluating shear resistance of reinforced concrete beams without stirrups. The CSCT explains shear resistance through the development critical shear crack. Both size and strain effects are naturally reflected in the opening of crack: increasing effective depth and longitudinal strain result in wider cracks. Rather than defining a governing mechanism, CSCT relates the efficiency of compressive zone and other shear transfer action is controlled to the location and geometry of crack. The closed-form equation in EN 1992-1-1-23 mirrors the basic idea of CSCT considering interface roughness, steel strain and effective depth. The SMCFT focuses on the capacity of transferring tensile stress of cracked concrete and inclination chord of concrete compression field. The Canadian standard reflects this idea in members without stirrups in simplified manner by factor β, which accounts for both strain and size effect. Strain effect is derived through average strain at mid-depth of beam, whereas size effect is represented by crack spacing parameter. Notably, experimental findings from MCFT further indicate that the size effect is governed by spacing between longitudinal reinforcement layers, which is also introduced in CSA A23.3:19. The *m*SM model follows the hypothesis that shear failure

in reinforced concrete beams without stirrups is governed by induced crack near neutral-axis level of cracked section. It describes shear resistance as a combination of the shear stresses transferred across crack (including residual tensile stress, aggregate interlock, and minor dowel action) and concrete compression zone above neutral axis. Accordingly, shear resistance is governed by both compression and tension zone, which are characterized by the relative depth of compressive zone, fracture energy, and crack width.

When compared with experiment results, changes in longitudinal reinforcement primarily affect the reference longitudinal strain and depth of compressive zone predicted by these models. Except for iterative *m*SM, strain effect in the remaining methods is evaluated as a function of longitudinal reinforcement ratio ρ_l and the elastic modulus of steel E_s. In the same context of CSCT and SMCFT, increasing longitudinal reinforcement ratio maintains minimal longitudinal strain within beams, hence crack opening is better controlled allowing shear stresses to be transferred continuously across crack's interface. Besides, the *m*SM reflects the control of crack width in tensile zone by mean strain difference between concrete and steel accumulated over crack spacing. The second important consequence of limiting reinforcement strain is the downward shift of neutral axis (as could be seen in Figure 4.5 on INCA2 software), which significantly increases the effectiveness of concrete compressive zone. This zone is clearly demonstrated through the contribution to shear capacity in *m*SM formulation, while it is experimentally calibrated in CSCT closed-form equation through a variable coefficient that depends on relevant span-to-depth ratio.

VGU
Vietnamese-German University

In simplified methods, size effect is generally presented through span-to-depth ratio a/d or crack spacing s_{cr}. In new EC2 formulation, the slenderness of structure is limited to 4. When lower than this limit, the use of effective depth d in this equation leads to more conservative prediction of shear strength. In such cases, the resistance may be adjusted by mechanical shear span a_v. Both CSA approaches account for size effect through crack spacing parameter s_z equal to effective depth d or spacing between longitudinal reinforcement layers. In simplified *m*SM, this effect is represented by ratio d_0/d considering the influence of concrete brittleness, member slenderness, and fracture energy. EN 1992-1-1:2023, simplified *m*SM, and iterative SMCFT generally predict higher resistance for the beams with higher longitudinal reinforcement ratio ρ_l. In particular, predicted shear capacities of each pair V26.01/V26.02 and V26.03/V26.04 are equal. Nevertheless, experimental shear capacity differs between individual beams due to the distribution longitudinal reinforcement.

Size effect is reflected differently in *m*SM iterative through crack spacing s_{cr}, which is considered through the distance from neutral axis to tensile reinforcement d - x and height of concrete tensile zone $h_{ct,ef}$. Thus, shear capacities predicted for beams with distinctive longitudinal reinforcement distribution by *m*SM may be not identical. In this case, iterative *m*SM yields the same shear resistance for beams V26.03 and V26.04. This can be attributed to relatively poor aggregate quality and low concrete strength, as observed through broken aggregate particles on the failure surfaces of splitting test specimen (Figure 3.7), resulting in lower fracture energy G_F. As shown in Equation 4.10, the limit crack width $w_c = 5.14 \cdot \frac{G_F}{f_{ct,ef}}$ in *m*SM decreases proportional to smaller G_F. Therefore, higher longitudinal reinforcement ratio although limits the width of critical shear crack in tension zone, there is no significant change in shear resistance.

5.2.3 Recommendation

The atypical distribution of reinforcing steel bars in the shear test has initially illustrated the influence of longitudinal reinforcement distribution on shear strength, post-crack behavior, and failure mode in beams without shear reinforcement. However, the observed tendencies are evidenced limitedly to small scale of 4 experiment beams and parameters related to materials are also not fully experimentally defined. Further tests are recommended to investigate within larger number of specimens the mutual influence between thickness of concrete cover and longitudinal reinforcement arrangements (layout, ratio...) on shear capacity of beams without stirrups, preferably employing various geometrical and material properties as well as extending to different testing setup such as cantilever or continuous beams. Besides, the influence of aggregate quality and concrete strength should be taken into consideration in parallel, since it also affects crack surface roughness and thus affecting the ability of shear transfer through crack.

Although considered models generally yield at more less accurate mean results, their abilities to distinguish the response of individual beams with different longitudinal reinforcement arrangements remain limited. It is necessary to validate experimentally the predictability of various models in shear capacity for beams with longitudinal reinforcement ratio exceeding 3.8%, for which EN 1992-1-1:2023 and iterative *m*SM offer overestimated shear resistance for higher reinforcement beams in the present tests. This observation is preliminary due to limited two specimens. Future investigations should cover wide variety of reinforcement distribution,

geometrical and material properties to determine whether the observed bias is systematic. The resulting data could be used to assess whether the existing formulations adequately reflect other effects of reinforcement distribution and concrete cover or need to be integrated more explicitly into shear strength models.

VGU
Vietnamese-German University

6. Conclusion

In conclusion, this bachelor thesis provides experimental investigation of the influence of longitudinal reinforcement distribution on shear capacity of slender members without shear reinforcement. Four beams with two different longitudinal reinforcement ratio 2.6% and 3.8% corresponding with two concrete cover thickness 24 mm and 74 mm, were tested. Five calculation methods are evaluated using both 4 testing specimens and database of 784 beams. Based on findings, this thesis answers two research questions mentioned earlier:

- The critical shear resistances of four experiment beams remains within relatively narrow range of 57.5 - 62.5 kN, while the ultimate shear resistances varied more considerably from 59.5 to 87.5 kN. This indicates that longitudinal reinforcement distribution exerts a minor influence on the initiation of critical shear state but significantly affects the post-cracking behavior and strengthens shear resistance after the first load drop.
- The increase of longitudinal reinforcement ratio from 2.6% to 3.8% by arranging two to three steel bars per layer, improves crack control and mitigates the propagation and opening of critical shear crack. The more highly reinforced beams maintain greater resistance after critical cracking and diagonal compressive strut or arch action gains more pronounced contribution in this stage. Furthermore, the experimental results also illustrates the effect of longitudinal reinforcement interacted with bottom concrete cover thickness, thus, both of these parameters should be considered together.
- For four experiment beams, the iterative SMCFT offers the closest overall prediction of shear capacity, with mean value μ_θ of 1.01 and δ_θ of 0.04. The EN 1992-1-1:2023 shows close agreement for the beams with $\rho_l = 2.6\%$ but overestimates the shear resistance of two highly-reinforced beams with $\rho_l = 3.8\%$ by approximately 9 - 11%. The CSA A23.3:2019 yields consistently conservative predictions and do not distinguish between different reinforcement arrangements of test specimens.
- Among 784 beams, both approaches of *m*SM provide the most favorable overall compromise between accuracy and result dispersion, with mean value μ_θ around 1.03 to 1.04 and δ_θ of 0.17 to 0.18. The new Eurocode 2 standard also attains satisfactory and comparatively stable predictions, with μ_θ of 1.09 and δ_θ of 0.18. The iterative SMCFT

Vietnamese-German University

remains reasonably accurate but greater scatter, in contrast, CSA A23.3:2019 illustrates the lowest accuracy as well as higher inconsistency in predicting shear strength.

- Among six investigated parameters, the experimental-to-calculated shear strength ratio of CSA A23.3:2019 increases in proportion to longitudinal reinforcement ratio ρ_l, yielding more conservative prediction, whereas other four methods remain relatively stable. The experimental-to-calculated ratio generally decreases with increasing effective depth d, span-to-depth ratio a/d, and concrete compressive strength f_c, which is clearly observed for CSA A23.3:2019. In contrast, there is no clear separate trend could be seen for longitudinal bar diameter ϕ_s or maximum aggregate size $a_{g,max}$. Consequently, d, a/d, and f_c show clearer variations in model performance than the effect of ϕ_s and $a_{g,max}$.
- By predicting shear strength of 784 beams, the iterative *m*SM indicates the separated contributions of tensile and compression zone to shear resistance, with calculated average V_{ct}/V_c and V_{cc}/V_c ratios of approximately 53% and 45%, respectively. The effectiveness of compressive zone tends to be more dominant with increasing longitudinal reinforcement ratio ρ_l, effective depth d, shear span-to-depth ratio a/d, and concrete compressive strength f_c, whereas bar diameter ϕ_s and maximum aggregate size $a_{g,max}$ show no clear tendency.

Vietnamese-German University

Bibliography

[1] G. N. J. Kani. "The Riddle of Shear Failure and its Solution". In: (Jan. 4, 1964). URL: https://www.concrete.org/publications/internationalconcreteabstractsportal.aspx?m=details&ID=7791 (visited on 04/03/2026).

[2] Davor Grandić, Paulo Sculac, and Ivana Stimac-Grandic. "Shear resistance of reinforced concrete beams in dependence on concrete strength in compressive struts". In: *Tehnicki Vjesnik* 22 (Aug. 1, 2015), pp. 925–934. DOI: 10.17559/TV-20140708125658.

[3] Jorg Schlaich, Schafer Kurt, and Jennewein Mattias. *Toward a Consistent Design of Structural Concrete*. Sept. 1987. DOI: https://doi.org/10.15554/pcij.05011987.74.150. (Visited on 04/04/2026).

[4] Aurelio Muttoni. *Behavior of Beams and Punching in Slabs without Shear Reinforcement*. ResearchGate. Jan. 1991. URL: https://www.researchgate.net/publication/37451974_Behavior_of_Beams_and_Punching_in_Slabs_without_Shear_Reinforcement (visited on 04/05/2026).

[5] Frank J. Vecchio and Michael P. Collins. "The Modified Compression-Field Theory for Reinforced Concrete Elements Subjected to Shear". In: (Jan. 3, 1986). URL: https://www.concrete.org/publications/internationalconcreteabstractsportal.aspx?m=details&ID=10416 (visited on 04/26/2026).

[6] *Eurocode 2: Design of concrete structures—Part 1-1: General rules and rules for buildings, bridges and civil engineering structures; English version EN 1992-1-1:2023; English translation of DIN EN 1992-1-1:2025-09*. Berlin, Germany, Sept. 2025.

[7] S Unnikrishna Pillai and Devdas Menon. *Reinforced Concrete Design - 3rd edition*. 2005. (Visited on 06/10/2026).

[8] M. Nadim Hassoun and Akthem Al-Manaseer. *Structural Concrete: Theory and Design*. Google-Books-ID: MSlHAAAAQBAJ. John Wiley & Sons, June 14, 2012. 1034 pp. ISBN: 978-1-118-20560-0.

[9] Vu Hong Nghiep. "Shear design of straight and haunched concrete beams without stirrups". PhD thesis. Shaker, 2011. ISBN: 978-3-8440-0844-9. DOI: 10.15480/882.1050. URL: http://tubdok.tub.tuhh.de/handle/11420/1052 (visited on 06/19/2026).

[10] S. Unnikrishna Pillai and Menon Devadas. *Reinforced concrete design*. 2nd ed. OCLC: 63502775. New Delhi: Tata McGraw Hill, 2003. ISBN: 978-0-07-049504-3.

VGU Vietnamese-German University

[11] Ataur Rahman and Tamon Ueda. “Shear Resisting Mechanism and Shear Strength Equation for Sandwich Beams”. In: *Journal of Materials Science Research* 7 (Jan. 31, 2018), p. 1. DOI: 10.5539/jmsr.v7n2p1.

[12] ASCE-ACI Committee 445 on Shear {and} Torsion. “Recent Approaches to Shear Design of Structural Concrete”. In: *Journal of Structural Engineering* 124.12 (Dec. 1, 1998), pp. 1375–1417. DOI: 10.1061/(ASCE)0733-9445(1998)124:12(1375). URL: https://ascelibrary.org/doi/10.1061/%28ASCE%290733-9445%281998%29124%3A12%281375%29 (visited on 04/16/2026).

[13] M. A. Mansur, K. C. G. Ong, and P. Paramasivam. “Shear Strength of Fibrous Concrete Beams Without Stirrups”. In: *Journal of Structural Engineering* 112.9 (Sept. 1, 1986), pp. 2066–2079. DOI: 10.1061/(ASCE)0733-9445(1986)112:9(2066). (Visited on 04/21/2026).

[14] T. Y. Lim, P. Paramasivam, and S. L. Lee. “Shear and moment capacity of reinforced steel-fibre-concrete beams”. In: *Magazine of Concrete Research* 39.140 (Sept. 1, 1987), pp. 148–160. ISSN: 0024-9831. DOI: 10.1680/macr.1987.39.140.148. (Visited on 04/21/2026).

[15] D. H. Monetti et al. “Long-term behavior of cracked fiber reinforced concrete under service conditions”. In: *Construction and Building Materials* 196 (Jan. 30, 2019), pp. 649–658. ISSN: 0950-0618. DOI: 10.1016/j.conbuildmat.2018.10.230. (Visited on 04/21/2026).

[16] Aurelio Muttoni and Miguel Fernández Ruiz. “Shear Strength of Members without Transverse Reinforcement as Function of Critical Shear Crack Width”. In: *ACI Structural Journal* 105 (Mar. 1, 2008).

[17] Christian Albrecht and Jürgen Schnell. “Zum Einfluss einzelner Traganteile auf die Querkrafttragfähigkeit von Stahlbetondecken mit integrierten Hohlräumen”. In: *Beton- und Stahlbetonbau* 112 (Mar. 1, 2017), pp. 133–143. DOI: 10.1002/best.201600054.

[18] R. C. Fenwick and Thomas Paulay. “Mechanisms of Shear Resistance of Concrete Beams”. In: *Journal of the Structural Division* 94.10 (Oct. 1, 1968), pp. 2325–2350. DOI: 10.1061/JSDEAG.0002092. (Visited on 04/20/2026).

[19] Adane Edom. “Mechanics of dowel action causing bond deterioration and splitting failure under cyclic service shear load”. In: (Sept. 15, 2023). URL: https://ynu.repo.nii.ac.jp/records/2000176 (visited on 06/05/2026).

[20] Dhanushka K. Palipana et al. “Framework for Quantification of Shear-Transfer Mechanisms from Deep Beam Experiments”. In: (). URL: https://www.concrete.org/publications/internationalconcreteabstractsportal.aspx?m=details&id=51734485 (visited on 04/21/2026).

VGU Vietnamese-German University

[21] Kim Jin-Keun and Yon-Dong. “Prediction of Shear Strength of Reinforced Concrete Beams without Web Reinforcement”. In: *ACI Materials Journal* 93.3 (1996). ISSN: 0889-325X. DOI: 10.14359/9805. URL: http://www.concrete.org/Publications/ACIMaterialsJournal/ACIJournalSearch.aspx?m=details&ID=9805 (visited on 04/21/2026).

[22] B. Martín-Pérez and S. J. Pantazopoulou. “Effect of bond, aggregate interlock and dowel action on the shear strength degradation of reinforced concrete”. In: *Engineering Structures* 23.2 (Feb. 1, 2001), pp. 214–227. ISSN: 0141-0296. DOI: 10.1016/S0141-0296(00)00004-3. URL: https://www.sciencedirect.com/science/article/pii/S0141029600000043 (visited on 04/21/2026).

[23] Qi Li et al. “Shear Capacity Calculation Methods for Reinforced Concrete Structure”. In: *Advances in Civil Engineering* 2025.1 (Jan. 1, 2025), p. 5088121. ISSN: 1687-8094. DOI: 10.1155/adce/5088121. (Visited on 04/21/2026).

[24] R. Taylor and R. S. Brewer. “The effect of the type of aggregate on the diagonal cracking of reinforced concrete beams”. In: *Magazine of Concrete Research* 15.44 (July 1, 1963), pp. 87–92. ISSN: 0024-9831. DOI: 10.1680/macr.1963.15.44.87. URL: https://doi.org/10.1680/macr.1963.15.44.87 (visited on 06/09/2026).

[25] H. P. J. Taylor. “Investigation of the Forces Carried Across Cracks in Reinforced Concrete Beams in Shear by Interlock of Aggregate”. In: (Nov. 1970). Number: TR 42.447 Tech. Rpt. URL: https://trid.trb.org/view/21744 (visited on 06/07/2026).

[26] Belkis Filian, Eva Lantsoght, and Yuguang Yang. *Shear Capacity of Steel Fibre Reinforced Concrete Beams*. June 5, 2019.

[27] James K. Wight and James G. MacGregor. *Reinforced Concrete: Mechanics and Design*. Google-Books-ID: xekuAAAAQBAJ. Pearson Education, Nov. 21, 2011. 1176 pp. ISBN: 978-0-13-300219-5.

[28] Houquan Lin et al. “Characterizing Splitting Failure of Concrete Influenced by Material Heterogeneity Based on Digital Image Processing Techniques”. In: *Buildings* 14.6 (June 2024), p. 1856. ISSN: 2075-5309. DOI: 10.3390/buildings14061856. URL: https://www.mdpi.com/2075-5309/14/6/1856 (visited on 07/25/2026).

[29] Ivan Rogovskii et al. “Technology of Producing Reinforced Concrete Columns of Circular Cross-Sectional and Investigation of Their Strain-Stress State at Transverse-Longitudinal Bending”. In: *Acta Polytechnica* 59 (Nov. 1, 2019), pp. 510–517. DOI: 10.14311/AP.2019.59.0510.

[30] Bamo Hasan and Jalal A Saeed. “Effect of Concrete Strength on Shear Capacity of Reinforced High-Strength Concrete Continuous Beams without Web Reinforcements”. In: *Advances in Civil Engineering* 2023 (May 4, 2023), pp. 1–10. DOI: 10.1155/2023/8784575.

[31] K. G. Moody et al. “Shear Strength of Reinforced Concrete Beams Part 2-Tests of Restrained Beams Without Web Reinforcement”. In: (). URL: https://www.concrete.org/publications/internationalconcreteabstractsportal.aspx?m=details&id=11686 (visited on 04/22/2026).

[32] Kani Gaspar. *Basic Facts Concerning Shear Failure*. SciSpace - Paper. Issue: 6 Pages: 675-692 Volume: 63. June 1, 1966. DOI: 10.14359/7644. URL: https://scispace.com/papers/basic-facts-concerning-shear-failure-21v76k0r68 (visited on 04/22/2026).

[33] Bogdan Andrzej Podgorniak-Stanik. “The influence of concrete strength, distribution of longitudinal reinforcement, amount of transverse reinforcement and member size on shear strength of reinforced concrete members”. In: (1998). URL: http://www.collectionscanada.ca/obj/s4/f2/dsk2/tape17/PQDD_0006/MQ34123.pdf (visited on 04/23/2026).

[34] Kani Gaspar. *How Safe are Our Large Reinforced Concrete Beams?* Jan. 3, 1967. URL: https://www.concrete.org/publications/internationalconcreteabstractsportal.aspx?m=details&id=7549 (visited on 04/23/2026).

[35] T. Shioya et al. “Shear Strength of Large Reinforced Concrete Beams”. In: (Jan. 1, 1990). URL: https://www.concrete.org/publications/internationalconcreteabstractsportal.aspx?m=details&id=2978 (visited on 04/23/2026).

[36] Michael P. Collins and Daniel Kuchma. “How Safe Are Our Large, Lightly Reinforced Concrete Beams, Slabs, and Footings?” In: (July 1, 1999). URL: https://www.concrete.org/publications/internationalconcreteabstractsportal.aspx?m=details&ID=684 (visited on 04/23/2026).

[37] Kim Jin-Keun and Park Yon-Dong. “Shear strength of reinforced high strength concrete beam without web reinforcement”. In: *Magazine of Concrete Research* 46.166 (Mar. 1, 1994), pp. 7–16. ISSN: 0024-9831. DOI: 10.1680/macr.1994.46.166.7. URL: https://dx.doi.org/10.1680/macr.1994.46.166.7 (visited on 04/23/2026).

[38] Z. P. Bazant and M. T. Kazemi. “Size Effect on Diagonal Shear Failure of Beams Without Stirrups”. In: *ACI Structural Journal* 88.3 (June 1991). ISSN: 0889-3241. URL: https://trid.trb.org/View/358154 (visited on 04/23/2026).

[39] Ngoc Linh Tran. “A mechanical model for the shear capacity of slender reinforced concrete members without shear reinforcement”. In: *Engineering Structures* 219 (June 27, 2020). DOI: 10.1016/j.engstruct.2020.110803.

[40] J. Walraven and H. Reinhardt. “Theory and Experiments on the Mechanical Behaviour of Cracks in Plain and Reinforced Concrete Subjected to Shear Loading”. In: 1981. URL: https://www.semanticscholar.org/paper/Theory-and-Experiments-on-

Vietnamese-German University

the-Mechanical-Behaviour-Walraven-Reinhardt/3456d769d4188a64ab6c1494c54408a48db648f7 (visited on 04/23/2026).

[41] Ashraf H. Elzanaty, Arthur H. Nilson, and Floyd O. Slate. "Shear Capacity of Reinforced Concrete Beams Using High-Strength Concrete". In: (Jan. 3, 1986). URL: https://www.concrete.org/publications/internationalconcreteabstractsportal.aspx?m=details&id=10432 (visited on 04/23/2026).

[42] H. P. J. Taylor. "Shear Strength of Large Beam". In: *Journal of the Structural Division* 98 (ST11 Nov. 1972). Number: Proc Paper 9329. URL: https://trid.trb.org/View/12458 (visited on 06/28/2026).

[43] F. Leondardt. "Reducing the shear reinforcement in reinforced concrete beams and slabs". In: *Magazine of Concrete Research* 17.53 (Dec. 1, 1965), pp. 187–198. ISSN: 0024-9831. DOI: 10.1680/macr.1965.17.53.187. URL: https://dx.doi.org/10.1680/macr.1965.17.53.187 (visited on 04/27/2026).

[44] Mohamed Zakaria et al. "Experimental Investigation on Shear Cracking Behavior in Reinforced Concrete Beams with Shear Reinforcement". In: *Journal of Advanced Concrete Technology* 7 (Feb. 26, 2009), pp. 79–96. DOI: 10.3151/jact.7.79.

[45] Dino Angelakos. "The influence of concrete strength and longitudinal reinforcement ratio on the shear strength of large-size reinforced concrete beams with, and without, transverse reinforcement". In: (1999). URL: http://www.collectionscanada.ca/obj/s4/f2/dsk1/tape8/PQDD_0003/MQ45934.pdf (visited on 06/07/2026).

[46] Monika Kaszubska, Renata Kotynia, and Joaquim A. O. Barros. "Influence of Longitudinal GFRP Reinforcement Ratio on Shear Capacity of Concrete Beams without Stirrups". In: *Procedia Engineering*. International Conference on Analytical Models and New Concepts in Concrete and Masonry Structures 193 (Jan. 1, 2017), pp. 361–368. ISSN: 1877-7058. DOI: 10.1016/j.proeng.2017.06.225. URL: https://www.sciencedirect.com/science/article/pii/S1877705817327893 (visited on 06/10/2026).

[47] Aurelio Muttoni. "Punching Shear, Draft Code Proposal". In: (1988). URL: https://infoscience.epfl.ch/handle/20.500.14299/63981 (visited on 04/26/2026).

[48] Aurelio Muttoni and Bruno Thürlimann. *Shear Tests on Beams and Slabs Without Shear Reinforcement*. Unpublished technical report. Zürich, Switzerland: Institut für Baustatik und Konstruktion, ETH Zürich, 1986.

[49] Francesco Cavagnis, Miguel Fernández Ruiz, and Aurelio Muttoni. "Shear failures in reinforced concrete members without transverse reinforcement: An analysis of the critical shear crack development on the basis of test results". In: *Engineering Structures* 103 (Nov. 15, 2015), pp. 157–173. ISSN: 0141-0296. DOI: 10.1016/j.engstruct.2015.09.015. (Visited on 04/04/2026).

Vietnamese-German University

[50] Abdullah Dönmez and Zdeněk P. Bažant. “Critique of critical shear crack theory for fib Model Code articles on shear strength and size effect of reinforced concrete beams”. In: *Structural Concrete* 20.4 (2019), pp. 1451–1463. ISSN: 1751-7648. (Visited on 06/12/2026).

[51] Aurelio Muttoni and Miguel Fernández Ruiz. “From experimental evidence to mechanical modeling and design expressions: The Critical Shear Crack Theory for shear design”. In: *Structural Concrete* 20.4 (2019), pp. 1464–1480. ISSN: 1751-7648. DOI: 10.1002/suco.201900193. (Visited on 06/12/2026).

[52] Aurelio Muttoni, Miguel Fernández Ruiz, and Francesco Cavagnis. *From detailed test observations to mechanical models and simple shear design expressions*. 2018, pp. 17–32. ISBN: 978-2-88394-125-0. DOI: 10.35789/fib.BULL.0085.Ch01.

[53] CEN/TC 250/SC 2. *Background document to FprEN 1992-1-1:2023-04 (Formal-Vote-Draft): Eurocode 2 – Design of concrete structures – Part 1-1: General rules and rules for buildings, bridges and civil engineering structures*. Background document / Committee document CEN/TC 250/SC 2 N2087. Brussels, Belgium: European Committee for Standardization (CEN), Mar. 31, 2023.

[54] Denis Mitchell and Michael P. Collins. “Diagonal Compression Field theory-A Rational Model For Structural Concrete in Pure Torsion”. In: (Jan. 8, 1974). URL: https://www.concrete.org/publications/internationalconcreteabstractsportal.aspx?m=details&id=7103 (visited on 04/30/2026).

VGU
Vietnamese-German University

[55] Herbert Wagner. *Flat sheet metal girders with very thin metal web. Part I : general theories and assumptions*. NTRS Author Affiliations: NTRS Report/Patent Number: NACA-TM-604 NTRS Document ID: 19930094812 NTRS Research Center: Legacy CDMS (CDMS). Feb. 1, 1931. URL: https://ntrs.nasa.gov/citations/19930094812 (visited on 04/30/2026).

[56] Evan Bentz, F.J. Vecchio, and M.P. Collins. “Simplified Modified Compression Field Theory of Calculating Shear Strength of Reinforced Concrete Elements”. In: *ACI Structural Journal* 103 (July 1, 2006), pp. 614–624.

[57] *Design of concrete structures CSA A23.3:19*. 2019.

[58] Fitik Birol, Reineck Karl-Heinz, and Kuchma Daniel A. *DAfStb-Heft 597 - DIN Media*. Aug. 2012. URL: https://www.dinmedia.de/de/fachliteratur/dafstb-heft-597/154635697 (visited on 06/30/2026).

[59] Szymon Cholostiakow et al. “Effect of beam depth on shear behavior of FRP RC beams”. In: *Journal of Composites for Construction* 23 (Nov. 24, 2018). DOI: 10.1061/(ASCE)CC.1943-5614.0000914.

Appendix A. Experimental work

The experimental program was conducted at the civil engineering laboratory of Vietnamese German University (VGU), including four specimens described in Figure 3.1 and Table 3.1. Properties of applied concrete and longitudinal reinforcement in this test are shown in Table 4.3 and 4.4. The following figures further illustrate the main stages of the experimental program, from formwork preparation to final shear tests.

Four beams were cast using prefabricated aluminum formworks, which were assembled and cleaned to remove the excess concrete residue. Before casting, the edges of the formwork were adjusted to ensure the beam straightness and to prevent misalignment. The joints between formwork panels were then sealed by clay to prevent water leakage, and all inner surfaces were sprayed with oil to facilitate the formwork removal after curing.



Formwork *Formwork and cylinder mold*

Figure A.1: *Formwork used in the experiment*

Each 1.5-meter bar was bended both ends ensuring middle distance equals 1.2-meter shear span. Following the designated beam cross-section, in which two steel bars were stacked vertically, special hooks were fabricated to align and fix the reinforcement in the correct position. The reinforcement cages were then placed on concrete spacers, ensuring that the reinforcing bars were centered within the formwork and that the effective depth d, was maintained at 210 mm.



Both end-bended steel bars with hooks *Longitudinal reinforcement placed on concrete spacer*

Figure A.2: *Longitudinal reinforcement details in the experiment*

The casting procedure was conducted using laboratory concrete mixer following sequence: half portion was spread evenly around the mixing bowl, then cement was poured evenly and finally, the rest sand portion. This step ensures that sand and cement were mixed uniformly and prevents the dispersion of cement dust. The finished concrete was poured into prepared molds and evenly spread with a trowel. After casting, all specimens were vibrated to eliminate air pockets and distribute concrete evenly. Additionally, 150-mm diameter cylinder specimens were also prepared to determine the strength and elastic modulus of concrete.

VGU
Vietnamese-German University



Rectangular formwork and cylinder mold *Casting procedure*

Concrete mixing *Longitudinal reinforcement*

Figure A.3: *Procedure of experimental works*

The preparation procedure, test setup, and instrumentation are described in detail in the ”Experimental program” section. Additional figures illustrating the support conditions, load cell, strain gauge locations... are provided as below:

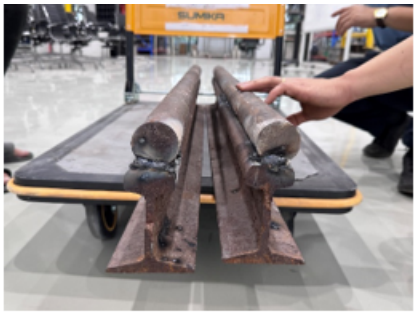

Supports of beams



Load cell



Strain gauge attached on reinforcement



Longitudinal reinforcement on spacer

Figure A.4: *Support and equipment used in the experiment*

VGU
Vietnamese-German University



Steel and rubber pads between beam and support



Full setup of shear test



Setup of shear test



Loading on beams

Figure A.5: *Shear test procedure*

Appendix B. Software application

Response-2000 software

The following appendix presents the Response-2000 analyses conducted for the four experimental beams. The material properties, cross-sectional dimensions, and longitudinal reinforcement details adopted in the software models are consistent with those described in the experimental program and calculation sections of this thesis. Based on these input data, Response-2000 was used to generate the moment–shear $M-V$ interaction diagrams presented below for each specimen. Similarly, Figure B.2 present moment–shear $M-V$ interaction diagrams of three additional beams with reinforcement of different material GFRP and BFRP.

Table B.1: *Material properties used in Response-2000 software*

Property	**Concrete**	**Steel**	**GFRP**	**BFRP**
Elastic modulus [MPa]	28,737	197,000	46,000	42,000
Strength [MPa]	$f_c = 56.52$	$f_y = 350$	$f_y = 758$	$f_y = 1,297$

VGU
Vietnamese-German University

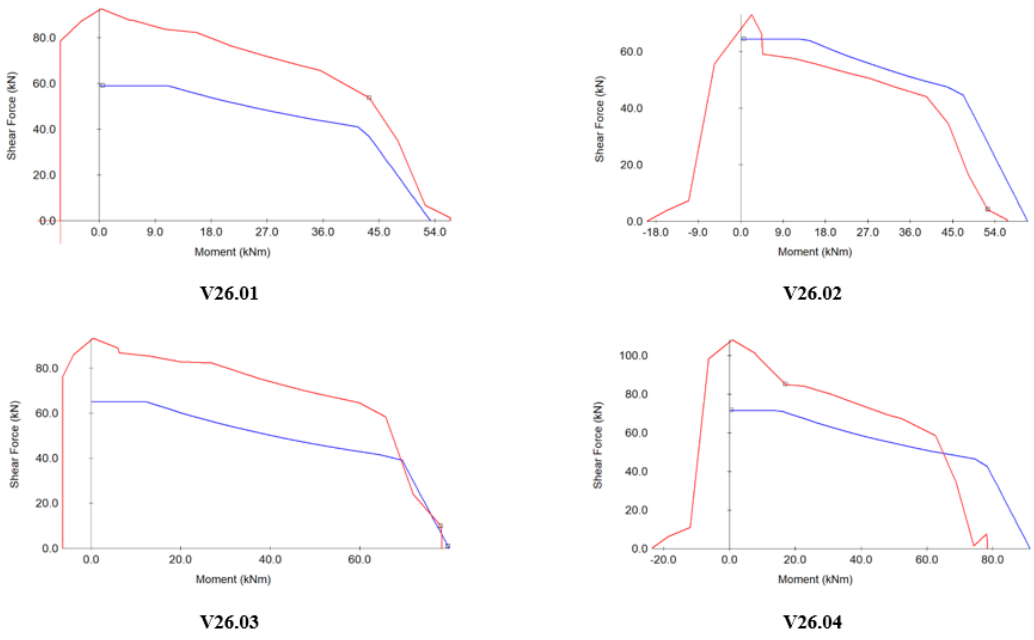

Figure B.1: *Bending moment-shear force interaction diagram of four experiment beams predicted by CSA 2014 (blue line) and MCFT (red line) on Response-2000 software*

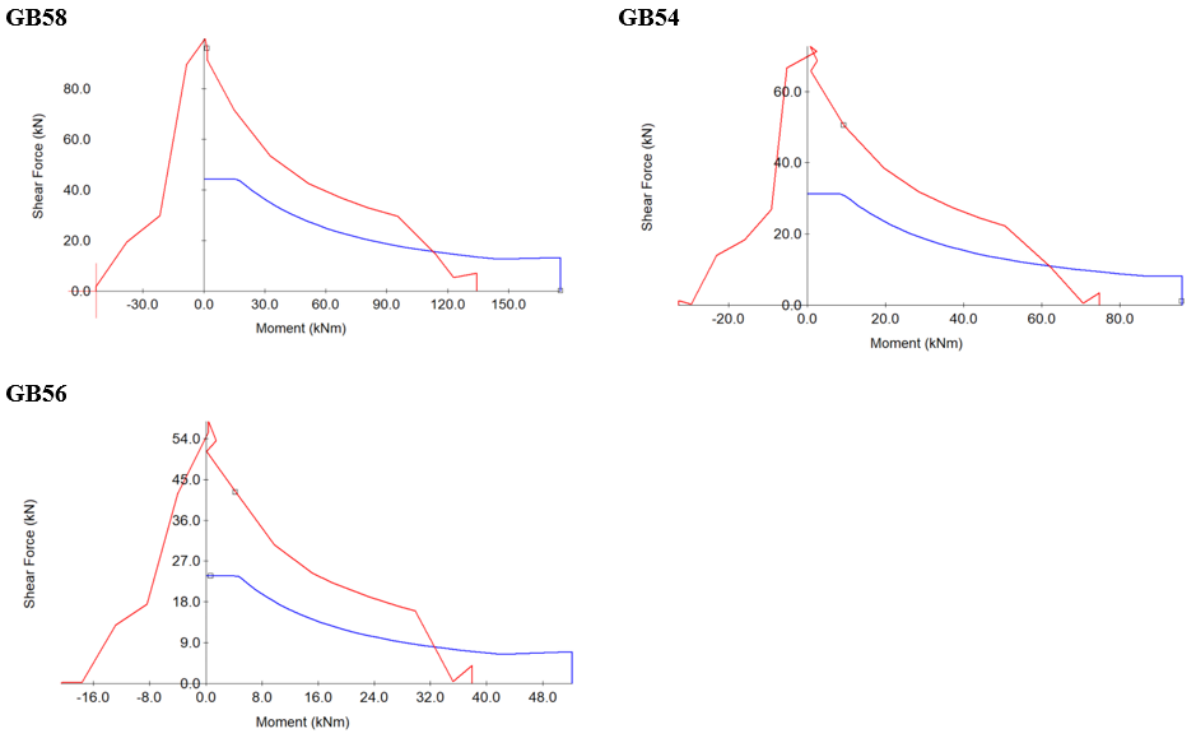

Figure B.2: *Bending moment-shear force interaction diagram of three beams GB58, GB54, and GB56 predicted by CSA 2014 (blue line) and MCFT (red line) on Response-2000 software*

VGU
Vietnamese-German University

INCA2 software

The INCA2 software is applied to evaluate depth of compressive zone and curvature of four experimental beams. The material properties, cross-sectional dimensions, and reinforcement parameters adopted in the numerical models are consistent with those described in the experimental program and calculation sections of this thesis. Based on these input data, the corresponding moment–curvature diagrams for each specimen is conducted by INCA2, as presented below. Besides, every part of a cross-section is calculated their relevant stress by INCA2, as shown in four testing beams cross-section in Figure B.4.

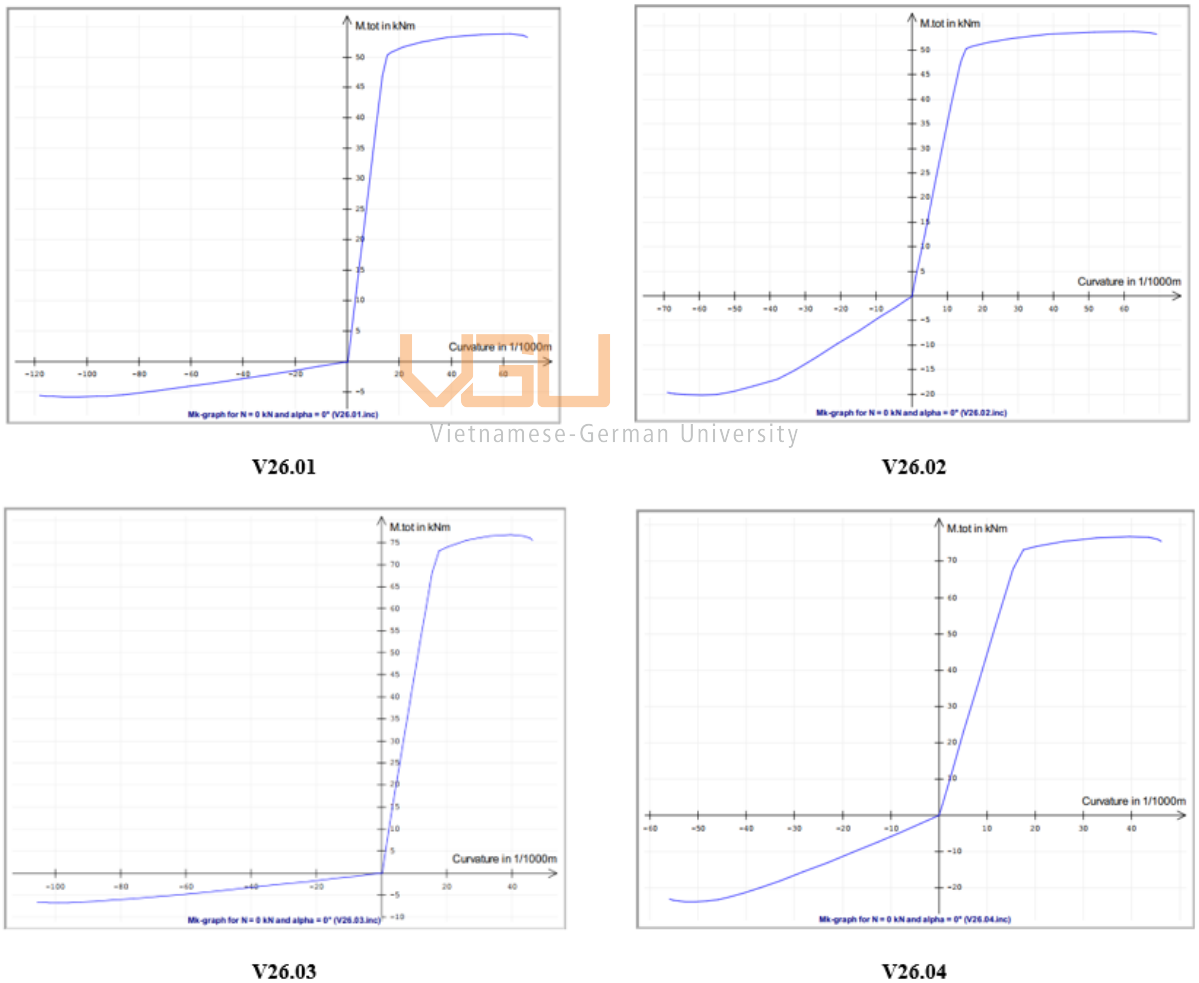

VGU
Vietnamese-German University

Figure B.3: *Moment-curvature diagram of four experiment beams, produced by INCA2 software*

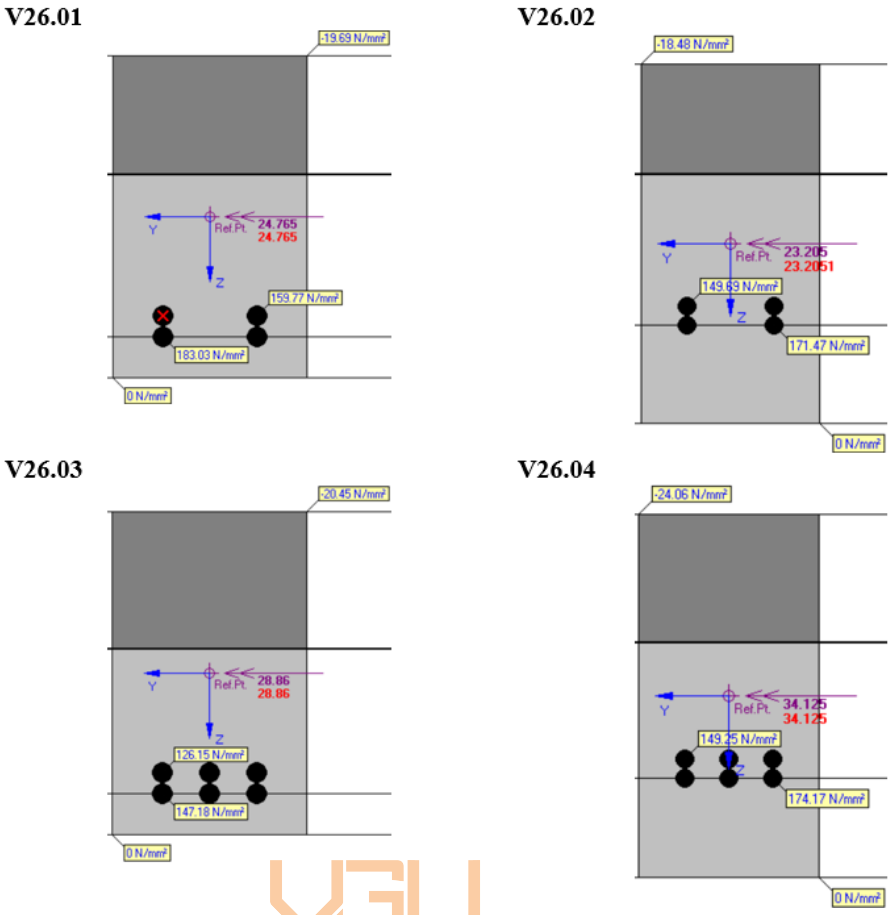

Figure B.4: *Stress of cross-section calculated by INCA2 for four experiment beams*

VGU
Vietnamese-German University

Appendix C. Database

Tables C.1 and C.2 summarize the main information and ranges of parameter in the database. The database comprises 784 specimens, of which 744 were tested under concentrated loading and 40 under distributed loading. It also includes several special groups, such as beams with non-rectangular cross-sections, compression reinforcement, and pre-stressing steel used as longitudinal reinforcement. Six investigated parameters include wide ranges of member size, material strength, reinforcement ratio, shear slenderness, bar diameter, and maximum aggregate size, thereby providing a broad basis for evaluating the applicability of the investigated prediction methods.

Table C.1: *General characteristics of the database*

Information	No. of specimens	Percentage
Beams under concentrated loading	744	94.90%
Beams under distributed loading	40	5.10%
Beams with non-rectangular cross-sections	64	8.20%
Beams with compression reinforcement	95	12.10%
Beams with prestressing steel as longitudinal reinforcement	5	0.60%
Total number of specimens	**784**	**100%**

Vietnamese-German University

Table C.2: *Minimum and maximum values of six investigated parameters in the database*

Parameter	Unit	Minimum	Maximum
Effective depth, d	mm	57.15	3000
Shear span-to-depth ratio, a/d	–	2.4	8.1
Longitudinal reinforcement ratio, ρ_l	%	0.139	6.635
Concrete compressive strength, f_c	MPa	12.25	132.05
Longitudinal reinforcement diameter, ϕ_s	mm	6	40
Maximum aggregate size, $a_{g,max}$	mm	2.5	51

Table C.3 shows the frequency distributions of experimental-to-calculated shear resistance ratios obtained using the five investigated methods. The results are classified into intervals with a step of 0.10. These dataset are represented through diagrams of Figure 5.2.

Table C.3: *Frequency distribution of the experimental-to-calculated shear resistance ratios, adopted in Figure 5.2*

V_{exp}/V_c		**EC2**	**CSA**	**SMCFT***	***m*SM**	***m*SM***
Upper	**Lower**	**Frequency**	**Frequency**	**Frequency**	**Frequency**	**Frequency**
0.45	0.55	0	0	0	1	1
0.55	0.65	2	8	6	4	11
0.65	0.75	12	19	8	23	25
0.75	0.85	36	27	28	65	73
0.85	0.95	118	37	73	140	148
0.95	1.05	202	38	171	197	202
1.05	1.15	182	68	228	172	148
1.15	1.25	107	94	109	109	99
1.25	1.35	67	108	67	40	37
1.35	1.45	24	103	39	18	20
1.45	1.55	12	80	20	10	10
1.55	1.65	8	52	11	2	4
1.65	1.75	4	36	5	1	3
1.75	1.85	6	35	5	0	2
1.85	1.95	0	16	2	1	1
1.95	2.05	0	14	5	0	0
2.05	2.15	2	7	2	1	0
2.15	2.25	1	2	1	0	0
2.25	2.35	0	12	3	0	0
2.35	2.45	0	6	0	0	0
2.45	2.55	1	3	1	0	0
Above 2.55	–	0	19	0	0	0

VGU Vietnamese-German University

In overall, the database covers wide range of geometric and material properties and is dominated by beams tested under concentrated loading. Thus, it offers sufficiently diverse basis for comparing the accuracy, precision, and applicability of the investigated shear resistance models.

Appendix D. Calculation procedure

This Appendix presents the detailed iterative calculation procedures used to determine the shear resistance according to the *m*SM and SMCFT approaches. The calculation sequences include the initial assumptions, evaluation of the relevant strain and crack parameters, and verification of the convergence criterion. Some important parameters obtained in the final iteration are also summarized in Table D.1, D.2 to demonstrate how the final shear resistance is determined and to ensure the transparency the calculations. In general, both iterative methods converge within a limited number of iterations, demonstrating numerical stability and competitive accuracy in predicting shear strength.

Iterative Calculation Methods

*m*SM iterative calculation

VGU
Vietnamese-German University

1. Define f_c and E_c:

$$f_c = 56.52\,\text{MPa}, \qquad E_c = 28,736\,\text{MPa}$$

2. Calculate f_{ct} and G_F:

$$f_{ct} = 0.3\,(f_{ck})^{2/3}, \qquad f_{ck} \leq 50\,\text{MPa}$$

$$G_F = 0.03\,f_c^{0.18} a_g^{0.32}$$

3. Calculate the effective concrete tensile strength:

$$f_{ct,ef} = f_{ct}\frac{1}{1+\nu}, \qquad \nu = 0.2$$

4. Calculate the initial shear force:

$$V_{initial} = \frac{2}{3} f_{ct,ef}\, b\, d$$

5. Calculate the relative depth of compressive zone:

$$k_x = \left(\sqrt{1+\frac{2}{n_e\rho_s}} - 1\right) n_e\rho_s,$$

where

$$n_e = \frac{E_s}{E_c}, \qquad \rho_s = \frac{A_{sl}}{b\,d}$$

6. Calculate the curvature:

$$\kappa = \frac{2M}{E_c\, b\, d^3 k_x^2 \left(1 - \frac{k_x}{3}\right)},$$

where

$$M = V_{initial}(a - d)$$

7. Calculate longitudinal reinforcement strain and stress:

$$\varepsilon_s = \kappa d(1 - k_x), \qquad \sigma_s = \frac{M}{z A_{sl}},$$

where

$$z = d\left(1 - \frac{k_x}{3}\right)$$

8. Calculate the mean strain difference:

$$\varepsilon_{sm} - \varepsilon_{cm} = \frac{1}{E_s}\left[\sigma_s - \beta_t \frac{f_{ct}}{\rho_{s,ef}}(1 + n_e \rho_{s,ef})\right] \geq (1 - \beta_t)\frac{\sigma_s}{E_s},$$

where

$$h_{ct,ef} = 2.5(h - d)$$

VGU Vietnamese-German University

9. Calculate the crack spacing:

$$s_{cr} = \max\left(s_{cr,1}, s_{cr,2}\right),$$

$$s_{cr,1} = 0.75 d(1 - k_x),$$

$$s_{cr,2} = \frac{1.5\phi_s}{4 k_b \rho_{s,ef}},$$

where

$$k_b = 0.97\left[\frac{1 + n_e \rho_{s,ef}}{\rho_{s,ef}^2}\frac{\phi_s}{E_s}\right]^{1/4}\sqrt{\frac{f_c^{3/4}}{f_{ct}}}$$

10. Calculate the crack width:

$$w_{cr} = s_{cr}\left(\varepsilon_{sm} - \varepsilon_{cm}\right)$$

11. Calculate the shear resistance:

$$V_c = \frac{2}{3} f_{ct,ef}\, b\, d\left[k_x + \frac{1.5 G_F}{f_{ct,ef} w_{cr}}(1 - k_x)\right]$$

12. If $V_{initial} \neq V_c$, return to Step 4 and repeat the calculation

Table D.1: *Key parameters obtained from the final iteration of the mSM calculation*

Parameters	**V26.01**	**V26.02**	**V26.03**	**V26.04**
Number of iterations	8	11	6	9
M [kN m]	22.00	21.73	26.56	26.56
k_x	0.44	0.44	0.51	0.51
$\varepsilon_{sm} - \varepsilon_{cm}$	0.000465	0.000172	0.000406	0.000256
s_{cr} [mm]	114.50	178.83	90.58	143.56
w_{cr} [mm]	0.0533	0.0548	0.0368	0.0368
V_c [kN]	56.41	55.71	68.09	68.09

SMCFT iterative calculation

1. Choose $V_{initial}$ randomly
2. Calculate the equivalent crack spacing:

$$s_{ze} = \frac{35 s_z}{15 + a_g}, \qquad s_z = d$$

3. Calculate the longitudinal strain:

$$\varepsilon_x = \frac{M/d_v + V_{initial}}{2 E_s A_s}$$

VGU Vietnamese-German University

4. Calculate the factor β:

$$\beta = \frac{0.4}{1 + 1500\varepsilon_x} \cdot \frac{1300}{1000 + s_{ze}}$$

5. Calculate the shear resistance:

$$V_c = \beta \sqrt{f_c'}\, b_w d_v$$

6. If $V_c \neq V_{initial}$, return to Step 3 and repeat the calculation

Table D.2: *Key parameters obtained from the final iteration of the SMCFT calculation*

Parameters	**V26.01 & V26.02**	**V26.03 & V26.04**
Number of iterations	10	11
M [kN m]	22.11	24.82
ε_x	0.000511	0.000383
β	0.24	0.27
V_c [kN]	56.45	63.63

Overall calculation of four experiment and 784 database beams following five calculation methods

All section properties, material properties, loading and geometry employed in calculating shear strength 788 beams without shear reinforcement following five methods are present through 9 sheets as below.

VGU
Vietnamese-German University

1	2	3	4	5	6	7	8	9	10	11	12	13	14	15	16	17	18	19	20	21	22	23	24	25	26	27	28	29	30	31
				Section properties				Loading and geometry			Longitudinal reinforcement							Concrete								EC2-2025	CSA 23.3.19	mSM	SMCFT_Iterative	mSM_Iterative
Notation	No.	Ref.	Specimen	bw	h	A	A_w	L	a	a/d	$ø_s$	No. bar	d	Es	f_y	A_{st}	ρ_l (%)	$a_{g,min}$	$a_{g,max}$	v	f_c	f_{ct}	Ec	Method	n_e	Vc	Vc	Vc	Vc	Vc
				mm	mm	mm^2	mm^2	mm	mm		mm		mm	MPa	MPa	mm^2		mm	mm		MPa	MPa	MPa		Es/Ec	kN	kN	kN	kN	kN
VGU	1	VGU	V26.01	150	250	37500	31500	1500	600	2.86	16	4	210	197000	350	804.25	0.026	2	16	0.2	56.52	0.00	28737	cyl/sp	6.86	59.57	44.03	52.37	56.45	56.41
VGU	2	VGU	V26.02	150	300	45000	31500	1500	600	2.86	16	4	210	197000	350	804.25	0.026	2	16	0.2	56.52	0.00	28737	cyl/sp	6.86	59.57	44.03	52.37	56.45	55.71
VGU	3	VGU	V26.03	150	250	37500	31500	1500	600	2.86	16	6	210	197000	350	1206.37	0.038	2	16	0.2	56.52	0.00	28737	cyl/sp	6.86	68.19	44.03	62.03	63.35	68.09
VGU	4	VGU	V26.04	150	300	45000	31500	1500	600	2.86	16	6	210	197000	350	1206.37	0.038	2	16	0.2	56.52	0.00	28737	cyl/sp	6.86	68.19	44.03	62.03	63.35	68.09
Adebar_1989_001_ST1	5	Adebar (1989) +	ST1	360	310	111600	100080	1625	813	2.92	20		278	197000	536	1570	0.0157	2	19	0.2	49.88	3.87	28737	cyl/sp	6.86	143.98	126.39	149.69	142.28	162.46
Adebar_1989_002_ST2	6	Adebar;	ST2	360	310	111600	100080	1625	813	2.92	20		278	197000	536	1570	0.0157	2	19	0.2	49.88	3.87	28737	cyl/sp	6.86	143.98	126.39	149.69	142.28	162.46
Adebar_1989_003_ST3	7	Collins (1994) +	ST3	290	310	89900	80620	1625	813	2.92	20		278	197000	536	1570	0.0195	2	19	0.2	46.84	4.05	28737	cyl/sp	6.86	122.07	98.66	134.32	120.37	146.61
Adebar_1989_005_ST16	8	Adebar;	ST16	290	210	60900	51620	1625	813	4.56	20		178	197000	536	1570	0.0304	2	19	0.2	48.93	3.33	28737	cyl/sp	6.86	94.48	70.18	92.38	82.80	84.56
Adebar_1989_007_ST23	9	Collins (1996)	ST23	290	310	89900	80620	1625	813	2.92	15		278	197000	484	800	0.0099	2	19	0.2	55.96	5.04	28737	cyl/sp	6.86	103.46	107.84	110.29	101.25	120.91
AhmadKhaloo_1986_001_A1	10	Ahmad;	A1	127	254	32258	25806.4	2032	813	4.00	25		203	197000	414	1013.41	0.0393	2	12.7	0.2	59.27	0.00	28737	cyl/sp	6.86	49.11	36.36	54.30	47.83	49.63
AhmadKhaloo_1986_002_A2	11	Kahloo	A2	127	254	32258	25806.4	1626	610	3.00	25		203	197000	414	1013.41	0.0393	2	12.7	0.2	59.27	0.00	28737	cyl/sp	6.86	55.12	36.36	61.94	51.88	58.52
AhmadKhaloo_1986_003_A3	12	Poveda (1986)	A3	127	254	32258	25806.4	1504	549	2.70	25		203	197000	414	1013.41	0.0393	2	12.7	0.2	59.27	0.00	28737	cyl/sp	6.86	56.63	36.36	65.52	53.34	63.12
AhmadKhaloo_1986_007_A7	13		A7	127	254	32258	26419.302	2071	832	4.00	16		208	197000	414	467.12	0.0177	2	12.7	0.2	59.27	0.00	28737	cyl/sp	6.86	38.23	37.05	39.36	37.62	38.73
AhmadKhaloo_1986_008_A8	14		A8	127	254	32258	26419.302	1655	624	3.00	16		208	197000	414	467.12	0.0177	2	12.7	0.2	59.27	0.00	28737	cyl/sp	6.86	42.91	37.05	44.61	41.55	45.84
AhmadKhaloo_1986_013_B1	15		B1	127	254	32258	25612.852	2020	807	4.00	29		202	197000	414	1289.45	0.0503	2	12.7	0.2	65.27	0.00	28737	cyl/sp	6.86	53.53	37.93	60.97	52.81	55.04
AhmadKhaloo_1986_014_B2	16		B2	127	254	32258	25612.852	1616	605	3.00	29		202	197000	414	1289.45	0.0503	2	12.7	0.2	65.27	0.00	28737	cyl/sp	6.86	60.08	37.93	69.61	56.99	64.93
AhmadKhaloo_1986_015_B3	17		B3	127	254	32258	25612.852	1495	545	2.70	29		202	197000	414	1289.45	0.0503	2	12.7	0.2	65.27	0.00	28737	cyl/sp	6.86	61.73	37.93	73.65	58.48	70.04
AhmadKhaloo_1986_019_B7	18		B7	127	254	32258	26419.302	2071	832	4.00	16		208	197000	414	593.80	0.0225	2	12.7	0.2	65.27	0.00	28737	cyl/sp	6.86	41.77	38.87	44.55	42.21	44.55
AhmadKhaloo_1986_020_B8	19		B8	127	254	32258	26419.302	1655	624	3.00	16		208	197000	414	593.80	0.0225	2	12.7	0.2	65.27	0.00	28737	cyl/sp	6.86	46.88	38.87	50.47	46.43	52.62
AhmadKhaloo_1986_021_B9	20		B9	127	254	32258	26419.302	1530	562	2.70	16		208	197000	414	593.80	0.0225	2	12.7	0.2	65.27	0.00	28737	cyl/sp	6.86	48.17	38.87	53.25	48.00	56.76
AhmadKhaloo_1986_025_C1	21	Ahmad;	C1	127	254	32258	23387.05	1880	737	4.00	22		184	197000	414	1551.79	0.0664	2	12.7	0.2	62.67	0.00	28737	cyl/sp	6.86	55.11	34.55	63.57	51.79	57.32
AhmadKhaloo_1986_026_C2	22	Kahloo	C2	127	254	32258	23387.05	1511	552	3.00	22		184	197000	414	1551.79	0.0664	2	12.7	0.2	62.67	0.00	28737	cyl/sp	6.86	61.85	34.55	73.02	55.46	68.95
AhmadKhaloo_1986_027_C3	23	Poveda (1986)	C3	127	254	32258	23387.05	1401	497	2.70	22		184	197000	414	1551.79	0.0664	2	12.7	0.2	62.67	0.00	28737	cyl/sp	6.86	63.55	34.55	77.44	56.76	75.03
AhmadKhaloo_1986_031_C7	24		C7	127	254	32258	26225.754	2058	826	4.00	19		207	197000	414	855.07	0.0326	2	12.7	0.2	62.67	0.00	28737	cyl/sp	6.86	46.94	37.87	51.41	46.73	50.05
AhmadKhaloo_1986_032_C8	25		C8	127	254	32258	26225.754	1645	620	3.00	19		207	197000	414	855.07	0.0326	2	12.7	0.2	62.67	0.00	28737	cyl/sp	6.86	52.68	37.87	58.47	50.95	59.04
AhmadKhaloo_1986_033_C9	26		C9	127	254	32258	26225.754	1522	558	2.70	19		207	197000	414	855.07	0.0326	2	12.7	0.2	62.67	0.00	28737	cyl/sp	6.86	54.13	37.87	61.78	52.49	63.64
AhmadPark_1995_007_B7N	27	Ahmad;	B7N	102	204	20808	18156	1774	659	3.70	13		178	197000	413	253.35	0.0140	2	12.7	0.2	41.45	0.00	28737	cyl/sp	6.86	24.24	21.95	23.53	22.21	23.21
AhmadPark_1995_015_B7H	28	Park;	B7H	102	204	20808	18156	1774	659	3.70	13		178	197000	413	253.35	0.0140	2	12.7	0.2	74.18	0.00	28737	cyl/sp	6.86	27.84	29.36	27.61	26.71	28.05
AhmadPark_1995_016_B8H	29	El-Dash (1995)	B8H	102	204	20808	18156	1774	659	3.70	13		178	197000	413	253.35	0.0140	2	12.7	0.2	76.80	0.00	28737	cyl/sp	6.86	27.95	29.88	27.80	27.00	28.31
AlAlusi_1957_002_12	30	Al-Alusi (1957)	12	76.2	146.05	11129.01	9677.4	1041	318	2.50	13		127	197000	366	253.35	0.0262	2	6.35	0.2	23.91	1.89	28737	cyl/sp	6.86	15.06	9.01	19.04	13.51	17.62
AlAlusi_1957_003_11	31		11	76.2	146.05	11129.01	9677.4	1270	432	3.40	13		127	197000	366	253.35	0.0262	2	6.35	0.2	27.19	2.50	28737	cyl/sp	6.86	14.54	9.61	16.63	13.04	14.95
AlAlusi_1957_004_2	32		2	76.2	146.05	11129.01	9677.4	1270	432	3.40	10		127	197000	366	142.51	0.0147	2	6.35	0.2	26.49	2.23	28737	cyl/sp	6.86	11.90	9.48	12.50	10.81	11.60
AlAlusi_1957_005_21	33		21	76.2	151.13	11516.106	9677.4	1270	432	3.40	13		127	197000	366	253.35	0.0262	2	6.35	0.2	27.78	2.49	28737	cyl/sp	6.86	14.64	9.71	16.64	13.14	14.54
AlAlusi_1957_006_15	34		15	76.2	151.13	11516.106	9677.4	1422	508	4.00	13		127	197000	366	253.35	0.0262	2	6.35	0.2	23.98	2.30	28737	cyl/sp	6.86	12.80	9.02	14.83	11.89	12.70
AlAlusi_1957_008_10	35		10	76.2	146.05	11129.01	9677.4	1422	508	4.00	13		127	197000	366	253.35	0.0262	2	6.35	0.2	27.19	2.30	28737	cyl/sp	6.86	13.35	9.61	14.96	12.43	13.46
AlAlusi_1957_009_4	36		4	76.2	146.05	11129.01	9677.4	1422	508	4.00	10		127	197000	366	142.51	0.0147	2	6.35	0.2	25.22	2.31	28737	cyl/sp	6.86	10.75	9.25	11.51	10.07	10.50
AlAlusi_1957_010_13	37		13	76.2	146.05	11129.01	9677.4	1422	508	4.00	13		127	197000	366	253.35	0.0262	2	6.35	0.2	27.29	2.27	28737	cyl/sp	6.86	13.37	9.62	14.92	12.45	13.45
AlAlusi_1957_012_18	38		18	76.2	146.05	11129.01	9677.4	1549	572	4.50	13		127	197000	366	253.35	0.0262	2	6.35	0.2	25.55	2.37	28737	cyl/sp	6.86	13.08	9.31	14.15	11.74	12.56
AlAlusi_1957_015_7	39		7	76.2	146.05	11129.01	9677.4	1549	572	4.50	13		127	197000	366	253.35	0.0262	2	6.35	0.2	24.18	2.17	28737	cyl/sp	6.86	12.84	9.06	13.79	11.51	12.26
AlAlusi_1957_016_24	40		24	76.2	146.05	11129.01	9677.4	1549	572	4.50	13		127	197000	366	253.35	0.0262	2	6.35	0.2	27.06	2.44	28737	cyl/sp	6.86	13.33	9.58	14.32	11.97	12.76
AlAlusi_1957_017_16	41		16	76.2	151.13	11516.106	9677.4	1549	572	4.50	13		127	197000	366	253.35	0.0262	2	6.35	0.2	26.73	2.34	28737	cyl/sp	6.86	13.27	9.52	14.14	11.92	12.21
AlAlusi_1957_018_17	42		17	76.2	146.05	11129.01	9677.4	1803	699	5.50	13		127	197000	366	253.35	0.0262	2	6.35	0.2	28.11	2.50	28737	cyl/sp	6.86	13.50	9.77	13.18	11.38	11.74
AlAlusi_1957_019_8	43		8	76.2	146.05	11129.01	9677.4	1803	699	5.50	13		127	197000	366	253.35	0.0262	2	6.35	0.2	24.96	2.27	28737	cyl/sp	6.86	12.98	9.20	12.74	10.93	11.28
AlAlusi_1957_020_19	44		19	76.2	146.05	11129.01	9677.4	1803	699	5.50	16		127	197000	366	395.87	0.0409	2	6.35	0.2	29.09	2.47	28737	cyl/sp	6.86	15.84	9.94	15.97	13.22	14.02
AlAlusi_1957_021_25	45		25	76.2	146.05	11129.01	9677.4	1803	699	5.50	13		127	197000	366	253.35	0.0262	2	6.35	0.2	24.70	2.16	28737	cyl/sp	6.86	12.93	9.16	12.56	10.89	11.16
AlAlusi_1957_022_9	46		9	76.2	146.05	11129.01	9677.4	2057	826	6.50	13		127	197000	366	253.35	0.0262	2	6.35	0.2	30.14	2.40	28737	cyl/sp	6.86	13.82	10.11	12.19	11.01	10.97
AlAlusi_1957_023_20	47		20	76.2	146.05	11129.01	9677.4	2057	826	6.50	16		127	197000	366	395.87	0.0409	2	6.35	0.2	25.91	2.46	28737	cyl/sp	6.86	15.25	9.38	14.74	12.08	12.78
AlAlusi_1957_025_23	48		23	76.2	146.05	11129.01	9677.4	2286	940	7.40	16		127	197000	366	395.87	0.0409	2	6.35	0.2	26.80	2.31	28737	cyl/sp	6.86	15.42	9.54	13.74	11.74	12.03
Angelakos_2000_001_DB0530	49	Angelakos;	DB0530	300	1000	300000	277500	5400	2662	2.88	30		925	197000	550	1400.00	0.0050	2	10	0.2	30.40	0.00	28737	cyl/sp	6.86	141.25	153.34	132.29	156.06	147.12
Angelakos_2000_002_DB120	50	Bentz;	DB120	300	1000	300000	277500	5400	2662	2.88	30		925	197000	550	2800.00	0.0101	2	10	0.2	19.95	0.00	28737	cyl/sp	6.86	154.65	124.22	150.14	169.03	162.66
Angelakos_2000_003_DB130	51	Collins (2000)	DB130	300	1000	300000	277500	5400	2662	2.88	30		925	197000	550	2800.00	0.0101	2	10	0.2	30.40	0.00	28737	cyl/sp	6.86	177.96	153.34	181.07	196.14	197.37
Angelakos_2000_004_DB140	52		DB140	300	1000	300000	277500	5400	2662	2.88	30		925	197000	550	2800.00	0.0101	2	10	0.2	36.10	0.00	28737	cyl/sp	6.86	188.45	167.09	196.32	208.19	213.95
Angelakos_2000_005_DB165	53		DB165	300	1000	300000	277500	5400	2662	2.88	30		925	197000	550	2800.00	0.0101	2	10	0.2	61.75	0.00	28737	cyl/sp	6.86	223.75	218.54	252.75	249.84	273.41
Angelakos_2000_006_DB180	54		DB180	300	1000	300000	277500	5400	2662	2.88	30		925	197000	550	2800.00	0.0101	2	10	0.2	76.00	0.00	28737	cyl/sp	6.86	229.25	242.45	267.78	267.71	289.03
Angelakos_2000_007_DB230	55		DB230	300	1000	300000	268500	5400	2662	2.97	30		895	197000	550	5600.00	0.0209	2	10	0.2	30.40	0.00	28737	cyl/sp	6.86	219.92	151.13	239.39	232.44	263.51
Aster_1974_002_2	56	Aster;	2	1000	277.5	277500	250000	2500	920	3.68	14		250	197000	543	1600.00	0.0064	2	30	0.2	25.57	2.41	28737	cyl/sp	6.86	218.81	243.43	200.12	200.02	200.99
Aster_1974_003_3	57	Koch (1974)	3	1000	284.25	284250	250000	2500	920	3.68	20		250	197000	525	2280.00	0.0091	2	30	0.2	25.96	2.71	28737	cyl/sp	6.86	247.46	245.26	243.77	229.86	225.36
Aster_1974_005_11	58		11	1000	534.25	534250	500000	4750	1825	3.65	20		500	197000	525	2280.00	0.0046	2	30	0.2	23.35	2.12	28737	cyl/sp	6.86	301.53	400.09	257.58	311.85	273.71
Aster_1974_006_12	59		12	1000	535	535000	500000	4750	1825	3.65	20		500	197000	525	3260.00	0.0065	2	30	0.2	25.96	2.71	28737	cyl/sp	6.86	351.90	421.85	334.94	370.05	354.94
Aster_1974_007_16	60		16	1000	789	789000	750000	7000	2750	3.67	24		750	197000	526	3140.00	0.0042	2	30	0.2	28.84	2.41	28737	cyl/sp	6.86	411.61	585.09	348.36	444.49	366.68
Lubell_2004_001_AT-1 - East	61	Lubell, Sherwood, Bentz	AT-1 - East	2016	1005	2026080	1846656	5400	2662	2.91	30		916	197000	465	9800.00	0.0076	2	10	0.2	60.93	6.21	28737	cyl/sp	6.86	1354.26	1452.58	1985.52	1319.24	2040.13
Lubell_2004_002_AT-1 West	62	Collins (2004)	AT-1 West	2016	1005	2026080	1846656	5400	2662	2.91	30		916	197000	465	9800.00	0.0076	2	10	0.2	61.37	6.21	28737	cyl/sp	6.86	1355.07	1457.81	1985.79	1322.21	2040.43
Lubell_2004_003_AT-2 / 250N	63		AT-2 / 250N	250	469	117250	109250	2600	1262	2.89	25		437	197000	465	1000.00	0.0092	2	10	0.2	35.82	3.66	28737	cyl/sp	6.86	91.89	93.30	102.52	100.31	111.13
Lubell_2004_004_AT-2/ 250W	64	Sherwood (2008)	AT-2/ 250W	252	471	118692	110628	2600	1262	2.87	25		439	197000	465	1000.00	0.0090	2	10	0.2	36.58	3.66	28737	cyl/sp	6.86	93.28	95.31	103.40	101.88	112.14
Lubell_2004_005_AT-2 /1000W	65		AT-2 /1000W	1002	471	471942	439878	2600	1262	2.87	25		439	197000	465	4000.00	0.0091	2	10	0.2	37.05	3.66	28737	cyl/sp	6.86	373.23	381.41	412.50	407.64	447.32
Lubell_2004_006_AT-2/1000N	66		AT-2/1000N	1002	470	470940	438876	2600	1262	2.88	25		438	197000	465	4000.00	0.0091	2	10	0.2	36.01	3.66	28737	cyl/sp	6.86	369.20	375.46	411.29	403.15	445.92
Lubell_2004_007_AT-2/3000	67		AT-2/3000	3005	472	1418360	1319195	2600	1262	2.87	25		439	197000	465	12000.00	0.0091	2	10	0.2	38.57	3.66	28737	cyl/sp	6.86	1134.56	1167.07	1239.64	1238.85	1347.09
Lubell_2004_008_AT-3/N1	68		AT-3/N1	697	339	236283	213979	2080	1002	3.26	25		307	197000	465	2000.00	0.0093	2	20	0.2	35.63	3.66	28737	cyl/sp	6.86	220.07	224.75	226.26	216.62	224.20
Lubell_2004_009_AT-3/N2	69		AT-3/N2	706	339	239334	216036	2080	1002	3.27	25		306	197000	465	2000.00	0.0093	2	20	0.2	35.25	3.66	28737	cyl/sp	6.86	220.76	225.87	227.22	217.05	224.00
Lubell_2004_010_AT-3/T1	70		AT-3/T1	700	338	236600	214200	2080	1002	3.27	25		306	197000	465	2000.00	0.0093	2	20	0.2	35.91	3.66	28737	cyl/sp	6.86	220.88	226.05	226.38	217.16	224.14
Lubell_2004_011_AT-3/T2	71		AT-3/T2	706	339	239334	216742	2080	1002	3.26	25		307	197000	465	2000.00	0.0092	2	20	0.2	35.25	3.66	28737	cyl/sp	6.86	221.17	226.44	227.73	217.65	225.23
Bernander_1957_001_A1	72	Bernander (1957)	A1	100	200	20000	16800	2100	700	4.17	15		168	197000	667	186.27	0.0111	2	14	0.2	27.66	2.54	28737	cyl/sp	6.86	17.59	16.90	17.57	16.11	15.01
Bernander_1957_002_A2	73		A2	100	200	20000	16800	2100	700	4.17	16		168	197000	905	196.07	0.0117	2	14	0.2	27.66	2.54	28737	cyl/sp	6.86	17.89	16.90	17.98	16.41	15.32
Bernander_1957_003_A3	74		A3	100	200	20000	16800	2100	700	4.17	8		168	197000	910	162.32	0.0097	2	14	0.2	26.19	2.54	28737	cyl/sp	6.86	16.50	16.44	16.44	15.05	15.95
Bernander_1957_004_A4	75		A4	100	200	20000	16800	2100	700	4.17	15		168	197000	667	186.27	0.0111	2	14	0.2	27.66	2.54	28737	cyl/sp	6.86	17.59	16.90	17.57	16.11	15.01
Bernander_1957_005_A5	76		A5	100	200	20000	16800	2100	700	4.17	16		168	197000	905	196.07	0.0117	2	14	0.2	27.66	2.54	28737	cyl/sp	6.86	17.89	16.90	17.98	16.41	15.32
Bernander_1957_006_A6	77		A6	100	200	20000	16800	2100	700	4.17	8		168	197000	910	162.32	0.0097	2	14	0.2	26.19	2.54	28737	cyl/sp	6.86	16.50	16.44	16.44	15.05	15.95
Bernhardt_1986_001_S6A	78	Bernhardt;	S6A	150	200	30000	23850	2550	400	2.52	20		159	197000	510	628.32	0.0263	2	16	0.2	78.00	0.00	28737	cyl/sp	6.86	53.37	41.07	62.40	51.86	59.84
Bernhardt_1986_003_S6C	79	Fynboe (1986)	S6C	150	200	30000	23850	2550	400	2.52	20		159	197000	510	628.32	0.0263	2	16	0.2	78.00	0.00	28737	cyl/sp	6.86	53.37	41.07	62.40	51.86	59.84
Bernhardt_1986_004_S9A	80		S9A	150	200	30000	23850	2550	550	3.46	20		159	197000	510	1256.64	0.0527	2	16	0.2	78.00	0.00	28737	cyl/sp	6.86	62.03	41.07	70.70	57.82	65.05
Bernhardt_1986_005_S9B	81		S9B	150	200	30000	23850	2550	550	3.46	20		159	197000	510	1256.64	0.0527	2	16	0.2	78.00	0.00	28737	cyl/sp	6.86	62.03	41.07	70.70	57.82	65.05
Bernhardt_1986_006_S9C	82		S9C	150	200	30000	23850	2550	550	3.46	20		159	197000	510	1256.64	0.0527	2	16	0.2	92.25	0.00	28737	cyl/sp	6.86	63.20	44.67	72.86	61.44	68.03
Bhal_1968_001_B1	83	Bhal (1968)	B1	240	350	84000	72000	1800	881	2.94	24		300	197000	426	904.78	0.0126	2	30	0.2	22.02	2.44	28737	cyl/sp	6.86	74.57	63.00	82.27	74.27	79.23
Bhal_1968_002_B2	84		B2	240	650	156000	144000	3600	1763	2.94	24		600	197000	426	1809.56	0.0126	2	30	0.2	28.12	2.71	28737	cyl/sp	6.86	128.43	119.75	135.70	143.49	146.80
Bhal_1968_003_B3	85		B3	240	950	228000	216000	5400	2644	2.94	24		900	197000	426	2714.34	0.0126	2	30	0.2	26.11	3.02	28737	cyl/sp	6.86	164.18	149.33	188.89	189.56	200.71
Bhal_1968_004_B4	86		B4	240	1250	300000	288000	7200	3525	2.94	24		1200	197000	426	3619.11	0.0126	2	30	0.2	23.95	2.38	28737	cyl/sp	6.86	193.24	167.67	207.84	224.01	218.68
Bhal_1968_005_B5	87		B5	240	650	156000	144000	3600	1763	2.94	24		600	197000	426	904.78	0.0063	2	30	0.2	25.26	2.40	28737	cyl/sp	6.86	98.36	113.50	94.18	109.20	103.21
Bhal_1968_006_B6	88		B6	240	650	156000	144000	3600	1763	2.94	12		600	197000	422	904.78	0.0063	2	30	0.2	23.49	2.94	28737	cyl/sp	6.86	95.99	109.43	101.47	106.70	111.70
Bhal_1968_007_B7	89		B7	240	950	228000	216000	5400	2644	2.94	24		900	197000	426	1357.17	0.0063	2	30	0.2	25.88	2.95	28737	cyl/sp	6.86	129.93	148.67	136.96	150.20	146.60
Bhal_1968_008_B8	90		B8	240	950	228000	216000	5400	2644	2.94	12		900	197000	422	1357.17	0.0063	2	30	0.2	26.34	2.28	28737	cy

Bresler_1963_001_0A-1	91	Bresler;	0A-1	309.88	556.26	172373.85	142857.78	3658	1753	3.80	29	461	197000	555	2578.91	0.0181	2	19.05	0.2	21.42	2.64	28737	cyl/sp	6.86	129.00	103.19	142.65	133.41	148.89
Bresler_1963_002_0A-2	92	Scordelis (1963)	0A-2	304.8	561.34	171096.43	142064.23	4572	2210	4.74	29	466	197000	555	3223.63	0.0227	2	19.05	0.2	22.54	2.89	28737	cyl/sp	6.86	132.21	104.88	149.91	135.02	154.73
Bresler_1963_003_0A-3	93		0A-3	307.34	556.26	170960.95	141842.94	6401	3124	6.77	29	462	197000	552	3868.36	0.0273	2	19.05	0.2	35.71	2.76	28737	cyl/sp	6.86	164.15	132.22	144.80	149.68	151.28
Cladera_2002_001_H 50/1	94	Cladera;	H 50/1	200	400	80000	72000	2160	1043	2.90	32	360	197000	500	1608.50	0.0223	2	12	0.2	47.41	0.00	28737	cyl/sp	6.86	97.82	77.74	106.42	103.02	116.80
Cladera_2002_002_H 50/5	95	Mari (2002)	H 50/5	200	400	80000	72000	2160	1043	2.90	32	360	197000	500	1608.50	0.0223	2	12	0.2	47.41	0.00	28737	cyl/sp	6.86	97.82	77.74	106.42	103.02	116.80
Cladera_2002_003_H 60/1	96		H 60/1	200	400	80000	72000	2160	1043	2.90	32	360	197000	500	1608.50	0.0223	2	12	0.2	57.76	0.00	28737	cyl/sp	6.86	104.48	85.81	114.50	110.43	125.97
Cladera_2002_004_H 75/1	97	Cladera (2002)	H 75/1	200	400	80000	72000	2160	1043	2.90	32	360	197000	500	1608.50	0.0223	2	12	0.2	65.46	0.00	28737	cyl/sp	6.86	106.38	91.35	117.49	115.34	129.30
Cladera_2002_005_H 100/1	98		H 100/1	200	400	80000	72000	2160	1043	2.90	32	360	197000	500	1608.50	0.0223	2	12	0.2	82.65	0.00	28737	cyl/sp	6.86	109.17	102.65	123.61	124.99	136.11
Cladera_2002_006_H 100/5	99		H 100/5	200	400	80000	72000	2160	1043	2.90	32	360	197000	500	1608.50	0.0223	2	12	0.2	82.65	0.00	28737	cyl/sp	6.86	109.17	102.65	123.61	124.99	136.11
Cao_2000_001_SB 2003/0	100	Cao (2000)	SB 2012/0	300	2000	600000	553500	10800	5325	2.89	30	1845	197000	436	8400.00	0.0152	2	10	0.2	26.08	0.00	28737	cyl/sp	6.86	306.75	181.44	334.97	295.78	363.38
Cao_2000_002_SB 2012/0	101		SB 2003/0	300	2000	600000	577500	10800	5325	2.77	30	1925	197000	436	2100.00	0.0036	2	10	0.2	28.55	0.00	28737	cyl/sp	6.86	204.22	192.07	195.49	210.99	207.87
Cederwall_1974_001_734-34	102	Cederwall; Hedman; Losberg (1974)	734-34	135	260	35100	31590	3000	800	3.42	12	234	197000	818	339.29	0.0107	2	16	0.2	27.81	0.00	28737	cyl/sp	6.86	32.62	30.31	31.15	31.19	33.34
Chana_1981_001_2.1a	103	Chana (1981)	2.1a	203	406	82418	72268	2152	1068	3.00	20	356	197000	478	1256.64	0.0174	2	20	0.2	36.98	3.02	28737	cyl/sp	6.86	89.93	74.54	93.33	91.85	103.51
Chana_1981_001_2.1b	104		2.1b	203	406	82418	72268	2152	1068	3.00	20	356	197000	478	1256.64	0.0174	2	20	0.2	36.98	3.02	28737	cyl/sp	6.86	89.93	74.54	93.33	91.85	103.51
Chana_1981_002_2.2a	105		2.2a	203	406	82418	72268	2152	1068	3.00	20	356	197000	478	1256.64	0.0174	2	10	0.2	31.20	2.57	28737	cyl/sp	6.86	76.25	61.96	81.32	80.78	90.07
Chana_1981_002_2.2b	106		2.2b	203	406	82418	72268	2152	1068	3.00	20	356	197000	478	1256.64	0.0174	2	10	0.2	31.20	2.57	28737	cyl/sp	6.86	76.25	61.96	81.32	80.78	90.07
Chana_1981_003_2.3a	107		2.3a	203	406	82418	72268	2152	1068	3.00	20	356	197000	478	1256.64	0.0174	2	20	0.2	33.90	2.75	28737	cyl/sp	6.86	87.37	71.37	90.10	89.14	99.60
Chana_1981_003_2.3b	108		2.3b	203	406	82418	72268	2152	1068	3.00	20	356	197000	478	1256.64	0.0174	2	20	0.2	33.90	2.75	28737	cyl/sp	6.86	87.37	71.37	90.10	89.14	99.60
Chana_1981_004_3.1a	109		3.1a	100	202	20200	17700		531	3.00	10	177	197000	421	314.16	0.0177	2	10	0.2	23.29	2.63	28737	cyl/sp	6.86	21.53	15.74	25.53	20.43	26.50
Chana_1981_004_3.1b	110		3.1b	100	202	20200	17700		531	3.00	10	177	197000	421	314.16	0.0177	2	10	0.2	23.29	2.63	28737	cyl/sp	6.86	21.53	15.74	25.53	20.43	26.50
Chana_1981_005_3.2a	111		3.2a	100	202	20200	17700		531	3.00	10	177	197000	421	314.16	0.0177	2	10	0.2	24.84	2.67	28737	cyl/sp	6.86	22.00	16.26	25.75	20.89	26.89
Chana_1981_005_3.2b	112		3.2b	100	202	20200	17700		531	3.00	10	177	197000	421	314.16	0.0177	2	10	0.2	24.84	2.67	28737	cyl/sp	6.86	22.00	16.26	25.75	20.89	26.89
Chana_1981_006_3.3a	113		3.3a	100	202	20200	17700		531	3.00	10	177	197000	421	314.16	0.0177	2	10	0.2	27.07	2.40	28737	cyl/sp	6.86	22.64	16.97	25.27	21.53	27.03
Chana_1981_006_3.3b	114		3.3b	100	202	20200	17700		531	3.00	10	177	197000	421	314.16	0.0177	2	10	0.2	27.07	2.40	28737	cyl/sp	6.86	22.64	16.97	25.27	21.53	27.03
Chana_1981_007_D1	115		D1	100	202	20200	17700		531	3.00	10	177	197000	421	314.16	0.0177	2	10	0.2	21.33	2.31	28737	cyl/sp	6.86	20.91	15.07	24.65	19.81	25.67
Chana_1981_008_D2	116		D2	100	202	20200	17700		531	3.00	10	177	197000	421	314.16	0.0177	2	10	0.2	21.87	2.48	28737	cyl/sp	6.86	21.08	15.26	25.09	19.98	26.00
Chana_1981_009_D3	117		D3	100	202	20200	17700		531	3.00	10	177	197000	421	314.16	0.0177	2	10	0.2	30.17	3.11	28737	cyl/sp	6.86	23.47	17.92	27.15	22.35	28.56
Chana_1981_010_4.1a	118		4.1a	60	121	7260	6360		318	3.00	6	106	197000	504	113.10	0.0178	2	5	0.2	19.78	2.90	28737	cyl/sp	6.86	8.10	5.49	10.38	7.19	9.90
Chana_1981_010_4.1b	119		4.1b	60	121	7260	6360		318	3.00	6	106	197000	504	113.10	0.0178	2	5	0.2	19.78	2.90	28737	cyl/sp	6.86	8.10	5.49	10.38	7.19	9.90
Chana_1981_011_4.2a	120	Chana (1981)	4.2a	60	121	7260	6360		318	3.00	6	106	197000	504	113.10	0.0178	2	5	0.2	19.78	2.90	28737	cyl/sp	6.86	8.10	5.49	10.38	7.19	9.90
Chana_1981_011_4.2b	121		4.2b	60	121	7260	6360		318	3.00	6	106	197000	504	113.10	0.0178	2	5	0.2	19.78	2.90	28737	cyl/sp	6.86	8.10	5.49	10.38	7.19	9.90
Chana_1981_012_4.3a	122		4.3a	60	121	7260	6360		318	3.00	6	106	197000	504	113.10	0.0178	2	5	0.2	33.41	3.29	28737	cyl/sp	6.86	9.65	7.13	11.10	8.62	11.15
Chana_1981_012_4.3b	123		4.3b	60	121	7260	6360		318	3.00	6	106	197000	504	113.10	0.0178	2	5	0.2	33.41	3.29	28737	cyl/sp	6.86	9.65	7.13	11.10	8.62	11.15
Chana_1981_013_4.4a	124		4.4a	60	121	7260	6360		318	3.00	6	106	197000	504	113.10	0.0178	2	5	0.2	33.41	3.29	28737	cyl/sp	6.86	9.65	7.13	11.10	8.62	11.15
Chana_1981_013_4.4b	125		4.4b	60	121	7260	6360		318	3.00	6	106	197000	504	113.10	0.0178	2	5	0.2	33.41	3.29	28737	cyl/sp	6.86	9.65	7.13	11.10	8.62	11.15
Chana_1958_001_IA1	126	Chang;	IA1	101.6	152.4	15483.84	13883.843	1168	559	4.09	16	137	197000	328	401.24	0.0289	2	25.4	0.2	26.21	0.00	28737	cyl/sp	6.86	23.17	14.62	25.14	19.02	23.02
Chana_1958_003_IB1	127	Kesler (1958)	IB1	101.6	152.4	15483.84	13883.843	762	356	2.60	13	137	197000	328	258.24	0.0186	2	25.4	0.2	26.21	0.00	28737	cyl/sp	6.86	23.30	14.62	27.19	19.08	25.73
Chana_1958_005_IC1	128		IC1	101.6	152.4	15483.84	13883.843	965	457	3.35	10	137	197000	328	329.05	0.0237	2	25.4	0.2	26.21	0.00	28737	cyl/sp	6.86	23.70	14.62	25.79	19.03	27.04
Chana_1958_006_IC2	129		IC2	101.6	152.4	15483.84	13883.843	965	457	3.35	10	137	197000	328	329.05	0.0237	2	25.4	0.2	26.21	0.00	28737	cyl/sp	6.86	23.70	14.62	25.79	19.03	27.04
Chana_1958_009_IIB1	130		IIB1	101.6	152.4	15483.84	13883.843	1168	559	4.09	10	137	197000	328	329.05	0.0237	2	25.4	0.2	16.77	0.00	28737	cyl/sp	6.86	18.69	11.69	20.72	15.33	21.32
Chana_1958_011_IIC1	131		IIC1	101.6	152.4	15483.84	13883.843	762	356	2.60	16	137	197000	328	401.24	0.0289	2	25.4	0.2	16.77	0.00	28737	cyl/sp	6.86	23.25	11.69	30.53	18.23	28.58
Chana_1958_027_4-21a	132		4-21a	101.6	152.4	15483.84	13883.843	1067	508	3.72	13	137	197000	328	258.24	0.0186	2	25.4	0.2	36.69	0.00	28737	cyl/sp	6.86	23.87	17.29	23.61	19.10	22.14
Chana_1958_029_4-22a	133		4-22a	101.6	152.4	15483.84	13883.843	1067	508	3.72	13	137	197000	328	258.24	0.0186	2	25.4	0.2	30.27	0.00	28737	cyl/sp	6.86	22.38	15.71	22.49	17.92	21.00
Chana_1958_031_4-23a	134		4-23a	101.6	152.4	15483.84	13883.843	1067	508	3.72	13	137	197000	328	258.24	0.0186	2	25.4	0.2	30.60	0.00	28737	cyl/sp	6.86	22.46	15.79	22.55	17.98	21.06
Chana_1958_037_5-21a	135		5-21a	101.6	152.4	15483.84	13883.843	1067	508	3.72	16	137	197000	328	401.24	0.0289	2	25.4	0.2	30.60	0.00	28737	cyl/sp	6.86	26.02	15.79	27.50	20.66	25.30
Chana_1958_038_5-21b	136		5-21b	101.6	152.4	15483.84	13883.843	1067	508	3.72	16	137	197000	328	401.24	0.0289	2	25.4	0.2	30.60	0.00	28737	cyl/sp	6.86	26.02	15.79	27.50	20.66	25.30
Chana_1958_039_5-22a	137		5-22a	101.6	152.4	15483.84	13883.843	1067	508	3.72	16	137	197000	328	401.24	0.0289	2	25.4	0.2	29.61	0.00	28737	cyl/sp	6.86	25.74	15.54	27.28	20.42	25.09
Chana_1958_040_5-22b	138		5-22b	101.6	152.4	15483.84	13883.843	1067	508	3.72	16	137	197000	328	401.24	0.0289	2	25.4	0.2	29.61	0.00	28737	cyl/sp	6.86	25.74	15.54	27.28	20.42	25.09
Chana_1958_041_5-23a	139		5-23a	101.6	152.4	15483.84	13883.843	1067	508	3.72	16	137	197000	328	401.24	0.0289	2	25.4	0.2	30.47	0.00	28737	cyl/sp	6.86	25.98	15.76	27.47	20.63	25.27
Chana_1958_042_5-23b	140		5-23b	101.6	152.4	15483.84	13883.843	1067	508	3.72	16	137	197000	328	401.24	0.0289	2	25.4	0.2	30.47	0.00	28737	cyl/sp	6.86	25.98	15.76	27.47	20.63	25.27
Collins_1999_001_B100	141	Collins;	B100	300	1000	300000	277500	5400	2662	2.88	30	925	197000	550	2800.00	0.0101	2	10	0.2	34.20	0.00	28737	cyl/sp	6.86	185.08	162.64	191.33	204.33	208.56
Collins_1999_002_B100H	142	Kuchma (1999)	B100H	300	1000	300000	277500	5400	2662	2.88	30	925	197000	550	2800.00	0.0101	2	10	0.2	93.10	0.00	28737	cyl/sp	6.86	237.39	268.34	283.33	286.19	305.11
Collins_1999_003_B100B	143		B100B	300	1000	300000	277500	5400	2662	2.88	30	925	197000	550	2800.00	0.0101	2	10	0.2	37.05	0.00	28737	cyl/sp	6.86	190.09	169.28	198.78	210.06	216.61
Collins_1999_004_B100L	144		B100L	300	1000	300000	277500	5400	2662	2.88	16	925	197000	483	2800.00	0.0101	2	10	0.2	37.05	0.00	28737	cyl/sp	6.86	190.09	169.28	198.78	210.06	216.61
Collins_1999_005_B100-R	145		B100-R	300	1000	300000	277500	5400	2662	2.88	30	925	197000	550	2800.00	0.0101	2	10	0.2	34.20	0.00	28737	cyl/sp	6.86	185.08	162.64	191.33	204.33	208.56
Collins_1999_006_B100HE	146		B100HE	300	1000	300000	277500	5400	2662	2.88	30	925	197000	550	2800.00	0.0101	2	10	0.2	93.10	0.00	28737	cyl/sp	6.86	237.39	268.34	283.33	286.19	305.11
Collins_1999_007_B100L-R	147		B100L-R	300	1000	300000	277500	5400	2662	2.88	16	925	197000	483	2800.00	0.0101	2	10	0.2	37.05	0.00	28737	cyl/sp	6.86	190.09	169.28	198.78	210.06	216.61
DiazdeCossio_1960_002_A-2	148	Diaz de Cossio;	A-2	152.4	304.8	46451.52	38709.6	1829	838	3.30	13	254	197000	469	380.03	0.0098	2	25.4	0.2	29.94	2.53	28737	cyl/sp	6.86	42.02	39.93	39.83	39.28	41.83
DiazdeCossio_1960_003_A-3	149	Siess (1960)	A-3	152.4	304.8	46451.52	38709.6	2337	1092	4.30	13	254	197000	452	380.03	0.0098	2	25.4	0.2	18.48	2.14	28737	cyl/sp	6.86	32.62	31.37	32.37	30.59	31.65
DiazdeCossio_1960_007_A-12	150		A-12	152.4	304.8	46451.52	38709.6	1829	838	3.30	29	254	197000	314	1289.45	0.0333	2	25.4	0.2	25.36	2.22	28737	cyl/sp	6.86	59.74	36.75	66.14	54.32	60.75
DiazdeCossio_1960_008_A-13	151		A-13	152.4	304.8	46451.52	38709.6	2337	1092	4.30	29	254	197000	393	1289.45	0.0333	2	25.4	0.2	21.03	1.95	28737	cyl/sp	6.86	51.19	33.47	55.12	47.28	49.32
DiazdeCossio_1960_009_A-14	152		A-14	152.4	304.8	46451.52	38709.6	2845	1346	5.30	29	254	197000	364	1289.45	0.0333	2	25.4	0.2	26.14	2.10	28737	cyl/sp	6.86	55.04	37.31	51.59	48.12	46.77
Drangsholt_1990_001_B11	153	Drangsholt;	B11	150	250	37500	33150	2300	663	3.00	16	221	197000	485	603.19	0.0182	2	16	0.2	51.30	3.39	28737	cyl/sp	6.86	52.65	43.70	53.16	50.51	57.19
Drangsholt_1990_003_B13	154	Thorenfeld (1992)	B13	150	250	37500	31050	2300	828	4.00	16	207	197000	485	1005.31	0.0324	2	16	0.2	51.30	3.39	28737	cyl/sp	6.86	54.41	41.46	56.94	52.30	57.69
Drangsholt_1990_004_B14	155		B14	150	250	37500	31050	2300	621	3.00	16	207	197000	485	1005.31	0.0324	2	16	0.2	51.30	3.39	28737	cyl/sp	6.86	61.08	41.46	65.63	56.92	68.56
Drangsholt_1990_006_B21	156		B21	150	250	37500	33150	2300	663	3.00	16	221	197000	485	603.19	0.0182	2	16	0.2	73.89	3.94	28737	cyl/sp	6.86	55.87	52.45	56.99	57.02	62.81
Drangsholt_1990_008_B23	157		B23	150	250	37500	31050	2300	828	4.00	16	207	197000	485	1005.31	0.0324	2	16	0.2	73.89	3.94	28737	cyl/sp	6.86	57.74	49.76	61.27	59.28	63.62
Drangsholt_1990_009_B24	158		B24	150	250	37500	31050	2300	621	3.00	16	207	197000	485	1005.31	0.0324	2	16	0.2	73.89	3.94	28737	cyl/sp	6.86	64.81	49.76	70.14	64.80	75.41
Drangsholt_1990_016_B43	159		B43	150	250	37500	31050	2300	828	4.00	16	207	197000	485	1005.31	0.0324	2	16	0.2	82.12	4.19	28737	cyl/sp	6.86	58.26	52.46	63.07	61.43	65.80
Drangsholt_1990_017_B44	160		B44	150	250	37500	31050	2300	621	3.00	16	207	197000	485	1005.31	0.0324	2	16	0.2	82.12	4.19	28737	cyl/sp	6.86	65.40	52.46	71.97	67.24	77.87
Drangsholt_1990_019_B51	161		B51	150	250	37500	33150	2300	663	3.00	16	221	197000	485	603.19	0.0182	2	16	0.2	92.82	4.38	28737	cyl/sp	6.86	57.20	58.79	59.90	61.44	66.20
Drangsholt_1990_021_B53	162		B53	150	250	37500	31050	2300	828	4.00	16	207	197000	485	1005.31	0.0324	2	16	0.2	92.82	4.38	28737	cyl/sp	6.86	59.12	55.77	64.59	64.01	67.93
Drangsholt_1990_022_B54	163		B54	150	250	37500	31050	2300	621	3.00	16	207	197000	485	1005.31	0.0324	2	16	0.2	92.82	4.38	28737	cyl/sp	6.86	66.36	55.77	73.55	70.16	80.34
Drangsholt_1990_024_B61	164		B61	300	500	150000	132600	4600	1326	3.00	32	442	197000	485	2412.74	0.0182	2	16	0.2	73.88	4.24	28737	cyl/sp	6.86	177.38	174.88	190.44	202.07	211.75
Drangsholt_1990_026_B63	165		B63	300	500	150000	124200	4600	1656	4.00	32	414	197000	485	4021.24	0.0324	2	16	0.2	73.88	4.24	28737	cyl/sp	6.86	183.32	167.33	207.92	210.50	226.08
Drangsholt_1990_027_B64	166		B64	300	500	150000	124200	4600	1242	3.00	32	414	197000	485	4021.24	0.0324	2	16	0.2	73.88	4.24	28737	cyl/sp	6.86	205.77	167.33	231.38	229.15	264.50
Elzanaty_1986_002_F11	167	Elzanaty;	F11	177.8	304.8	54193.44	47983.775	3239	1080	4.00	19	270	197000	434	570.05	0.0119	2	12.7	0.2	19.66	0.00	28737	cyl/sp	6.86	38.60	36.49	37.76	39.92	38.58
Elzanaty_1986_003_F12	168	Nilson;	F12	177.8	304.8	54193.44	47701.518	3219	1073	4.00	22	268	197000	434	1163.84	0.0244	2	12.7	0.2	19.66	0.00	28737	cyl/sp	6.86	48.87	36.33	52.14	49.75	54.64
Elzanaty_1986_004_F8	169	Slate (1986)	F8	177.8	304.8	54193.44	48548.29	3277	1092	4.00	13	273	197000	434	451.29	0.0093	2	12.7	0.2	38.00	0.00	28737	cyl/sp	6.86	44.65	51.18	42.66	45.58	45.75
Elzanaty_1986_005_F13	170		F13	177.8	304.8	54193.44	47983.775	3239	1080	4.00	19	270	197000	434	570.05	0.0119	2	12.7	0.2	38.00	0.00	28737	cyl/sp	6.86	48.08	50.73	47.26	49.43	48.33
Elzanaty_1986_006_F14	171		F14	177.8	304.8	54193.44	47701.518	3219	1073	4.00	22	268	197000	434	1163.84	0.0244	2	12.7	0.2	38.00	0.00	28737	cyl/sp	6.86	60.88	50.51	64.60	62.72	67.25
Elzanaty_1986_007_F1	172		F1	177.8	304.8	54193.44	47983.775	3239	1080	4.00	19	270	197000	434	570.05	0.0119	2	12.7	0.2	62.24	0.00	28737	cyl/sp	6.86	56.08	64.93	56.54	57.74	58.44
Elzanaty_1986_008_F2	173		F2	177.8	304.8	54193.44	47701.518	3219	1073	4.00	22	268	197000	434	1163.84	0.0244	2	12.7	0.2	62.24	0.00	28737	cyl/sp	6.86	71.01	64.64	76.72	74.17	80.46
Elzanaty_1986_009_F10	174		F10	177.8	304.8	54193.44	47419.26	3200	1067	4.00	25	267	197000	434	1520.12	0.0321	2	12.7	0.2	62.24	0.00	28737	cyl/sp	6.86	77.46	64.36	85.58	80.53	88.50
Elzanaty_1986_010_F9	175		F9	177.8	304.8	54193.44	47701.518	3219	1073	4.00	22	268	197000	434	775.90	0.0163	2	12.7	0.2	75.34	0.00	28737	cyl/sp	6.86	62.99	71.12	67.42	68.56	69.45
Elzanaty_1986_011_F15	176		F15	177.8	304.8	54193.44	47701.518	3219	1073	4.00	22	268	197000	434	1163.84	0.0244	2	12.7	0.2	75.34	0.00	28737	cyl/sp	6.86	72.11	71.12	80.07	79.05	84.80
Elzanaty_1986_015_F6	177		F6	177.8	304.8	54193.44	47701.518	4829	1610	6.00	22	268	197000	434	1163.84	0.0244	2	12.7	0.2	60.28	0.00	28737	cyl/sp	6.86	70.90	63.61	67.02	63.84	68.34
Feldman_1955_002_L-2	178	Feldman;	L-2	152.4	304.8	46451.52	38477.342	2438	762	3.02	29	252	197000	310	1290.32	0.0335	2	25.4	0.2	20.44	1.61	28737	cyl/sp	6.86	56.73	32.83	64.82	51.03	59.49
Feldman_1955_003_L-2A	179	Siess (1955)	L-2A	152.4	304.8	46451.52	38477.342	2438	762	3.02	29	252	197000	283	1290.32	0.0335	2	25.4	0.2	34.86	2.64	28737	cyl/sp	6.86	67.77	42.87	73.90	62.33	69.78
Feldman_1955_004_L-3	180		L-3	152.4	304.8	46451.52	38477.342	2946	1016	4.02	29	252	197000	310	1290.32	0.0335	2	25.4	0.2	26.60	2.14	28737	cyl/sp	6.86	55.26	37.45	59.17	52.25	53.80
Feldman_1955_005_L-4	181		L-4	152.4	304.8	46451.52	38477.342	3454	1270	5.03	29	252	197000	303	1290.32	0.0335	2	25.4	0.2	24.50	2.14	28737	cyl/sp	6.86	53.77	35.95	52.81	47.62	47.18
Feldman_1955_006_L-5	182		L-5	152.4	304.8	46451.52	38477.342	3962	1524	6.04	29	252	197000	331	1290.32	0.0335	2	25.4	0.2	26.53	2.39	28737	cyl/sp	6.86	55.21	37.41	50.68	46.33	45.18
Feldman_1955_009_L2R	183		L2R	152.4	304.8	46451.52	38477.342	1524	724	2.87	29	252	197000	310	1290.32	0.0335	2	25.4	0.2	20.44	1.61	28737	cyl/sp	6.86	57.47	32.83	67.01	51.65	61.72

Ferguson_1953_005_A5	190		A5	101.6	241.3	24516.08	21290.28	1626	711	3.39	25	210	197000	276	1013.41	0.0476	2	6.35	0.2	43.11	0.00	28737	cyl/sp	6.86	38.53	23.93	43.44	36.82	42.79
Ferguson_1953_006_A6	191		A6	101.6	241.3	24516.08	21290.28	1626	711	3.39	25	210	197000	276	1013.41	0.0476	2	6.35	0.2	36.76	0.00	28737	cyl/sp	6.86	36.54	22.10	41.34	34.65	40.46
Ferguson_1953_007_D1	192		D1	177.8	241.3	42903.14	37257.99	1626	711	3.39	25	210	197000	276	1013.41	0.0272	2	6.35	0.2	29.74	0.00	28737	cyl/sp	6.86	49.45	34.79	53.31	48.57	49.57
Ferguson_1953_008_D2	193		D2	177.8	241.3	42903.14	37257.99	1626	711	3.39	25	210	197000	276	1013.41	0.0272	2	6.35	0.2	28.11	0.00	28737	cyl/sp	6.86	48.52	33.81	52.41	47.58	48.61
Ferguson_1953_009_N1	194		N1	107.95	190.5	20564.475	19193.51	2134	711	4.00	19	178	197000	276	570.05	0.0297	2	15.875	0.2	19.66	0.00	28737	cyl/sp	6.86	24.94	16.29	27.92	22.86	28.74
Ferguson_1953_010_N2	195		N2	107.95	190.5	20564.475	19193.51	2134	711	4.00	19	178	197000	276	570.05	0.0297	2	15.875	0.2	19.59	0.00	28737	cyl/sp	6.86	24.91	16.26	27.89	22.83	28.71
Ferguson_1953_011_N3	196		N3	107.95	190.5	20564.475	19193.51	2134	711	4.00	19	178	197000	276	570.05	0.0297	2	15.875	0.2	16.64	0.00	28737	cyl/sp	6.86	23.59	14.99	26.77	21.52	27.46
Ferguson_1953_012_G4	197		G4	107.95	139.7	15080.615	12338.685	2134	711	6.22	19	114	197000	276	570.05	0.0462	2	15.875	0.2	21.75	0.00	28737	cyl/sp	6.86	22.26	11.72	21.39	15.94	15.83
Ferguson_1953_013_G5	198		G5	107.95	139.7	15080.615	12338.685	2134	711	6.22	19	114	197000	276	570.05	0.0462	2	15.875	0.2	20.64	0.00	28737	cyl/sp	6.86	21.88	11.41	21.10	15.64	15.58
Ferguson_1953_014_G6	199		G6	107.95	139.7	15080.615	12338.685	2134	711	6.22	19	114	197000	276	570.05	0.0462	2	15.875	0.2	20.77	0.00	28737	cyl/sp	6.86	21.92	11.45	21.13	15.68	15.60
Ferguson_1953_015_B1	200		B1	101.6	241.3	24516.08	21290.28	1626	711	3.39	25	210	197000	276	1013.41	0.0476	2	6.35	0.2	33.91	0.00	28737	cyl/sp	6.86	35.57	21.22	40.35	33.59	39.37
Ferguson_1953_016_B2	201		B2	101.6	241.3	24516.08	21290.28	1626	711	3.39	25	210	197000	276	1013.41	0.0476	2	6.35	0.2	31.84	0.00	28737	cyl/sp	6.86	34.83	20.57	39.61	32.79	38.57
Ferguson_1953_017_B3	202		B3	101.6	241.3	24516.08	21290.28	1626	711	3.39	25	210	197000	276	1013.41	0.0476	2	6.35	0.2	38.00	0.00	28737	cyl/sp	6.86	36.95	22.47	41.76	35.09	40.93
Ferguson_1953_018_B4	203		B4	101.6	241.3	24516.08	21290.28	1626	711	3.39	25	210	197000	276	1013.41	0.0476	2	6.35	0.2	41.21	0.00	28737	cyl/sp	6.86	37.96	23.40	42.83	36.19	42.10
Ferguson_1953_019_B5	204		B5	101.6	241.3	24516.08	21290.28	1626	711	3.39	25	210	197000	276	1013.41	0.0476	2	6.35	0.2	38.98	0.00	28737	cyl/sp	6.86	37.26	22.76	42.09	35.44	41.29
Ferguson_1953_020_C1	205		C1	101.6	241.3	24516.08	21290.28	1626	711	3.39	25	210	197000	276	1013.41	0.0476	2	6.35	0.2	31.84	0.00	28737	cyl/sp	6.86	34.83	20.57	39.61	32.79	38.57
Ferguson_1953_021_C2	206		C2	101.6	241.3	24516.08	21290.28	1626	711	3.39	25	210	197000	276	1013.41	0.0476	2	6.35	0.2	31.84	0.00	28737	cyl/sp	6.86	34.83	20.57	39.61	32.79	38.57
Ferguson_1953_022_L1	207		L1	107.95	190.5	20564.475	17137.063	2134	711	4.48	19	159	197000	276	570.05	0.0333	2	15.875	0.2	20.64	0.00	28737	cyl/sp	6.86	24.41	15.18	26.16	21.05	22.07
Ferguson_1953_023_L2	208		L2	107.95	190.5	20564.475	17137.063	2134	711	4.48	19	159	197000	276	570.05	0.0333	2	15.875	0.2	21.49	0.00	28737	cyl/sp	6.86	24.74	15.49	26.44	21.36	22.32
Ferguson_1953_024_L3	209		L3	107.95	190.5	20564.475	17137.063	2134	711	4.48	19	159	197000	276	570.05	0.0333	2	15.875	0.2	21.10	0.00	28737	cyl/sp	6.86	24.59	15.34	26.31	21.22	22.21
Ferguson1_1956_001_F2	210	Ferguson (1956)	F2	100.838	209.55	21130.603	19055.962	1524	610	3.23	16	189	197000	310	395.87	0.0208	2	6.35	0.2	27.84	0.00	28737	cyl/sp	6.86	23.69	17.66	25.36	23.21	26.31
Gabrielsson_1993_002_SAR3	211	Gabrielsson (1993)	SAR3	200	298	59600	52000	2500	1100	4.23	16	260	197000	652	1608.50	0.0309	2	16	0.2	130.15	3.26	28737	cyl/sp	6.86	96.02	105.48	88.26	112.27	93.75
Gabrielsson_1993_003_HP1	212		HP1	200	238	47600	40000	1900	800	4.00	16	200	197000	686	1206.37	0.0302	2	16	0.2	132.05	3.53	28737	cyl/sp	6.86	80.19	86.25	77.25	90.83	83.36
Gabrielsson_1993_004_HP3	213		HP3	200	238	47600	40000	1900	800	4.00	16	200	197000	661	1608.50	0.0402	2	16	0.2	118.75	3.53	28737	cyl/sp	6.86	86.32	81.79	86.77	96.59	93.41
Gabrielsson_1993_005_HP5	214		HP5	200	238	47600	40000	1900	800	4.00	16	200	197000	661	1608.50	0.0402	2	16	0.2	102.60	3.06	28737	cyl/sp	6.86	84.07	76.02	82.53	91.91	88.51
Ghannoum_1998_003_N155 (N)	215	Ghannoum (1998)	N155 (N)	400	155	62000	51000	1138	319	2.50	16	128	197000	444	1000.00	0.0196	2	20	0.2	32.48	2.77	28737	cyl/sp	6.86	93.46	59.29	111.31	77.25	91.37
Ghannoum_1998_004_N155 (S)	216		N155 (S)	400	155	62000	51000	1138	319	2.50	16	128	197000	444	600.00	0.0118	2	20	0.2	32.48	2.77	28737	cyl/sp	6.86	78.83	59.29	88.05	65.66	71.40
Ghannoum_1998_005_N220 (N)	217		N220 (N)	400	220	88000	76000	1450	475	2.50	20	190	197000	433	1500.00	0.0197	2	20	0.2	32.48	2.77	28737	cyl/sp	6.86	122.20	83.72	141.32	111.04	132.37
Ghannoum_1998_006_N220 (S)	218		N220 (S)	400	220	88000	76000	1450	475	2.50	20	190	197000	433	900.00	0.0118	2	20	0.2	32.48	2.77	28737	cyl/sp	6.86	103.07	83.72	111.97	94.61	101.71
Ghannoum_1998_007_N350 (N)	219		N350 (N)	400	350	140000	125000	2063	781	2.50	25	313	197000	436	2500.00	0.0200	2	20	0.2	32.48	2.77	28737	cyl/sp	6.86	171.03	124.84	192.84	170.97	211.38
Ghannoum_1998_008_N350 (S)	220		N350 (S)	400	350	140000	125000	2063	781	2.50	25	313	197000	436	1500.00	0.0120	2	20	0.2	32.48	2.77	28737	cyl/sp	6.86	144.25	124.84	153.16	146.35	160.71
Ghannoum_1998_009_N485 (N)	221		N485 (N)	400	485	194000	176000	2700	1100	2.50	30	440	197000	385	3500.00	0.0199	2	20	0.2	32.48	2.77	28737	cyl/sp	6.86	214.44	160.21	239.20	224.80	265.34
Ghannoum_1998_010_N485 (S)	222		N485 (S)	400	485	194000	176000	2700	1100	2.50	30	440	197000	385	2100.00	0.0119	2	20	0.2	32.48	2.77	28737	cyl/sp	6.86	180.86	160.21	190.34	193.14	213.42
Ghannoum_1998_011_N960 (N)	223		N960 (N)	400	960	384000	355600	4945	2223	2.50	30	889	197000	385	7000.00	0.0197	2	20	0.2	32.48	2.77	28737	cyl/sp	6.86	341.56	246.76	382.55	370.87	422.03
Ghannoum_1998_012_N960 (S)	224		N960 (S)	400	960	384000	355600	4945	2223	2.50	30	889	197000	385	4200.00	0.0118	2	20	0.2	32.48	2.77	28737	cyl/sp	6.86	288.08	246.76	305.81	322.38	339.52
Ghannoum_1998_013_H90 (N)	225		H90 (N)	400	90	36000	26000	825	163	2.50	11	65	197000	648	500.00	0.0192	2	10	0.2	55.62	3.14	28737	cyl/sp	6.86	63.61	40.88	72.33	48.20	54.44
Ghannoum_1998_014_H90 (S)	226		H90 (S)	400	90	36000	26000	825	163	2.50	11	65	197000	648	300.00	0.0115	2	10	0.2	55.62	3.14	28737	cyl/sp	6.86	53.65	40.88	57.15	40.47	41.78
Ghannoum_1998_015_H155 (N)	227		H155 (N)	400	155	62000	51000	1138	319	2.50	16	128	197000	444	1000.00	0.0196	2	10	0.2	55.62	3.14	28737	cyl/sp	6.86	100.32	74.23	108.18	90.27	96.08
Ghannoum_1998_016_H155 (S)	228		H155 (S)	400	155	62000	51000	1138	319	2.50	16	128	197000	444	600.00	0.0118	2	10	0.2	55.62	3.14	28737	cyl/sp	6.86	84.62	74.23	85.69	76.06	75.53
Ghannoum_1998_017_H220 (N)	229		H220 (N)	400	220	88000	76000	1450	475	2.50	20	190	197000	433	1500.00	0.0197	2	10	0.2	55.62	3.14	28737	cyl/sp	6.86	131.17	102.98	138.32	128.33	138.75
Ghannoum_1998_018_H220 (S)	230		H220 (S)	400	220	88000	76000	1450	475	2.50	20	190	197000	433	900.00	0.0118	2	10	0.2	55.62	3.14	28737	cyl/sp	6.86	110.64	102.98	109.78	108.44	107.13
Ghannoum_1998_019_H350 (N)	231		H350 (N)	400	350	140000	125000	2063	781	2.50	25	313	197000	436	2500.00	0.0200	2	10	0.2	55.62	3.14	28737	cyl/sp	6.86	183.58	149.16	190.78	193.98	214.43
Ghannoum_1998_020_H350 (S)	232		H350 (S)	400	350	140000	125000	2063	781	2.50	25	313	197000	436	1500.00	0.0120	2	10	0.2	55.62	3.14	28737	cyl/sp	6.86	154.84	149.16	151.85	164.83	168.94
Ghannoum_1998_021_H485 (N)	233		H485 (N)	400	485	194000	176000	2700	1100	2.50	30	440	197000	385	3500.00	0.0199	2	10	0.2	55.62	3.14	28737	cyl/sp	6.86	230.18	186.82	238.72	251.02	266.82
Ghannoum_1998_022_H485 (S)	234		H485 (S)	400	485	194000	176000	2700	1100	2.50	30	440	197000	385	2100.00	0.0119	2	10	0.2	55.62	3.14	28737	cyl/sp	6.86	194.14	186.82	190.41	214.28	215.22
Ghannoum_1998_023_H960 (N)	235		H960 (N)	400	960	384000	355600	4945	2223	2.50	30	889	197000	385	7000.00	0.0197	2	10	0.2	55.62	3.14	28737	cyl/sp	6.86	366.63	271.75	390.01	398.49	431.18
Ghannoum_1998_024_H960 (S)	236		H960 (S)	400	960	384000	355600	4945	2223	2.50	30	889	197000	385	4200.00	0.0118	2	10	0.2	55.62	3.14	28737	cyl/sp	6.86	309.23	271.75	312.68	344.87	347.75
Grimm_1997_001_S 1.1	237	Grimm, R. (1997)	S 1.1	300	200	60000	45900	1540	570	3.73	14	153	197000	660	615.75	0.0134	2	16	0.2	85.60	5.80	28737	cyl/sp	6.86	76.04	83.28	82.33	71.28	79.31
Grimm_1997_002_S 1.2	238		S 1.2	300	200	60000	45600	1540	570	3.75	16	152	197000	517	1005.31	0.0220	2	16	0.2	86.64	3.80	28737	cyl/sp	6.86	89.34	83.32	86.76	85.23	79.93
Grimm_1997_003_S 1.3	239		S 1.3	300	200	60000	43800	1540	570	3.90	28	146	197000	487	1847.26	0.0422	2	16	0.2	89.02	4.26	28737	cyl/sp	6.86	107.34	81.60	113.80	101.53	93.19
Grimm_1997_004_S 2.2	240		S 2.2	300	400	120000	104400	3260	1230	3.53	25	348	197000	469	1963.50	0.0188	2	16	0.2	86.69	3.80	28737	cyl/sp	6.86	149.21	160.50	146.02	168.44	159.62
Grimm_1997_005_S 2.4	241		S 2.4	300	400	120000	98400	3260	1230	3.75	28	328	197000	487	3694.51	0.0375	2	16	0.2	89.40	4.33	28737	cyl/sp	6.86	178.83	156.16	193.79	199.40	209.31
Grimm_1997_006_S 3.2	242		S 3.2	300	800	240000	215400	6860	2630	3.66	28	718	197000	487	3694.51	0.0172	2	16	0.2	89.04	4.26	28737	cyl/sp	6.86	233.33	258.18	255.57	282.50	272.60
Grimm_1997_007_S 3.3	243		S 3.3	300	800	240000	223800	6860	2630	3.53	28	746	197000	487	1847.26	0.0083	2	16	0.2	89.68	5.01	28737	cyl/sp	6.86	189.41	264.60	216.66	226.26	227.43
Grimm_1997_008_S 3.4	244		S 3.4	300	800	240000	207000	6860	2630	3.81	28	690	197000	487	7389.03	0.0357	2	16	0.2	89.40	4.33	28737	cyl/sp	6.86	287.64	253.03	332.23	342.16	357.89
Grimm_1997_009_S 4.1	245		S 4.1	300	200	60000	45900	1540	570	3.73	14	153	197000	660	615.75	0.0134	2	16	0.2	105.36	5.39	28737	cyl/sp	6.86	78.33	92.40	80.60	75.97	78.37
Grimm_1997_010_S 4.2	246		S 4.2	300	200	60000	45600	1540	570	3.75	16	152	197000	517	1005.31	0.0220	2	16	0.2	105.36	5.39	28737	cyl/sp	6.86	91.90	91.88	99.31	90.76	93.68
Grimm_1997_011_S 4.3	247		S 4.3	300	200	60000	43800	1540	570	3.90	28	146	197000	487	1847.26	0.0422	2	16	0.2	105.36	5.39	28737	cyl/sp	6.86	110.05	88.77	124.71	107.58	105.40
Haddadin_1971_001_A1	248	Haddadin; Hong;	A1	177.8	469.9	83548.22	67741.8	1905	953	2.50	29	381	197000	517	2578.91	0.0381	2	16	0.2	28.01	2.14	28737	cyl/sp	6.86	98.40	57.66	116.73	96.20	131.68
Haddadin_1971_002_C1	249	Mattock (1971)	C1	177.8	469.9	83548.22	67741.8	3239	1619	4.25	29	381	197000	517	2578.91	0.0381	2	16	0.2	24.63	2.48	28737	cyl/sp	6.86	80.06	54.07	91.11	81.04	93.36
Haddadin_1971_003_E1	250		E1	177.8	469.9	83548.22	67741.8	1905	953	2.50	29	381	197000	517	2578.91	0.0381	2	16	0.2	13.23	1.30	28737	cyl/sp	6.86	76.64	39.63	101.28	71.00	108.40
Haddadin_1971_004_J1	251		J1	177.8	469.9	83548.22	67741.8	1905	953	2.50	29	381	197000	517	2578.91	0.0381	2	16	0.2	24.37	2.23	28737	cyl/sp	6.86	93.94	53.78	116.67	91.02	129.09
Hallgreen1_1994_001_B90SB5-2-33	252	Hallgren (1994)	B90SB5-2-33	156	232	36192	29836.066	2000	700	3.66	12	191	197000	651	678.00	0.0227	2	18	0.2	31.16	3.06	28737	cyl/sp	6.86	44.13	31.85	47.83	39.67	47.31
Hallgreen1_1994_002_B90SB6-2-33	253		B90SB6-2-33	156	235	36660	30249.307	2000	700	3.61	12	194	197000	651	678.00	0.0224	2	18	0.2	31.16	3.06	28737	cyl/sp	6.86	44.47	32.21	48.29	40.15	48.04
Hallgreen1_1994_003_B90SB9-2-31	254		B90SB9-2-31	156	233	36348	29917.808	2000	700	3.65	12	192	197000	651	678.00	0.0227	2	18	0.2	29.55	2.88	28737	cyl/sp	6.86	43.42	31.08	46.95	39.04	46.39
Hallgreen1_1994_004_B90SB10-2-31	255		B90SB10-2-31	157	234	36738	30275.482	2000	700	3.63	12	193	197000	651	666.62	0.0220	2	18	0.2	29.55	2.88	28737	cyl/sp	6.86	43.49	31.42	46.95	39.19	46.44
Hallgreen1_1994_005_B90SB13-2-86	256		B90SB13-2-86	163	233	37979	31260.274	2000	700	3.65	12	192	197000	630	678.00	0.0217	2	18	0.2	81.89	6.03	28737	cyl/sp	6.86	57.18	54.07	67.12	56.59	69.46
Hallgreen1_1994_006_B90SB14-2-86	257		B90SB14-2-86	158	235	37130	30637.119	2000	700	3.61	12	194	197000	630	678.00	0.0221	2	18	0.2	81.89	6.03	28737	cyl/sp	6.86	56.35	52.89	66.41	56.00	69.12
Hallgreen1_1994_007_B90SB17-2-45	258		B90SB17-2-45	157	232	36424	30027.322	2000	700	3.66	12	191	197000	630	678.00	0.0226	2	18	0.2	42.66	3.24	28737	cyl/sp	6.86	49.21	37.50	49.80	44.35	50.75
Hallgreen1_1994_008_B90SB18-2-45	259		B90SB18-2-45	155	235	36425	30055.402	2000	700	3.61	12	194	197000	630	678.00	0.0226	2	18	0.2	42.66	3.24	28737	cyl/sp	6.86	49.17	37.45	49.92	44.51	51.21
Hallgreen1_1994_009_B90SB21-2-85	260		B90SB21-2-85	155	235	36425	30055.402	2000	700	3.61	12	194	197000	630	678.00	0.0226	2	18	0.2	80.37	5.40	28737	cyl/sp	6.86	55.55	51.40	62.38	54.97	65.42
Hallgreen1_1994_010_B90SB22-2-85	261		B90SB22-2-85	158	234	36972	30468.32	2000	700	3.63	12	193	197000	630	678.00	0.0223	2	18	0.2	80.37	5.40	28737	cyl/sp	6.86	56.09	52.16	62.83	55.39	65.68
Hallgreen1_1994_011_B91SC1-2-62	262		B91SC1-2-62	156	234	36504	30082.645	2000	700	3.63	12	193	197000	443	678.00	0.0225	2	18	0.2	58.71	4.95	28737	cyl/sp	6.86	54.76	44.01	59.12	49.52	60.47
Hallgreen1_1994_012_B91SC2-2-62	263		B91SC2-2-62	155	237	36735	30392.157	2000	700	3.57	12	196	197000	443	678.00	0.0223	2	18	0.2	58.71	4.95	28737	cyl/sp	6.86	55.04	44.34	59.58	50.04	61.41
Hallgreen1_1994_013_B91SC3-2-69	264		B91SC3-2-69	155	235	36425	30055.402	2000	700	3.61	12	194	197000	443	678.00	0.0226	2	18	0.2	65.65	4.68	28737	cyl/sp	6.86	55.07	46.45	58.13	51.42	60.50
Hallgreen1_1994_014_B91SC4-2-69	265		B91SC4-2-69	156	236	36816	30417.827	2000	700	3.59	12	195	197000	443	678.00	0.0223	2	18	0.2	65.65	4.68	28737	cyl/sp	6.86	55.48	46.97	58.57	51.90	61.09
Hallgreen1_1994_015_B91SD1-4-61	266		B91SD1-4-61	156	247	38532	30249.307	2000	700	3.61	16	194	197000	494	1206.00	0.0399	2	18	0.2	57.76	4.32	28737	cyl/sp	6.86	66.19	43.86	71.72	59.21	70.45
Hallgreen1_1994_016_B91SD2-4-61	267		B91SD2-4-61	156	248	38688	30417.827	2000	700	3.59	16	195	197000	494	1206.00	0.0396	2	18	0.2	57.76	4.32	28737	cyl/sp	6.86	66.40	44.06	72.00	59.50	70.92
Hallgreen1_1994_017_B91SD3-4-66	268		B91SD3-4-66	156	248	38688	30417.827	2000	700	3.59	16	195	197000	494	1206.00	0.0396	2	18	0.2	62.42	4.41	28737	cyl/sp	6.86	67.21	45.80	72.86	61.16	72.22
Hallgreen1_1994_018_B91SD4-4-66	269		B91SD4-4-66	155	248	38440	30222.841	2000	700	3.59	16	195	197000	494	1206.00	0.0399	2	18	0.2	62.42	4.41	28737	cyl/sp	6.86	66.92	45.51	72.58	60.88	71.97
Hallgreen1_1994_019_B91SD5-4-58	270		B91SD5-4-58	156	249	38844	30502.793	2000	700	3.58	16	196	197000	494	1206.00	0.0395	2	18	0.2	55.39	4.59	28737	cyl/sp	6.86	65.58	43.24	73.57	58.75	72.09
Hallgreen1_1994_020_B91SD6-4-58	271		B91SD6-4-58	150	249	37350	29329.609	2000	700	3.58	16	196	197000	494	1206.00	0.0411	2	18	0.2	55.39	4.59	28737	cyl/sp	6.86	63.88	41.58	71.90	57.13	70.53
Hallgreen2_1996_003_B3	272	Hallgren (1996)	B3	262	240	62880	54496	1350	550	2.64	16	208	197000	632	402.13	0.0074	2	18	0.2	87.78	5.85	28737	cyl/sp	6.86	73.81	96.21	80.34	75.36	84.89
Hallgreen2_1996_005_B5	273		B5	283	240	67920	59713	1350	550	2.61	20	211	197000	604	628.32	0.0105	2	18	0.2	86.74	6.30	28737	cyl/sp	6.86	90.84	104.52	106.86	94.69	108.59
Hallgreen2_1996_007_B7	274		B7	337	240	80880	70096	1350	550	2.64	16	208	197000	630	402.12	0.0057	2	18	0.2	80.75	6.66	28737	cyl/sp	6.86	86.64	118.69	97.33	85.47	100.75
Hamadi_1976_001_G1	275	Hamadi (1976)	G1	100	400	40000	37000	2560	1255	3.39	20	370	197000	400	628.32	0.0170	2	20	0.2	28.82	0.00	28737	cyl/sp	6.86	40.29	33.35	39.56	40.94	41.78
Hamadi_1976_002_G2	276		G2	100	400	40000	37200	2560	1255	3.37	16	372	197000	460	402.12	0.0108	2	20	0.2	22.34	0.00	28737	cyl/sp	6.86	31.99	29.48	29.87	32.63	31.42
Hamadi_1976_004_G4a	277		G4a	100	400	40000	37200	4440	2195	5.90	16	372	197000	800	402.12	0.0108	2	20	0.2	20.86	0.00	28737	cyl/sp	6.86	28.66	28.48	22.43	26.16	23.05
Hamadi_1976_005_G4b	278		G4b	100	400	40000	37200	4440	1280	3.44	16	372	197000	800	402.12	0.0108	2	20	0.2	19.91	0.00	28737	cyl/sp	6.86	30.64	27.83	28.49	31.20	29.85
Hanson1_1958_001_8A-X	279	Hanson (1958)	8A-X	152.4	304.8	46451.52	40645.08	1981	660	2.48	25	267	197000	333	1013.41	0.0249	2	16	0.2	24.24	0.00	28737	cyl/sp	6.86	55.18	35.38	65.42	53.43	67.43
Hanson1_1958_002_8A	280		8A	152.4	304.8	46451.52	40645.08	1981	660	2.48	25	267	197000	333	1013.41	0.0249	2	16	0.2	26.34	0.00	28737	cyl/sp	6.86	56.73	36.87	66.77	55.11	68.98
Hanson1_1958_003_8B	281		8B	152.4	304

Hedmann_1978_001_A4	289	Hedmann; Losberg (1978)	A4	152	296.66667	45093.333	40584		1321	4.95	13	267	197000	611	507.00	0.0125	2	13	0.2	18.90	0.00	28737	cyl/sp	6.86	33.00	30.43	29.23	31.63	30.39
Hedmann_1978_002_B4	290		B4	152	296.66667	45093.333	40584		1321	4.95	13	267	197000	611	507.00	0.0125	2	13	0.2	27.98	0.00	28737	cyl/sp	6.86	37.60	37.02	33.60	35.87	35.15
Hedmann_1978_003_BW4	291		BW4	152	296.66667	45093.333	40584		1321	4.95	13	267	197000	611	507.00	0.0125	2	13	0.2	26.78	0.00	28737	cyl/sp	6.86	37.06	36.21	33.06	35.38	34.57
Hedmann_1978_004_B2	292		B2	152	296.66667	45093.333	40584		1321	4.95	22	267	197000	645	901.00	0.0222	2	13	0.2	27.83	0.00	28737	cyl/sp	6.86	45.47	36.92	43.28	43.64	45.08
Islam_1998_001_M100-S0	293	Islam;	M100-S0	150	250	37500	30450	2200	800	3.94	25	203	197000	532	981.75	0.0322	2	10	0.2	79.14	0.00	28737	cyl/sp	6.86	57.35	48.51	61.65	58.10	57.97
Islam_1998_002_M80-S0	294	Pam;	M80-S0	150	250	37500	30450	2200	800	3.94	25	203	197000	532	981.75	0.0322	2	10	0.2	68.59	0.00	28737	cyl/sp	6.86	56.23	45.17	59.83	55.33	55.66
Islam_1998_003_M60-S0	295	Kwan (1998)	M60-S0	150	250	37500	31050	2200	800	3.86	20	207	197000	554	628.32	0.0202	2	10	0.2	48.26	0.00	28737	cyl/sp	6.86	44.97	38.46	45.40	43.22	42.77
Islam_1998_004_M40-S0	296		M40-S0	150	250	37500	30750	2200	800	3.90	25	205	197000	320	981.75	0.0319	2	10	0.2	32.68	0.00	28737	cyl/sp	6.86	45.58	31.41	48.11	43.02	42.65
Islam_1998_005_M25-S0	297		M25-S0	150	250	37500	31050	2200	800	3.86	20	207	197000	350	628.32	0.0202	2	10	0.2	25.27	0.00	28737	cyl/sp	6.86	36.25	27.83	36.80	34.71	33.29
Johnson_1989_001_6	298	Johnson; Ramirez (1989)	6	304.8	609.6	185806.08	164206.12	4255	1670	3.10	32	539	197000	525	4086.34	0.0249	2	19.05	0.2	53.07	0.00	28737	cyl/sp	6.86	222.43	177.07	239.32	237.47	263.52
Kani_1967_001_40	299	Kani (1967)	40	151.638	152.4	23109.631	21183.829	1952	747	5.35	19	140	197000	388	548.39	0.0259	2	19.05	0.2	25.09	0.00	28737	cyl/sp	6.86	31.90	21.34	30.02	25.01	27.30
Kani_1967_002_41	300		41	152.4	152.4	23225.76	21522.538	1137	340	2.41	19	141	197000	381	561.29	0.0261	2	19.05	0.2	25.88	0.00	28737	cyl/sp	6.86	38.94	21.99	49.19	32.49	47.31
Kani_1967_003_43	301		43	151.384	152.4	23070.922	20763.829	2083	813	5.93	19	137	197000	392	567.74	0.0273	2	19.05	0.2	26.60	0.00	28737	cyl/sp	6.86	32.67	21.59	29.40	24.65	25.66
Kani_1967_007_47	302		47	151.13	152.4	23032.212	19961.25	1814	678	5.13	19	132	197000	392	567.74	0.0284	2	19.05	0.2	23.52	0.00	28737	cyl/sp	6.86	30.93	19.60	30.26	24.18	24.47
Kani_1967_008_48	303		48	151.13	152.4	23032.212	20153.186	1814	678	5.09	19	133	197000	392	567.74	0.0282	2	19.05	0.2	23.52	0.00	28737	cyl/sp	6.86	31.03	19.77	30.45	24.40	25.04
Kani_1967_009_52	304		52	152.4	152.4	23225.76	21096.732	1544	544	3.93	19	138	197000	392	567.74	0.0269	2	19.05	0.2	23.59	0.00	28737	cyl/sp	6.86	33.31	20.63	35.31	27.18	31.54
Kani_1967_012_55	305		55	150.368	152.4	22916.083	20242.54	1270	406	3.02	19	135	197000	392	567.74	0.0280	2	19.05	0.2	23.85	0.00	28737	cyl/sp	6.86	34.93	19.97	41.02	28.60	34.68
Kani_1967_013_56	306		56	153.162	152.4	23341.889	21046.603	1409	476	3.46	19	137	197000	403	561.29	0.0267	2	19.05	0.2	25.88	0.00	28737	cyl/sp	6.86	35.26	21.58	38.67	29.01	33.98
Kani_1967_014_57	307		57	153.162	152.4	23341.889	21241.119	1952	747	5.39	19	139	197000	375	554.84	0.0261	2	19.05	0.2	25.09	0.00	28737	cyl/sp	6.86	32.16	21.42	30.20	25.11	26.94
Kani_1967_015_58	308		58	152.4	152.4	23225.76	21096.732	1409	476	3.44	19	138	197000	417	561.29	0.0266	2	19.05	0.2	25.88	0.00	28737	cyl/sp	6.86	35.29	21.61	38.77	29.11	34.71
Kani_1967_016_59	309		59	154.432	152.4	23535.437	21574.15	1203	373	2.67	19	140	197000	392	567.74	0.0263	2	19.05	0.2	25.29	0.00	28737	cyl/sp	6.86	37.89	21.82	45.95	31.53	42.51
Kani_1967_017_60	310		60	154.94	152.4	23612.856	21487.699	1271	407	2.93	19	139	197000	392	567.74	0.0264	2	19.05	0.2	25.42	0.00	28737	cyl/sp	6.86	37.03	21.81	43.21	30.73	39.02
Kani_1967_018_81	311		81	153.416	304.8	46761.197	42085.077	4170	1628	5.93	25	274	197000	343	1161.29	0.0276	2	19.05	0.2	26.14	0.00	28737	cyl/sp	6.86	52.41	38.60	46.17	46.04	47.67
Kani_1967_020_83	312		83	155.956	304.8	47535.389	42306.496	2542	814	3.00	25	271	197000	343	1161.29	0.0274	2	19.05	0.2	26.08	0.00	28737	cyl/sp	6.86	59.21	38.85	65.04	56.48	68.58
Kani_1967_021_84	313		84	151.13	304.8	46064.424	40958.95	3085	1085	4.00	25	271	197000	342	1161.29	0.0284	2	19.05	0.2	26.08	0.00	28737	cyl/sp	6.86	51.64	37.62	54.57	50.97	56.62
Kani_1967_023_91	314		91	154.432	304.8	47070.874	41500.82	4170	1628	6.06	25	269	197000	364	1122.58	0.0270	2	19.05	0.2	26.08	0.00	28737	cyl/sp	6.86	51.65	38.19	45.03	44.91	45.02
Kani_1967_025_93	315		93	154.94	304.8	47225.712	42267.012	4441	1763	6.46	25	273	197000	372	1122.58	0.0266	2	19.05	0.2	28.76	0.00	28737	cyl/sp	6.86	53.75	40.72	45.77	45.89	46.80
Kani_1967_027_95	316		95	153.416	304.8	46761.197	42201.98	2271	678	2.47	25	275	197000	338	1161.29	0.0275	2	19.05	0.2	24.04	0.00	28737	cyl/sp	6.86	60.31	37.10	71.83	57.33	77.52
Kani_1967_028_96	317		96	153.162	304.8	46683.778	42132.109	3085	1085	3.94	25	275	197000	335	1161.29	0.0276	2	19.05	0.2	24.04	0.00	28737	cyl/sp	6.86	53.63	37.04	54.20	50.62	56.77
Kani_1967_029_97	318		97	152.4	304.8	46451.52	42116.045	2545	815	2.95	25	276	197000	366	1129.03	0.0268	2	19.05	0.2	25.88	0.00	28737	cyl/sp	6.86	58.22	38.38	64.10	55.79	68.31
Kani_1967_030_98	319		98	153.162	304.8	46683.778	42054.303	2273	679	2.47	25	275	197000	366	1129.03	0.0268	2	19.05	0.2	24.90	0.00	28737	cyl/sp	6.86	60.28	37.64	71.26	57.50	77.08
Kani_1967_031_99	320		99	152.4	304.8	46451.52	41419.272	2273	679	2.50	25	272	197000	366	1129.03	0.0273	2	19.05	0.2	24.90	0.00	28737	cyl/sp	6.86	59.71	37.15	70.46	56.80	75.65
Kani_1967_034_63	321		63	154.432	609.6	94141.747	83825.381	5356	2170	4.00	29	543	197000	352	2322.58	0.0277	2	19.05	0.2	24.90	0.00	28737	cyl/sp	6.86	85.96	61.75	84.97	88.40	90.03
Kani_1967_035_64	322		64	156.21	609.6	95225.616	84433.38	9697	4340	8.03	29	541	197000	352	2322.58	0.0275	2	19.05	0.2	24.44	0.00	28737	cyl/sp	6.86	81.93	61.71	65.39	71.75	67.09
Kani_1967_036_65	323		65	149.606	609.6	91199.818	82649.835	3734	1359	2.46	29	552	197000	374	2329.03	0.0282	2	19.05	0.2	25.62	0.00	28737	cyl/sp	6.86	96.44	61.37	109.63	99.19	120.60
Kani_1967_037_66	324		66	156.21	609.6	95225.616	84552.412	7527	3255	6.01	29	541	197000	352	2322.58	0.0275	2	19.05	0.2	25.09	0.00	28737	cyl/sp	6.86	82.69	62.59	72.88	79.39	75.57
Kani_1967_041_71	325		71	154.94	609.6	94451.424	84297.896	4271	1628	2.99	29	544	197000	373	2245.16	0.0266	2	19.05	0.2	26.01	0.00	28737	cyl/sp	6.86	92.60	63.42	98.29	96.32	106.73
Kani_1967_043_74	326		74	152.4	609.6	92903.04	79741.776	4277	1631	3.12	29	523	197000	366	2264.51	0.0284	2	19.05	0.2	25.88	0.00	28737	cyl/sp	6.86	89.60	60.67	94.71	92.42	104.19
Kani_1967_044_75	327		75	152.4	609.6	92903.04	79857.905	4277	1631	3.11	29	524	197000	367	2264.51	0.0284	2	19.05	0.2	25.94	0.00	28737	cyl/sp	6.86	89.75	60.80	94.89	92.61	104.35
Kani_1967_045_76	328		76	152.4	609.6	92903.04	78890.165	3734	1359	2.63	29	518	197000	372	2264.51	0.0287	2	19.05	0.2	29.22	0.00	28737	cyl/sp	6.86	97.15	64.02	108.16	100.32	123.25
Kani_1967_046_79	329		79	153.162	609.6	93367.555	85197.894	8626	3805	6.84	29	556	197000	381	2316.12	0.0272	2	19.05	0.2	24.83	0.00	28737	cyl/sp	6.86	82.00	62.12	69.09	75.82	70.92
Kani_1967_048_3042	330		3042	153.924	1219.2	187664.14	168506.76	7506	2737	2.50	32	1095	197000	375	4554.83	0.0270	2	19.05	0.2	25.09	0.00	28737	cyl/sp	6.86	152.64	91.35	168.99	155.80	189.56
Kani_1967_049_3043	331		3043	153.67	1219.2	187354.46	167838.37	8585	3277	3.00	32	1092	197000	376	4554.83	0.0271	2	19.05	0.2	25.62	0.00	28737	cyl/sp	6.86	146.22	92.05	155.08	150.96	169.65
Kani_1967_050_3044	332		3044	152.4	1219.2	185806.08	167225.47	10759	4364	3.98	32	1097	197000	376	4554.83	0.0272	2	19.05	0.2	28.04	0.00	28737	cyl/sp	6.86	140.47	95.71	143.79	145.77	152.39
Kani_1967_051_3045	333		3045	154.94	1219.2	188902.85	169225.47	12954	5461	5.00	32	1092	197000	381	4567.73	0.0270	2	19.05	0.2	26.86	0.00	28737	cyl/sp	6.86	133.20	95.03	131.82	136.83	137.60
Kani_1967_052_3046	334		3046	154.94	1219.2	188902.85	170012.56	17394	7681	7.00	32	1097	197000	360	4593.54	0.0270	2	19.05	0.2	25.36	0.00	28737	cyl/sp	6.86	131.11	92.53	116.88	122.35	119.93
Kani_1967_053_3047	335		3047	154.94	1219.2	188902.85	169619.02	19548	8758	8.00	32	1095	197000	376	4554.83	0.0269	2	19.05	0.2	25.36	0.00	28737	cyl/sp	6.86	130.64	92.43	112.79	117.17	115.23
Kani_1967_054_271	336		271	611.124	304.8	186270.6	164228.57	4176	1631	6.07	32	269	197000	377	4509.67	0.0275	2	19.05	0.2	25.62	0.00	28737	cyl/sp	6.86	204.22	149.80	178.08	177.42	168.15
Kani_1967_055_272	337		272	610.87	304.8	186193.18	165401.6	3632	1359	5.02	32	271	197000	377	4509.67	0.0273	2	19.05	0.2	25.62	0.00	28737	cyl/sp	6.86	204.68	150.62	193.55	189.08	185.89
Kani_1967_056_273	338		273	612.14	304.8	186580.27	166056.44	3089	1087	4.01	32	271	197000	377	4509.67	0.0272	2	19.05	0.2	25.81	0.00	28737	cyl/sp	6.86	205.61	151.74	216.26	203.27	209.93
Kani_1967_057_274	339		274	612.14	304.8	186580.27	165434.51	2545	815	3.02	32	270	197000	377	4509.67	0.0273	2	19.05	0.2	25.81	0.00	28737	cyl/sp	6.86	230.18	151.29	252.38	219.43	246.93
KaniHuggins_1979_002_266	340	Kani; Huggins;	266	153.162	304.8	46683.778	41587.465	2261	673	2.48	8	272	197000	396	207.10	0.0050	2	19.05	0.2	17.17	0.00	28737	cyl/sp	6.86	30.13	30.98	29.57	29.74	32.82
KaniHuggins_1979_003_267	341	Wittkopp (1979)	267	153.416	304.8	46761.197	41305.724	2813	949	3.53	8	269	197000	400	212.90	0.0052	2	19.05	0.2	19.66	0.00	28737	cyl/sp	6.86	29.05	32.99	24.84	27.36	27.04
KaniHuggins_1979_004_268	342		268	153.162	304.8	46683.778	42171.012	2546	816	2.96	8	275	197000	396	207.10	0.0049	2	19.05	0.2	19.07	0.00	28737	cyl/sp	6.86	29.90	33.01	26.99	28.96	29.35
KaniHuggins_1979_007_246	343		246	153.162	304.8	46683.778	42015.4	2819	952	3.47	8	274	197000	400	212.90	0.0051	2	19.05	0.2	26.21	0.00	28737	cyl/sp	6.86	32.25	38.59	27.39	30.29	29.87
KaniHuggins_1979_008_248	344		248	153.162	304.8	46683.778	43182.494	2271	678	2.41	8	282	197000	400	212.90	0.0049	2	19.05	0.2	26.21	0.00	28737	cyl/sp	6.86	35.76	39.42	34.20	35.36	37.85
KaniHuggins_1979_015_179	345		179	153.162	304.8	46683.778	40459.274	2271	678	2.57	8	264	197000	400	212.90	0.0053	2	19.05	0.2	30.73	0.00	28737	cyl/sp	6.86	36.23	40.57	33.91	35.11	40.41
KaniHuggins_1979_016_180	346		180	153.416	304.8	46761.197	41305.724	2813	949	3.53	8	269	197000	400	212.90	0.0052	2	19.05	0.2	32.76	0.00	28737	cyl/sp	6.86	34.44	42.59	29.14	31.94	32.44
KaniHuggins_1979_019_143	347	Kani; Huggins;	143	153.67	304.8	46838.616	42154.754	3085	1085	3.96	10	274	197000	428	313.55	0.0074	2	19.05	0.2	16.77	0.00	28737	cyl/sp	6.86	30.76	30.97	26.76	29.17	28.16
KaniHuggins_1979_025_149	348	Wittkopp (1979)	149	152.654	304.8	46528.939	41449.53	2271	678	2.50	10	272	197000	380	322.58	0.0078	2	19.05	0.2	17.10	0.00	28737	cyl/sp	6.86	34.73	30.82	36.18	34.53	39.45
KaniHuggins_1979_026_150	349		150	153.416	304.8	46761.197	41890.239	2271	678	2.48	10	273	197000	380	322.58	0.0077	2	19.05	0.2	17.10	0.00	28737	cyl/sp	6.86	34.97	31.11	36.44	34.81	39.63
KaniHuggins_1979_027_151	350		151	153.924	304.8	46916.035	41950.755	2273	679	2.49	10	273	197000	382	325.81	0.0078	2	19.05	0.2	18.34	0.00	28737	cyl/sp	6.86	35.94	32.28	37.20	35.75	40.69
KaniHuggins_1979_028_152	351		152	149.352	304.8	45522.49	40325.339	2545	815	3.02	10	270	197000	384	318.71	0.0079	2	19.05	0.2	18.67	0.00	28737	cyl/sp	6.86	33.34	31.37	31.99	32.60	34.63
KaniHuggins_1979_029_153	352		153	152.4	304.8	46451.52	41535.401	2545	815	2.99	10	273	197000	384	316.77	0.0076	2	19.05	0.2	18.67	0.00	28737	cyl/sp	6.86	33.91	32.25	32.47	33.22	35.02
KaniHuggins_1979_031_103	353		103	155.194	304.8	47303.131	42493.98	2542	814	2.97	10	274	197000	423	313.55	0.0074	2	19.05	0.2	27.98	0.00	28737	cyl/sp	6.86	39.26	40.34	36.69	38.29	40.30
KaniHuggins_1979_033_105	354		105	152.4	304.8	46451.52	41419.272	2273	679	2.50	10	272	197000	383	320.00	0.0077	2	19.05	0.2	24.90	0.00	28737	cyl/sp	6.86	39.22	37.15	39.53	38.93	44.24
KaniHuggins_1979_034_106	355		106	153.67	304.8	46838.616	41139.918	2271	678	2.53	10	268	197000	422	313.55	0.0076	2	19.05	0.2	27.32	0.00	28737	cyl/sp	6.86	40.05	38.78	39.86	39.56	45.46
KaniHuggins_1979_035_107	356		107	154.432	304.8	47070.874	41226.24	3627	1356	5.08	10	267	197000	422	313.55	0.0076	2	19.05	0.2	25.22	0.00	28737	cyl/sp	6.86	33.32	37.37	27.03	29.78	28.70
KaniHuggins_1979_039_111	357		111	153.924	304.8	46916.035	41872.561	2271	678	2.49	10	272	197000	368	316.77	0.0076	2	19.05	0.2	25.68	0.00	28737	cyl/sp	6.86	39.80	38.14	39.95	39.50	44.82
KaniHuggins_1979_040_112	358		112	152.908	304.8	46606.358	41751.529	2271	678	2.48	10	273	197000	368	316.77	0.0076	2	19.05	0.2	25.68	0.00	28737	cyl/sp	6.86	39.72	38.00	39.93	39.45	44.67
KaniHuggins_1979_043_115	359		115	152.4	304.8	46451.52	41380.562	2273	679	2.50	10	272	197000	383	318.71	0.0077	2	19.05	0.2	24.90	0.00	28737	cyl/sp	6.86	39.14	37.13	39.42	38.84	44.16
KaniHuggins_1979_044_116	360		116	152.4	304.8	46451.52	41303.143	2545	815	3.01	10	271	197000	384	320.64	0.0078	2	19.05	0.2	25.09	0.00	28737	cyl/sp	6.86	37.45	37.22	35.29	36.52	38.74
KaniHuggins_1979_048_163	361		163	155.956	304.8	47535.389	42504.56	2271	678	2.49	10	273	197000	378	321.29	0.0076	2	19.05	0.2	33.61	0.00	28737	cyl/sp	6.86	44.18	44.27	43.60	43.72	49.66
KaniHuggins_1979_049_163'	362		163'	151.638	304.8	46219.262	41212.176	2271	678	2.50	10	272	197000	378	321.29	0.0078	2	19.05	0.2	33.61	0.00	28737	cyl/sp	6.86	43.28	42.95	42.86	42.84	48.86
KaniHuggins_1979_052_166	363		166	151.892	304.8	46296.682	41204.047	2545	815	3.01	10	271	197000	377	321.93	0.0078	2	19.05	0.2	33.61	0.00	28737	cyl/sp	6.86	41.26	42.96	38.49	40.07	42.77
KaniHuggins_1979_053_166'	364		166'	153.67	304.8	46838.616	42154.754	2545	815	2.97	10	274	197000	379	320.00	0.0076	2	19.05	0.2	33.61	0.00	28737	cyl/sp	6.86	41.77	43.85	38.93	40.66	42.96
KaniHuggins_1979_058_121	365		121	152.4	304.8	46451.52	41496.691	2545	815	2.99	16	272	197000	330	767.74	0.0185	2	19.05	0.2	19.33	0.00	28737	cyl/sp	6.86	46.05	32.78	49.33	44.59	52.40
KaniHuggins_1979_059_122	366		122	149.86	304.8	45677.328	41299.917	3089	1087	3.94	16	276	197000	343	761.29	0.0184	2	19.05	0.2	18.87	0.00	28737	cyl/sp	6.86	42.38	32.15	41.26	40.44	43.03
KaniHuggins_1979_060_123	367		123	155.448	304.8	47380.55	42168.69	3085	1085	4.00	16	271	197000	346	754.84	0.0179	2	19.05	0.2	14.61	0.00	28737	cyl/sp	6.86	37.59	28.99	38.56	37.37	40.04
KaniHuggins_1979_061_124	368		124	154.432	304.8	47070.874	41893.078	3627	1356	5.00	16	271	197000	345	754.84	0.0180	2	19.05	0.2	14.61	0.00	28737	cyl/sp	6.86	37.42	28.80	34.01	34.72	35.08
KaniHuggins_1979_062_126	369		126	155.448	304.8	47380.55	42326.625	2542	814	2.99	16	272	197000	346	754.84	0.0178	2	19.05	0.2	15.46	0.00	28737	cyl/sp	6.86	43.09	29.91	46.80	41.57	49.23
KaniHuggins_1979_066_130	370		130	153.416	304.8	46761.197	42279.915	3898	1492	5.41	16	276	197000	346	754.84	0.0179	2	19.05	0.2	17.10	0.00	28737	cyl/sp	6.86	39.47	31.34	34.34	35.82	35.37
KaniHuggins_1979_067_131	371		131	151.13	304.8	46064.424	41419.595	2273	679	2.48	16	274	197000	401	767.74	0.0185	2	19.05	0.2	17.23	0.00	28737	cyl/sp	6.86	46.42	30.85	54.32	44.93	57.92
KaniHuggins_1979_068_132	372		132	153.67	304.8	46838.616	41608.304	2273	679	2.51	16	271	197000	417	754.84	0.0181	2	19.05	0.2	17.56	0.00	28737	cyl/sp	6.86	46.62	31.37	54.08	45.14	57.99
KaniHuggins_1979_069_133	373		133	153.924	304.8	46916.035	42068.045	3632	1359	4.97	16	273	197000	508	761.29	0.0181	2	19.05	0.2	18.87	0.00	28737	cyl/sp	6.86	40.88	32.81	37.13	38.10	38.48
KaniHuggins_1979_076_27	374		27	152.4	304.8	46451.52	41341.853	2271	678	2.50	16	271	197000	396	774.19	0.0187	2	19.05	0.2	28.30	0.00	28737	cyl/sp	6.86	54.92	39.56	61.35	53.82	67.45
KaniHuggins_1979_077_28	375		28	152.4	304.8	46451.52	41341.853	2271	678	2.50	16	271	197000	396	774.19	0.0187	2	19.05	0.2	27.71	0.00	28737	cyl/sp	6.86	54.53	39.14	61.02	53.42	67.02
KaniHuggins_1979_078_29	376		29	152.4	304.8	46451.52	41341.853	3356	1221	4.50	16	271	197000	350	774.19	0.0187	2	19.05	0.2	23.32	0.00	28737	cyl/sp	6.86	43.72	35.91	41.77	42.05	43.72
KaniHuggins_1979_079_30	377		30	152.4	304.8	46451.52	41341.853	3356	1221	4.50	16	271	197000	350	774.19	0.0187	2	19.05	0.2	23.91	0.00	28737	cyl/sp	6.86	44.09	36.36	42.11	42.41	44.10
KaniHuggins_1979_084_35	378		35	155.194	304.8	47303.131	41823.852	2819	953	3.53	16	269	197000	491	761.29	0.0182	2	19.05	0.2	24.77	0.00	28737	cyl/sp	6.86	48.34	37.49	48.17	46.51	51.31
KaniHuggins_1979_085_36	379		36	152.908	304.8	46606.358	41751.529	2819	953	3.49	16	273	197000	491	761.29	0.0182	2	19.05	0.2	24.77	0.00	28737	cyl/sp	6.86	48.22	37.32	48.22	46.56	51.15
KaniHuggins_1979_087_182	380		182	154.686	304.8	47148.293	41529.788	3627	1356	5.05	15	268	197000	386	748.39	0.0180	2	19.05	0.

KaniHuggins_1979_108_206	388		206	152.4	304.8	46451.52	41187.014	2273	679	2.51	19	270	197000	381	1122.58	0.0273	2	19.05	0.2	33.41	0.00	28737	cyl/sp	6.86	65.51	42.85	75.32	63.02	83.10		
KaniHuggins_1979_110_208	389		208	156.718	304.8	47767.646	43110.301	3356	1221	4.44	19	275	197000	379	1154.84	0.0268	2	19.05	0.2	33.94	0.00	28737	cyl/sp	6.86	57.94	45.03	57.84	55.97	60.57		
KaniHuggins_1979_112_210	390		210	154.432	304.8	47070.874	41971.529	2273	679	2.50	19	272	197000	381	1122.58	0.0267	2	19.05	0.2	33.41	0.00	28737	cyl/sp	6.86	66.32	43.62	76.23	63.94	83.92		
KaniHuggins_1979_113_211	391		211	153.162	304.8	46683.778	41315.143	2545	815	3.02	19	270	197000	381	1129.03	0.0273	2	19.05	0.2	33.41	0.00	28737	cyl/sp	6.86	62.71	43.00	67.73	60.24	73.35		
KaniHuggins_1979_114_212	392		212	155.194	304.8	47303.131	42415.141	2545	815	2.98	19	273	197000	381	1129.03	0.0266	2	19.05	0.2	33.41	0.00	28737	cyl/sp	6.86	63.75	44.02	68.91	61.49	74.30		
KaniHuggins_1979_115_213	393		213	154.178	304.8	46993.454	42489.915	3360	1223	4.44	19	276	197000	381	1129.03	0.0266	2	19.05	0.2	34.86	0.00	28737	cyl/sp	6.86	57.43	44.96	57.29	55.52	59.99		
KaniHuggins_1979_116_214	394		214	153.416	304.8	46761.197	41695.4	2273	679	2.50	19	272	197000	412	1129.03	0.0271	2	19.05	0.2	34.20	0.00	28737	cyl/sp	6.86	66.67	43.84	76.60	64.28	84.41		
KaniHuggins_1979_117_215	395		215	154.432	304.8	47070.874	42246.109	2273	679	2.48	19	274	197000	412	1129.03	0.0267	2	19.05	0.2	34.20	0.00	28737	cyl/sp	6.86	67.23	44.35	77.30	64.95	84.95		
KaniHuggins_1979_119_709	396		709	152.4	304.8	46451.52	42541.85	3633	1359	4.87	25	279	197000	379	1155.93	0.0272	2	19.05	0.2	25.49	0.00	28737	cyl/sp	6.86	51.96	38.38	49.75	48.71	51.52		
KaniHuggins_1979_120_666	397		666	154.94	304.8	47225.712	42857.334	2546	816	2.95	25	277	197000	348	1155.93	0.0270	2	19.05	0.2	27.84	0.00	28737	cyl/sp	6.86	60.81	40.50	66.69	58.41	71.21		
KaniHuggins_1979_121_675	398		675	152.4	304.8	46451.52	42193.464	2548	817	2.95	25	277	197000	378	1155.93	0.0274	2	19.05	0.2	25.29	0.00	28737	cyl/sp	6.86	58.26	37.99	64.41	55.72	68.52		
KaniHuggins_1979_122_718	399		718	151.638	304.8	46219.262	42483.205	3632	1359	4.85	25	280	197000	392	1155.93	0.0272	2	19.05	0.2	25.22	0.00	28737	cyl/sp	6.86	51.67	38.10	49.57	48.53	51.29		
KaniHuggins_1979_123_742	400		742	152.4	304.8	46451.52	41264.434	3633	1359	5.02	25	271	197000	507	1155.93	0.0280	2	19.05	0.2	33.15	0.00	28737	cyl/sp	6.86	56.15	42.75	53.40	51.98	54.55		
KaniHuggins_1979_124_744	401		744	152.4	304.8	46451.52	40993.466	3631	1358	5.05	25	269	197000	465	1155.93	0.0282	2	19.05	0.2	34.72	0.00	28737	cyl/sp	6.86	56.90	43.53	54.08	52.52	54.63		
KaniHuggins_1979_125_746	402		746	152.4	304.8	46451.52	40877.338	3629	1357	5.06	25	268	197000	474	1155.93	0.0283	2	19.05	0.2	29.48	0.00	28737	cyl/sp	6.86	53.83	40.02	50.97	49.55	51.25		
KaniHuggins_1979_127_502	403		502	152.4	304.8	46451.52	43741.848	2539	812	2.83	25	287	197000	373	1155.93	0.0264	2	19.05	0.2	24.11	0.00	28737	cyl/sp	6.86	58.65	38.15	65.61	56.49	68.93		
KaniHuggins_1979_129_504	404		504	150.876	304.8	45987.005	41196.692	2542	814	2.98	25	273	197000	346	1155.93	0.0281	2	19.05	0.2	24.90	0.00	28737	cyl/sp	6.86	57.16	36.92	63.26	54.41	67.56		
Kawano_1998_001_A-1a	405	Kawano; Watanabe (1998)	A-1a	105	330	34650	31500	2200	900	3.00	16	300	197000	370	402.12	0.0128	2	20	0.2	23.56	0.00	28737	cyl/sp	6.86	32.22	27.05	32.21	32.03	34.43		
Kawano_1998_002_A-1b	406		A-1b	105	330	34650	31500	2200	900	3.00	16	300	197000	370	402.12	0.0128	2	20	0.2	23.56	0.00	28737	cyl/sp	6.86	32.22	27.05	32.21	32.03	34.43		
Kawano_1998_003_A-2a	407		A-2a	176	570	100320	88000	3600	1500	3.00	16	500	197000	370	1206.37	0.0137	2	20	0.2	25.94	0.00	28737	cyl/sp	6.86	80.26	68.72	78.98	85.75	87.47		
Kawano_1998_004_A-2b	408		A-2b	176	570	100320	88000	3600	1500	3.00	16	500	197000	370	1206.37	0.0137	2	20	0.2	25.94	0.00	28737	cyl/sp	6.86	80.26	68.72	78.98	85.75	87.47		
Kawano_1998_005_A-3a	409		A-3a	350	1050	367500	332500	6500	2850	3.00	25	950	197000	360	3926.99	0.0118	2	20	0.2	19.67	0.00	28737	cyl/sp	6.86	212.45	173.91	200.90	233.98	218.99		
Kawano_1998_006_A-3b	410		A-3b	350	1050	367500	332500	6500	2850	3.00	25	950	197000	360	3926.99	0.0118	2	20	0.2	19.57	0.00	28737	cyl/sp	6.86	212.11	173.49	200.51	233.57	218.53		
Kawano_1998_007_A-4a	411		A-4a	600	2200	1320000	1200000	13000	6000	3.00	35	2000	197000	360	14431.69	0.0120	2	40	0.2	21.09	0.00	28737	cyl/sp	6.86	638.10	557.70	637.12	779.73	697.49		
Kawano_1998_008_A-4b	412		A-4b	600	2200	1320000	1200000	13000	6000	3.00	35	2000	197000	360	14431.69	0.0120	2	40	0.2	21.95	0.00	28737	cyl/sp	6.86	646.61	568.89	649.70	791.01	711.64		
KimPark_1994_001_CTL-1	413	Kim,	CTL-1	170	300	51000	45900	1890	810	3.00	19	270	197000	477	860.00	0.0187	2	25	0.2	49.40	0.00	28737	cyl/sp	6.86	73.25	60.02	74.21	70.22	80.77		
KimPark_1994_002_CTL-2	414	Park (1994)	CTL-2	170	300	51000	45900	1890	810	3.00	19	270	197000	477	860.00	0.0187	2	25	0.2	49.40	0.00	28737	cyl/sp	6.86	73.25	60.02	74.21	70.22	80.77		
KimPark_1994_003_P1.0-1	415		P1.0-1	170	300	51000	46240	1904	816	3.00	14	272	197000	477	468.00	0.0101	2	25	0.2	49.40	0.00	28737	cyl/sp	6.86	59.95	60.38	56.62	57.06	62.04		
KimPark_1994_004_P1.0-2	416		P1.0-2	170	300	51000	46240	1904	816	3.00	14	272	197000	477	468.00	0.0101	2	25	0.2	49.40	0.00	28737	cyl/sp	6.86	59.95	60.38	56.62	57.06	62.04		
KimPark_1994_005_P3.4-1	417		P3.4-1	170	300	51000	45390	1869	801	3.00	25	267	197000	477	1520.00	0.0335	2	25	0.2	49.40	0.00	28737	cyl/sp	6.86	88.24	59.48	94.84	82.87	102.05		
KimPark_1994_006_P3.4-2	418		P3.4-2	170	300	51000	45390	1869	801	3.00	25	267	197000	477	1520.00	0.0335	2	25	0.2	49.40	0.00	28737	cyl/sp	6.86	88.24	59.48	94.84	82.87	102.05		
KimPark_1994_007_P4.6-1	419		P4.6-1	170	300	51000	43350	1785	765	3.00	25	255	197000	477	2027.00	0.0468	2	25	0.2	49.40	0.00	28737	cyl/sp	6.86	95.65	57.30	106.11	86.95	109.84		
KimPark_1994_008_P4.6-2	420		P4.6-2	170	300	51000	43350	1785	765	3.00	25	255	197000	477	2027.00	0.0468	2	25	0.2	49.40	0.00	28737	cyl/sp	6.86	95.65	57.30	106.11	86.95	109.84		
KimPark_1994_011_A4.5-1	421		A4.5-1	170	300	51000	45900	2700	1215	4.50	19	270	197000	477	860.00	0.0187	2	25	0.2	49.40	0.00	28737	cyl/sp	6.86	65.26	60.02	62.12	61.17	65.31		
KimPark_1994_012_A4.5-2	422		A4.5-2	170	300	51000	45900	2700	1215	4.50	19	270	197000	477	860.00	0.0187	2	25	0.2	49.40	0.00	28737	cyl/sp	6.86	65.26	60.02	62.12	61.17	65.31		
KimPark_1994_013_A6.0-1	423		A6.0-1	170	300	51000	45900	3510	1620	6.00	19	270	197000	477	860.00	0.0187	2	25	0.2	49.40	0.00	28737	cyl/sp	6.86	65.26	60.02	56.23	55.09	58.20		
KimPark_1994_014_A6.0-2	424		A6.0-2	170	300	51000	45900	3510	1620	6.00	19	270	197000	477	860.00	0.0187	2	25	0.2	49.40	0.00	28737	cyl/sp	6.86	65.26	60.02	56.23	55.09	58.20		
KimPark_1994_015_D142-1	425		D142-1	170	170	28900	24140	994	426	3.00	14	142	197000	477	452.00	0.0187	2	25	0.2	49.40	0.00	28737	cyl/sp	6.86	47.72	34.71	49.20	39.35	44.39		
KimPark_1994_016_D142-2	426		D142-2	170	170	28900	24140	994	426	3.00	14	142	197000	477	452.00	0.0187	2	25	0.2	49.40	0.00	28737	cyl/sp	6.86	47.72	34.71	49.20	39.35	44.39		
KimPark_1994_017_D550-1	427		D550-1	300	620	186000	165000	3850	1650	3.00	22	550	197000	477	3097.00	0.0188	2	25	0.2	49.40	0.00	28737	cyl/sp	6.86	207.85	180.08	213.90	223.28	236.90		
KimPark_1994_018_D550-2	428		D550-2	300	620	186000	165000	3850	1650	3.00	22	550	197000	477	3097.00	0.0188	2	25	0.2	49.40	0.00	28737	cyl/sp	6.86	207.85	180.08	213.90	223.28	236.90		
KimPark_1994_019_D915-1	429		D915-1	300	1000	300000	274500	6405	2745	3.00	29	915	197000	477	5139.00	0.0187	2	25	0.2	49.40	0.00	28737	cyl/sp	6.86	291.57	246.45	311.60	323.95	337.61		
KimPark_1994_020_D915-2	430		D915-2	300	1000	300000	274500	6405	2745	3.00	29	915	197000	477	5139.00	0.0187	2	25	0.2	49.40	0.00	28737	cyl/sp	6.86	291.57	246.45	311.60	323.95	337.61		
Krefeld_1966_003_ 11A2	431	Krefeld;	11A2	152.4	381	58064.4	47845.066	1829	851	2.71	32	314	197000	366	1583.46	0.0331	2	16	0.2	28.70	0.00	28737	cyl/sp	6.86	69.78	43.52	80.54	68.14	80.96		
Krefeld_1966_004_ 12A2	432	Thurston (1966)	12A2	152.4	304.8	46451.52	36232.186	1829	851	3.58	32	238	197000	366	1583.46	0.0437	2	16	0.2	28.57	0.00	28737	cyl/sp	6.86	59.31	35.11	65.31	54.15	56.44		
Krefeld_1966_005_ 18A2	433		III-18A2	152.4	381	58064.4	48154.742	1829	851	2.69	29	316	197000	386	1282.60	0.0266	2	16	0.2	18.34	0.00	28737	cyl/sp	6.86	56.25	34.96	65.52	54.93	65.98		
Krefeld_1966_006_ 18B2	434		18B2	152.4	381	58064.4	48154.742	1829	851	2.69	29	316	197000	386	1282.60	0.0266	2	16	0.2	18.87	0.00	28737	cyl/sp	6.86	56.78	35.46	65.99	55.53	66.49		
Krefeld_1966_007_ 18C2	435		18C2	152.4	381	58064.4	48154.742	1829	851	2.69	29	316	197000	386	1282.60	0.0266	2	16	0.2	21.49	0.00	28737	cyl/sp	6.86	59.30	37.84	68.24	58.35	69.03		
Krefeld_1966_008_ 18D2	436		18D2	152.4	381	58064.4	48154.742	1829	851	2.69	29	316	197000	386	1282.60	0.0266	2	16	0.2	20.97	0.00	28737	cyl/sp	6.86	58.81	37.38	67.80	57.80	68.52		
Krefeld_1966_009_13A2	437		IV-13A2	152.4	381	58064.4	48619.258	1829	851	2.67	22	319	197000	366	387.95	0.0080	2	16	0.2	18.93	0.00	28737	cyl/sp	6.86	38.38	35.77	38.40	39.68	38.47		
Krefeld_1966_010_14A2	438		14A2	152.4	304.8	46451.52	37006.378	1829	851	3.50	22	243	197000	366	387.95	0.0105	2	16	0.2	19.66	0.00	28737	cyl/sp	6.86	33.16	29.62	31.74	31.92	27.65		
Krefeld_1966_011_15A2	439		15A2	152.4	381	58064.4	48154.742	1829	851	2.69	29	316	197000	386	641.30	0.0133	2	16	0.2	19.13	0.00	28737	cyl/sp	6.86	45.28	35.71	48.27	46.36	46.34		
Krefeld_1966_012_15B2	440		15B2	152.4	381	58064.4	48154.742	1829	851	2.69	29	316	197000	386	641.30	0.0133	2	16	0.2	19.66	0.00	28737	cyl/sp	6.86	45.69	36.19	48.62	46.80	46.76		
Krefeld_1966_013_16A2	441		16A2	152.4	304.8	46451.52	36541.862	1829	851	3.55	29	240	197000	386	641.30	0.0175	2	16	0.2	21.10	0.00	28737	cyl/sp	6.86	39.85	30.38	40.42	38.10	33.82		
Krefeld_1966_014_ 17A2	442		17A2	152.4	304.8	46451.52	37006.378	1829	851	3.50	22	243	197000	366	775.90	0.0210	2	16	0.2	20.90	0.00	28737	cyl/sp	6.86	42.64	30.54	44.34	40.64	40.35		
Krefeld_1966_015_18E2	443		18E2	152.4	381	58064.4	48154.742	1829	851	2.69	29	316	197000	386	1282.60	0.0266	2	16	0.2	18.80	0.00	28737	cyl/sp	6.86	56.72	35.40	65.93	55.45	66.43		
Krefeld_1966_016_19A2	444		19A2	152.4	304.8	46451.52	36541.862	1829	851	3.55	29	240	197000	386	1282.60	0.0351	2	16	0.2	19.52	0.00	28737	cyl/sp	6.86	48.93	29.23	54.06	44.87	46.66		
Krefeld_1966_017_ 20A2	445		20A2	152.4	304.8	46451.52	36232.186	1829	851	3.58	32	238	197000	366	1583.46	0.0437	2	16	0.2	19.98	0.00	28737	cyl/sp	6.86	52.65	29.37	59.35	47.22	49.98		
Krefeld_1966_018_21A2	446		21A2	203.2	304.8	61935.36	48309.581	1829	851	3.58	32	238	197000	366	2375.19	0.0492	2	16	0.2	18.93	0.00	28737	cyl/sp	6.86	71.71	38.12	82.22	63.24	69.47		
Krefeld_1966_020_2AC	447		2AC	152.4	304.8	46451.52	38709.6	2438	1156	4.55	25	254	197000	394	506.71	0.0131	2	16	0.2	21.88	0.00	28737	cyl/sp	6.86	35.27	32.37	32.54	33.90	28.52		
Krefeld_1966_021_ 3AC	448		3AC	152.4	304.8	46451.52	38941.858	2438	1156	4.52	22	256	197000	366	775.90	0.0199	2	16	0.2	19.79	0.00	28737	cyl/sp	6.86	39.39	30.92	38.36	37.95	36.18		
Krefeld_1966_022_4AC	449		4AC	152.4	304.8	46451.52	38709.6	2438	1156	4.55	25	254	197000	394	1013.41	0.0262	2	16	0.2	15.66	0.00	28737	cyl/sp	6.86	39.75	27.38	40.15	37.66	37.23		
Krefeld_1966_023_ 5AC	450		5AC	152.4	304.8	46451.52	38477.342	2438	1156	4.58	29	252	197000	386	1282.60	0.0333	2	16	0.2	17.43	0.00	28737	cyl/sp	6.86	44.46	28.75	45.86	41.55	41.49		
Krefeld_1966_024_ 6AC	451		6AC	152.4	304.8	46451.52	38167.666	2438	1156	4.61	32	250	197000	366	1583.46	0.0415	2	16	0.2	21.69	0.00	28737	cyl/sp	6.86	51.17	31.87	53.38	47.27	47.26		
Krefeld_1966_027_ 3CC	452		3CC	152.4	304.8	46451.52	38941.858	3048	1461	5.72	22	256	197000	366	775.90	0.0199	2	16	0.2	19.46	0.00	28737	cyl/sp	6.86	39.17	30.66	34.10	34.99	31.91		
Krefeld_1966_028_4CC	453		4CC	152.4	304.8	46451.52	38709.6	3048	1461	5.75	25	254	197000	394	1013.41	0.0262	2	16	0.2	19.52	0.00	28737	cyl/sp	6.86	42.78	30.57	38.29	37.97	35.14		
Krefeld_1966_029_5CC	454		5CC	152.4	304.8	46451.52	38477.342	3048	1461	5.78	29	252	197000	386	1282.60	0.0333	2	16	0.2	19.33	0.00	28737	cyl/sp	6.86	46.02	30.28	42.17	40.41	37.93		
Krefeld_1966_035_ 3GC	455		V-3GC	152.4	304.8	46451.52	38941.858	4267	2070	8.10	22	256	197000	379	775.90	0.0199	2	16	0.2	21.33	0.00	28737	cyl/sp	6.86	40.38	32.10	30.44	31.96	28.31		
Krefeld_1966_043_ 6C	456		VII-6C	152.4	304.8	46451.52	38477.342	1829	851	3.37	29	252	197000	386	1282.60	0.0333	2	16	0.2	19.13	0.00	28737	cyl/sp	6.86	50.05	30.12	55.82	46.48	51.15		
Krefeld_1966_044_ 3AAC	457		VIII- 3AAC	152.4	304.8	46451.52	38941.858	1829	851	3.33	22	256	197000	366	775.90	0.0199	2	16	0.2	32.82	0.00	28737	cyl/sp	6.86	51.02	39.83	52.37	49.69	51.19		
Krefeld_1966_045_ 4AAC	458		4AAC	152.4	304.8	46451.52	38709.6	1829	851	3.35	25	254	197000	394	1013.41	0.0262	2	16	0.2	27.75	0.00	28737	cyl/sp	6.86	52.55	36.45	55.87	50.41	53.00		
Krefeld_1966_046_ 5AAC	459		5AAC	152.4	304.8	46451.52	38477.342	1829	851	3.37	29	252	197000	386	1282.60	0.0333	2	16	0.2	31.19	0.00	28737	cyl/sp	6.86	58.90	38.46	63.81	55.80	59.65		
Krefeld_1966_047_ 6AAC	460		6AAC	152.4	304.8	46451.52	38167.666	1829	851	3.40	32	250	197000	366	1583.46	0.0415	2	16	0.2	32.69	0.00	28737	cyl/sp	6.86	63.89	39.13	70.45	59.52	64.61		
Krefeld_1966_048_ 3AC	461	Krefeld;	3AC	152.4	304.8	46451.52	38941.858	2438	1156	4.52	22	256	197000	366	775.90	0.0199	2	16	0.2	30.27	0.00	28737	cyl/sp	6.86	45.38	38.24	44.05	43.83	41.93		
Krefeld_1966_049_ 4AC	462	Thurston (1966)	4AC	152.4	304.8	46451.52	38709.6	2438	1156	4.55	25	254	197000	394	1013.41	0.0262	2	16	0.2	28.96	0.00	28737	cyl/sp	6.86	48.79	37.23	48.60	46.78	45.31		
Krefeld_1966_050_ 5AC	463		5AC	152.4	304.8	46451.52	38477.342	2438	1156	4.58	29	252	197000	386	1282.60	0.0333	2	16	0.2	31.19	0.00	28737	cyl/sp	6.86	53.98	38.46	54.93	51.26	50.42		
Krefeld_1966_051_ 6AC	464		6AC	152.4	304.8	46451.52	38167.666	2438	1156	4.61	32	250	197000	366	1583.46	0.0415	2	16	0.2	32.43	0.00	28737	cyl/sp	6.86	58.51	38.97	60.55	54.80	54.55		
Krefeld_1966_052_ 4CC	465		4CC	152.4	304.8	46451.52	38709.6	3048	1461	5.75	25	254	197000	394	1013.41	0.0262	2	16	0.2	36.49	0.00	28737	cyl/sp	6.86	52.70	41.80	47.95	46.93	44.75		
Krefeld_1966_053_ 5CC	466		5CC	152.4	304.8	46451.52	38477.342	3048	1461	5.78	29	252	197000	386	1282.60	0.0333	2	16	0.2	35.58	0.00	28737	cyl/sp	6.86	56.40	41.08	52.25	49.98	47.91		
Krefeld_1966_054_ 6CC	467		6CC	152.4	304.8	46451.52	38167.666	3048	1461	5.83	32	250	197000	366	1583.46	0.0415	2	16	0.2	36.49	0.00	28737	cyl/sp	6.86	60.86	41.34	57.29	53.43	51.64		
Krefeld_1966_056_ 5EC	468		5EC	152.4	304.8	46451.52	38477.342	3658	1765	6.99	29	252	197000	386	1282.60	0.0333	2	16	0.2	35.58	0.00	28737	cyl/sp	6.86	56.40	41.08	48.79	47.01	44.64		
Krefeld_1966_057_ 6EC	469		6EC	152.4	304.8	46451.52	38167.666	3658	1765	7.05	32	250	197000	366	1583.46	0.0415	2	16	0.2	32.10	0.00	28737	cyl/sp	6.86	58.32	38.78	50.85	48.24	45.46		
Krefeld_1966_059_ 4AAC	470		4AAC	152.4	304.8	46451.52	38709.6	1829	851	3.35	25	254	197000	394	1013.41	0.0262	2	16	0.2	12.25	0.00	28737	cyl/sp	6.86	40.02	24.22	44.95	37.27	43.09		
Krefeld_1966_060_ 5AAC	471		5AAC	152.4	304.8	46451.52	38477.342	1829	851	3.37	29	252	197000	386	1282.60	0.0333	2	16	0.2	14.61	0.00	28737	cyl/sp	6.86	45.75	26.32	52.10	41.93	47.94		
Krefeld_1966_062_3AC	472		3AC	152.4	304.8	46451.52	38941.858	2438	1156	4.52	22	256	197000	366	775.90	0.0199	2	16	0.2	13.04	0.00	28737	cyl/sp	6.86	34.27	25.10	33.80	32.83	32.53		
Krefeld_1966_067_4CC	473		4CC	152.4	304.8	46451.52	38709.6	3048	1461	5.75	25	254	197000	394	1013.41	0.0262	2	16	0.2	16.25	0.00	28737	cyl/sp	6.86	40.24	27.89	36.03	35.63	33.17		
Krefeld_1966_072_ C	474		X-C	203.2	533.4	108386.88	98064.32	3048	1461	3.03	25	483	197000	394	1520.12	0.0155	2	16	0.2	15.92	0.00	28737	cyl/sp	6.86	76.88	58.25	77.91	81.44	82.74		
Krefeld_1966_073_PCA	475		XI-PCA	152.4	304.8	46451.52	38167.666	3658	1765	7.05	32	250	197000	366	1583.46	0.0415	2	16	0.2	34.46	0.00	28737	cyl/sp	6.86	59.71	40.17	52.28	49.43	46.92		
Krefeld_1966_074_PCB	476		PCB	152.4	304.8	46451.52	38167.666	3658	1765	7.05	32	250	197000	366	1583.46	0.0415	2	16	0.2	34.46	0.00	28737	cyl/sp	6.86	59.71	40.17	52.28	49.43	46.92		
Krefeld_1966_075_OCA	477		s-I-OCa	152.4	304.8	46451.52	38709.6	3048	1461	5.75	25	254	197000	394	1013.41	0.0262	2	16	0.2	33.94	0.00	28737	cyl/sp	6.86	51.44	40.31	46.63	45.81	43.39		
Krefeld_1966_076_ OCB	478		OCb	152.4	304.8	46451.52	38709.6	3048

Kung_1985_008_E-1	487		E-1	140	230	32200	28000	1500	500	2.50	14	200	197000	492	307.88	0.0110	2	30	0.2	18.93	0.00	28737	cyl/sp	6.86	31.51	24.25	35.82	28.93	35.00
KuhlmannEhmann_2001_001_A6-L	488	Kuhlmann; Ehmann (2001)	A6-L	402	303	121806	100500	2002	715	2.86	20	250	197000	579	1570.80	0.0156	2	16	0.2	47.12	2.86	28737	cyl/sp	6.86	143.27	123.74	140.16	141.32	144.33
KuhlmannEhmann_2001_002_A6-R	489		A6-R	402	303	121806	100500	2002	1215	4.86	20	250	197000	579	1570.80	0.0156	2	16	0.2	47.12	2.86	28737	cyl/sp	6.86	126.11	123.74	109.15	117.41	105.90
KuhlmannZilch_2002_001_B1/l	490	Kuhlmann; Zilch;	B1/l	400	302	120800	100000	2000	715	2.86	25	250	197000	554	1924.23	0.0192	2	16	0.2	45.22	3.61	28737	cyl/sp	6.86	150.71	120.62	163.36	148.28	160.07
KuhlmannZilch_2002_002_B1/r	491	Ehmann et al. (2002)	B1/r	400	302	120800	100000	2000	1215	4.86	25	250	197000	554	1924.23	0.0192	2	16	0.2	45.22	3.61	28737	cyl/sp	6.86	132.65	120.62	130.31	124.25	120.77
KuhlmannZilch_2002_003_C3	492		C3	400	301	120400	100000	2000	965	3.86	20	250	197000	559	1570.80	0.0157	2	16	0.2	41.27	3.47	28737	cyl/sp	6.86	127.17	115.23	127.61	121.78	123.61
KuhlmannZilch_2002_004_C6	493		C6	400	302	120800	100000	2000	965	3.86	20	250	197000	559	1570.80	0.0157	2	16	0.2	42.09	3.52	28737	cyl/sp	6.86	128.01	116.38	128.39	122.57	124.43
Kulkarni_1998_005_B4JL20-S	494	Kulkarni;	B4JL20-S	102	178	18156	15504	1672	760	5.00	10	152	197000	518	213.77	0.0138	2	9.5	0.2	38.55	0.00	28737	cyl/sp	6.86	19.10	18.19	17.46	16.60	16.84
Kulkarni_1998_007_B3SE03-S	495	Shah (1998)	B3SE03-S	102	178	18156	15504	1673	684	4.50	10	152	197000	518	213.77	0.0138	2	9.5	0.2	41.40	0.00	28737	cyl/sp	6.86	19.56	18.85	18.70	17.65	18.18
Kulkarni_1998_011_B3NO15-S	496		B3NO15-S	102	178	18156	15504	1368	608	4.00	10	152	197000	518	213.77	0.0138	2	9.5	0.2	39.56	0.00	28737	cyl/sp	6.86	19.26	18.43	19.42	18.16	18.99
Kulkarni_1998_013_B3NO30-S	497		B3NO30-S	102	178	18156	15504	1216	532	3.50	10	152	197000	518	213.77	0.0138	2	9.5	0.2	41.40	0.00	28737	cyl/sp	6.86	21.15	18.85	21.00	19.33	20.81
Laupa_1953_002_ S2	498	Laupa;	S2	152.4	304.8	46451.52	40954.757	2743	1295	4.82	19	269	197000	284	855.07	0.0209	2	25.4	0.2	25.55	0.00	28737	cyl/sp	6.86	48.53	38.62	44.96	44.61	47.03
Laupa_1953_003_ S3	499	Siess (1953)	S3	152.4	304.8	46451.52	40412.822	2743	1295	4.89	25	265	197000	410	1013.41	0.0251	2	25.4	0.2	30.73	0.00	28737	cyl/sp	6.86	54.38	41.90	51.05	49.59	49.85
Laupa_1953_004_S4	500		S4	152.4	304.8	46451.52	40141.855	2743	1295	4.92	29	263	197000	309	1282.60	0.0320	2	25.4	0.2	29.29	0.00	28737	cyl/sp	6.86	57.75	40.68	55.41	52.20	53.05
Laupa_1953_005_ S5	501		S5	152.4	304.8	46451.52	39909.598	2743	1295	4.95	32	262	197000	315	1583.46	0.0397	2	25.4	0.2	28.37	0.00	28737	cyl/sp	6.86	61.18	39.85	59.82	54.62	56.20
Laupa_1953_008_ S11	502		S11	152.4	304.8	46451.52	40683.79	2743	1295	4.85	22	267	197000	328	775.90	0.0191	2	25.4	0.2	14.02	0.00	28737	cyl/sp	6.86	38.38	28.46	35.60	35.06	36.48
Laupa_1953_009_ S13	503		S13	152.4	304.8	46451.52	39909.598	2743	1295	4.95	32	262	197000	304	1583.46	0.0397	2	25.4	0.2	24.90	0.00	28737	cyl/sp	6.86	58.58	37.33	57.43	52.11	53.84
Leonhardt_1962_004_P4	504	Leonhardt; Walther (1962)	P4	500	165	82500	72500	1500	490	3.38	12	145	197000	427	1017.88	0.0140	2	30	0.2	12.67	0.00	28737	cyl/sp	6.86	79.80	53.34	89.69	65.83	84.35
Leonhardt_1962_018_4l	505		4l	190	320	60800	51300	1700	670	2.48	26	270	197000	465	1061.86	0.0207	2	30	0.2	28.89	2.87	28737	cyl/sp	6.86	74.40	52.41	89.67	72.17	87.34
Leonhardt_1962_019_4r	506		4r	190	320	60800	51300	1700	670	2.48	26	270	197000	465	1061.86	0.0207	2	30	0.2	28.89	2.87	28737	cyl/sp	6.86	74.40	52.41	89.67	72.17	87.34
Leonhardt_1962_020_5l	507		5l	190	320	60800	51300	1950	810	3.00	26	270	197000	465	1061.86	0.0207	2	30	0.2	28.89	2.87	28737	cyl/sp	6.86	70.77	52.41	80.08	68.31	75.91
Leonhardt_1962_021_5r	508		5r	190	320	60800	51300	1950	810	3.00	26	270	197000	465	1061.86	0.0207	2	30	0.2	28.89	2.87	28737	cyl/sp	6.86	70.77	52.41	80.08	68.31	75.91
Leonhardt_1962_022_6l	509		6l	190	320	60800	51300	2350	1100	4.07	26	270	197000	465	1061.86	0.0207	2	30	0.2	28.89	2.87	28737	cyl/sp	6.86	63.05	52.41	68.77	62.12	63.53
Leonhardt_1962_023_6r	510		6r	190	320	60800	51300	2350	1100	4.07	26	270	197000	465	1061.86	0.0207	2	30	0.2	28.89	2.87	28737	cyl/sp	6.86	63.05	52.41	68.77	62.12	63.53
Leonhardt_1962_024_ 7-1	511		7-1	190	320	60800	52820	3100	1350	4.86	26	278	197000	465	1061.86	0.0201	2	30	0.2	28.61	2.84	28737	cyl/sp	6.86	63.46	53.43	64.03	59.39	60.43
Leonhardt_1962_025_ 7-2	512		7-2	190	320	60800	52820	3100	1350	4.86	26	278	197000	465	1061.86	0.0201	2	30	0.2	28.61	2.84	28737	cyl/sp	6.86	63.46	53.43	64.03	59.39	60.43
Leonhardt_1962_026_ 8-1	513		8-1	190	320	60800	52820	3600	1620	5.83	26	278	197000	465	1061.86	0.0201	2	30	0.2	31.87	2.90	28737	cyl/sp	6.86	65.79	56.39	60.54	57.77	57.37
Leonhardt_1962_027_ 8-2	514		8-2	190	320	60800	52060	3600	1620	5.91	26	274	197000	465	1061.86	0.0204	2	30	0.2	31.87	2.90	28737	cyl/sp	6.86	65.47	55.72	59.99	57.03	55.96
Leonhardt_1962_028_ EA1	515		EA1	190	320	60800	51300	2000	750	2.78	24	270	197000	440	1105.84	0.0216	2	30	0.2	19.39	0.00	28737	cyl/sp	6.86	64.06	42.94	73.36	61.23	71.67
Leonhardt_1962_029_ EA2	516		EA2	190	320	60800	51300	2000	750	2.78	16	270	197000	430	911.06	0.0178	2	30	0.2	19.39	0.00	28737	cyl/sp	6.86	60.05	42.94	67.14	58.01	72.57
Leonhardt_1962_030_ D1/1	517		D1/1	50	80	4000	3500	520	210	3.00	6	70	197000	451	56.55	0.0162	2	15	0.2	28.06	0.00	28737	cyl/sp	6.86	6.34	3.94	7.36	4.61	6.17
Leonhardt_1962_031_ D1/2	518		D1/2	50	80	4000	3500	520	210	3.00	6	70	197000	451	56.55	0.0162	2	15	0.2	28.06	0.00	28737	cyl/sp	6.86	6.34	3.94	7.36	4.61	6.17
Leonhardt_1962_032_ D2/1	519		D2/1	100	160	16000	14000	1040	420	3.00	12	140	197000	427	226.19	0.0162	2	15	0.2	29.73	0.00	28737	cyl/sp	6.86	20.53	15.09	22.18	17.92	20.55
Leonhardt_1962_033_ D2/2	520		D2/2	100	160	16000	14000	1040	420	3.00	12	140	197000	427	226.19	0.0162	2	15	0.2	29.73	0.00	28737	cyl/sp	6.86	20.53	15.09	22.18	17.92	20.55
Leonhardt_1962_034_ D3/1	521	Leonhardt; Walther (1962)	D3/1	150	240	36000	31500	1560	630	3.00	18	210	197000	413	508.94	0.0162	2	15	0.2	32.09	0.00	28737	cyl/sp	6.86	41.39	32.97	43.33	39.51	42.48
Leonhardt_1962_035_ D3/2l	522		D3/2l	150	240	36000	31500	1560	630	3.00	18	210	197000	413	508.90	0.0162	2	15	0.2	32.09	0.00	28737	cyl/sp	6.86	41.39	32.97	43.32	39.50	42.48
Leonhardt_1962_036_ D3/2r	523		D3/2r	150	240	36000	31500	1560	630	3.00	18	210	197000	413	508.90	0.0162	2	15	0.2	32.09	0.00	28737	cyl/sp	6.86	41.39	32.97	43.32	39.50	42.48
Leonhardt_1962_037_ D4/1	524		D4/1	200	320	64000	56000	2080	840	3.00	24	280	197000	439	938.00	0.0168	2	15	0.2	32.83	0.00	28737	cyl/sp	6.86	68.18	55.63	70.75	68.55	72.14
Leonhardt_1962_038_ D4/2l	525		D4/2l	200	320	64000	56000	2080	840	3.00	24	280	197000	439	938.00	0.0168	2	15	0.2	32.83	0.00	28737	cyl/sp	6.86	68.18	55.63	70.75	68.55	72.14
Leonhardt_1962_039_ D4/2r	526		D4/2r	200	320	64000	56000	2080	840	3.00	24	280	197000	439	938.00	0.0168	2	15	0.2	32.83	0.00	28737	cyl/sp	6.86	68.18	55.63	70.75	68.55	72.14
Leonhardt_1962_040_ C1	527		C1	100	180	18000	15000	1000	450	3.00	16	150	197000	425	199.00	0.0133	2	30	0.2	36.39	0.00	28737	cyl/sp	6.86	23.44	18.64	24.25	19.75	20.51
Leonhardt_1962_041_ C2	528		C2	150	330	49500	45000	2000	900	3.00	16	300	197000	425	603.20	0.0134	2	30	0.2	36.39	0.00	28737	cyl/sp	6.86	56.00	50.62	56.07	55.70	60.56
Leonhardt_1962_042_ C3	529		C3	200	500	100000	90000	3000	1350	3.00	16	450	197000	425	1206.30	0.0134	2	30	0.2	36.39	0.00	28737	cyl/sp	6.86	97.84	92.49	97.35	104.91	106.57
Leonhardt_1962_043_ C4	530		C4	225	670	150750	135000	4000	1800	3.00	16	600	197000	425	1809.60	0.0134	2	30	0.2	36.39	0.00	28737	cyl/sp	6.86	133.35	127.70	133.04	148.86	146.77
Leonhardt_1962_044_E6	531		E6	190	320	60800	51300	2000	750	2.78	20	270	197000	425	1231.50	0.0240	2	30	0.2	26.88	2.73	28737	cyl/sp	6.86	74.04	50.56	87.84	71.01	89.92
Marti_1977_001_PS6	532	Marti; Pralong;	PS6	400	180	72000	66800	2380	640	3.83	14	167	197000	542	1231.50	0.0184	2	16	0.2	27.86	3.53	28737	cyl/sp	6.86	90.07	68.23	102.67	79.46	101.56
Marti_1977_003_PS11	533	Thürlimann (1977)	PS11	400	180	72000	66800	2380	640	3.83	14	167	197000	542	923.63	0.0138	2	16	0.2	28.06	3.80	28737	cyl/sp	6.86	82.02	68.47	92.74	72.28	88.51
Mathey_1963_017_ IIIa- 17	534	Mathey;	IIIa- 17	203.2	457.2	92903.04	81857.901	3658	1524	3.78	32	403	197000	505	2083.22	0.0254	2	25.4	0.2	27.78	0.00	28737	cyl/sp	6.86	98.90	73.56	97.66	98.81	104.09
Mathey_1963_018_ IIIa-18	535	Watstein (1963)	IIIa-18	203.2	457.2	92903.04	81857.901	3658	1524	3.78	32	403	197000	505	2083.22	0.0254	2	25.4	0.2	23.91	0.00	28737	cyl/sp	6.86	94.08	68.25	92.94	93.66	98.71
Mathey_1963_019_ Va-19	536		Va-19	203.2	457.2	92903.04	81857.901	3658	1524	3.78	19	403	197000	690	762.58	0.0093	2	25.4	0.2	22.34	0.00	28737	cyl/sp	6.86	65.79	65.97	57.77	66.25	62.26
Mathey_1963_020_ Va-20	537		Va-20	203.2	457.2	92903.04	81857.901	3658	1524	3.78	19	403	197000	690	762.58	0.0093	2	25.4	0.2	24.31	0.00	28737	cyl/sp	6.86	67.67	68.81	59.46	68.07	64.26
Mathey_1963_021_ VIb-21	538	Mathey;	VIb-21	203.2	457.2	92903.04	81857.901	2896	1143	2.84	19	403	197000	707	688.39	0.0084	2	25.4	0.2	24.83	0.00	28737	cyl/sp	6.86	70.59	69.55	66.59	73.19	74.55
Mathey_1963_022_ VIb-22	539	Watstein (1963)	VIb-22	203.2	457.2	92903.04	81857.901	2896	1143	2.84	19	403	197000	707	688.39	0.0084	2	25.4	0.2	24.50	0.00	28737	cyl/sp	6.86	70.27	69.09	66.32	72.87	74.20
Mathey_1963_023_ VIb-23	540		VIb-23	203.2	457.2	92903.04	81857.901	2896	1143	2.84	19	403	197000	707	688.39	0.0084	2	25.4	0.2	29.02	0.00	28737	cyl/sp	6.86	74.36	75.19	69.88	76.99	78.89
Mathey_1963_024_ VIa-24	541		VIa-24	203.2	457.2	92903.04	81857.901	3658	1524	3.78	13	403	197000	696	383.23	0.0047	2	25.4	0.2	25.03	0.00	28737	cyl/sp	6.86	54.33	69.82	43.66	52.86	48.36
Mathey_1963_025_ VIa-25	542		VIa-25	203.2	457.2	92903.04	81857.901	3658	1524	3.78	13	403	197000	696	383.23	0.0047	2	25.4	0.2	24.50	0.00	28737	cyl/sp	6.86	53.94	69.09	43.33	52.52	47.96
Moayer2_1974_001_P41	543	Moayer; Regan (1974)	P41	149.86	320.04	47961.194	41870.884	1981	977	3.50	16	279	197000	641	791.73	0.0189	2	19	0.2	41.80	0.00	28737	cyl/sp	6.86	57.77	48.35	57.34	56.20	62.32
Moody_1954_013_A1	544	Moody;	A1	177.8	304.8	54193.44	46516.036	1600	775	2.96	36	262	197000	310	1007.39	0.0217	2	25.4	0.2	28.83	0.00	28737	cyl/sp	6.86	66.01	46.83	70.05	62.36	62.41
Moody_1954_014_A2	545	Viest; Elstner;	A2	177.8	304.8	54193.44	47419.26	1600	775	2.90	25	267	197000	310	1013.41	0.0214	2	25.4	0.2	29.48	0.00	28737	cyl/sp	6.86	67.39	48.11	71.69	64.03	71.74
Moody_1954_015_A3	546	Hognestad (1954)	A3	177.8	304.8	54193.44	47645.066	1600	775	2.89	22	268	197000	310	1060.92	0.0223	2	25.4	0.2	29.48	0.00	28737	cyl/sp	6.86	68.62	48.29	73.45	65.15	77.09
Moody_1954_016_A4	547		A4	177.8	304.8	54193.44	48006.356	1600	775	2.87	19	270	197000	310	1140.09	0.0237	2	25.4	0.2	29.94	0.00	28737	cyl/sp	6.86	70.96	48.96	76.60	67.30	82.95
Moody_1954_017_B1	548		B1	177.8	304.8	54193.44	47419.26	1600	775	2.90	25	267	197000	310	760.06	0.0160	2	25.4	0.2	20.11	0.00	28737	cyl/sp	6.86	53.90	39.73	57.01	51.40	55.01
Moody_1954_018_B2	549		B2	177.8	304.8	54193.44	47645.066	1600	775	2.89	22	268	197000	310	775.90	0.0163	2	25.4	0.2	20.51	0.00	28737	cyl/sp	6.86	54.78	40.27	58.04	52.28	58.81
Moody_1954_019_B3	550		B3	177.8	304.8	54193.44	48006.356	1600	775	2.87	19	270	197000	310	767.98	0.0160	2	25.4	0.2	18.28	0.00	28737	cyl/sp	6.86	52.77	38.26	56.47	50.39	60.19
Moody_1954_020_B4	551		B4	177.8	304.8	54193.44	48277.323	1600	775	2.85	16	272	197000	310	791.73	0.0164	2	25.4	0.2	15.92	0.00	28737	cyl/sp	6.86	51.08	35.87	55.62	48.64	58.74
Moody_1954_025_1	552		1	152.4	304.8	46451.52	40877.338	2743	914	3.41	22	268	197000	310	775.90	0.0190	2	25.4	0.2	34.86	0.00	28737	cyl/sp	6.86	56.67	45.04	56.13	53.66	57.50
Moody_1954_026_2	553		2	152.4	304.8	46451.52	40877.338	2743	914	3.41	22	268	197000	310	775.90	0.0190	2	25.4	0.2	15.86	0.00	28737	cyl/sp	6.86	43.58	30.38	45.12	40.81	46.63
Moody_1954_027_3	554		3	152.4	304.8	46451.52	40877.338	2743	914	3.41	22	268	197000	310	775.90	0.0190	2	25.4	0.2	24.50	0.00	28737	cyl/sp	6.86	50.39	37.76	50.67	47.55	51.69
Moody_1954_028_4	555		4	152.4	304.8	46451.52	40877.338	2743	914	3.41	22	268	197000	310	775.90	0.0190	2	25.4	0.2	14.61	0.00	28737	cyl/sp	6.86	42.41	29.16	44.18	39.64	45.99
Moody_1954_029_5	556		5	152.4	304.8	46451.52	40877.338	2743	914	3.41	22	268	197000	310	775.90	0.0190	2	25.4	0.2	29.16	0.00	28737	cyl/sp	6.86	53.40	41.19	53.23	50.49	54.37
Moody_1954_030_6	557		6	152.4	304.8	46451.52	40877.338	2743	914	3.41	22	268	197000	310	775.90	0.0190	2	25.4	0.2	15.00	0.00	28737	cyl/sp	6.86	42.79	29.55	44.48	40.02	46.19
Moody_1954_031_7	558		7	152.4	304.8	46451.52	40877.338	2743	914	3.41	22	268	197000	310	775.90	0.0190	2	25.4	0.2	29.35	0.00	28737	cyl/sp	6.86	53.52	41.33	53.34	50.61	54.48
Moody_1954_033_9	559		9	152.4	304.8	46451.52	40877.338	2743	914	3.41	22	268	197000	310	775.90	0.0190	2	25.4	0.2	39.11	0.00	28737	cyl/sp	6.86	58.89	47.71	58.15	55.80	59.73
Moody_1954_034_10	560	Moody; Viest et al. (1954)	10	152.4	304.8	46451.52	40877.338	2743	914	3.41	22	268	197000	310	775.90	0.0190	2	25.4	0.2	22.73	0.00	28737	cyl/sp	6.86	49.15	36.38	49.64	46.33	50.65
Moody_1954_035_11	561		11	152.4	304.8	46451.52	40877.338	2743	914	3.41	22	268	197000	310	775.90	0.0190	2	25.4	0.2	36.23	0.00	28737	cyl/sp	6.86	57.41	45.92	56.79	54.37	58.23
Moody_1954_036_12	562		12	152.4	304.8	46451.52	40877.338	2743	914	3.41	22	268	197000	310	775.90	0.0190	2	25.4	0.2	19.20	0.00	28737	cyl/sp	6.86	46.45	33.43	47.43	43.67	48.54
Moody_1954_037_13	563		13	152.4	304.8	46451.52	40877.338	2743	914	3.41	22	268	197000	310	775.90	0.0190	2	25.4	0.2	35.90	0.00	28737	cyl/sp	6.86	57.23	45.71	56.63	54.20	58.05
Moody_1954_038_14	564		14	152.4	304.8	46451.52	40877.338	2743	914	3.41	22	268	197000	310	775.90	0.0190	2	25.4	0.2	21.42	0.00	28737	cyl/sp	6.86	48.18	35.31	48.84	45.38	49.87
Moody_1954_039_15	565		15	152.4	304.8	46451.52	40877.338	2743	914	3.41	22	268	197000	310	775.90	0.0190	2	25.4	0.2	35.51	0.00	28737	cyl/sp	6.86	57.02	45.46	56.44	54.00	57.85
Moody_1954_040_16	566		16	152.4	304.8	46451.52	40877.338	2743	914	3.41	22	268	197000	310	775.90	0.0190	2	25.4	0.2	15.53	0.00	28737	cyl/sp	6.86	43.28	30.06	44.88	40.51	46.46
Morrow_1957_025_ B40 B4	567	Morrow;	B40 B4	304.8	406.4	123870.72	112257.84	2388	1105	3.00	22	368	197000	378	2121.84	0.0189	2	25.4	0.2	33.02	0.00	28737	cyl/sp	6.86	141.65	112.48	144.32	143.48	155.68
Morrow_1957_026_ B56 B2	568	Viest (1957)	B56 B2	304.8	406.4	123870.72	112257.84	3200	1511	4.10	22	368	197000	471	2121.84	0.0189	2	25.4	0.2	13.96	0.00	28737	cyl/sp	6.86	94.70	73.12	93.39	96.61	96.53
Morrow_1957_028_ B56 A4	569		B56 A4	304.8	406.4	123870.72	114193.32	3200	1511	4.03	25	375	197000	330	2802.73	0.0245	2	25.4	0.2	23.72	0.00	28737	cyl/sp	6.86	124.71	96.57	126.61	128.23	131.95
Morrow_1957_029_ B56 B4	570		B56 B4	304.8	406.4	123870.72	112257.84	3200	1511	4.10	22	368	197000	441	2121.84	0.0189	2	25.4	0.2	25.88	0.00	28737	cyl/sp	6.86	116.35	99.58	113.91	119.68	119.57
Morrow_1957_030_ B56 E4	571		B56 E4	304.8	406.4	123870.72	112257.84	3200	1511	4.10	19	368	197000	429	1425.11	0.0127	2	25.4	0.2	26.99	0.00	28737	cyl/sp	6.86	103.34	101.70	96.71	106.23	101.97
Morrow_1957_031_ B56 A6	572		B56 A6	308.102	406.4	125212.65	109561.07	3200	1511	4.25	29	356	197000	439	4237.05	0.0387	2	25.4	0.2	37.87	0.00	28737	cyl/sp	6.86	165.59	118.55	172.23	164.58	182.82
Morrow_1957_032_ B56 B6	573		B56 B6	304.8	406.4	123870.72	113264.29	3200	1511	4.07	22	372	197000	466	2121.84	0.0187	2	25.4	0.2	43.44	0.00	28737	cyl/sp	6.86	138.69	129.88	138.27	143.46	145.50
Morrow_1957_033_ B70 B2	574		B70 B2	304.8	406.4	123870.72	111328.81	3912	1867	5.11	22	365	197000	462	2121.84	0.0191	2	25.4	0.2	15.53	0.00	28737	cyl/sp	6.86	97.86	76.65	85.99	93.36	88.75
Morrow_1957_034_ B70 A4	575		B70 A4	304.8	406.4	123870.72	112257.84	3912	1867	5.07	25	368	197000	436	2802.73	0.0250	2	25.4	0.2	25.88	0.00	28737	cyl/sp	6.86	127.66	99.58	117.09	122.24	121.56
Morrow_1957_035_ B70 A6	576		B70 A6	304.8	406.4	123870.72	108386.88	3912	1867	5.25	29	356	197000	435	4237.05	0.0391	2	25.4	0.2	42.72	0.00	28737	cyl/sp	6.86	171.14	124.56	164.98	160.34	172.86
Morrow_1957_036_ B84 B4	577		B84 B4	304.8	406.4	123870.72	110786.88	4623	2223	6.11	22	363	197000	465	2121.84	0.0192	2	25.4	0.2	25.88	0.00	28737	cyl/sp	6.86	115.84	98.58	95.82	104.07	99.16
Morrow_1957_037_ B113 B4	578		B113 B4	304.8	406.4

Mphonde_1984_008_AO-15-3b	586		AO-15-3b	152.4	336.55	51290.22	45483.78	2134	1041	3.49	25	298	197000	414	1520.12	0.0334	2	9.525	0.2	91.28	0.00	28737	cyl/sp	6.86	80.10	70.09	90.44	89.10	97.70
Mphonde_1984_009_AO-15-3c	587		AO-15-3c	152.4	336.55	51290.22	45483.78	2134	1041	3.49	25	298	197000	414	1520.12	0.0334	2	9.525	0.2	89.48	0.00	28737	cyl/sp	6.86	79.79	69.40	90.04	88.48	97.27
Mphonde_1984_010_AO-3-2	588		AO-3-2	152.4	336.55	51290.22	45483.78	1492	721	2.41	25	298	197000	414	1520.12	0.0334	2	9.525	0.2	20.06	0.00	28737	cyl/sp	6.86	57.50	32.86	72.21	55.60	78.51
Mphonde_1984_011_AO-7-2	589		AO-7-2	152.4	336.55	51290.22	45483.78	1492	721	2.41	25	298	197000	414	1520.12	0.0334	2	9.525	0.2	44.00	0.00	28737	cyl/sp	6.86	74.71	48.67	89.34	75.53	101.10
Mphonde_1984_012_AO-11-2	590		AO-11-2	152.4	336.55	51290.22	45483.78	1492	721	2.41	25	298	197000	414	1520.12	0.0334	2	9.525	0.2	77.25	0.00	28737	cyl/sp	6.86	85.44	64.48	102.76	93.22	117.90
Mphonde_1984_013_AO-15-2a	591		AO-15-2a	152.4	336.55	51290.22	45483.78	1492	721	2.41	25	298	197000	414	1520.12	0.0334	2	9.525	0.2	81.61	0.00	28737	cyl/sp	6.86	86.22	66.28	103.86	95.12	119.24
Mphonde_1984_014_AO-15-2b	592		AO-15-2b	152.4	336.55	51290.22	45483.78	1492	721	2.41	25	298	197000	414	1520.12	0.0334	2	9.525	0.2	67.62	0.00	28737	cyl/sp	6.86	83.87	60.33	100.15	88.75	114.71
Niwa_1987_001_1	593	Niwa;	1	600	2100	1260000	1200000	12000	5968	2.98	23	2000	197000	999	3324.00	0.0028	2	25	0.2	25.76	2.17	28737	cyl/sp	6.86	418.68	509.39	359.83	452.36	388.61
Niwa_1987_002_2	594	Yamada et al. (1987)	2	600	2100	1260000	1200000	12000	5968	2.98	23	2000	197000	999	1662.00	0.0014	2	25	0.2	24.93	2.05	28737	cyl/sp	6.86	328.71	501.14	251.35	340.51	279.28
Niwa_1987_003_3	595		3	300	1100	330000	300000	6000	2984	2.98	23	1000	197000	999	415.50	0.0014	2	25	0.2	23.37	1.93	28737	cyl/sp	6.86	101.32	177.89	73.25	104.37	90.74
Podgorniak_1998_001_BRL100	596	Podgorniak-Stanik (1998)	BRL100	300	1000	300000	277500	5400	2663	2.88	30	925	197000	550	1404.31	0.0051	2	10	0.2	89.30	0.00	28737	cyl/sp	6.86	187.10	262.81	206.71	219.21	226.72
Podgorniak_1998_001_BRH100	597		BRH100	300	1000	300000	268500	5400	2663	2.97	30	895	197000	550	8425.85	0.0314	2	10	0.2	89.30	0.00	28737	cyl/sp	6.86	333.48	259.02	430.29	385.68	469.21
Podgorniak_1998_002_BN100	598		BN100	300	1000	300000	277500	5400	2663	2.88	30	925	197000	550	2106.46	0.0076	2	10	0.2	35.15	0.00	28737	cyl/sp	6.86	169.87	164.88	170.72	188.31	187.29
Podgorniak_1998_003_BH100	599		BH100	300	1000	300000	277500	5400	2663	2.88	30	925	197000	550	2106.46	0.0076	2	10	0.2	94.05	0.00	28737	cyl/sp	6.86	216.33	269.70	251.10	259.49	271.87
Podgorniak_1998_004_BN50	600		BN50	300	500	150000	135000	2700	1313	2.92	25	450	197000	486	1096.05	0.0081	2	10	0.2	35.15	0.00	28737	cyl/sp	6.86	107.09	112.94	104.09	116.90	116.62
Podgorniak_1998_005_BH50	601		BH50	300	500	150000	135000	2700	1313	2.92	25	450	197000	486	1096.05	0.0081	2	10	0.2	94.05	0.00	28737	cyl/sp	6.86	136.39	184.74	143.36	159.60	161.30
Podgorniak_1998_006_BN25	602		BN25	300	250	75000	67500	1352	664	2.95	16	225	197000	437	603.19	0.0089	2	10	0.2	35.15	0.00	28737	cyl/sp	6.86	69.46	70.00	68.24	69.18	69.62
Podgorniak_1998_007_BH25	603		BH25	300	250	75000	67500	1352	664	2.95	16	225	197000	437	603.19	0.0089	2	10	0.2	94.05	0.00	28737	cyl/sp	6.86	88.46	114.49	88.76	94.09	95.26
Rajagopalan_1968_001_S-13	604	Rajagopalan;	S-13	152.146	311.15	47340.228	40306.823	2540	1118	4.22	17	265	197000	655	696.77	0.0173	2	12.7	0.2	22.54	2.57	28737	cyl/sp	6.86	38.69	32.97	42.88	39.17	42.46
Rajagopalan_1968_002_S-1	605	Ferguson (1968)	S-1	153.924	311.15	47893.453	39800.437	2337	1016	3.93	16	259	197000	655	567.74	0.0143	2	12.7	0.2	34.72	2.82	28737	cyl/sp	6.86	43.95	40.66	42.84	43.06	43.87
Rajagopalan_1968_003_S-2	606		S-2	153.924	311.15	47893.453	40816.951	2337	1016	3.83	13	265	197000	655	400.00	0.0098	2	12.7	0.2	31.45	2.87	28737	cyl/sp	6.86	38.37	39.43	37.21	37.60	39.06
Rajagopalan_1968_004_S-3	607		S-3	152.4	311.15	47419.26	40645.08	2540	1118	4.19	12	267	197000	524	329.03	0.0081	2	12.7	0.2	27.52	2.56	28737	cyl/sp	6.86	32.31	36.68	31.11	32.31	32.65
Rajagopalan_1968_005_S-4	608		S-4	152.4	311.15	47419.26	40877.338	2540	1118	4.17	10	268	197000	524	258.06	0.0063	2	12.7	0.2	31.45	2.46	28737	cyl/sp	6.86	31.21	39.38	27.73	30.78	30.11
Rajagopalan_1968_006_S-5	609		S-5	152.4	311.15	47419.26	39909.598	2540	1118	4.27	9	262	197000	1779	210.97	0.0053	2	12.7	0.2	26.53	2.37	28737	cyl/sp	6.86	27.36	35.53	24.33	26.45	25.83
Rajagopalan_1968_007_S-9	610		S-9	151.892	311.15	47261.196	39737.985	2540	1118	4.27	9	262	197000	1779	210.97	0.0053	2	12.7	0.2	23.85	2.29	28737	cyl/sp	6.86	26.34	33.54	23.83	25.54	25.08
Rajagopalan_1968_008_S-6	611		S-6	150.876	311.15	46945.067	40353.597	2540	1118	4.18	8	267	197000	1779	140.64	0.0035	2	12.7	0.2	29.48	2.57	28737	cyl/sp	6.86	24.76	37.67	21.00	23.37	23.17
Rajagopalan_1968_009_S-7	612		S-7	152.4	311.15	47419.26	40877.338	2540	1118	4.17	7	268	197000	1779	103.23	0.0025	2	12.7	0.2	27.19	2.77	28737	cyl/sp	6.86	21.91	36.62	18.72	20.18	20.78
Rajagopalan_1968_010_S-12	613		S-12	153.162	311.15	47656.356	41120.627	2540	1118	4.16	7	268	197000	1779	103.23	0.0025	2	12.7	0.2	28.17	2.59	28737	cyl/sp	6.86	22.25	37.48	18.35	20.46	20.54
Regan_1971_001_R1	614	Regan (1971)	R1	152	304	46208	41344	1828	889	3.27	16	272	197000	630	603.19	0.0146	2	19	0.2	24.60	0.00	28737	cyl/sp	6.86	44.95	36.85	44.71	43.78	47.79
Regan_1971_002_R2	615		R2	152	304	46208	41344	1828	889	3.27	16	272	197000	630	603.19	0.0146	2	19	0.2	24.60	0.00	28737	cyl/sp	6.86	44.95	36.85	44.71	43.78	47.79
Regan_1971_003_R3	616		R3	152	304	46208	41344	1828	889	3.27	16	272	197000	630	603.19	0.0146	2	19	0.2	23.25	0.00	28737	cyl/sp	6.86	44.11	35.82	44.00	42.95	46.93
Regan_1971_007_R7	617		R7	152	304	46208	41344	1828	889	3.27	16	272	197000	630	603.19	0.0146	2	19	0.2	26.40	0.00	28737	cyl/sp	6.86	46.02	38.17	45.63	44.84	48.89
Regan_1971_008_R29	618		R29	152	304	46208	41344	1828	889	3.27	16	272	197000	630	603.19	0.0146	2	19	0.2	28.43	0.00	28737	cyl/sp	6.86	47.17	39.61	46.64	45.97	50.07
Regan_1971_009_K3	619		K3	152	305	46360	41344	3655	1803	6.63	16	272	197000	630	1608.50	0.0389	2	19	0.2	31.05	0.00	28737	cyl/sp	6.86	61.29	41.40	53.70	51.69	55.39
Rehm_1978_001_P 1	620	Rehm; Eligehausen; Neubert (1978)	P 1	900	340	306000	281700	3000	1000	3.19	11	313	197000	564	3421.19	0.0121	2	30	0.2	22.50	2.60	28737	cyl/sp	6.86	280.57	247.16	303.66	280.02	324.01
Reinneck_1978_002_N6	621	Reineck; Koch;	N6	500	250	125000	113000	2500	565	2.50	12	226	197000	501	887.20	0.0079	2	16	0.2	24.49	2.45	28737	cyl/sp	6.86	110.37	102.47	119.33	107.56	127.70
Reinneck_1978_003_N7	622	Schlaich (1978)	N7	500	250	125000	112500	2500	563	2.50	14	225	197000	441	1569.00	0.0139	2	16	0.2	23.39	2.81	28737	cyl/sp	6.86	131.24	99.79	159.47	127.30	168.64
Reinneck_1978_004_N8	623		N8	500	250	125000	113000	2500	791	3.50	12	226	197000	501	887.20	0.0079	2	16	0.2	24.49	2.45	28737	cyl/sp	6.86	101.36	102.47	98.46	95.29	101.81
Remmel_1991_002_2	624	Remmel (1991)	2	150	200	30000	24750	1026	505	3.06	14	165	197000	523	461.81	0.0187	2	16	0.2	80.82	4.77	28737	cyl/sp	6.86	46.48	43.14	50.32	45.44	50.09
Remmel_1991_003_3	625		3	150	200	30000	24750	1840	660	4.00	14	165	197000	523	461.81	0.0187	2	16	0.2	80.82	4.77	28737	cyl/sp	6.86	41.62	43.14	44.74	41.30	43.01
Remmel_1991_005_5	626		5	150	200	30000	24000	995	490	3.06	25	160	197000	554	981.75	0.0409	2	16	0.2	80.27	4.73	28737	cyl/sp	6.86	59.12	41.89	68.88	56.64	61.45
Remmel_1991_006_6	627		6	150	200	30000	24000	1750	640	4.00	25	160	197000	554	981.75	0.0409	2	16	0.2	80.27	4.73	28737	cyl/sp	6.86	52.93	41.89	60.83	52.29	52.89
Rosenbusch_2002_001_1.2 / 1	628	Rosenbusch;	1.2 / 1	200	300	60000	52000	1800	875	3.37	28	260	197000	550	1847.26	0.0355	2	16	0.2	41.25	3.07	28737	cyl/sp	6.86	88.41	59.38	95.17	84.61	95.48
Rosenbusch_2002_003_2.3 / 1	629		2.3 / 1	200	300	60000	52400	2300	650	2.48	16	262	197000	550	603.19	0.0115	2	16	0.2	37.61	2.68	28737	cyl/sp	6.86	63.99	57.04	65.95	64.27	73.12
Rosenbusch_2002_004_2.4 / 1	630		2.4 / 1	200	300	60000	52000	2250	625	2.40	20	260	197000	550	942.48	0.0181	2	16	0.2	37.61	2.68	28737	cyl/sp	6.86	74.73	56.70	82.36	74.42	88.97
Rosenbusch_2002_005_2.6 / 1	631		2.6 / 1	200	300	60000	52000	2250	1025	3.94	20	260	197000	550	942.48	0.0181	2	16	0.2	38.28	2.57	28737	cyl/sp	6.86	66.45	57.21	62.06	64.03	63.87
Ruesch_1962_001_X	632	Ruesch;	X	90	134	12060	9990	1250	400	3.60	11	111	197000	481	264.74	0.0265	2	30	0.2	21.86	2.04	28737	cyl/sp	6.86	17.55	9.89	20.53	13.25	16.85
Ruesch_1962_002_Y	633	Haugli (1962)	Y	120	229	27480	23880	2240	717	3.60	16	199	197000	407	633.72	0.0265	2	30	0.2	21.86	2.04	28737	cyl/sp	6.86	34.56	22.24	38.48	30.35	37.57
Ruesch_1962_003_Z	634		Z	180	301	54180	47160	2960	947	3.62	23	262	197000	412	1246.43	0.0264	2	30	0.2	23.02	2.53	28737	cyl/sp	6.86	63.21	43.23	71.58	59.13	69.80
Salandra_1989_003_LR-2.59-NS	635	Salandra;	LR-2.59-NS	101.6	203.2	20645.12	17419.32	1345	444	2.59	13	171	197000	414	253.35	0.0145	2	12.7	0.2	52.03	0.00	28737	cyl/sp	6.86	28.13	23.75	30.10	26.46	30.72
Salandra_1989_004_LR-3.63-NS	636	Ahmad (1989)	LR-3.63-NS	101.6	203.2	20645.12	17419.32	1702	622	3.63	13	171	197000	414	253.35	0.0145	2	12.7	0.2	50.38	0.00	28737	cyl/sp	6.86	25.59	23.37	25.02	23.28	24.24
Salandra_1989_007_HR-2.59-NS	637		HR-2.59-NS	101.6	203.2	20645.12	17419.32	1345	444	2.59	13	171	197000	414	253.35	0.0145	2	12.7	0.2	64.72	0.00	28737	cyl/sp	6.86	29.61	26.49	31.61	28.43	32.91
Salandra_1989_008_HR-3.63-NS	638		HR-3.63-NS	101.6	203.2	20645.12	17419.32	1702	622	3.63	13	171	197000	414	253.35	0.0145	2	12.7	0.2	66.62	0.00	28737	cyl/sp	6.86	27.28	26.88	26.92	25.45	26.57
Scholz_1994_002_A-2	639	Scholz (1994)	A-2	200	400	80000	74400	3500	1116	3.00	16	372	197000	500	603.19	0.0081	2	16	0.2	76.37	4.91	28737	cyl/sp	6.86	80.72	105.45	84.41	88.87	91.36
Scholz_1994_005_B-2	640		B-2	200	400	80000	73600	3500	1104	3.00	25	368	197000	500	1472.62	0.0200	2	16	0.2	80.28	4.87	28737	cyl/sp	6.86	108.75	107.15	123.84	123.66	133.76
Scholz_1994_006_B-3	641		B-3	200	400	80000	73600	3500	1472	4.00	25	368	197000	500	1472.62	0.0200	2	16	0.2	80.28	4.87	28737	cyl/sp	6.86	96.89	107.15	112.34	112.16	117.83
Scholz_1994_008_C-2	642		C-2	200	400	80000	73200	3500	1098	3.00	28	366	197000	500	2463.01	0.0336	2	16	0.2	79.71	4.91	28737	cyl/sp	6.86	128.77	106.36	153.61	144.13	166.62
Scholz_1994_009_C-3	643		C-3	200	400	80000	73200	3500	1464	4.00	28	366	197000	500	2463.01	0.0336	2	16	0.2	79.71	4.91	28737	cyl/sp	6.86	114.72	106.36	138.79	132.28	146.05
Scholz_1994_011_D-2	644		D-2	200	400	80000	72400	3500	1086	3.00	16	362	197000	500	1407.43	0.0194	2	16	0.2	91.96	5.37	28737	cyl/sp	6.86	108.21	113.36	127.68	126.48	139.42
Scholz_1994_012_D-3	645		D-3	200	400	80000	72400	3500	1448	4.00	16	362	197000	500	1407.43	0.0194	2	16	0.2	91.96	5.37	28737	cyl/sp	6.86	96.41	113.36	116.56	114.48	122.92
Shin_1999_003_MHB 2.5-0	646	Shin; Lee;	MHB 2.5-0	125	250	31250	26875	1075	526	2.45	25	215	197000	410	1013.41	0.0377	2	19	0.2	49.40	0.00	28737	cyl/sp	6.86	58.97	35.57	69.69	53.80	69.56
Shin_1999_006_HB 2.5-0	647	Moon; Ghosh (1999)	HB 2.5-0	125	250	31250	26875	1075	526	2.45	25	215	197000	410	1013.41	0.0377	2	13	0.2	69.35	0.00	28737	cyl/sp	6.86	59.59	40.57	71.71	59.34	74.10
Swamy_1971_001_M1N3D	648	Swamy;	M1N3D	152.4	228.6	34838.64	26128.98	3124	514	3.00	19	171	197000	414	1140.09	0.0436	2	38.1	0.2	20.95	2.63	28737	cyl/sp	6.86	48.31	24.71	66.90	39.91	54.52
Swamy_1971_002_M1N3	649	Qureshi (1971)	M1N3	152.4	228.6	34838.64	26128.98	3124	514	3.00	19	171	197000	414	1140.09	0.0436	2	19.05	0.2	27.93	2.58	28737	cyl/sp	6.86	50.88	27.00	62.20	42.74	53.24
Swamy_1971_003_M1N3A	650		M1N3A	152.4	228.6	34838.64	26128.98	3124	514	3.00	19	171	197000	414	1140.09	0.0436	2	19.05	0.2	29.05	2.67	28737	cyl/sp	6.86	51.55	27.54	62.80	43.39	54.01
Swamy_1971_004_M1N3B	651		M1N3B	152.4	228.6	34838.64	26128.98	3124	514	3.00	19	171	197000	414	1140.09	0.0436	2	9.525	0.2	26.44	2.43	28737	cyl/sp	6.86	44.95	24.83	56.03	40.06	48.58
Swamy_1971_005_M2N3A	652		M2N3A	76.2	114.3	8709.66	6522.5676	1562	257	3.01	10	86	197000	414	285.02	0.0437	2	19.05	0.2	29.05	2.67	28737	cyl/sp	6.86	16.22	7.43	20.93	11.50	15.98
Swamy_1971_006_M2N3	653		M2N3	76.2	114.3	8709.66	6522.5676	1562	257	3.01	10	86	197000	414	285.02	0.0437	2	9.525	0.2	30.07	2.81	28737	cyl/sp	6.86	14.76	7.33	19.25	11.38	15.06
Swamy_1971_007_M2N3B	654		M2N3B	76.2	114.3	8709.66	6522.5676	1562	257	3.01	10	86	197000	414	285.02	0.0437	2	9.525	0.2	29.33	2.86	28737	cyl/sp	6.86	14.64	7.24	19.26	11.27	15.04
Swamy_1971_008_M2N3C	655		M2N3C	76.2	114.3	8709.66	6522.5676	1562	257	3.01	10	86	197000	414	285.02	0.0437	2	6.35	0.2	27.70	2.61	28737	cyl/sp	6.86	13.74	6.92	17.90	10.89	14.03
Swamy_1971_009_M3N3B	656		M3N3B	50.8	76.2	3870.96	2903.22	1041	171	3.00	6	57	197000	414	126.68	0.0436	2	9.525	0.2	29.33	2.86	28737	cyl/sp	6.86	7.46	3.34	10.19	5.16	7.41
Swamy_1971_010_M3N3	657		M3N3	50.8	76.2	3870.96	2903.22	1041	171	3.00	6	57	197000	414	126.68	0.0436	2	6.35	0.2	28.40	2.72	28737	cyl/sp	6.86	7.06	3.25	9.54	5.05	7.00
Swamy_1971_011_M3N3C	658		M3N3C	50.8	76.2	3870.96	2903.22	1041	171	3.00	6	57	197000	414	126.68	0.0436	2	6.35	0.2	27.70	2.61	28737	cyl/sp	6.86	7.00	3.21	9.47	5.01	6.92
Swamy_1971_012_M1N8	659		M1N8	152.4	228.6	34838.64	26128.98	3124	1372	8.00	19	171	197000	414	1140.09	0.0436	2	19.05	0.2	30.72	2.76	28737	cyl/sp	6.86	46.79	28.32	40.28	33.70	33.38
Swamy_1971_015_M3N4	660		M1N4	152.4	228.6	34838.64	26128.98	3124	686	4.00	19	171	197000	414	1140.09	0.0436	2	19.05	0.2	29.05	2.89	28737	cyl/sp	6.86	45.93	27.54	54.61	40.43	45.65
Swamy_1971_016_M2N4	661		M2N4	76.2	114.3	8709.66	6522.5676	1562	343	4.01	10	86	197000	414	285.02	0.0437	2	9.525	0.2	27.93	2.67	28737	cyl/sp	6.86	12.84	7.07	16.06	10.30	12.19
Swamy_1971_017_M3N4	662		M3N4	50.8	76.2	3870.96	2903.22	1041	229	4.00	6	57	197000	414	126.68	0.0436	2	6.35	0.2	28.16	2.67	28737	cyl/sp	6.86	6.27	3.24	8.01	4.69	5.76
Taylor1_1968_001_1A	663	Taylor (1968)	1A	203.2	406.4	82580.48	75161.14	4572	1118	3.02	22	370	197000	350	775.90	0.0103	2	9.525	0.2	27.41	0.00	28737	cyl/sp	6.86	62.53	59.24	61.60	67.13	66.91
Taylor1_1968_002_2A	664		2A	203.2	406.4	82580.48	75161.14	4572	1118	3.02	22	370	197000	350	1163.84	0.0155	2	9.525	0.2	31.55	0.00	28737	cyl/sp	6.86	75.01	63.55	77.64	80.17	84.01
Taylor1_1968_005_5A	665		5A	203.2	406.4	82580.48	75161.14	4572	914	2.47	22	370	197000	350	775.90	0.0103	2	9.525	0.2	28.45	0.00	28737	cyl/sp	6.86	66.74	60.35	69.89	72.57	77.92
Taylor1_1968_007_1B	666		1B	203.2	406.4	82580.48	75161.14	4572	1118	3.02	22	370	197000	350	775.90	0.0103	2	9.525	0.2	27.41	0.00	28737	cyl/sp	6.86	62.53	59.24	61.60	67.13	66.91
Taylor1_1968_008_2B	667		2B	203.2	406.4	82580.48	75161.14	4572	1118	3.02	22	370	197000	350	1163.84	0.0155	2	9.525	0.2	31.55	0.00	28737	cyl/sp	6.86	75.01	63.55	77.64	80.17	84.01
Taylor1_1968_009_3B	668		3B	203.2	406.4	82580.48	75161.14	4572	1118	3.02	22	370	197000	350	775.90	0.0103	2	9.525	0.2	30.00	0.00	28737	cyl/sp	6.86	64.43	61.97	63.56	69.17	69.20
Taylor1_1968_011_5B	669		5B	203.2	406.4	82580.48	75161.14	4572	914	2.47	22	370	197000	350	775.90	0.0103	2	9.525	0.2	28.45	0.00	28737	cyl/sp	6.86	66.74	60.35	69.89	72.57	77.92
Taylor1_1968_012_6B	670		6B	203.2	406.4	82580.48	75161.14	4572	1295	3.50	22	370	197000	350	775.90	0.0103	2	9.525	0.2	26.38	0.00	28737	cyl/sp	6.86	59.57	58.11	56.44	63.06	60.41
Taylor2_1972_001_A1	671	Taylor (1972)	A1	400	1000	400000	372000	6500	2800	3.01	40	930	197000	420	5026.55	0.0135	2	38	0.2	27.30	0.00	28737	cyl/sp	6.86	289.02	276.95	293.12	348.77	314.04
Taylor2_1972_002_A2	672		A2	400	1000	400000	372000	6500	2800	3.01	40	930	197000	420	5026.55	0.0135	2	19	0.2	21.47	0.00	28737	cyl/sp	6.86	255.15	202.52	247.44	279.60	264.54
Taylor2_1972_003_B1	673		B1	200	500	100000	93000	3250	1400	3.01	20	465	197000	420	1256.64	0.0135	2	38	0.2	25.50	0.00	28737	cyl/sp	6.86	88.99	82.64	91.14	98.44	96.69
Taylor2_1972_004_B2	674		B2	200	500	100000	93000	3250	1400	3.01	20	465	197000	420	1256.64	0.0135	2	19	0.2	20.93	0.00	28737	cyl/sp	6.86	79.69	66.17	78.73	84.49	83.35
Taylor2_1972_005_B3	675		B3	200	500	100000	93000	3250	1400	3.01	20	465	197000	420	1256.64	0.0135	2	9	0.2	27.00	0.00	28737	cyl/sp	6.86	77.55	66.23	78.78	84.54	84.19
Walraven_1978_001_A1	676	Walraven (1978)	A1	200	150	30000	25000	1750	375	3.00	10	125	197000	440	207.35	0.0083	2	16	0.2	22.90	2.24	28737	cyl/sp	6.86	28.24	24.11	29.94	23.67	24.92
Walraven_1978_002_A2	677		A2	200	450	90000	84000	3520	1260

Lubell_2006_001_AW1	685	Lubell (2006)	AW1	1170	590	690300	629460	3700	1774	3.30	25	538	197000	467	5000.00	0.0079	2	10	0.2	35.06	3.90	28737	cyl/sp	6.86	452.78	488.92	520.42	493.65	565.28
Lubell_2006_002_AW4	686		AW4	1168	590	689120	591008	3700	1774	3.51	25	506	197000	467	10000.00	0.0169	2	10	0.2	37.91	0.00	28737	cyl/sp	6.86	564.79	489.87	581.78	610.36	644.02
Lubell_2006_003_AW8	687		AW8	1169	591	690879	592683	3700	1812	3.57	25	507	197000	467	10000.00	0.0169	2	10	0.2	37.43	3.62	28737	cyl/sp	6.86	560.58	487.77	645.51	604.91	712.05
Lubell_2006_004_AX6	688		AX6	703	338	237614	202464	2080	1002	3.48	25	288	197000	467	3500.00	0.0173	2	10	0.2	38.95	0.00	28737	cyl/sp	6.86	237.70	207.11	241.41	243.63	241.63
Lubell_2006_005_AX7	689		AX7	704	335	235840	202048	2080	1002	3.49	20	287	197000	413	2100.00	0.0104	2	10	0.2	38.95	0.00	28737	cyl/sp	6.86	200.28	206.90	191.99	204.10	195.93
Lubell_2006_006_AX8	690		AX8	705	339	238995	203745	2080	1002	3.47	25	289	197000	467	3500.00	0.0172	2	10	0.2	38.95	0.00	28737	cyl/sp	6.86	238.62	208.22	242.38	244.78	242.93
Lubell_2006_007_AY1	691		AY1	249	467	116283	108066	2600	1262	2.91	15	434	197000	900	354.00	0.0033	2	10	0.2	38.67	0.00	28737	cyl/sp	6.86	66.24	96.14	57.54	68.90	64.48
Sherwood_2008_001_L-10N1	692	Sherwood (2008)	L-10N1	300	1510	453000	420000	8100	4012	2.87	30	1400	197000	452	3500.00	0.0083	2	9.5	0.2	36.48	0.00	28737	cyl/sp	6.86	232.63	194.48	249.62	247.99	271.68
Sherwood_2008_002_L-10N2	693	Sherwood;Bentz;	L-10N2	300	1510	453000	420000	8100	4012	2.87	30	1400	197000	452	3500.00	0.0083	2	9.5	0.2	38.29	0.00	28737	cyl/sp	6.86	236.41	199.24	256.31	252.19	278.68
Sherwood_2008_003_L-10H	694	Collins (2007)	L-10H	300	1510	453000	420000	8100	4012	2.87	30	1400	197000	452	3500.00	0.0083	2	9.5	0.2	69.92	0.00	28737	cyl/sp	6.86	279.18	269.25	341.90	309.72	366.54
Sherwood_2008_004_L-20N1	695		L-20N1	300	1510	453000	420000	8100	4012	2.87	30	1400	197000	452	3500.00	0.0083	2	19	0.2	29.83	0.00	28737	cyl/sp	6.86	241.76	216.12	236.43	266.78	258.34
Sherwood_2008_005_L-20N2	696		L-20N2	300	1510	453000	420000	8100	4012	2.87	30	1400	197000	452	3500.00	0.0083	2	19	0.2	31.54	0.00	28737	cyl/sp	6.86	246.29	222.23	243.08	271.93	265.54
Sherwood_2008_006_L-40N1	697		L-40N1	300	1510	453000	420000	8100	4012	2.87	30	1400	197000	452	3500.00	0.0083	2	38	0.2	26.70	0.00	28737	cyl/sp	6.86	243.57	259.34	238.28	302.01	260.12
Sherwood_2008_007_L-40N2	698		L-40N2	300	1510	453000	420000	8100	4012	2.87	30	1400	197000	452	3500.00	0.0083	2	38	0.2	27.08	0.00	28737	cyl/sp	6.86	244.72	261.18	239.80	303.45	261.82
Sherwood_2008_008_L-50N1	699		L-50N1	300	1510	453000	420000	8100	4012	2.87	30	1400	197000	452	3500.00	0.0083	2	51	0.2	38.95	0.00	28737	cyl/sp	6.86	276.26	346.00	290.95	365.60	317.82
Sherwood_2008_009_L-50N2	700		L-50N2	300	1510	453000	420000	8100	4012	2.87	30	1400	197000	452	3500.00	0.0083	2	51	0.2	38.10	0.00	28737	cyl/sp	6.86	274.23	342.18	287.92	362.96	314.54
Sherwood_2008_010_L-50N2R	701		L-50N2R	300	1510	453000	420000	8100	4012	2.87	30	1400	197000	452	3500.00	0.0083	2	51	0.2	38.10	0.00	28737	cyl/sp	6.86	274.23	342.18	287.92	362.96	314.54
Sherwood_2008_011_S-10N1	702		S-10N1	122	330	40260	34160	1620	780	2.78	10	280	197000	494	285.20	0.0083	2	9.5	0.2	39.81	0.00	28737	cyl/sp	6.86	33.58	35.41	33.10	34.87	39.61
Sherwood_2008_012_S-10N2	703		S-10N2	122	330	40260	34160	1620	780	2.78	10	280	197000	494	285.20	0.0083	2	9.5	0.2	39.81	0.00	28737	cyl/sp	6.86	33.58	35.41	33.10	34.87	39.61
Sherwood_2008_013_S-10H	704		S-10H	122	330	40260	34160	1620	780	2.78	10	280	197000	494	285.20	0.0083	2	9.5	0.2	73.44	0.00	28737	cyl/sp	6.86	39.41	48.09	39.66	42.28	48.52
Sherwood_2008_014_S-20N1	705		S-20N1	122	330	40260	34160	1620	780	2.78	10	280	197000	494	285.20	0.0083	2	19	0.2	37.24	0.00	28737	cyl/sp	6.86	36.50	37.22	35.00	36.00	41.34
Sherwood_2008_015_S-20N2	706		S-20N2	122	330	40260	34160	1620	780	2.78	10	280	197000	494	285.20	0.0083	2	19	0.2	36.20	0.00	28737	cyl/sp	6.86	36.15	36.69	34.70	35.67	40.90
Sherwood_2008_016_S-40N1	707		S-40N1	122	330	40260	34160	1620	780	2.78	10	280	197000	494	285.20	0.0083	2	38	0.2	27.65	0.00	28737	cyl/sp	6.86	34.55	34.86	34.99	34.52	40.09
Sherwood_2008_017_S-40N2	708		S-40N2	122	330	40260	34160	1620	780	2.78	10	280	197000	494	285.20	0.0083	2	38	0.2	27.65	0.00	28737	cyl/sp	6.86	34.55	34.86	34.99	34.52	40.09
Sherwood_2008_018_S-50N1	709		S-50N1	122	330	40260	34160	1620	780	2.78	10	280	197000	494	285.20	0.0083	2	51	0.2	41.33	0.00	28737	cyl/sp	6.86	39.51	43.98	40.48	39.99	47.48
Sherwood_2008_019_S-50N2	710		S-50N2	122	330	40260	34160	1620	780	2.78	10	280	197000	494	285.20	0.0083	2	51	0.2	41.33	0.00	28737	cyl/sp	6.86	39.51	43.98	40.48	39.99	47.48
Sherwood_2008_020_L-20L	711		L-20L	295	1510	445450	427750	8100	4012	2.77	26	1450	197000	880	1088.00	0.0025	2	19	0.2	33.63	0.00	28737	cyl/sp	6.86	172.08	228.89	149.16	185.24	160.86
Sherwood_2008_021_L-20LR	712		L-20LR	295	1510	445450	427750	8100	4012	2.77	26	1450	197000	880	1088.00	0.0025	2	19	0.2	33.63	0.00	28737	cyl/sp	6.86	172.08	228.89	149.16	185.24	160.86
Thiele_2010_001_T1-ohne	713	Thiele (2010)	T1_ohne	400	300	120000	99200	2100	1030	4.15	14	248	197000	581	923.63	0.0093	2	16	0.2	24.32	0.00	28737	cyl/sp	6.86	84.24	87.91	77.87	82.43	76.84
Thiele_2010_002_T7_70_oben	714		T7_70_oben	400	350	140000	118800	2100	1030	3.47	16	297	197000	580	1608.50	0.0135	2	16	0.2	23.40	0.00	28737	cyl/sp	6.86	115.16	98.98	112.06	115.08	121.58
Thiele_2010_003_T9-ohne	715		T9_ohne	400	200	80000	66800	1700	830	4.97	16	167	197000	632	1608.50	0.0241	2	16	0.2	39.68	0.00	28737	cyl/sp	6.86	104.57	81.42	99.81	89.62	90.09
Thiele_2010_004_T13-ohne	716		T13_ohne	400	250	100000	86800	1700	830	3.82	16	217	197000	632	1608.50	0.0185	2	16	0.2	40.35	0.00	28737	cyl/sp	6.86	121.61	101.86	119.41	113.55	120.92
Thiele_2010_005_T10_40_oben	717		T10_40_oben	400	250	100000	66800	1700	830	4.97	16	167	197000	632	1608.50	0.0241	2	16	0.2	39.68	0.00	28737	cyl/sp	6.86	104.57	81.42	99.81	89.62	85.78
Injaganeri_2007_001_H20-0-0	718	Injaganeri (2007)	H20-0-0	150	200	30000	24150	966	464	2.88	16	161	197000	521	603.19	0.0250	2	16	0.2	47.88	0.00	28737	cyl/sp	6.86	46.76	32.52	51.30	41.77	47.68
Injaganeri_2007_002_H40-0-0	719		H40-0-0	150	400	60000	51750	2070	1016	2.95	16	345	197000	521	1206.37	0.0233	2	16	0.2	55.58	0.00	28737	cyl/sp	6.86	79.39	63.86	85.30	81.95	96.09
Injaganeri_2007_003_H60-0-0	720		H60-0-0	150	600	90000	80400	3216	1589	2.97	20	536	197000	595	2513.27	0.0313	2	16	0.2	55.58	0.00	28737	cyl/sp	6.86	117.25	85.88	131.81	124.52	145.11
Winkler_2011_001_SB2	721	Winkler (2011)	SB 2	150	240	36000	30000	1601	782	3.91	10	200	197000	573	358.12	0.0119	2	16	0.2	33.35	2.61	28737	cyl/sp	6.86	34.83	32.50	32.55	31.71	33.48
Winkler_2011_002_SB3	722		SB 3	150	345	51750	45000	2400	1175	3.92	12	300	197000	566	530.94	0.0118	2	16	0.2	33.35	2.61	28737	cyl/sp	6.86	45.45	44.64	42.21	44.73	45.79
Winkler_2011_003_SB4	723		SB 4	225	495	111375	101250	3600	1769	3.93	12	450	197000	567	1218.96	0.0120	2	16	0.2	33.35	2.61	28737	cyl/sp	6.86	89.86	89.17	84.28	93.74	89.49
Winkler_2011_004_SB5	724		SB 5	300	647	194100	180000	4800	2363	3.94	16	600	197000	590	2158.26	0.0120	2	16	0.2	33.35	2.61	28737	cyl/sp	6.86	144.89	142.52	137.73	155.11	144.79
Winkler_2011_005_SB6	725		SB 6	450	950	427500	405000	7200	3550	3.94	20	900	197000	571	4860.06	0.0120	2	16	0.2	33.35	2.61	28737	cyl/sp	6.86	284.75	266.80	279.71	308.71	290.52
Rosenbusch_2003_001_1.1-1	726	Rosenbusch (2003)	1.1-1	200	300	60000	52000	1800	875	3.37	12	260	197000	550	339.29	0.0065	2	16	0.2	41.25	0.00	28737	cyl/sp	6.86	50.26	59.38	44.92	47.84	48.58
Rosenbusch_2003_002_1.2-1	727		2.1-1	200	300	60000	52000	1800	875	3.37	28	260	197000	550	1847.26	0.0355	2	16	0.2	41.25	0.00	28737	cyl/sp	6.86	88.41	59.38	95.47	84.61	95.68
Tureyen_2002_001_V-S-1	728	Tureyen; Frosch (2002)	V-S-1	457.2	406.4	185806.08	164757.74	2438	1181	3.28	16	360	197000	524	1583.46	0.0096	2	19.05	0.2	38.85	3.13	28737	cyl/sp	6.86	165.24	172.36	157.77	167.80	174.60
Tureyen_2002_002_V-S-2	729	Tureyen (2001)	V-S-2	457.2	426.72	195096.38	164757.74	2438	1181	3.28	16	360	197000	524	3166.92	0.0192	2	19.05	0.2	39.31	3.53	28737	cyl/sp	6.86	209.00	173.37	224.83	213.08	252.82
Tureyen_2002_003_V-D-2	730		V-D-2	457.2	406.4	185806.08	164757.74	2438	1181	3.28	16	360	197000	745	593.80	0.0036	2	19.05	0.2	41.47	3.37	28737	cyl/sp	6.86	121.78	178.07	103.80	116.65	113.84
bentz_2005_001_SBB1.1	731	Bentz; Buckley (2005)	SBB1.1	104	103	10712	8736	495	235	2.80	10	84	197000	400	142.00	0.0163	2	10	0.2	33.82	0.00	28737	cyl/sp	6.86	15.25	10.46	17.50	12.30	13.69
bentz_2005_002_SBB1.2	732		SBB1.2	105	103	10815	8820	495	235	2.80	10	84	197000	400	142.00	0.0161	2	10	0.2	33.82	0.00	28737	cyl/sp	6.86	15.35	10.56	17.59	12.38	13.75
bentz_2005_003_SBB1.3	733		SBB1.3	104	103	10712	8736	495	235	2.80	10	84	197000	400	142.00	0.0163	2	10	0.2	33.82	0.00	28737	cyl/sp	6.86	15.25	10.46	17.50	12.30	13.69
bentz_2005_004_SBB2.1	734		SBB2.1	106	206	21836	17808	990	483	2.87	10	168	197000	400	284.00	0.0159	2	10	0.2	32.59	0.00	28737	cyl/sp	6.86	24.05	18.93	26.01	22.79	26.75
bentz_2005_005_SBB2.2	735		SBB2.2	105	206	21630	17640	990	483	2.87	10	168	197000	400	284.00	0.0161	2	10	0.2	32.59	0.00	28737	cyl/sp	6.86	23.90	18.75	25.87	22.65	26.63
bentz_2005_006_SBB2.3	736		SBB2.3	106	204	21624	17596	990	483	2.91	10	166	197000	400	284.00	0.0161	2	10	0.2	32.59	0.00	28737	cyl/sp	6.86	23.88	18.75	25.78	22.56	26.34
bentz_2005_007_SBB3.1	737		SBB3.1	105	378	39690	34965	1980	978	2.94	15	333	197000	400	542.00	0.0155	2	10	0.2	34.30	0.00	28737	cyl/sp	6.86	37.67	32.12	39.32	39.86	43.65
bentz_2005_008_SBB3.2	738		SBB3.2	101	378	38178	33633	1980	978	2.94	15	333	197000	400	542.00	0.0161	2	10	0.2	34.30	0.00	28737	cyl/sp	6.86	36.71	30.90	38.48	38.81	42.68
bentz_2005_009_SBB3.3	739		SBB3.3	101	378	38178	33633	1980	978	2.94	15	333	197000	400	542.00	0.0161	2	10	0.2	34.30	0.00	28737	cyl/sp	6.86	36.71	30.90	38.48	38.81	42.68
Tanimura_2005_011_45	740	Tanimura; Sato (2005)	45	300	450	135000	120000	2400	1000	2.50	29	400	197000	750	2642.08	0.0220	2	16	0.2	92.34	0.00	28737	cyl/sp	6.86	189.83	182.71	222.86	227.17	255.27
Sneed_2007_001_1-1	741	Sneed (2007);	1-1	304.8	306.324	93367.555	71109.535	1397	679	2.91	19	233	197000	431	855.07	0.0120	2	9.525	0.2	62.77	4.28	28737	cyl/sp	6.86	95.50	97.21	98.27	97.22	102.32
Sneed_2007_002_1-2	742	Sneed, Ramirez (2008);	1-2	306.324	611.124	187201.95	162887.48	3162	1537	2.89	25	532	197000	453	2026.83	0.0124	2	9.525	0.2	62.77	4.07	28737	cyl/sp	6.86	168.47	168.75	179.32	188.55	206.29
Sneed_2007_003_1-3	743	Sneed, Ramirez (2010)	1-3	304.8	762	232257.6	207568.62	4064	1965	2.89	29	681	197000	474	2578.91	0.0124	2	9.525	0.2	61.78	4.03	28737	cyl/sp	6.86	197.36	190.30	215.04	221.41	240.46
Sneed_2007_004_1-4	744		1-4	306.324	914.4	280102.67	251816.19	4928	2375	2.89	36	822	197000	475	4029.54	0.0160	2	9.525	0.2	71.02	4.50	28737	cyl/sp	6.86	248.52	224.60	300.35	285.43	330.30
Sneed_2007_005_2-1	745		2-1	203.2	306.324	62245.037	47728.937	1397	679	2.89	16	235	197000	483	593.80	0.0124	2	9.525	0.2	65.12	3.76	28737	cyl/sp	6.86	65.05	66.35	63.93	66.93	72.15
Sneed_2007_006_2-2	746		2-2	407.924	608.076	248048.79	215006.71	3162	1537	2.92	29	527	197000	474	2578.91	0.0120	2	9.525	0.2	61.59	4.10	28737	cyl/sp	6.86	219.42	221.48	233.45	244.16	269.48
Sneed_2007_007_2-3	747		2-3	508	762	387096	347560.6	4064	1965	2.87	29	684	197000	474	4513.09	0.0130	2	9.525	0.2	64.73	4.16	28737	cyl/sp	6.86	336.81	325.42	374.30	382.04	416.33
Sneed_2007_008_2-4	748		2-4	612.902	914.4	560437.59	502759.22	4928	2375	2.90	36	820	197000	475	8059.08	0.0160	2	9.525	0.2	69.25	3.97	28737	cyl/sp	6.86	494.91	443.32	555.26	565.27	613.76
Feldman_1955_001_D-1	749	Feldman; Siess (1955)	D-1	152.4	304.8	46451.52	38477.342	2794	699	2.77	29	252	197000	295	1289.45	0.0335	2	25.4	0.2	29.29	2.29	28737	cyl/sp	6.86	65.37	39.30	74.69	59.72	70.30
Feldman_1955_002_D-2	750		D-2	152.4	304.8	46451.52	38477.342	2794	699	2.77	29	252	197000	307	1289.45	0.0335	2	25.4	0.2	36.62	2.39	28737	cyl/sp	6.86	70.43	43.94	76.51	64.92	73.80
Feldman_1955_003_D-3	751		D-3	152.4	304.8	46451.52	38477.342	3353	838	3.32	29	252	197000	314	1289.45	0.0335	2	25.4	0.2	31.58	2.66	28737	cyl/sp	6.86	64.06	40.81	69.71	58.60	64.49
Feldman_1955_006_D-6	752		D-6	152.4	304.8	46451.52	38477.342	2794	699	2.77	29	252	197000	310	1289.45	0.0335	2	25.4	0.2	22.60	2.07	28737	cyl/sp	6.86	59.96	34.52	71.89	54.12	65.99
Krefeld_1996_020_2AU	753	Krefeld;	2AU	152.4	304.8	46451.52	38709.6	2438	610	2.40	25	254	197000	394	506.71	0.0131	2	16	0.2	20.11	0.00	28737	cyl/sp	6.86	40.85	31.03	46.32	40.53	42.71
Krefeld_1996_022_4AU	754	Thurston (1966)	4AU	152.4	304.8	46451.52	38709.6	2438	610	2.40	25	254	197000	273	1013.41	0.0262	2	16	0.2	16.97	0.00	28737	cyl/sp	6.86	48.63	28.50	61.26	45.65	58.80
Krefeld_1996_023_5AU	755		5AU	152.4	304.8	46451.52	38477.342	2438	610	2.41	29	252	197000	268	1289.45	0.0335	2	16	0.2	19.59	0.00	28737	cyl/sp	6.86	55.07	30.48	70.19	50.64	66.04
Krefeld_1996_026_2CU	756		2CU	152.4	304.8	46451.52	38709.6	3048	762	3.00	25	254	197000	370	506.71	0.0131	2	16	0.2	19.79	0.00	28737	cyl/sp	6.86	38.28	30.78	39.69	37.64	35.56
Krefeld_1996_027_3CU	757		3CU	152.4	304.8	46451.52	38941.858	3048	762	2.98	22	256	197000	319	775.90	0.0199	2	16	0.2	19.46	0.00	28737	cyl/sp	6.86	44.03	30.66	48.25	42.68	46.63
Krefeld_1996_028_4CU	758		4CU	152.4	304.8	46451.52	38709.6	3048	762	3.00	25	254	197000	276	1013.41	0.0262	2	16	0.2	19.52	0.00	28737	cyl/sp	6.86	48.02	30.57	54.26	45.64	51.24
Krefeld_1996_029_5CU	759		5CU	152.4	304.8	46451.52	38477.342	3048	762	3.02	29	252	197000	224	1289.45	0.0335	2	16	0.2	19.39	0.00	28737	cyl/sp	6.86	51.73	30.33	60.09	48.02	55.44
Krefeld_1996_030_6CU	760		6CU	152.4	304.8	46451.52	38167.666	3048	762	3.04	32	250	197000	174	1634.54	0.0428	2	16	0.2	19.52	0.00	28737	cyl/sp	6.86	55.85	30.24	66.50	50.38	59.72
Krefeld_1996_031_3EU	761		3EU	152.4	304.8	46451.52	38941.858	3658	914	3.58	22	256	197000	349	775.90	0.0199	2	16	0.2	16.71	0.00	28737	cyl/sp	6.86	40.05	28.41	41.48	38.38	39.61
Krefeld_1996_032_4EU	762		4EU	152.4	304.8	46451.52	38709.6	3658	914	3.60	25	254	197000	327	1013.41	0.0262	2	16	0.2	19.23	0.00	28737	cyl/sp	6.86	45.73	30.34	48.44	43.27	45.20
Krefeld_1996_035_3GU	763		3GU	152.4	304.8	46451.52	38941.858	4267	1067	4.17	22	256	197000	379	775.90	0.0199	2	16	0.2	21.49	0.00	28737	cyl/sp	6.86	40.49	32.22	40.99	40.03	38.82
Krefeld_1996_037_5GU	764		5GU	152.4	304.8	46451.52	38477.342	4267	1067	4.23	29	252	197000	260	1289.45	0.0335	2	16	0.2	20.21	0.00	28737	cyl/sp	6.86	46.80	30.96	50.06	44.88	45.41
Krefeld_1996_039_3JU	765		3JU	152.4	304.8	46451.52	38941.858	4877	1219	4.77	22	256	197000	379	775.90	0.0199	2	16	0.2	21.10	0.00	28737	cyl/sp	6.86	40.24	31.93	38.13	38.14	35.90
Krefeld_1996_048_4AU	766		4AU	152.4	304.8	46451.52	38709.6	2438	610	2.40	25	254	197000	298	1013.41	0.0262	2	16	0.2	30.07	0.00	28737	cyl/sp	6.86	58.85	37.94	70.01	56.75	69.43
Krefeld_1996_049_5AU	767		5AU	152.4	304.8	46451.52	38477.342	2438	610	2.41	29	252	197000	306	1289.45	0.0335	2	16	0.2	30.07	0.00	28737	cyl/sp	6.86	63.53	37.77	77.54	59.85	75.12
Krefeld_1996_050_6AU	768		6AU	152.4	304.8	46451.52	38167.666	2438	610	2.43	32	250	197000	278	1634.54	0.0428	2	16	0.2	32.43	0.00	28737	cyl/sp	6.86	70.16	38.97	87.08	64.51	82.78
Krefeld_1996_051_4CU	769		4CU	152.4	304.8	46451.52	38709.6	3048	762	3.00	25	254	197000	314	1013.41	0.0262	2	16	0.2	30.66	0.00	28737	cyl/sp	6.86	55.81	38.31	61.14	53.89	58.92
Krefeld_1996_052_5CU	770		5CU	152.4	304.8	46451.52	38477.342	3048	762	3.02	29	252	197000	254	1289.45	0.0335	2	16	0.2	30.66	0.00	28737	cyl/sp	6.86	60.27	38.13	67.68	57.13	63.83
Krefeld_1996_053_6CU	771		6CU	152.4	304.8	46451.52	38206.375	3048	762	3.04	32	251	197000	249	1634.54	0.0428	2	16	0.2	34.99	0.00	28737	cyl/sp	6.86	67.88	40.51	77.39	63.26	71.96
Krefeld_1996_063_4CU	772		4CU	152.4	304.8	46451.52	38709.6	3048	762	3.00	25	254	197000	251	1013.41	0.0262	2	16	0.2	16.25	0.00	28737	cyl/sp	6.86	45.17	27.89	51.83	42.60	48.90
Krefeld_1996_067_4EU	773		4EU	152.4	304.8	46451.52	38709.6	3658	914	3.60	25	254	197000	231	1013.41	0.0262	2	16	0.2	13.56	0.00	28737	cyl/sp	6.86	40.71	25.48	44.11	38.04	41.64
Leonhardt_1962_007_14/1	774	Leonhardt;	14/1	190	320	60800	51870	3000	750	2.75	26	273	197000	465	1061.86	0.0205	2	30	0.2	30.67	2.97	28737	cyl/sp	6.86	74.11	54.50	85.45	72.06	83.01
Leonhardt_1962_008_14/2	775	Walther (1962)	14/2	190	320	60800	51870	3000	750	2.75	26	273	197000	465	1061.86	0.0205	2	30	0.2	30.67	2.97	28737	cyl/sp	6.86	74.11	54.50	85.45	72.06	83.01
Leonhardt_1962_009_15/1	776		15/1	190	320	60800	51680	4000	1000	3.68	26	272	197000	465	1061.86	0.0205	2	30

Shioya_1985_005_2-5	784	Akiyama (1985)	2-5	500	1200	600000	500000	12000	3000	3.00	10	1000	197000	370	1996.40	0.0040	2	25	0.2	20.81	2.01	28737	cyl/sp	6.86	230.90	279.76	203.20	256.40	265.91
Shioya_1985_006_2-6	785		2-6	1000	2100	2100000	2000000	24000	6000	3.00	16	2000	197000	370	7960.00	0.0040	2	25	0.2	27.08	2.46	28737	cyl/sp	6.86	799.49	870.38	761.90	873.37	812.77
Shioya_1985_007_2-7	786		2-7	1500	3140	4710000	4500000	36000	9000	3.00	25	3000	197000	360	18252.00	0.0041	2	25	0.2	23.09	1.97	28737	cyl/sp	6.86	1499.54	1371.82	1389.05	1566.31	1475.41
Shioya_1989_004_3-4	787	Shioya (1989)	3-4	300	655	196500	180000	7200	1800	3.00	6	600	197000	440	768.00	0.0043	2	2.5	0.2	25.94	1.70	28737	cyl/sp	6.86	83.86	95.83	66.84	91.68	74.89
Shioya_1989_006_3-6	788		3-6	500	1200	600000	500000	12000	3000	3.00	10	1000	197000	370	1996.40	0.0040	2	5	0.2	26.79	1.58	28737	cyl/sp	6.86	202.65	216.45	160.20	217.85	209.47

Vietnamese-German University

Structural Concrete Research Group

Bachelor Thesis Series

A. Shear, Punching, Torsion

[2026] **Dang My Kao Kim, Nguyen**

Shear and Punching Shear Design of Reinforced Concrete Structures according to the New Generation of Eurocode 2.
Vietnamese-German University, **BCE-2026-01**.

Supervisors: Dr.-Ing. habil. Ngoc Linh Tran, Prof.-Ing. Christian Kulas

[2026] **Viet Hung, Nguyen**

Effect of longitudinal reinforcement distribution on the shear strength of slender concrete members without shear reinforcement.
Vietnamese-German University, **BCE-2026-04**.

Supervisors: Dr.-Ing. habil. Ngoc Linh Tran, Prof.-Ing. Christian Kulas

VGU
Vietnamese-German University

B. Cracking

[2026] **Ngoc Anh Thu, Nguyen**

Cracking in Reinforced Concrete Structures.
Vietnamese-German University, **BCE-2026-02**.

Supervisors: Dr.-Ing. habil. Ngoc Linh Tran, Prof.-Ing. Christian Kulas